

# **Investigation of the Impact of Three Different Reference Particulate Matter on Human Monocytic THP-1 and Lung Epithelial A549 Cells**

## **Kumulative Dissertation**

zur

Erlangung des akademischen Grades  
doctor rerum naturalium (Dr. rer. nat.)  
der Mathematisch-Naturwissenschaftlichen Fakultät  
der Universität Rostock

vorgelegt von

**Xin Cao**

geb. am 03. Jan 1990 in Shandong

München und Rostock, October 2021

**Gutachter:**

Prof. Dr. Ralf Zimmermann, Universität Rostock, Institut für Chemie

Prof. Dr. Jeroen Buters, Technische Universität München, Zentrum Allergie und Umwelt

**Jahr der Einreichung:** 2021

**Jahr der Verteidigung:** 2022



## ERKLÄRUNG

Ich versichere hiermit an Eides statt, dass ich die vorliegende Arbeit selbstständig angefertigt und ohne fremde Hilfe verfasst habe. Dazu habe ich keine außer den von mir angegebenen Hilfsmitteln und Quellen verwendet und die den benutzten Werken inhaltlich und wörtlich entnommenen Stellen habe ich als solche kenntlich gemacht.

Die vorliegende Dissertation wurde bisher in gleicher oder ähnlicher Form keiner anderen Prüfungsbehörde vorgelegt und auch nicht veröffentlicht.

München, October, 2021

---





## Contributions to Publications

**First authorship publications:**

**Title:** Adenine Derivatization for LC-MS/MS Epigenetic DNA Modifications Studies on Monocytic THP-1 Cells Exposed to Reference Particulate Matter

**Author:** Xin Cao, Jutta Lintelmann, Sara Padoan, Stefanie Bauer, Anja Huber, Ajit Mudan, Sebastian Oeder, Thomas Adam, Sebastiano Di Bucchianico, Ralf Zimmermann

**Journal:** Analytical biochemistry, 618: 114127

**Year:** 2021

**Contribution:** For this publication, Xin Cao carried out the experiments, made data process, and wrote the manuscript.

**Title:** A comparative study of persistent DNA oxidation and chromosomal instability induced in vitro by oxidizers and reference airborne particles

**Authors:** Xin Cao, Sara Padoan, Stephanie Binder, Stefanie Bauer, Jürgen Orasche, Corina-Marcela Rus, Ajit Mudan, Anja Huber, Evelyn Kuhn, Sebastian Oeder, Jutta Lintelmann, Thomas Adam, Sebastiano Di Bucchianico, Ralf Zimmermann

**Journal:** Mutation Research - Genetic Toxicology and Environmental Mutagenesis

**Year:** Accepted (2022)

**Contribution:** For this publication, Xin Cao carried out the experiments, made data process, and wrote the manuscript.

**Co-authorship publications:**

**Title:** Analysis of PAHs Associated with PM10 and PM2.5 from Different Districts in Nanjing

**Authors:** Xiansheng Liu, Jürgen Schnelle-Kreis, Brigitte Schlöter-Hai, Lili Ma, Pengfei Tai, Xin Cao, Cencen Yu, Thomas Adam, Ralf Zimmermann

**Journal:** Aerosol and Air Quality Research, 19(10): 2294–2307

**Year:** 2019

<p><b>Contributions:</b> For this publication, Xin Cao helped to make data process and revise the manuscript.</p>
---

München, October 2021

---

---

## Acknowledgements

This study was supported by Helmholtz Virtual Institute of Complex Molecular System in Environment Health (HICE). I have been working full time at the Cooperation Group Comprehensive Molecular Analysis (CMA) within the framework of the Joint Mass Spectrometry Center (JMSC) of the Helmholtz Zentrum München and the University of Rostock. I acknowledge the financial supports from China Scholarship council (CSC).

I am sincerely grateful to my supervisor, Prof. Dr. Ralf Zimmermann for giving me this valuable opportunity to work with outstanding colleagues at CMA. This worthwhile experience of studying abroad opened my eyes and made me become a confident researcher. It will have a lasting impact on my academic life. I really appreciate what you have done for me.

I would also like to give my special thanks to my advisor Dr. Jutta Lintelmann for the encouragement and support when I came to CMA. Many thanks to my advisor Dr. Sebastiano Di Bucchianico for your technical guidance. Thank you for welcoming me in your “Aerosol Mutagenesis” group. I am very grateful to Dr. Christoph Bisig, Dr. Brigitte Schlöter-Hai, Dr. Uwe Kaefer, and Stephanie Binder for proofreading my dissertation, Dr. Stefanie Bauer for revising my manuscripts, Dr. Sara Padoan for analyzing metal elements, Dr. Jürgen Orasche for giving valuable information about particulate matter, Xiao Wu, Anja Huber, Evelyn Kuhn, Dr. Sebastian Oeder, and other bio-group, and all other members of CMA are acknowledged for giving me great help.

Finally, I give my deepest thanks to my devoted family, especially to my parents and wife for their love, encouragement, and support. You are my light in the darkness when I am sailing on the sea. Thank you for being my family.



## Zusammenfassung

Luftverschmutzung ist eines der größten Gesundheitsprobleme der Welt. Jedes Jahr werden Tausende von Todesfällen auf verschmutzte Luft zurückgeführt. Feinstaub (PM) ist ein sehr wichtiger Bestandteil der Luftverschmutzung. Es enthält komplexe anorganische und organische Stoffe wie Metalle und polyzyklische aromatische Kohlenwasserstoffe (PAK). Toxikologische Studien zeigen, dass PM Zytotoxizität, Entzündung und Genotoxizität in Zellen induzieren kann. Die Auswirkungen von PM auf die menschliche Gesundheit sind jedoch sehr komplex und noch nicht vollständig verstanden. Im Zuge dieser Arbeit fanden wir zunächst heraus, dass PM verschiedenen Ursprungs unterschiedliche Zusammensetzungen an PAKs enthielten, die unterschiedliche toxische und mutagene Äquivalente aufwiesen (Publikation 1). Um zu verstehen, wie sich PM verschiedenen Ursprungs auf Zellen auswirken, und welche Komponenten bei den biologischen Effekten eine Rolle spielen, wurden in-vitro-Experimente an verschiedenen Zelltypen durchgeführt (Publikation 2 und 3).

Wir untersuchten den Einfluss von drei Referenz-PM, d. h. Feinstaub ERM-CZ100 (CZ100), Urban Dust SRM1649 (UD 1649), und Diesel PM SRM2975 (Diesel PM 2975), auf humane monozytäre THP-1-Zellen und A549 Lungenepithelzellen. Sowohl oxidative DNA-Schäden in Form von 8-Hydroxy-2'-desoxyguanosin (8-OHdG) Läsionen, als auch das Lipidperoxidationsprodukt Malondialdehyd (MDA) wurden in beiden Zelltypen mittels Flüssigchromatographie-Tandem-Massenspektrometrie (LC-MS/MS) analysiert, um die oxidative Kapazität der drei verschiedenen PM. Der Zytokinese-Block-Mikronukleus-Zytom Assay (CBMN Cyt, OECD 487) wurde durchgeführt, um in beiden Zelllinien die Genotoxizität (basierend auf Chromosomenschäden) der verschiedenen PM und Oxidationsmittel zu untersuchen. Kontaminationen durch Metallelemente in den PM Proben wurden unter Verwendung von Massenspektrometrie mit induktiv gekoppeltem Plasma (ICP-MS) analysiert. Die Auswirkungen von PM auf epigenetische DNA-Modifikationen wie Cytosin-Methylierung, Cytosin-Hydroxymethylierung und Adenin-Methylierung wurden in menschlichen monozytären THP-1-Zellen untersucht. Die Korrelation zwischen verschiedenen toxikologischen Ereignissen und PM-Komponenten wurden untersucht, um eine potenzielle Verbindung zwischen ihnen herzustellen.

Die drei verschiedenen PM wiesen unterschiedliche Verunreinigungen durch Metallelemente und PAHs auf und zeigten unterschiedliche schädliche Wirkungen auf beide Zelltypen. Alle PM induzierten oxidative DNA-Schäden in Form von 8-OHdG. Nur CZ100 zeigte eine oxidative Kapazität, Lipide zu oxidieren, was sich in Form erhöhter MDA Level widerspiegelte. In A549 Zellen generierte Diesel PM 2975 die höchste Genotoxizität im Vergleich zu den beiden anderen PM. CZ100 und UD 1649 verringerten das Cytosin-Methylierungs Level. Während alle PM das Cytosin-Hydroxymethylierungs Level erhöhten, wurde eine erhöhte Adenin-Methylierung nur durch CZ100 induziert. Die Ergebnisse zeigten, dass THP-1 Zellen gegenüber oxidativen Bedingungen sensibler waren als A549 Zellen. Während die persistenten 8-OHdG DNA-Schäden eine potenziell treibende Kraft für Chromosomenschäden darstellen, waren die verringerten Cytosin-Methylierungsniveaus eher auf

Metallelemente wie As, Cr und Cd in PM zurückzuführen. Die erhöhte Cytosin-Hydroxymethylierung und N6-Methyladenin waren reversibel und hatten potenziell biologische Funktionen als Reaktion auf die PM-Exposition.

## Abstract

Air pollution has been one of the biggest environmental issues in the world. Every year, polluted air caused thousands of deaths. Particulate matter (PM) is a very important component of air pollutants. It contains complex inorganic and organic substances such as metals and polycyclic aromatic hydrocarbons (PAHs). Toxicological studies show that PM induces cytotoxicity, inflammation, and genotoxicity. However, the impact of PM on human health is very complex, and the underlying mechanisms are not yet fully understood. In this thesis, we firstly found PM, collected from different districts, contained diverse PAHs, and exhibited different toxic and mutagenic equivalent (Publication 1). To understand how PM from different sources impact cells and which components play a key role in the observed adverse effects, *in vitro* experiments on distinct cell types were conducted (Publication 2 and 3).

We investigated the impact of three reference PM, encompassing fine dust ERM-CZ100 (CZ100), urban dust SRM1649 (UD 1649), and diesel PM SRM2975 (diesel PM 2975) on human monocytic THP-1 cells and lung epithelial A549 cells, respectively. 8-Hydroxy-2'-deoxyguanosine (8-OHdG) is used as the oxidative DNA damage marker and malondialdehyde (MDA) is served as the biomarker of lipid peroxidation. Liquid chromatography tandem mass spectrometry (LC-MS/MS) was used to evaluate the mentioned oxidative stress inducing potential, respectively. Additionally, cytokinesis-block micronucleus cytome (CBMN Cyt, OECD 487) assay was performed to evaluate their genotoxicity (in terms of chromosomal instability). To know much more about the observed adverse effects, inductively coupled plasma mass spectrometry (ICP-MS) was used to analyze the metals in the samples. The effects of PM on epigenetic DNA modifications such as cytosine methylation, cytosine hydroxymethylation, and adenine methylation were investigated in human monocytic THP-1 cells. The associations between the different toxicological events and PM components were studied to explore their potential interplay.

Three reference PM, containing different metal elements and PAHs, showed different capacities to induce adverse effects on the cells. All PM had the oxidative potential to oxidize DNA, which was demonstrated by the detection of 8-OHdG. Only CZ100 was capable of inducing lipid peroxidation generating MDA. Diesel PM 2975 induced the highest genotoxicity compared to the other PM on A549 cells, while CZ100 and UD 1649 decreased cytosine methylation levels. All PM increased cytosine hydroxymethylation levels, increased adenine methylation level was only induced by CZ100. These results indicated that THP-1 cells were more sensitive towards oxidative conditions than that of A549 cells. The persistent DNA damage, depicted by increased 8-OHdG levels, was a potential driving force for chromosome damage. The decreased cytosine methylation levels were due to the presence of metals such as As, Cr, and Cd contained in PM. The increased cytosine hydroxymethylation and N6-methyladenine were reversible and had potential functions in response to PM exposure.





## Contents

1 Introduction .....	1
1.1 Particulate matter and human health.....	1
1.2 Toxicology of particulate matter .....	2
1.2.1 Genotoxicity .....	2
1.2.2 Epigenetic DNA modifications .....	4
1.3 Motivation.....	5
2 Methodology .....	7
2.1 Reference particulate matter .....	7
2.1.1 Fine dust ERM-CZ100 .....	7
2.1.2 Urban dust SRM1649.....	7
2.1.3 Diesel PM SRM2975 .....	7
2.2 Cell culture.....	8
2.3 Trypan blue exclusion assay .....	8
2.4 Particle deposition analysis.....	9
2.5 Sample preparations.....	10
2.5.1 Solid-phase extraction.....	10
2.5.2 Liquid-liquid extraction .....	11
2.5.3 Chemical derivatization .....	12
2.6 Liquid chromatography.....	15
2.7 Hybrid triple quadrupole/linear ion trap mass spectrometry .....	17
2.8 Inductively coupled plasma mass spectrometry .....	20
2.9 Cytokinesis-block micronucleus cytome assay .....	21
2.10 Calculation of toxic equivalent and mutagenic equivalent .....	22
3 Results and discussion.....	25
3.1 PM analysis from Nanjing city .....	25
3.2 Cell viability assay.....	26
3.3 Particle deposition analysis.....	27
3.4 Quantification of 8-hydroxy-2'-deoxyguanosine and malondialdehyde .....	27
3.5 Cytokinesis-block micronucleus cytome assay .....	29
3.6 Correlation between 8-OHdG persistency and chromosomal instabilities .....	32
3.7 Epigenetic DNA modifications analysis methods development .....	33
3.8 Epigenetic DNA modifications measurement.....	34
4 Conclusion and outlook.....	39
5 References .....	40
6 Appendix .....	50
6.1 List of abbreviations .....	50
6.2 List of figures.....	52
6.3 List of tables .....	54
6.4 List of publications .....	55
6.4.1 Publication 1.....	55
6.4.2 Publication 2.....	70
6.4.3 Publication 3.....	93
6.5 Contributions to conferences .....	104
6.6 Curriculum vitae .....	105



# 1 Introduction

Air is polluted by aerosols from both anthropogenic and natural sources, for instance, fossil fuels burning from transports and industries, biomass burning from agricultural land and households, as well as volcanic eruptions and forest fires. Particulate matter (PM) is a very important component of air pollution. It contains harmful inorganic substances (e.g. heavy metals) and toxic organic substances (e.g. polycyclic aromatic hydrocarbons, PAHs) (Wang et al., 2020; He et al., 2014). Together with the gases in air (e.g. NO<sub>x</sub>, SO<sub>2</sub>, and volatile organic compounds), PM severely impacts human health. It is a driving force for different health impairments such as pulmonary diseases and cardiovascular diseases thus leading to increased morbidity and mortality (Valavanidis et al., 2008). Toxicological studies show that PM causes cytotoxicity, genotoxicity, and inflammation in cells (Park et al., 2018; Steenhof et al., 2011). However, the impact of PM on human health is much more complicated than we know and the mechanism of how PM induces adverse effects is still not yet fully understood (Anderson et al., 2012). A better understanding of how PM impacts cells and which components of PM induce the adverse effects can help to understand how air pollution effects human health.

In this thesis, we studied diverse PM collected from different districts in Nanjing city (Publication 1). We found that PAH components in collected PM varied in the collected places such as the traffic area and the industrial area. Based on toxic and mutagenic equivalent calculation, PM<sub>10</sub> showed higher toxic and mutagenic potential than PM<sub>2.5</sub> in all places. To understand how PM from different sources impacts cells, *in vitro* studies are necessary. In the following studies (Publication 2 and 3), three standard reference PM (i.e. fine dust ERM-CZ100, CZ100; urban dust SRM1649, UD 1649; diesel PM SRM2975, diesel PM 2975) were used for cell exposure studies. Human monocytic THP-1 cells were used to study the immune cell-related response. Lung epithelial A549 cells were used to investigate the lung cell-related activity. The components (e.g. PAHs and metals) of PM were confirmed either from certificates or by chemical analysis. Different toxicological endpoints (e.g. oxidative DNA damage, lipid oxidation damage, and genotoxicity) were studied and their associations with PAHs or metals were explored to reveal their potential interplay.

## 1.1 Particulate matter and human health

PM can be categorized into PM<sub>10</sub> (< 10 µm), PM<sub>2.5</sub> (< 2.5 µm), and PM<sub>0.1</sub> (< 0.1 µm) based on their aerodynamic diameters (Colbeck and Lazaridis, 2014). Inhalation of PM impacts human health (Brunekreef and Forsberg, 2005) and the increased PM in the ambient air is related to different diseases (Kim et al., 2015). In several countries, an increase of 10 µg/m<sup>3</sup> PM<sub>2.5</sub> was associated with increased lung cancer mortality, including the USA with an increase of 8% (Arden Pope III et al., 2002), Japan with an increase of 24% (Katanoda et al., 2011), and northern China with an increase of 3.4%-6.0% (Chen et al., 2016). Especially, the older and the chronically ill population are susceptible to the inhalation of PM (Gouveia and Fletcher, 2000). The Air Pollution on Health: a European approach II

study showed that an increase of  $10 \mu\text{g}/\text{m}^3$   $\text{PM}_{10}$  was associated with a 0.8% increase of daily mortality for the elderly which was 0.2% higher compared to the all ages daily mortality (Aga et al., 2003). The concentration of ambient PM varies in different regions. The annual  $\text{PM}_{2.5}$  concentrations in New Delhi, Beijing, and Hanoi are higher than that in Lima, Singapore, and Munich with the health protection limit of  $25 \mu\text{g}/\text{m}^3$  set by European Union (EU) (**Figure 1.1**). According to the World Air Quality Report in 2019 (<https://www.iqair.cn/cn-en/node/10136>), about 90% of the global population breathes unsafe air without meeting WHO annual  $\text{PM}_{2.5}$  target of  $10 \mu\text{g}/\text{m}^3$ . And particulate matter pollution is an important risk factor for the global burden of disease (GBD 2019 Risk Factor Collaborators, 2020). So the study of the impact of particulate matter on human health is very in demand.

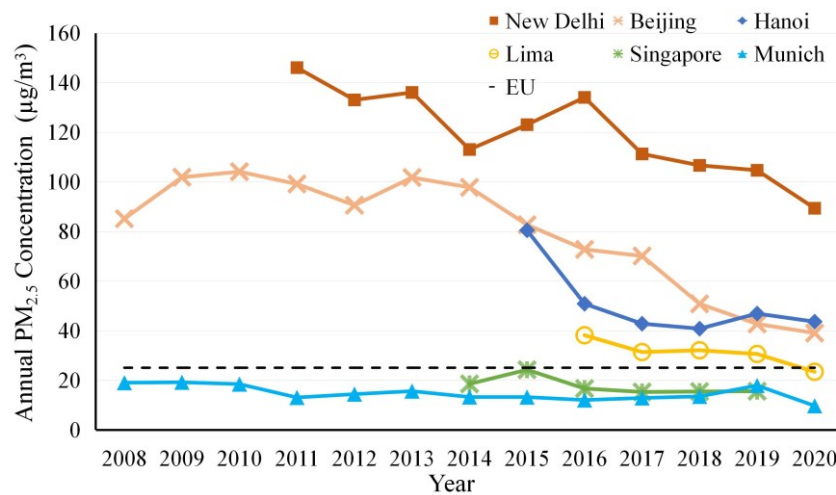


**Figure 1.1:** Annual  $\text{PM}_{2.5}$  concentrations in different cities (2008-2020). New Delhi data in 2011 from a report (Mandal et al., 2014) and in 2012-2016 from a report (Sharma et al., 2018) and in 2017-2020 from <https://www.airnow.gov>; Beijing data from <http://www.stateair.net> (2008-2017) and <https://www.airnow.gov> (2018-2020); Hanoi data from <https://www.airnow.gov>; Lima data from <https://www.airnow.gov>; Singapore data from <https://smartairfilters.com/en>; Munich data from <https://www.lfu.bayern.de/index.htm>

## 1.2 Toxicology of particulate matter

### 1.2.1 Genotoxicity

Genotoxicity is a broader term and it refers to the capability of substances to damage genetic information (Boobis et al., 2017). PM is a complex mixture containing inorganic and organic components which can damage DNA and chromosome leading to genotoxicity such as oxidative DNA damage, DNA adducts, DNA single- and double-strand breaks, and chromosomal abnormalities (Schins and Knaapen, 2007; Da Silva et al., 2015) (**Figure 1.2**).

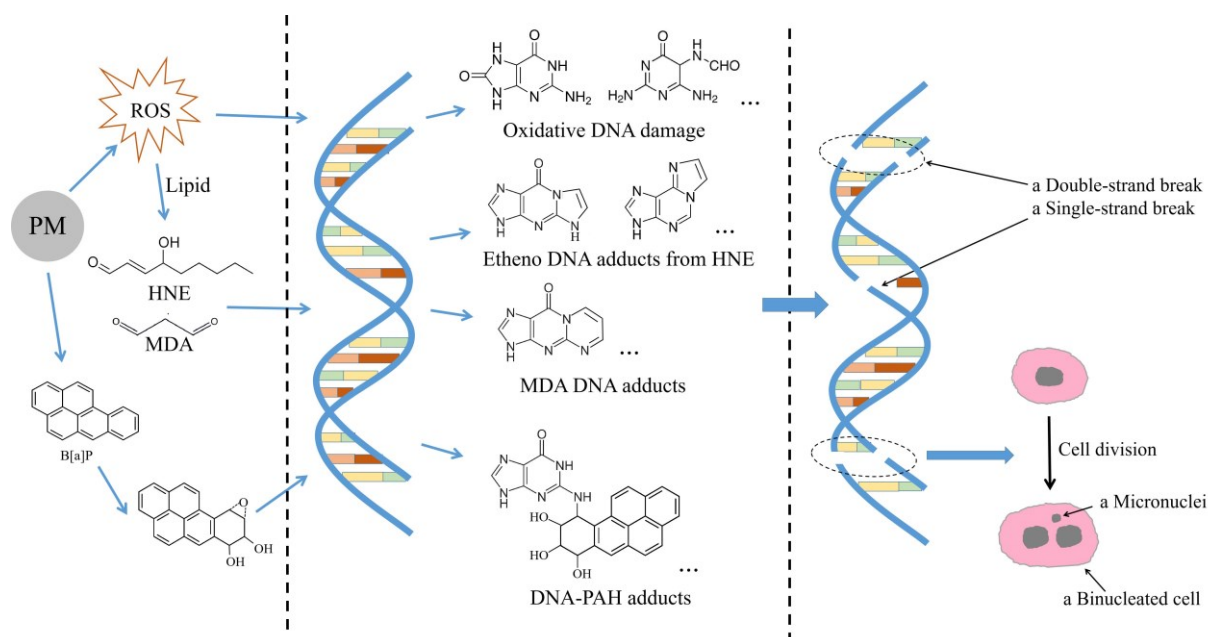


**Figure 1.2:** Illustration of possible genotoxicity induced by PM. (ROS, reactive oxygen species; HNE, 4-hydroxynoneal; MDA, malondialdehyde; B[a]P, benzo[a]pyrene)

Different components in PM can induce reactive oxygen species (ROS) in cells. Transition metals (e.g. iron and copper) can act as catalyst in Fenton reactions to produce ROS (Winterbourn, 1995; Vidrio et al., 2008). Quinones in PM can induce ROS by redox reactions (Chung et al., 2006; Wang et al., 2018). PAHs can be metabolized by cytochrome P450 family 1 subfamily A (CYP1A) proteins into redox-active epoxide intermediates producing ROS as well (Harvey, 1996). Free radicals are very reactive and can destruct cell organelles and components. For instance, ROS can oxidize bases on DNA (e.g. guanine) inducing hydroxyl or carbonyl groups to guanine forming 8-oxoguanine which is the most commonly used biomarker for DNA oxidation, or break the molecular structure of guanine generating Fapy-guanine (Cadet and Wanger, 2013). The produced 8-oxoguanine can further lead to DNA mutation by inducing G:C to T:A transversion mutations (Kornyushyna et al., 2002).

ROS can also lead to lipid peroxidation, which produces aldehydes such as malondialdehyde (MDA) and 4-hydroxynoneal (HNE) (Ayala et al., 2014). The produced MDA and HNE can further react with DNA forming DNA adducts. For example, MDA can react with guanine forming pyrimido[1,2-a]purin-10(3H)-one adduct which can cause G-T or G-A mutations (Dedon et al., 1998; Fink et al., 1997). HNE can react with guanine and adenine to produce 1,N<sup>2</sup>-etheno-guanine and 1,N<sup>6</sup>-etheno-adenine adducts (De Oliveira et al., 2018) which can lead to G-A mutation and A-G mutations, respectively (Marnett and Plastaras, 2001).

DNA adducts can also be induced by exogenous PAHs from PM (Sevastyanova et al., 2008). Cellular metabolisms of PAHs can generate highly reactive intermediates such as diol-PAH and epoxide-PAH (Godschalk et al., 2003) that can form DNA-PAH adducts. For instance, PAHs in urban PM formed stable bulky DNA adducts in lung embryonic L132 cells (Abbas et al., 2013) and in lung epithelial A549

cells (Billet et al., 2008). A comparison *in vitro* study about the extracted fractions of urban PM showed that PAHs and nitro-PAHs were the major contributors to DNA adducts compared to bases, acids, and aliphatic substances in rat hepatocyte cells and hamster lung V79NH cells (Topinka et al., 2000). The produced DNA-PAH adducts were mutagenic inducing G-T mutation (Barnes et al., 2018; Zhang et al., 2012).

Furthermore, the excision of DNA adducts or DNA damage (such as 8-oxoguanine) can induce gaps on DNA structures to produce DNA single- and double-strand breaks (Fenech and Neville, 1992; Fenech et al., 2011). It can contribute to chromosomal abnormalities such as micronuclei.

### 1.2.2 Epigenetic DNA modifications

Epigenetic DNA modifications refer to heritable changes by affecting gene activities and expressions but without changing the DNA sequence (Handy et al., 2011). Cytosine methylation and cytosine hydroxymethylation are two important epigenetic DNA modification processes (**Figure 1.3a**). They play an important role in gene regulation (Guibert and Weber, 2013). Cytosine methylation can silence gene transcriptions to suppress gene expression. Cytosine hydroxymethylation can activate the cytosine demethylation process (namely, transformation of 5-cytosine to 5-hydroxymethylcytosine which can further be oxidized into 5-formylcytosine and 5-carboxycytosine) and modulate the binding of chromatin effectors to influence gene expression. Furthermore, aberrant changes of cytosine methylation levels (Wilson et al., 2007; Hansen et al., 2011; Ehrlich, 2009) and cytosine hydroxymethylation levels (Dao et al., 2014) are related to different diseases such as cancer and can be regarded as useful markers. Adenine methylation (**Figure 1.3b**) is another important epigenetic modification and was first found in prokaryotes such as bacteria (Luo et al., 2015). It plays an important role in the restriction-modification system to remove foreign pathogenic DNA and protect host DNA (Naito et al., 1995). It was also observed in unicellular eukaryotes such as tetrahymena (Hattman, 2005) and in higher and multicellular eukaryotes such as plants and mammals (Parashar et al., 2018). The function of adenine methylation in eukaryotes is not yet fully understood. But adenine methylation is linked to gene expression in eukaryotes and may be a potential epigenetic marker (Sun et al, 2015a).

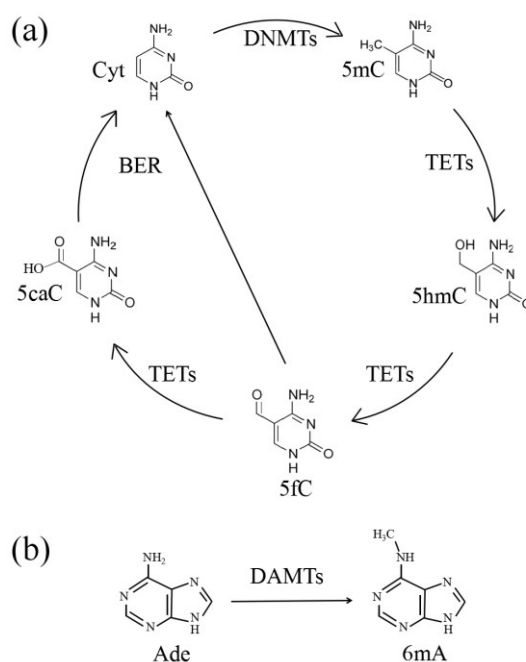


**Figure 1.3:** (a) Epigenetic cytosine modifications; (b) epigenetic adenine modification. (Cyt, cytosine; 5mC, 5-methylcytosine; 5hmC, 5-hydroxymethylcytosine; 5fC, 5-formylcytosine; 5caC, 5-carboxycytosine; DNMTs, DNA methyltransferases; TETs, tel-eleven translocations; BER, base excision repair; Ade, adenine, 6mA, N6-methyladenine; DAMTs, DNA N6 adenine methyltransferases)

The research on epigenetic DNA modifications, induced by PM exposure, only focused on cytosine methylation and cytosine hydroxymethylation. The published cytosine methylation data are contradictory. Indoor PM exposure was associated with global cytosine hypomethylation in placental tissues (Janssen et al., 2013). An increase of global methylation in male C57BL/CBA mice germ-line DNA was observed after in-situ exposure to PM exhausted by steel mills and highway transportation (Yauk et al., 2008). A study revealed a reduced DNA Alu methylation (DNA Alu sequences are repetitive short interspersed DNA elements named after the endonuclease *Arthrobacter luteus* and encompassing 10% of the primate DNA, Sukapan et al., 2014) in human blood samples after exposure to street PM (Bellavie et al., 2013). Traffic-related pollutants strongly increased DNA Alu methylation in human blood samples (Bind et al., 2012). Cytosine hydroxymethylation changes exposed to PM were also reported with contradictions. For instance, 5hmC levels in human blood samples were positively associated with ambient PM<sub>10</sub> but not with PM<sub>2.5</sub> levels (Sanchez-Guerra et al., 2015). In contrast, 5hmC levels in human buccal cells were negatively associated with ambient PM<sub>10</sub> and PM<sub>2.5</sub> (De Nys et al., 2017). Based on the above research, the effects of PM on cytosine methylation and hydroxymethylation are still not yet fully understood. Furthermore, the impact of PM on adenine methylation is still not studied yet.

### 1.3 Motivation

PM is a central component of air pollution, related to different pulmonary diseases and cardiovascular



---

diseases. Understanding how PM interacts with cells can help to elucidate its impacts on human health and to evaluate the air pollution exposure risk. However, even with large research efforts until now, the effects of PM on cells are still not yet fully understood.

More work are still needed to study the difference between diverse PM collected from different sources and which components in PM cause the adverse cytotoxicity and genotoxicity effects in cells. The impact of PM on epigenetic DNA modifications is still not clear and further studies are in demand to elucidate their potential associations.

Based on these points, we studied PM collected from different districts in Nanjing city. It was found that PM from different sources contains diverse PAH components and exhibited different toxic and mutagenic equivalents. In the following studies, we investigated the impact of three reference PM *in vitro* to study their potential adverse effects in human monocytic THP-1 and lung epithelial A549 cells. Toxicological events such as cytotoxicity, oxidative DNA damage, lipid peroxidation, genotoxicity, and epigenetic DNA modifications were investigated to compare their different effects. The association between different toxicological events were also studied to explore their potential interplay.

## 2 Methodology

### 2.1 Reference particulate matter

In this thesis, three different reference PM were used for cell exposure. That is fine dust ERM-CZ100, urban dust SRM1649, and diesel PM SRM 2975 (**Figure 2.1**). All three reference PM were collected from different sources containing different components and are agglomerates without a uniform size distribution. Information of PAH contents, particle size distribution for three PM, and metal contents in CZ100 and UD 1649 are from their respective certificates. Information of metal contents in diesel PM 2975 is reported by Ball et al., 2000.

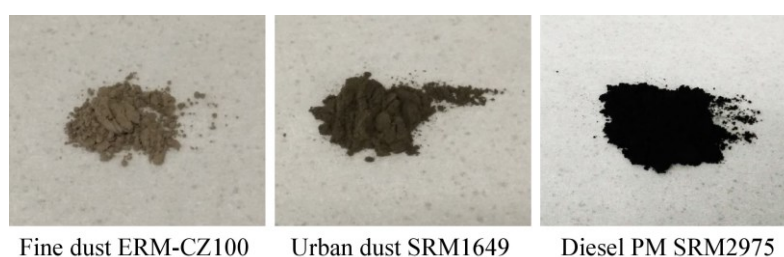


**Figure 2.1:** Three different reference PM.

#### 2.1.1 Fine dust ERM-CZ100

Fine dust ERM CZ-100 is road dust collected in 2010 from the tunnel called Wislostrada in Poland. Most of the dust is from tunnel walls and small parts are from sidewalks which are inaccessible to the public. Collected dust was sieved by a 0.5 mm sieve followed by a 0.25 mm sieve. Filtrated dust was triturerated into fine dust by using a jet mill. The final produced PM<sub>10</sub>-like dust was filled into vials under an argon atmosphere. CZ100 contains some high amounts of metals such as iron (38 g/kg), magnesium (13 g/kg), and aluminium (34 g/kg), which could be originated from tire and brake abrasion from vehicles.

#### 2.1.2 Urban dust SRM1649

Urban dust SRM1649 are ambient particles collected from an urban area in Washington, D.C. in 1976/1977. The collection period lasted for more than one year. The collected dust was filtrated by a 63 µm sieve and mixed well by using a V-blender before the final bottling. Urban dust SRM1649 used in the study was firstly issued in 1982 and the same particles were re-issued in 1999 as SRM1649a and again in 2009 as SRM1649b. Urban dust SRM1649 includes PAHs, their derivatives, and metal elements. The amount of Cd (569 mg/kg) in urban dust SRM1649 is very high, which may be related to the extensive use of Cd in plastics and vehicle brakes until the late 20th century.

#### 2.1.3 Diesel PM SRM2975

Diesel PM SRM2975 was produced by diesel-powered forklifts from Donaldson Company, Inc in 2000.

Collected particles were firstly mixed well by using a V-blender for 1 hour and then bottled for distribution. Diesel PM SRM2975 comprises high amounts of PAHs, their derivatives, and few metals. High concentrations of nitro-PAHs are certified for diesel PM SRM2975, which is related to freshly collected particles and without exposure to any atmospheric photo-oxidation reactions. The filtrated particles originate directly from the exhaust pipe, therefore, the found metals like iron (0.9 mg/kg), cobalt (0.1 mg/kg), and nickel (0.5 mg/kg) are typical for metal abrasion from the engine. In addition, different alkylated PAHs are certified for diesel PM SRM2975, which is a typical non-combustion-related release of lubrication oil.

## 2.2 Cell culture

Human monocytic THP-1 and lung epithelial A549 cells were cultured in Roswell Park Memorial Institute (RPMI) 1649 medium with 10% fetal bovine serum (FBS), 1% penicillin/streptomycin solution, and 2 mM L-glutamine under 37°C in a humid condition with 5% CO<sub>2</sub>. Cells were seeded in culture flasks (T25 or T75 or T175) 24 hours prior to substance exposure. The seeding density of monocytic THP-1 and epithelial A549 cells were 0.12 and 0.06 million cells/cm<sup>2</sup>, respectively. PM stock solution (1 mg/mL) was prepared in medium without FBS. Menadione and 3-chloro-1,2-propanediol (3-MCPD) stock solutions (1 mg/mL) were prepared in dimethyl sulphoxide (DMSO) and water, respectively. 5-aza-2'-deoxycytidine (5-azadC) and tert-butyl hydroperoxide (TBHP) stock solutions (1 mg/mL) were prepared in water, respectively. The PM and other substance stock solutions were diluted in the culture medium (with FBS) to reach the final exposure concentrations. For the epigenetic experiment, 2 mL of CZ100 or UD 1649 stocking solution were added to T75 flasks containing 8 mL culture medium to reach 200 µg/mL. 0.4 mL of diesel PM 2975 stock solution was added to a T75 flask containing 9.6 mL culture medium to reach 40 µg/mL. 23 µL of 5-azadC or 90 µL of TBHP stocking solution were added to T75 flasks containing 10 mL culture medium to reach 2.3 µg/mL or 9 µg/mL, respectively.

## 2.3 Trypan blue exclusion assay

Trypan blue exclusion assay was used to measure cell viability of human monocytic THP-1 and lung epithelial A549 cells exposed to different concentrations of PM and oxidizers for 24 hours. This assay is simple and widely used to determine cytotoxicity by counting the number of alive cells and dead cells in a cell suspension (Strober, 2015). The principle is that trypan blue is a large molecule with negative charge. Viable cells with intact cell membranes can block the entry of trypan blue through the cell membrane. On the contrary, trypan blue can penetrate dead cells membrane to color the cell into blue (**Figure 2.2a**). The colored cells can be distinguished by a light microscopy. Briefly, a cell suspension was diluted to an appropriate density (200-2000 cells per mL). Then 20 µL of the cell suspension was mixed with 20 µL of 0.4% trypan blue solution. An aliquot of 20 µL of the mixture was transferred to a hemacytometer. The following counting step was operated by using the hemacytometer (**Figure 2.2b**) with the cell viability calculation shown in eq. 2.1.

$$\text{Cell viability}\% = (\text{alive cells}) / (\text{alive cells} + \text{dead cells}) \cdot 100\% \quad (\text{eq. 2.1})$$

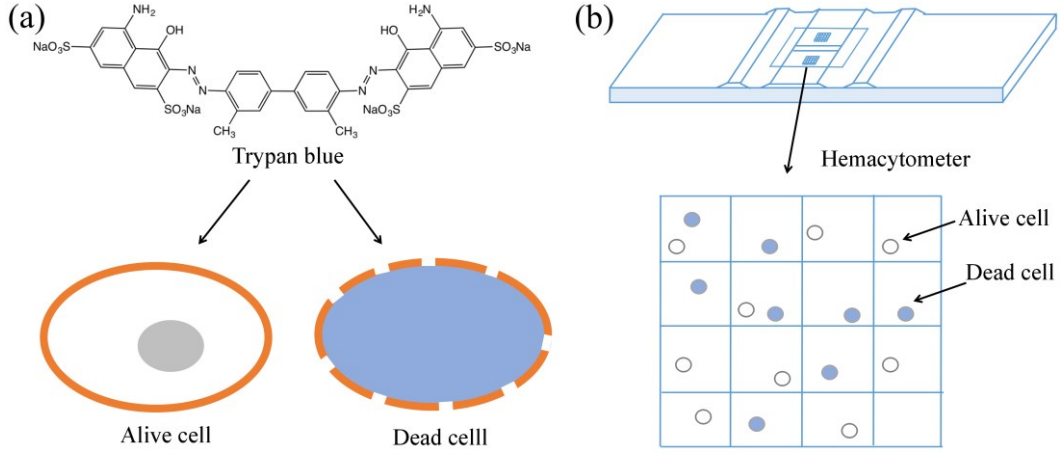


**Figure 2.2:** (a) The difference between an alive cell and a dead cell stained by trypan blue; (b) Counting cells by using a hemacytometer.

## 2.4 Particle deposition analysis

Particle deposition was explored on A549 cells exposed to different PM. After PM exposure, the epithelial A549 cells were washed by phosphate-buffered saline (PBS). After treatment by trypsin, cells were centrifuged (144 rcf for 20 mins) to get the pellet. The pellet was hydrolyzed in 4 N KOH:ethanol (1:1, v/v) solution at room temperature overnight (Rudd and Strom, 1981). The hydrolysate solution was centrifuged (9390 rcf for 20 mins) again and the pellet was resuspended in water for analysis by using a photometer with a 748 nm wavelength. For calibration curves, different amounts of standard particles were hydrolyzed and analyzed according to the sample preparation process. The standard curves for CZ100 (15-105  $\mu\text{g/mL}$ ), UD 1649 (15-105  $\mu\text{g/mL}$ ), and diesel PM 2975 (3-21  $\mu\text{g/mL}$ ) were set up for quantification, respectively. In principle, the particles in the solution absorb and scatter part of the incident light which lead to a lower intensity of the transmitted light, which can be measured photometrically (**Figure 2.3**). The intensity difference between the incident and transmitted light correlates with the concentration of the analyte, the absorption coefficient, and the path distance of light in the solution, which obey the Lambert-Beer's law (eq. 2.2).

$$A = \varepsilon \cdot l \cdot c \quad (\text{eq. 2.2})$$

A is the absorbance.  $\varepsilon$  is the absorption coefficient.  $l$  is the path distance of light.  $c$  is the concentration of the analyte.

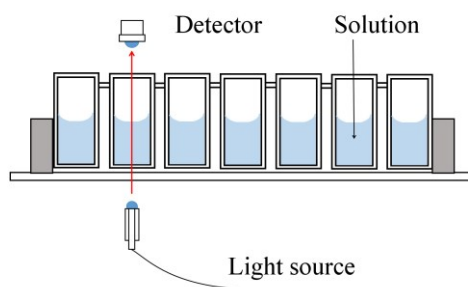


**Figure 2.3:** Illustration of the work mechanism of a photometer.

## 2.5 Sample preparations

After cell exposure, the medium and cells were collected for further sample preparations prior to liquid chromatography tandem mass spectrometry (LC-MS/MS) system. Different sample preparation methods were used to either remove impurities, concentrate target molecules, increase the target retention time on LC, or improve the target sensitivity on MS. For the analysis of oxidative DNA damage (8-OHdG), solid-phase extraction was used. For the measurement of oxidative lipid damage (MDA), chemical derivatization and liquid-liquid extraction were applied. For the evaluation of epigenetic DNA modifications, chemical derivatization methods were developed.

### 2.5.1 Solid-phase extraction

Solid-phase extraction (SPE) was used to prepare 8-OHdG samples. SPE is widely used in sample preparation for semivolatile or nonvolatile target analytes. It can effectively remove impurities and enrich the target analytes especially for low concentrations of analytes. Normally, a cartridge is packaged with stationary/solid phase such as modified silica particles which have different functional groups on the surface depending on the desired selectivity. The analytes in the mobile phase which interact with the solid phase (e.g. via van der Waals force, pi-pi interaction, dipole-dipole interaction, and electrostatic attraction) can be adsorbed on the solid phase. The typical extraction steps include conditioning, equilibration, loading, washing, and eluting (**Figure 2.4**). The conditioning step can remove the trapped air in the package materials and activate the functional groups on the surface of the stationary phase. Subsequently, the SPE cartridge is purged with the desired solvent to equilibrate the stationary phase for the following adsorption process. In the loading step, the sample solution is transferred to the SPE cartridge. Target analytes are selectively adsorbed to the stationary phase, whereas unwanted parts of the matrix pass through the solid bed. In the following washing step, the cartridge is washed by solutions to remove the undesired impurities from the stationary phase. Finally, the desired analyte is desorbed by disrupting the interaction between the analyte and stationary phase with appropriate eluents. In addition to the purification of the target analytes, the analyte concentration can be increased when re-dissolved in a small volume solution.

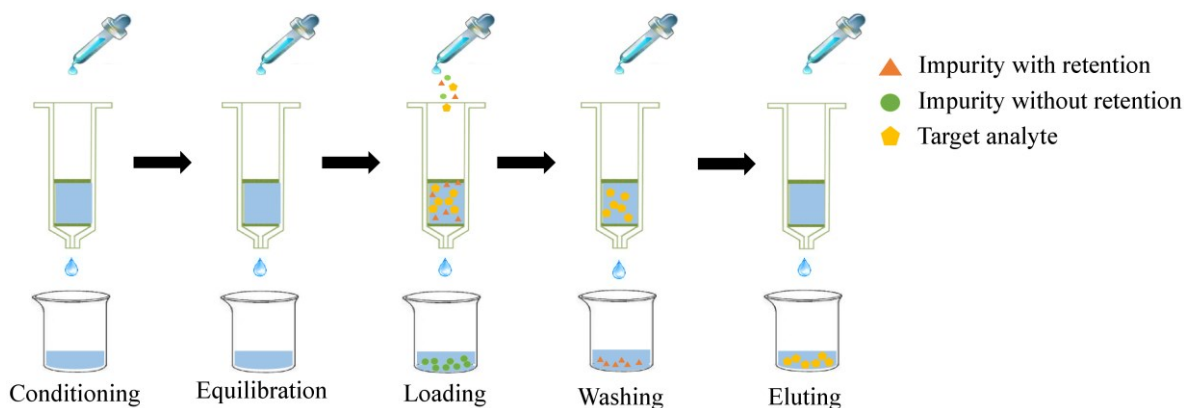


**Figure 2.4:** Illustration of the work mechanism of a solid-phase extraction.

Based on different work mechanisms, SPE can be divided into normal-phase SPE, reverse-phase SPE, and ion-exchange SPE. Normal-phase SPE is used to extract polar analytes dispersed in non-polar or mid-polar solution. The surface of the stationary phase is normally modified with hydrophilic groups such as -CN and -NH<sub>2</sub>. When a sample is loaded on the cartridge, target analytes can retain on the stationary phase via hydrophilic interaction. In contrast, reverse-phase SPE can separate non-polar or mid-polar target analytes dissolved in polar or moderately polar solution. The hydrophobic groups (i.e. C8 and C18) on the stationary phase can interact with the target analytes by hydrophobic interaction. Ion-exchange SPE is designed to separate target analytes with charge (either positive or negative) via electrostatic interaction.

In this thesis, LiChrolut-EN cartridge was used for the 8-OHdG sample preparation. The package material is polymeric sorbent particles (i.e. ethylvinyl benzene-divinylbenzene) which has a huge surface area of 1200 m<sup>2</sup>/g. This sorbent has an extra hydrophilic function to adsorb polar organic compounds.

### 2.5.2 Liquid-liquid extraction

Liquid-liquid extraction (LLE) was used to prepare MDA adducts in samples after chemical derivatization. This method is widely used to separate an analyte (**Figure 2.5**) based on its different solubility in the aqueous phase and in the immiscible organic solvent. Depending on its partition coefficient ( $K_d$ ), the analytes transfer from the aqueous phase into another immiscible organic solvent (eq. 2.3). A high value of  $K_d$  is helpful for the analyte transfer process from water to the organic phase. LLE can be repeated for several times to reach a good extraction. The collected organic solvent phase containing the target analyte can be concentrated for the further measurement.

$$K_d = (Con_{(org)} \cdot V_{(org)}) / (Con_{(aq)} \cdot V_{(aq)}) \quad (\text{eq. 2.3})$$

$K_d$  is the partition coefficient.  $Con_{(org)}$  and  $Con_{(aq)}$  are the concentration of the analyte in the organic phase and the aqueous phase, respectively.  $V_{(org)}$  and  $V_{(aq)}$  are the volumes of the analyte in the organic phase and the aqueous phase, respectively.

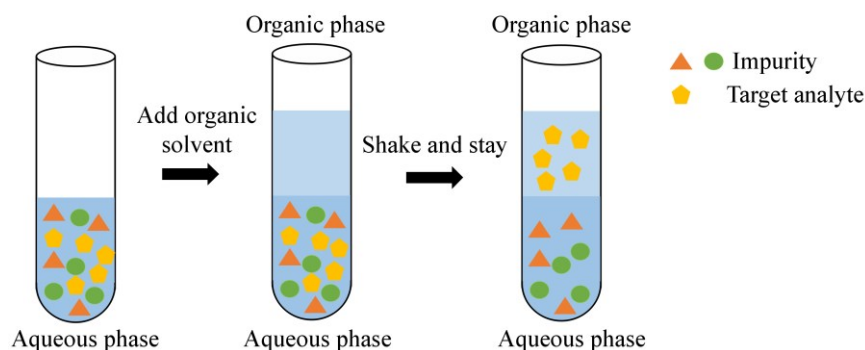


**Figure 2.5:** Illustration of the work mechanism of a liquid-liquid extraction.

### 2.5.3 Chemical derivatization

Chemical derivatization is a very useful technique to convert an analyte into a different species (Holländer, 2017). The newly produced compound can show different physico-chemical characteristics in terms of solubility, boiling point, and reactive ability. In most cases, derivatization is used to adapt the physical or chemical properties of target analytes in order to improve their analytical accessibility. This technique is widely used in the sample preparation prior to LC-MS/MS when the original target analytes are difficult to be analyzed directly because of, for example, the poor ionization efficiency in MS source, the bad retention time on liquid chromatography, and unsuitable ion fragments on MS. In this thesis, chemical derivatization is used for MDA (**Figure 2.6a**), cytosine modifications (**Figure 2.6b**), and adenine modifications analysis prior to LC-MS/MS (**Figure 2.6c**).

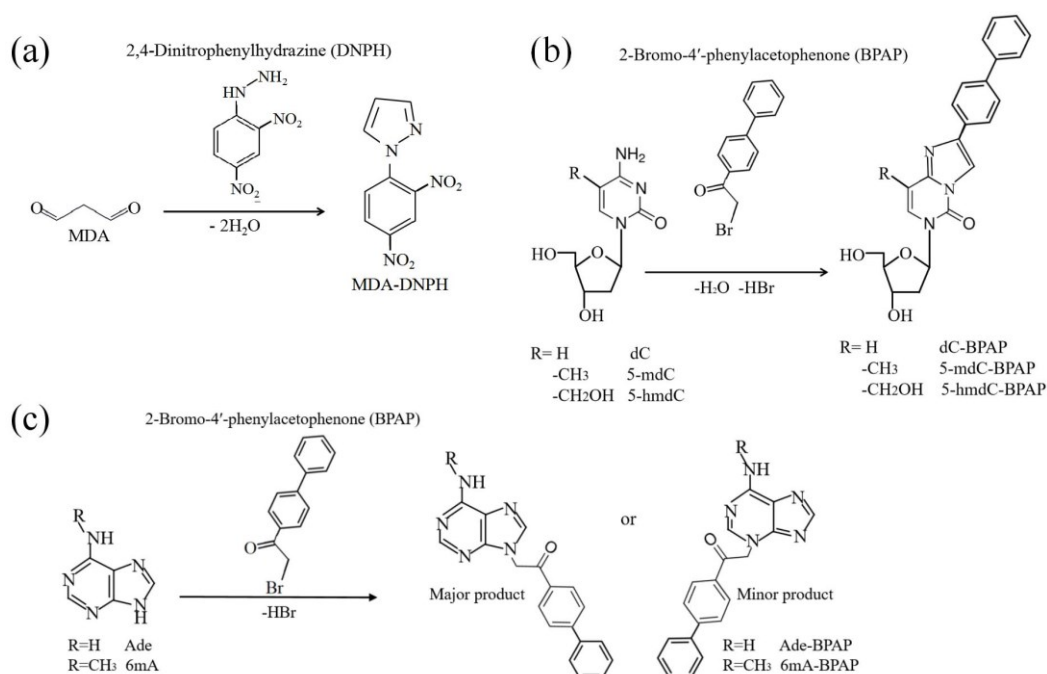


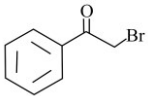
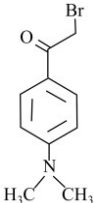
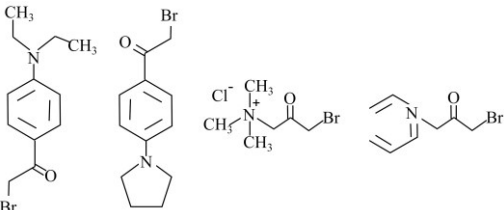
**Figure 2.6:** Illustration of the chemical derivatization for (a) MDA; (b) cytosine modifications; (c) adenine modifications (the quantification was based on the major adduct).

(1) MDA is a small molecule which lacks appropriately visible chromophore for spectrum analysis. It has poor retention time on LC and is difficult to be analyzed directly on MS without chemical derivatization. MDA with two aldehyde groups can selectively react with 2,4-dinitrophenylhydrazine (DNPH) on the hydrazine group forming a five-membered ring (**Figure 2.6a**). The produced MDA adduct has an adequate retention time on LC and a good ionization performance on MS, which is widely used to evaluate MDA levels in biological samples (Chen et al., 2011; Wu et al., 2011).

(2) 2'-Deoxycytidine (dC) and its modifications such as 5-methyl-2'-deoxycytidine (5-mdC) and 5-hydroxymethyl-2'-deoxycytidine (5-hmdC) are polar molecules showing poor retention time on reverse phase chromatography. In recent reports, cytosine was found to selectively react with the bromacetone group forming a robust five-membered ring (**Table 2.1**). As a result, the retention time of the new adducts was improved on LC. Significantly increased sensitivity of new adducts on MS was achieved. In this study 2-bromo-4'-phenylacetophenone (BPAP) including a bromacetone function group was used to react with cytosine and its modifications for chemical derivatization (**Figure 2.6b**).

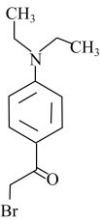
(3) Adenine (Ade) and its modification N6-methyladenine (6mA) have poor retention time on LC and poor sensitivity on MS. Chemical derivatization for Ade and 6mA is an effective way to increase their retention time on LC and improve their detection limit on MS. In this study, Ade and 6mA reacted with BPAP forming new adducts prior to LC-MS/MS for measurement (**Figure 2.6c**).

**Table 2.1:** Derivative reagents used for cytosine and its modifications.

Targets	Derivative reagents	Reference
cytidine; dC; 5-methylcytidine; 5-mdC;		(Torres et al., 2011)
5-mdC; 5-hmdC; 5-formyl-2'-deoxycytidine; 5-carboxy-2'-deoxycytidine;		(Tang et al., 2015)
5-methylcytidine; 5-hydroxymethylcytidine; 5-formylcytidine; 5-carboxycytidine;		(Huang et al., 2016)



**Table 2.1**(continued): Derivative reagents used for cytosine and its modifications.

5-mdC;		(Xiong et al., 2017)
5-hmdC;		
5-formyl-2'-deoxycytidine;		
5-carboxy-2'-deoxycytidine;		
5-methylcytidine;		
5-hydroxymethylcytidine;		
5-formylcytidine;		
5-carboxycytidine;		

Internal standard method is widely used in MS analysis for the accurate and precious quantification. Briefly the constant amount of internal standard is spiked in both samples and standard solutions at the beginning of sample preparation process. The calibration curve is set up by x-axis (the concentration ratio between the target analyte and internal standard) and y-axis (the area ratio between the target analyte and internal standard). Based on the detected area ratio between the target analyte and internal standard in samples, the concentration of the target analyte can be calculated. This method can compensate the loss of the target analyte during sample preparation such as SPE, LLE, and chemical derivatization. It can also correct the influence of matrix effect in samples on MS either due to ion-suppression or ion-promotion. In general, the internal standard should have similar physico-chemical characteristics to the target analyte, which can be distinguished by MS without effecting the target analyte. The isotope labeled internal standard is regarded as the gold standard because it has nearly the same physico-chemical characteristics as its native counterpart.

In this study, isotope labeled internal standard  $^{15}\text{N}_5$ -8-OHdG and  $\text{d}_2$ -MDA (**Figure 2.7a**) were used for the target analytes quantification. However, the corresponding isotope labeled internal standard is very expensive and sometimes not available. The suitable internal standard as the substitution of isotope labeled internal standard is necessary. In cytosine modifications and adenine modifications analysis, 2-bromo-2'-acetonaphthone (BAN) which has a similar physico-chemical properties to BPAP reacted with 5-mdC, Ade, and 6mA forming new adducts and were used as an internal standards for quantification (**Figure 2.7b,c**).

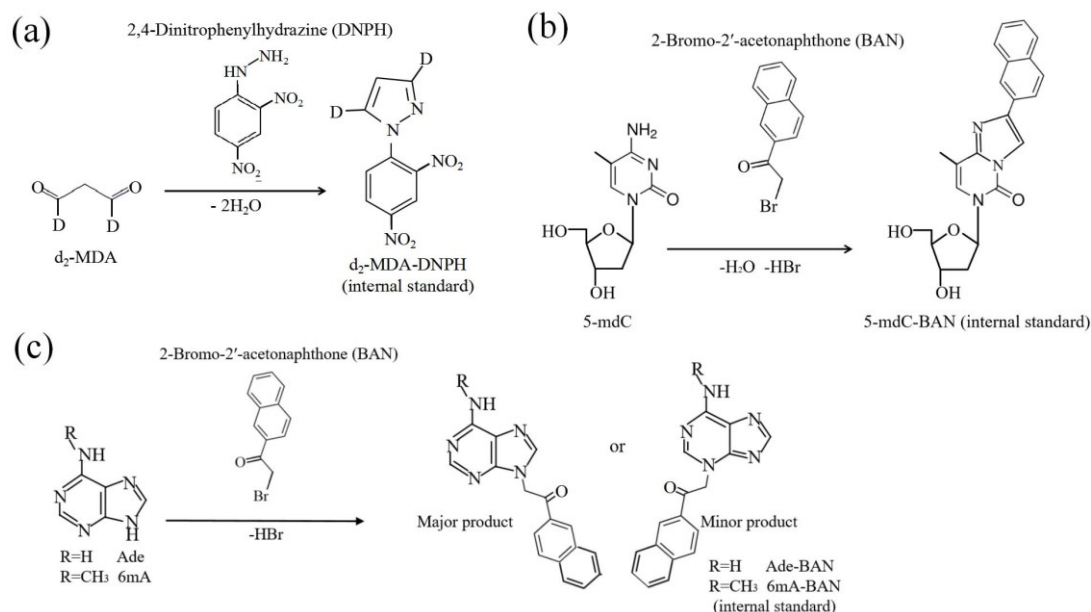


**Figure 2.7:** Illustration of a chemical derivatization for (a)  $d_2$ -MDA; (b) 5-mdC; (c) Ade and 6mA.

## 2.6 Liquid chromatography

For this thesis, liquid chromatography (LC) was used for the analysis of target compounds, such as 2'-deoxyguanosine (dG), 8-OHdG, MDA, cytosine and adenine modification. The LC was either used with ultraviolet detection (LC-UV) or mass spectrometry (LC-MS) depending on the target analytes. LC is an effectively analytical technique to separate and analyze targets which are unstable at high temperature, nonvolatile, and have high boiling points or high molecular weights. A typical LC mainly includes four components that is a pump system, an autosampler, a column compartment, and a detector system shown in **Figure 2.8**. The pump connected to different solvents can steady supply the flow of mobile phase for analysis. The function of an autosampler is for automatic sample injection with a constant volume. The column compartment can contain and keep stable temperature for columns. The detector (eg. UV or MS) can qualitatively and quantitatively detect the target analytes.

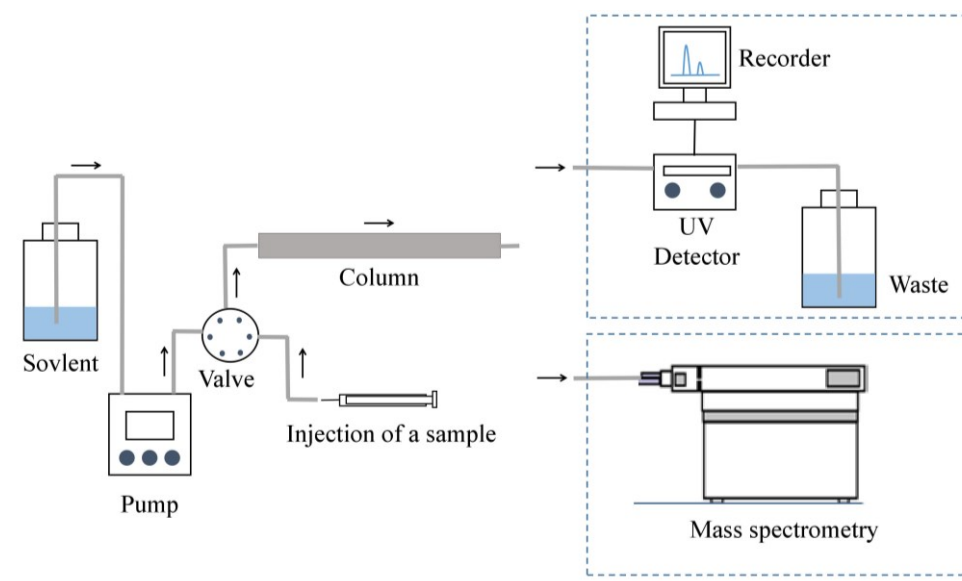


**Figure 2.8:** Illustration of the work mechanism of a liquid chromatography and its complementary connection with either a UV detector or mass spectrometer.

The column is an important part for in LC system. Normally, columns are packaged with small porous silica particles (regarded as stationary phase) with high surface area and high mechanical strength. The surface of silica particles can be further modified with different groups for various separation selectivities. Based on the interaction between molecules and stationary phase, different analytes are eluted with various retention time according to their physico-chemical characteristics (**Figure 2.9**). The interaction mechanisms are same to SPE including via van der Waals force, hydrophobic or hydrophilic interaction, pi-pi interaction, hydrogen bonding, dipole-dipole interaction, and electrostatic attraction.

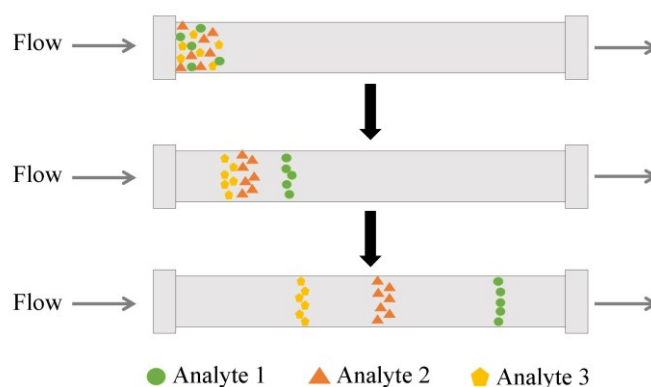


**Figure 2.9:** Illustration of the work mechanism of a column.

Depending on the physico-chemical characteristics of target analytes, different columns were chosen in this study. A Kinetex® C18 column (2.6  $\mu\text{m}$ , 100  $\text{\AA}$ , 100 $\times$ 2.1 mm i.d., Phenomenex, USA) was used to separate cytosine modifications and MDA adducts. Reversed phase C18 columns are the most used column with octadecyl-bonded silica particles as stationary phase (**Figure 2.10a**). It shows good separation efficiency, robust reproducibility, and good column lifetime and is widely used in various analysis including pharmaceuticals, vitamins, fatty acids, and steroids.

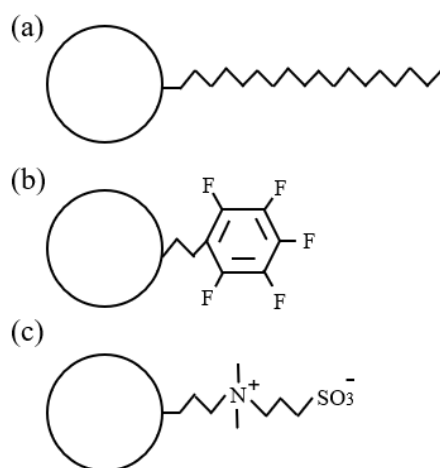


**Figure 2.10:** Illustration of the stationary phase for (a) C18; (b) F5 ;(c) Eurospher HILIC.

A Kinetex® F5 column (2.6  $\mu\text{m}$ , 100 Å, 100×3.0 mm i.d., Phenomenex, USA) was used to separate adenine modifications. The stationary phase is modified with pentafluorophenyl function group (**Figure 2.10b**) showing the good separation ability for isomers which have the same molecule weight but different molecule structure. In our study, the derivatized adenine and N6-methyladenine products had two isomers which can not be directly distinguished by MS. F5 column successfully separated the isomers prior to MS for the accurate quantification.

A Eurospher II 100-3 HILIC column (3  $\mu\text{m}$ , 100 Å, 100×3 mm i.d., Knauer, Germany) was selected for the separation of dG and 8-OHdG. The stationary phase was modified with polar ammonium-sulfonic acid functional groups (**Figure 2.10c**). This column belongs to hydrophilic interaction columns. During analysis, a thin water layer forms on the surface of stationary phase. Thus hydrophilic analytes can partition between the mobile phase and the water layer leading to the increased retention time. The column is suitable for the analysis of polar and ionic analytes which have poor retention time on reversed phase columns.

## 2.7 Hybrid triple quadrupole/linear ion trap mass spectrometry

In this thesis, a hybrid triple quadrupole/linear ion trap mass spectrometry (4000 QTRAP system) combined with an LC system was used for the analysis of 8-OHdG, MDA, cytosine modifications, and adenine modifications samples. The 4000 QTRAP system is suitable for the quantitative analysis of molecules with small weights such as drugs and cell metabolite products. It analyzes ions (either with positive charge or with negative charge) generated from molecules by measuring their mass to charge ratio ( $m/z$ ). It can identify an unknown substance according to its  $m/z$  or quantitatively measure a known substance by detecting the identified  $m/z$ . The basic components of a mass spectrometer include an ionization source, a mass analyzer (working in a high vacuum condition to avoid ion collisions with molecules from the air), and a detection system (**Figure 2.11**).

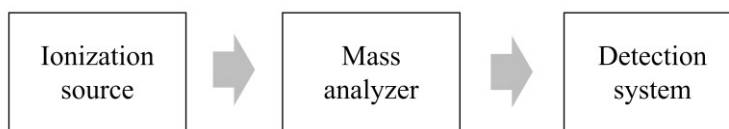


**Figure 2.11:** Illustration of the basic components of mass spectrometry.

(1) In the ion source, analytes are transformed to charged species. This process enables the manipulation of analytes movement in electric fields. In the field of mass spectrometry, several different ionization techniques are used, depending on physical-chemical properties of analytes or the sample matrix. A commonly applied technique for the coupling with LC is electrospray ionization (ESI). In our study, a 4000 QTRAP system with a Turbo V™ Ion Source was operated in ESI mode. The sensitivity is related to target analytes and the flow rate. The mobile phase can be a pure aqueous solution or an organic solvent. The sensitivity of ESI can be further improved by increasing the source temperature (up to 750°C). The mechanism of ESI in positive mode includes several steps (Ho et al., 2003) (**Figure 2.12**). Firstly, the liquid flow containing target analytes sprays from the tip and generates droplets with positive polarity as the predominant. Secondly, with the evaporation of solvents, droplets become smaller and smaller. The electrical field in the droplet increases dramatically. Finally, when the electrical field is high enough, positive ions are ejected from droplets into the gas phase. The ejected ions pass through a skimmer cone and are transferred into the mass analyzer for further analysis. ESI is a kind of soft ionization technique since it will not destroy the structure of the target molecules. In general, ESI in positive mode introduces a positive ion charge (e.g.  $H^+$ ,  $NH_4^+$ , and  $Na^+$ ) to the target molecule (M) generating a positive precursor ion (e.g.  $[M+H]^+$ ,  $[M+NH_4]^+$ , and  $[M+Na]^+$ ). ESI in negative mode removes a proton from the target molecule (M) generating a negative precursor ion ( $[M-H]^-$ ).

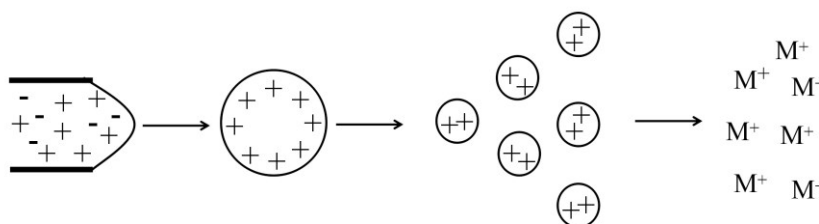


**Figure 2.12:** Illustration of the mechanism of the electrospray ionization in positive model.

(2) The mass analyzer of a 4000 QTRAP is a hybrid triple quadrupole/linear ion trap system. It contains two separation components consisting of a quadrupole (regarded as Q1) and a linear ion trap (LIT, regarded as Q3) as well as a collision component that is Q2. In this study, the measurement works under multiple reaction monitoring (MRM) mode. The illustration of MRM is shown in **Figure 2.13**. When a sample mixture enters the mass analyzer, different ions firstly pass through Q0 to reach Q1. Q1 can generate an electric field to filter target ions based on the specific mass to charge ratio. Only the selected ions (precursor ions) can enter the Q2. In Q2, precursor ions are collided with nitrogen gas and broken into fragment ions. Subsequently, the fragment ions enter into Q3. Q3 can generate a radio frequency

field to filter selected fragment ions and let the selected fragment ions pass through (Zhang et al., 2005). MRM mode has high sensitivity and selectivity and can efficiently reduce the background noise and matrix components in samples. Typical precursor ions and fragment ions used in this study for 8-OHdG, 5-mdC-BPAP (a cytosine modification adduct), and 6mA-BPAP (an adenine modification adduct) are shown in **Figure 2.14**.

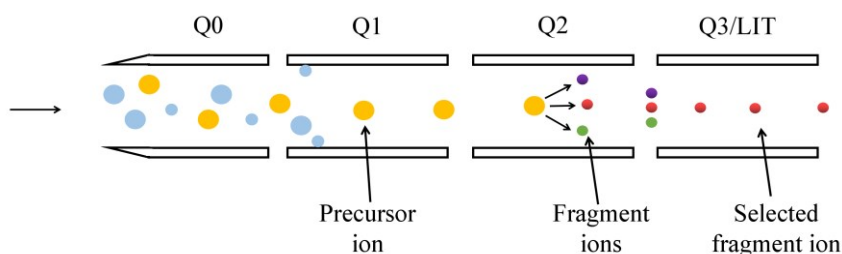


**Figure 2.13:** Illustration of the work mechanism of multiple reaction monitoring.

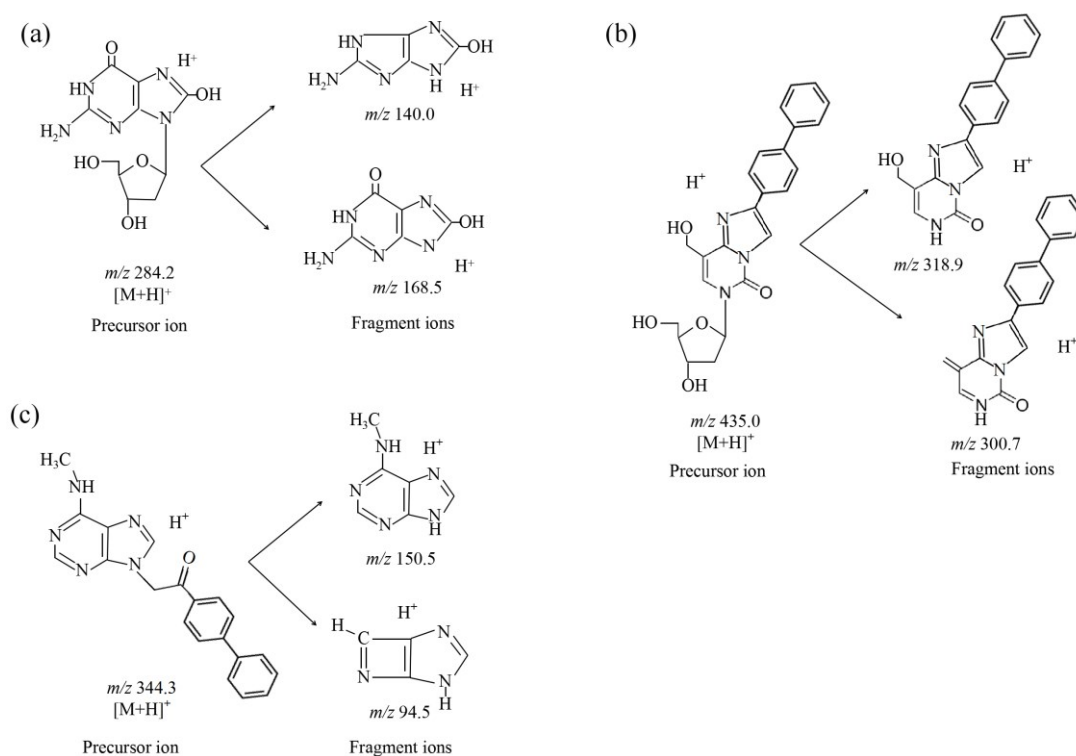


**Figure 2.14:** Typical precursor ions and fragment ions from (a) 8-OHdG; (b) 5-hmdC-BPAP; (c) 6mA-BPAP analyzed in MRM positive mode.

(3) The detector system of the 4000 QTRAP consists a channel electron multiplier (CEM). When an ion enters and collides the CEM, the inner surface of the CEM emits 1-3 electrons which further collide the CEM and induce more electrons (**Figure 2.15**). This process is called secondary emission. So a small signal intensity can be amplified by several orders of magnitude. The displayed signals can subsequently be transferred to a computer and used as quantitative signals for data processing.

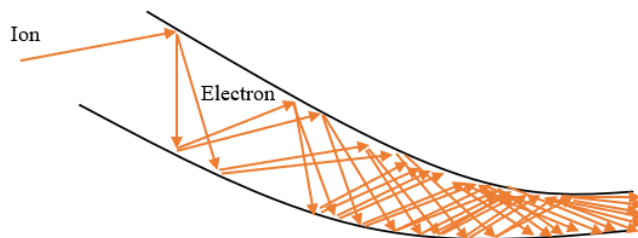


**Figure 2.15:** Illustration of a channel electron multiplier.

## 2.8 Inductively coupled plasma mass spectrometry

In this study, inductively coupled plasma mass spectrometry (Agilent 7700 Series ICP-MS system) was used to analyze metal elements in samples. ICP-MS with high sensitivity is a robust method for trace metals analysis. Samples consisting of either particles or cells were first digested by strong acid hydrolysis (i.e. a mixture of 69% nitric acid and 30% hydrogen peroxide) and the hydrolysate solution was diluted and injected into the nebulizer. The nebulized drops were transferred to an ICP torch for ionization.

(1) The ionization process of the Agilent 7700 ICP-MS is realized in an ICP torch (Leonhard et al., 2002) (**Figure 2.16**). A sample mixture is carried by inert Ar gas after the sample nebulization. At the end of the torch, a radio frequency coil induces a strong radio frequency field in high megahertz. When Ar gas passes through the radio frequency coil, Ar is ionized into a plasma state ( $\text{Ar} \rightarrow \text{Ar}^+ + \text{e}^-$ ). The electrons move with high velocity around the magnetic field and generate high temperatures. Metal elements (M) in mixtures can be immediately ionized ( $\text{M} + \text{Ar}^+ \rightarrow \text{M}^+ + \text{Ar}$ ).

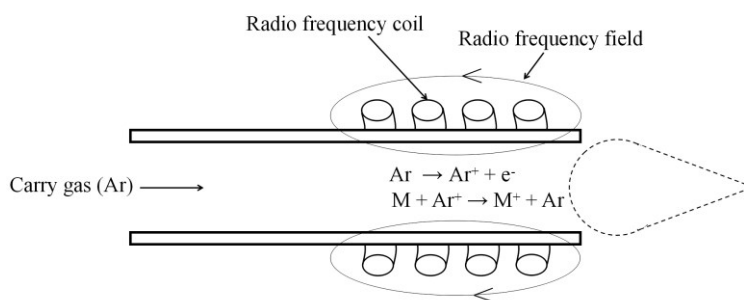


**Figure 2.16:** Illustration of the work mechanism of an inductively coupled plasma torch.

(2) After the ionization process, generated ions ( $\text{M}^+$ ) pass through an octopole reaction system to remove the interference. The octopole reaction system can increase the transmissions of ions. It works effectively with an inert He gas condition and a kinetic energy discrimination voltage to remove the polyatomic interference. Afterwards, the ions enter a quadrupole mass analyzer which generates an electric field to filter target ions based on  $m/z$  (**Figure 2.17**). The quadrupole mass analyzer with hyperbolic rod profile has a high sensitivity and resolution for ions filtration. Finally, the selected ions pass through the mass analyzer to reach the detector.

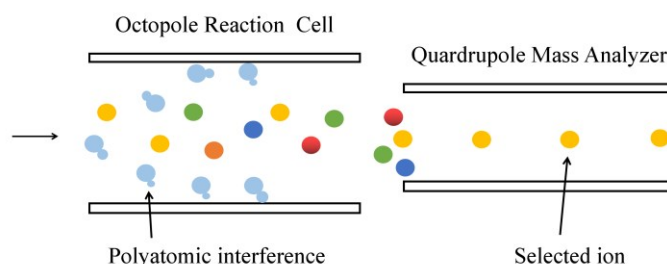


**Figure 2.17:** Illustration of the work mechanism of an octopole reaction cell and a quadrupole mass analyzer.

(3) The detector system of the Agilent 7700 ICP-MS consists an electron multiplier system. It acquires ion signals and makes amplifications. The amplified signals can be further transferred to a computer for the data processing.

## 2.9 Cytokinesis-block micronucleus cytome assay

Cytokinesis-block micronucleus cytome assay (CBMN assay) was used in this study to measure genotoxicity based on chromosome damage (Fenech, 2007; OECD 487, 2016). The illustration of CBMN assay is shown in **Figure 2.18**. Cells were seeded 24 hours prior to PM or oxidizer exposure. Cytochalasin B was added after 44 hours after seeding to make sure cells underwent at least one cell division (A549 and THP-1 cells have a doubling time of 24 hours and 36 hours, respectively). Cytochalasin B inhibited cytoplasm division but did not block nuclear division. After fixation of the cell samples on microscopy slides, cells were stained with Giemsa. Giemsa stain entered cells and attached to DNA phosphate groups to color the nucleus and chromosomes.

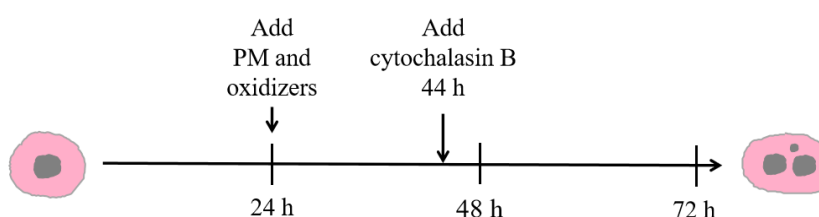


**Figure 2.18:** Illustration of cytokinesis-block micronucleus cytome assay duration.

Mononucleated cells (MONO, one nuclei), binucleated cells (BN, two nuclei), and Multinucleated cells (three or more than three nuclei) were distinguished (**Figure 2.19**). Based on their counts, cytokinesis-block proliferation index (CBPI) was calculated to evaluate the cell proliferation (eq. 2.4).

$$CBPI = \frac{\text{No. mononucleated cells} + 2 \cdot \text{No. binucleated cells} + 3 \cdot \text{No. multinucleated cells}}{\text{Total number of cells}} \quad (\text{eq. 2.4})$$

Apoptosis refers to the programmed cell death. It includes nuclear structure changes such as the nuclear fragmentation and chromatin condensation (Elmore, 2007). Necrosis is the unprogrammed cell death and includes alterations such as the loss of cell membrane integrity and uncontrolled release of cell



organelle (Fink and Cookson, 2005). Analysis of apoptotic and necrotic cells was used to evaluate and distinguish the cell cytotoxicity (**Figure 2.19**).

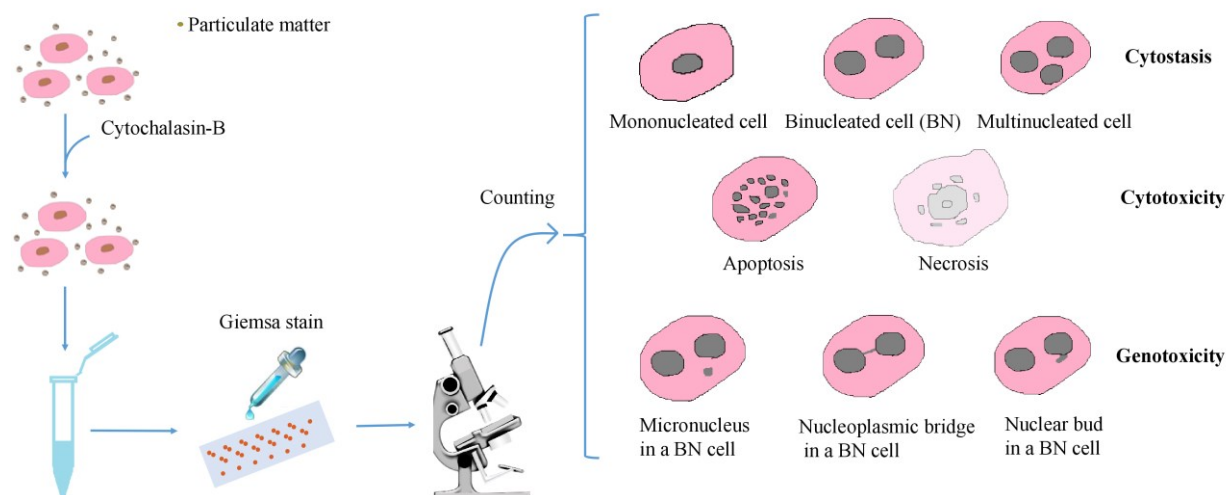


**Figure 2.19:** Illustration of cytokinesis-block micronucleus cytome assay procedures.

Genotoxicity events on chromosomes in CBMN assay include the formation of micronuclei (MN) in MONO or in BN, nucleoplasmic bridge (NPB), or nuclear bud (NBUD) in BN. These chromosomal aberration are makers of different chromosomal instabilities resulting from different genotoxic mechanisms (Fenech et al., 2011) (**Figure 2.19**).

For example, MN can be generated from chromosome fragments or whole chromosomes which are not appropriately attached to spindles during the mitosis phase. Misrepair of DNA and unrepaired DNA strand breaks, the excision of 8-oxoguanine from the complementary DNA double-strand, the dysfunction of the spindle apparatus, and the error of mitosis check points can also lead to MN formation as well (Fenech et al., 2011; Rosefort et al., 2004; Kirsch-Volders and Fenech, 2001).

NPB can be formed when a dicentric chromosome is pulled by spindles to two directions in a cell during anaphase. Telomere end fusions and fault repair of chromosome breaks can also lead to dicentric chromosomes (Fenech et al., 2011; Di Bucchianico et al., 2018).

NBUD can be produced by the elimination of the amplified DNA in the synthesis phase of the cell cycle. It can also be formed when a NPB breaks between two nuclei and the residue still attach to one nucleus. (Fenech et al., 2011; Di Bucchianico et al., 2018).

## 2.10 Calculation of toxic equivalent and mutagenic equivalent

Toxic equivalent (TEQ) and mutagenic equivalent (MEQ) of PAHs were calculate based on the toxic equivalency factor (TEF) and the mutagenic equivalency factor (MEF) for each PAH shown in **Table 2.2** (Nisbet and Lagoy, 1992; Durant et al., 1996; Delistraty, 1997). A toxic equivalency factor represents the toxicity capacity of a PAH, while different PAHs have their corresponding TEF values. Thus a mixture of PAHs can be described in a single value (eq. 2.5) to evaluate its total toxic capacity. This

concept is also applied to MEQ (eq. 2.6). Benzo[a]pyrene (B[a]P) widely exists in environment such as cigarette smoke and burnt food (Risner, 1988; Lintas and De Matthaëis, 1979) and belongs to Group 1 (i.e. carcinogenic to humans) by International Agency for Research on Cancer (IARC, <https://monographs.iarc.who.int/agents-classified-by-the-iarc/>). It is usually used as a surrogate to evaluate the PAH mixtures, which TEF and MEF are regarded as 1. PAHs showing higher factors than 1 are more toxic or mutagenic than B[a]P. PAHs showing a smaller factor than 1 are less toxic or mutagenic than B[a]P. The toxic and mutagenic equivalency values are useful for the risk assessment of PAH mixtures.

$$\sum B[a]P_{TEQ} = \sum_{i=1}^n C_i \cdot TEF_i \quad (\text{eq. 2.5})$$

$$\sum B[a]P_{MEQ} = \sum_{i=1}^n C_i \cdot MEF_i \quad (\text{eq. 2.6})$$

$C_i$  represents the concentration of a PAH,  $TEF_i$  is the corresponding toxic equivalency factor for the PAH,  $MEF_i$  is the corresponding mutagenic equivalency factor for the PAH.

**Table 2.2:** Toxic equivalency factor (No. 1-17 from Nisbet and Lagoy, 1992; No. 18-33 from Delistraty, 1997) and mutagenic equivalency factor (Durant et al., 1996) for PAHs and their derivatives.

Number	Substance	TEF	MEF
1	Naphthalene	0.001	-
2	Acenaphthylene	0.001	0.00056
3	Acenaphthene	0.001	-
4	Fluorene	0.001	-
5	Phenanthrene	0.001	-
6	Anthracene	0.01	-
7	Fluoranthene	0.001	-
8	Pyrene	0.001	-
9	Benz[a]anthracene	0.1	0.082
10	Chrysene	0.01	0.017
11	Benzo[b]fluoranthene	0.1	0.25
12	Benzo[k]fluoranthene	0.1	0.11
13	Benzo[a]pyrene	1	1
14	Diben[a,h]anthracene	5	0.29
15	Benzo[ghi]perylene	0.01	0.19
16	Indeno[1,2,3-cd]pyrene	0.1	0.31
17	2-Methylnaphthalene	0.001	-
18	Benzo[j]fluoranthene	0.1	0.26
19	Dibenz[a,j]acridine	0.1	-
20	Dibenz[a,h]acridine	0.1	-
21	Dibenzo[a,e]pyrene	1	2.9
22	Dibenzo[a,h]pyrene	10	-

**Table 2.2** (continued): Toxic equivalency factor (No. 1-17 from Nisbet and Lagoy, 1992; No. 18-33 from Delistraty, 1997) and mutagenic equivalency factor (Durant et al., 1996) for PAHs and their derivatives

23	Dibenzo[a,i]pyrene	10	-
24	Dibenzo[a,l]pyrene	10	24
25	1,6-Dinitropyrene	10	0.28
26	1,8-Dinitropyrene	1	0.046
27	5-Methylchrysene	1	-
28	6-Nitrochrysene	10	-
29	2-Nitrofluorene	0.01	0.025
30	1-Nitropyrene	0.1	-
31	4-Nitropyrene	0.1	-
32	5-Nitroacenaphthene	0.01	-
33	7H-Dibenzo[c,g]carbazole	1.0	-
34	1,3-Dinitropyrene	-	0.031
35	9-Nitroanthracene	-	0.0032
36	2-Nitrofluoranthene	-	0.05
37	3-Nitrofluoranthene	-	0.0026

### 3 Results and discussion

#### 3.1 PM analysis from Nanjing city

Different PM were collected in Nanjing city from five districts with different regional setting: an industrial district, a traffic district, a residential district, a business district, and a background district (Publication 1). The analyzed total amounts of PAHs in  $PM_{2.5}$  and  $PM_{10}$  varied in the five places with the following order: industrial district > residential district > traffic district > business district > background district (**Table 3.1** and **Table 3.2**). The components of PAHs differed in both  $PM_{2.5}$  and  $PM_{10}$  in all five districts. Based on TEQ and MEQ calculation,  $PM_{2.5}$  from an industrial district showed the highest TEQ ( $5.21 \text{ ng}\cdot\text{m}^{-3}$ ) and MEQ ( $6.31 \text{ ng}\cdot\text{m}^{-3}$ ), respectively (**Table 3.1**). While  $PM_{10}$  from the business district and the residential district showed the highest TEQ ( $9.74 \text{ ng}\cdot\text{m}^{-3}$ ) and MEQ ( $14.08 \text{ ng}\cdot\text{m}^{-3}$ ), respectively (**Table 3.2**). This indicated that the collected PM showed distinct toxic and mutagenic equivalent values due to their different PAH constitutions.

**Table 3.1:** Concentrations of PAHs in  $PM_{2.5}$  and the calculated TEQ and MEQ of  $PM_{2.5}$ .

District	$PM_{2.5} (\text{ng}\cdot\text{m}^{-3})$	TEQ ( $\text{ng}\cdot\text{m}^{-3}$ )	MEQ ( $\text{ng}\cdot\text{m}^{-3}$ )
industrial district	50.00	5.21	6.31
residential district	21.11	2.80	2.20
traffic district	17.13	2.38	2.78
business district	16.33	3.33	2.78
background district	14.02	1.94	1.57

**Table 3.2:** Concentrations of PAHs in  $PM_{10}$  and the calculated TEQ and MEQ of  $PM_{10}$ .

District	$PM_{10} (\text{ng}\cdot\text{m}^{-3})$	TEQ ( $\text{ng}\cdot\text{m}^{-3}$ )	MEQ ( $\text{ng}\cdot\text{m}^{-3}$ )
industrial district	93.08	9.44	13.53
residential district	61.03	8.64	14.08
traffic district	48.31	6.11	8.78
business district	44.13	9.74	11.49
background district	38.45	7.01	8.11

### 3.2 Cell viability assay

Cytotoxicity was assessed in THP-1 and A549 cells after exposure to different concentrations of PM and oxidizers (Publication 2). All compounds decreased cell viability with dose-dependent effects in both cell lines (**Figure 3.1**). Cell viability decreased moderately with increasing doses of PM and there was no big difference in two cell types.

Diesel PM 2975 showed higher cytotoxicity than other PM. Diesel PM 2975 decreased cell viability to 80% at about 80  $\mu\text{g/mL}$ , while CZ100 or UD 1649 decreased cell viability to 80% at about 400  $\mu\text{g/mL}$  (**Figure 3.1a-c**). It would have been interesting to look at the impact of higher concentrations of PM on cell viability, but this was not possible due to the limited solubility. Therefore, exposure concentrations (200  $\mu\text{g/mL}$  of CZ100 or UD 1649, 40  $\mu\text{g/mL}$  of diesel PM 2975) which had 90% cell viability were used for the cell exposure experiments. Compared to the other PM, diesel PM 2975 contains much less metal elements but has higher PAHs and nitro-PAHs. The observed stronger cytotoxicity induced by diesel PM 2975 could be attributed to its highly toxic organic components i.e. PAHs and nitro-PAHs. Especially, nitro-PAHs are more toxic than PAHs (Bandowe and Meusel, 2017). Rossner compared the cytotoxicity of benzo[a]pyrene, 1-nitropyrene, and 3-nitrofluoranthene in A549 cells. Both nitro-PAHs showed higher cytotoxicity than benzo[a]pyrene (Rossner et al., 2016). 1-nitropyrene also promoted inflammation and cause apoptosis and necrosis in BEAS-2B cells (Øvrevik et al., 2010). Furthermore, the TEQ (in terms of PAHs and nitro-PAHs, based on  $\text{pg/mL}$  in medium) of diesel PM 2975 was 2.379  $\text{pg/mL}$  higher than CZ100 and UD 1649 (0.43 and 1.123  $\text{pg/mL}$ ), which also indicated the cytotoxicity of diesel PM 2975 was higher than CZ100 and UD 1649.

Two oxidizers severely reduced cell viability in THP-1 cells than A549 cells (**Figure 3.1d,e**). The cell viability of THP-1 decreased to 80% after exposure to about 2.5  $\mu\text{g/mL}$  of menadione and 3  $\mu\text{g/mL}$  of 3-MCPD. A549 cells viability reduced to 80% after treatment with 6.5  $\mu\text{g/mL}$  of menadione and 10  $\mu\text{g/mL}$  of 3-MCPD. In order to gain comparable results to the PM exposure and avoid strong cytotoxicity, 2  $\mu\text{g/mL}$  of menadione or 3-MCPD which had 90% cell viability were selected for further exposure experiments.

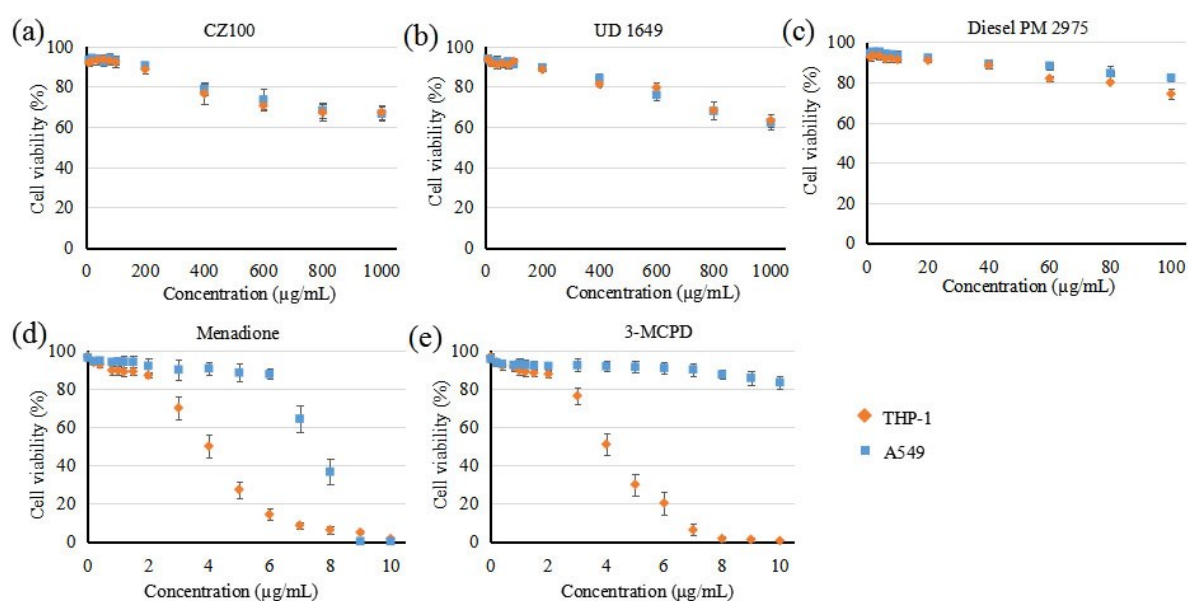


**Figure 3.1:** Cell viability of THP-1 and A549 cells after 24 hours exposure to (a) CZ100; (b) UD 1649; (c) diesel PM 2975; (d) menadione; (e) 3-MCPD. (mean  $\pm$  standard error of mean,  $n=3$ )

### 3.3 Particle deposition analysis

Particle deposition was explored on A549 cells exposed to three reference PM at the selected concentrations. All particles are agglomerates with different sizes (based on 90% of volume distribution) of 17.57  $\mu\text{m}$ , 43.2  $\mu\text{m}$ , and 70  $\mu\text{m}$  for CZ100, UD 1649, and diesel PM 2975, respectively. Three PM showed different particle deposition. Even though the exposure concentrations of CZ100 and UD 1649 were the same, their particle deposition differed a lot.

**Table 3.3:** Particle deposition values for A549 cells exposed to different PM. (mean  $\pm$  standard error of mean,  $n=3$ )

Target	Exposure concentration	Nominal concentration	Precipitate concentration	% Deposition
CZ100	200 $\mu\text{g/mL}$	40 $\mu\text{g/cm}^2$	$25.9 \pm 2.2 \mu\text{g/cm}^2$	64.7%
UD 1649	200 $\mu\text{g/mL}$	40 $\mu\text{g/cm}^2$	$33.9 \pm 1.7 \mu\text{g/cm}^2$	84.7%
Diesel PM 2975	40 $\mu\text{g/mL}$	8 $\mu\text{g/cm}^2$	$6.1 \pm 0.3 \mu\text{g/cm}^2$	76.3%

### 3.4 Quantification of 8-hydroxy-2'-deoxyguanosine and malondialdehyde

The base levels of 8-OHdG in THP-1 and A549 cells are about five oxidized bases per one million normal bases (namely, 8-OHdG/ $10^6$  dG). Both PM and oxidizers increased 8-OHdG productions in two cell types. After exposure to PM for 4 h in THP-1 cells, the 8-OHdG levels increased 11-, 13-, and 15-fold in CZ100, UD 1649, and diesel PM 2975 groups, respectively, compared to the negative control group (**Figure 3.2a**). In contrast, A549 cells showed a 12-, 8-, and 15-fold increase in 8-OHdG levels upon treatment with CZ100, UD1549, and diesel PM 2975 groups, respectively, compared to the

negative group (**Figure 3.2b**). Persistently increased 8-OHdG in cells were observed after exposure to PM for 72 h. For THP-1 cells, 8-OHdG increased 3-, 2-, and 3-fold in CZ100, UD 1649, and diesel PM 2975 groups, respectively (**Figure 3.2a**). In A549 cells, 8-OHdG increased 1-, 2-, and 3-fold in CZ100, UD 1649, and diesel PM 2975 groups, respectively (**Figure 3.2b**). The results indicated that persistent DNA oxidation condition existed in both cell types during the short and long PM exposures.

In previous studies based on cell free experiments, UD 1649 oxidized dG to produce 8-OHdG in buffer solution but ion chelators did not reduce the oxidation process (Prahalad et al., 2001), which indicated that the oxidation capacity of UD 1649 could be due to its aqueous extraction fractions. 8-OHdG levels did not increase in isolated calf thymus DNA treated together with diesel PM 2975 and H<sub>2</sub>O<sub>2</sub> (Danielsen et al., 2008), which indicated the aqueous extraction fractions in diesel PM 2975 were neglectful in the oxidation of dG. In this study, we observed that UD 1649 and diesel PM 2975 increased 8-OHdG induction in both cell types, which could be explained by their organic components such as PAHs. Since PAHs can be metabolized into epoxide intermediates via CYP1A1 cellular metabolism (Harvey, 1996) and the metabolized epoxide products can further induce reactive oxygen species (ROS). This assumption is supported by the following studies. UD 1649 was shown to cause CYP1A1 expression in murine embryonic fibroblasts (Dumax-Vorzet et al., 2015). Diesel PM 2975 induced CYP1A1 expression in Sprague Dawley rats alveolar macrophages (Zhao et al., 2006).

The background of MDA levels in THP-1 and A549 was about 0.3 ng/mL per a million cells. After exposure to CZ100 for 4, 48, and 72 hours, the MDA increased 2.2-, 1.6-, and 1.5-fold, respectively, compared to the negative control group (**Figure 3.2c**). In A549 cells, increased MDA was only observed in the CZ100 group for 4 hours which was about 2-fold of the background level (**Figure 3.2d**). THP-1 cells generated higher 8-OHdG and MDA levels than A549 cells, which indicated that THP-1 cells were more sensitive to oxidative condition induced by PM and oxidizers. CZ100 induced comparable 8-OHdG and higher MDA than the other PM, which indicated that the oxidative capacity of CZ100 was higher than UD 1649 and diesel PM 2975.

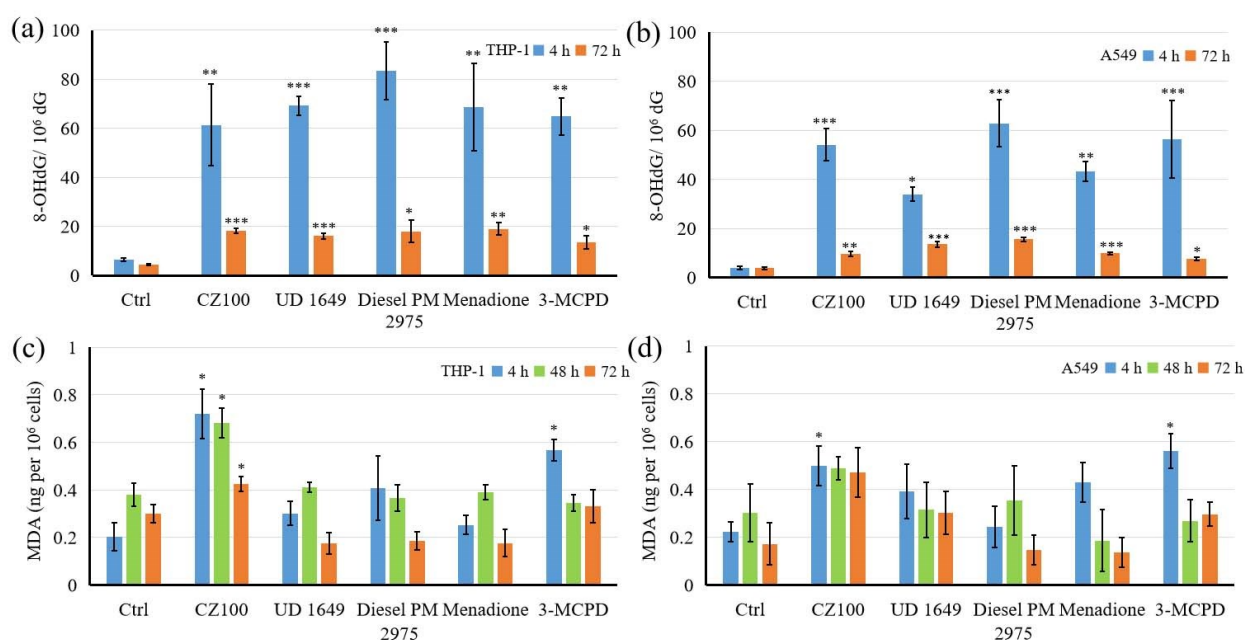


**Figure 3.2:** (a) 8-OHdG in THP-1 cells; (b) 8-OHdG in A549 cells; (c) MDA in THP-1 cells; (d) MDA in A549 cells. (exposed to 200  $\mu\text{g/mL}$  of CZ100 or UD 1649, or 40  $\mu\text{g/mL}$  of diesel PM 2975, or 2  $\mu\text{g/mL}$  of menadione or 3-MCPD) mean  $\pm$  standard error of mean,  $n=3$ . Analysis of variance was used, \* =  $p$ -value  $< 0.05$ , \*\* =  $p$ -value  $< 0.01$ , \*\*\* =  $p$ -value  $< 0.001$ .

### 3.5 Cytokinesis-block micronucleus cyto assay

A microscopic image of THP-1 cells shows mononucleated, binucleated, and polynucleated cells in **Figure 3.3a** used for cytokinesis-block proliferation index (CBPI) calculation. Mitotic cells were used for the cell cycle activity assessment to evaluate the cellular proliferation (**Figure 3.3b**). Apoptotic cells and necrotic cells were used to evaluate cytotoxicity (**Figure 3.3c,d**). The production of micronuclei (MN) in mononucleated (MONO) and binucleated (BN) cells (**Figure 3.3e,f**) are markers for aneuploidogenic and clastogenic events (Rosefort et al., 2004; Kirsch-Volder and Fenech, 2001). Nucleoplasmic bridges (NPB) and nuclear buds (NBUD) in **Figure 3.3g,h** are markers for DNA misrepair or telomere end-fusion and the elimination of amplified DNA, respectively (Di Bucchianico et al., 2018).



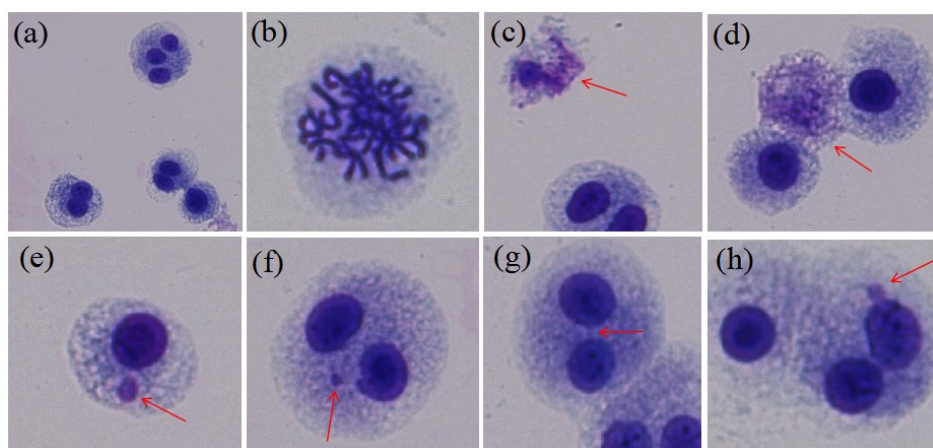


**Figure. 3.3:** Typical microscope graphic of THP-1 cells (a) mononucleated, binucleated and polynucleated cells; (b) a mitotic cell; (c) an apoptotic cell; (d) a necrotic cell; (e) a micronucleus in a mononucleated cell; (f) a micronucleus in a binucleated cell; (g) a nucleoplasmic bridge in a binucleated cell; (h) a nuclear bud in a binucleated cell.

The background CBPI was about 1.7% in both cell types, and no significant changes were observed in both cell types after exposure to PM (**Figure 3.4a**). All three PM reduced the mitotic capacity in THP-1 cells from 4.7% to about 2.8% (**Figure 3.4b**). Cytotoxic effects (apoptosis and necrosis) were not observed in both cell types (**Figure 3.4c,d**).

Diesel PM 2975, menadione, and 3-MCPD induced the similar increase of MN in MONO A549 cells (from 4 to 26) and in BN A549 cells (from 5 to 20), while this phenomenon was not observed in the other PM or in THP-1 cells (**Figure 3.4e,f**). NPB increased in THP-1 cells (from 2 to 7) and A549 cells (from 4 to 15) after exposure to CZ100, menadione, and 3-MCPD, respectively. An increase of NPB was also observed in A549 cells induced by diesel PM 2975 but not for UD 1649 (**Figure 3.4g**). No changes of NBUD frequency in both cell types after exposure to PM and oxidizers were observed (**Figure 3.4h**). Based on the above results, different PM and oxidizers showed different genotoxic effects in two cell lines. In general, diesel PM 2975 showed stronger mutagenicity (based on chromosome instabilities) compared to CZ100 and UD 1649.

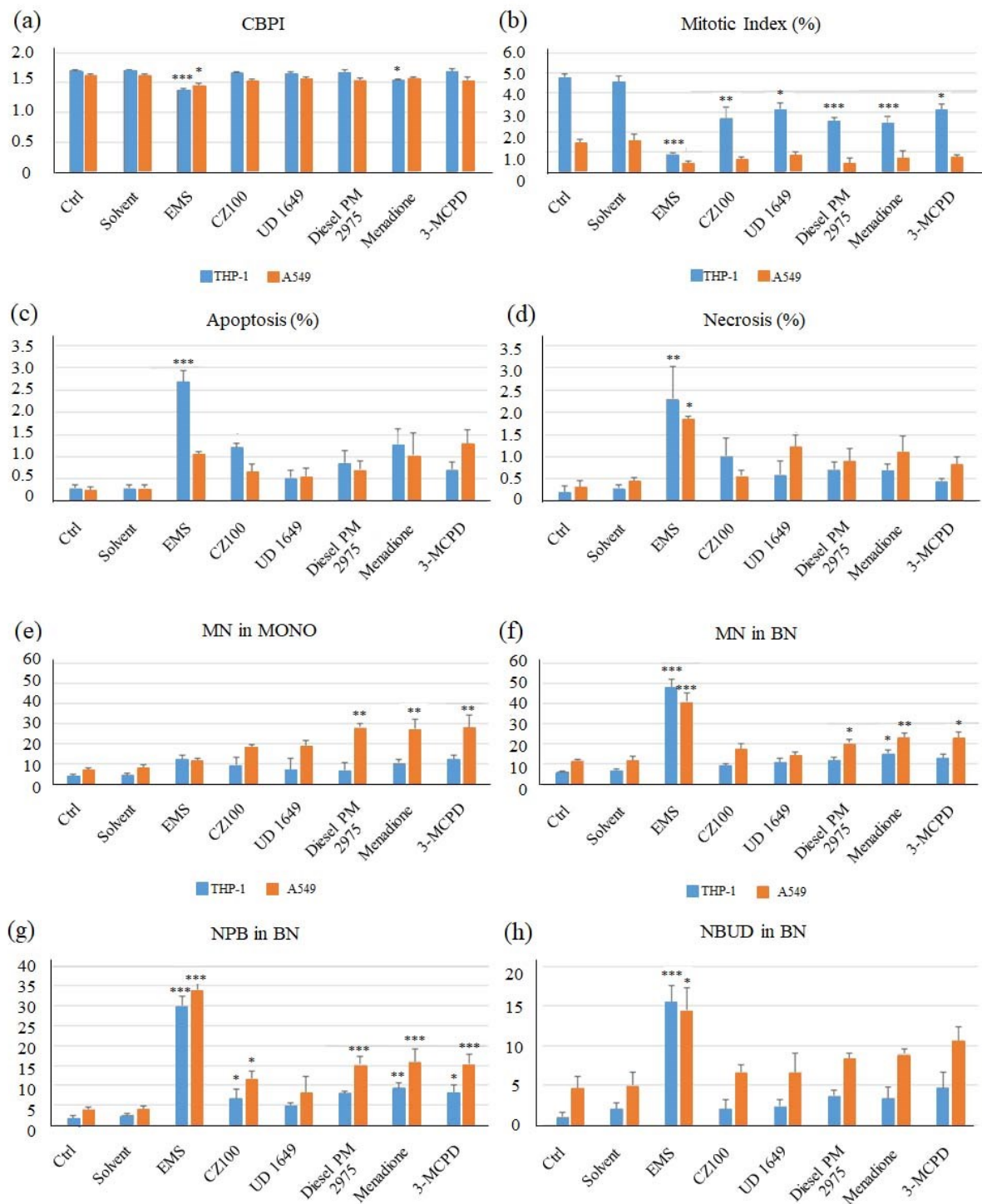


**Figure 3.4:** (a) cytokinesis-block proliferation index (CBPI); (b) mitotic%; (c) apoptotic%; (d) necrotic%; (e) MN in MONO; (f) MN in BN; (g) NPB in BN; (h) NBUD in BN. Exposed to 200  $\mu\text{g/mL}$  of CZ100 or UD 1649, or 40  $\mu\text{g/mL}$  of diesel PM 2975, 2  $\mu\text{g/mL}$  of menadione or 3-MCPD, mean  $\pm$  standard error of mean,  $n=3$ . Solvent control = 0.2% DMSO, positive control = 300  $\mu\text{g/mL}$  of ethyl-methanesulfonate (EMS). Analysis of variance was used, \*,  $p < 0.05$ ; \*\*,  $p < 0.01$ ; \*\*\*,  $p < 0.001$ .

Previous reports studied the genotoxicity of PM and oxidizers mainly by using the comet assay to evaluate single- double-strand breaks in DNA. UD 1649 showed dose-dependent effects on DNA

damage in murine embryonic fibroblast cells (Dumax-Vorzet et al., 2015). Diesel PM 2975 induced DNA damage in various different cell lines, including hamster lung fibroblasts V79 cells, lung epithelial A549 cells, macrophages, bronchial epithelial HBEC3 cells, respectively (Shi et al., 2009; Danielsen et al., 2008; Jantzen et al., 2012; Rynning et al., 2018). 3-MCPD was reported to cause DNA damage in embryonic kidney HEK293 cells (Sun et al., 2015b; Ji et al., 2017). Increased DNA damage in neuroblast-like SH-SY5Y cells was also observed upon treatment with menadione (Luukkonen et al., 2011). These studies indicated that both PM and oxidizers induced DNA damage in different cell types. Additionally, an increased MN frequency was observed after exposure to organic extraction of diesel PM 2975 but not to the washed particles alone in V79 fibroblasts (Shi et al., 2009) indicating that the genotoxicity induced by diesel PM 2975 was mainly due to its organic components. In our experiments, diesel PM 2975 induced stronger genotoxicity compared to CZ100 and UD 1649. This could be attributed to its high concentrations of PAHs and especially nitro-PAHs. A comparison study between the effects of 1-nitropyrene, 3-nitrobenzanthrone, and benzo[a]pyrene on bronchial epithelial BEAS-2B cells showed that both nitro-PAHs caused stronger genotoxicity than benzo[a]pyrene (Cervena et al., 2017). 1-Nitropyrene and 3-nitrofluoranthene (two important components in diesel PM 2975) were very genotoxic and induced strong ROS generation and DNA damage in A549 cells (Shang et al., 2017; Hu et al., 2020).

### 3.6 Correlation between 8-OHdG persistency and chromosomal instabilities

Production and excision of 8-OHdG that occurred on DNA strands may be a factor in chromosomal instabilities such as MN, NPB, and BUND. To explore their potential associations, correlations were made between 8-OHdG persistency and chromosomal instabilities. 8-OHdG persistency was evaluated based on the ratio between 72 hours and 4 hours values of 8-OHdG. Small ratios refer to the weak DNA oxidation persistency, while high ratios refer to strong DNA oxidation persistency. PM and oxidizers showed different 8-OHdG persistency in **Table 3.4**. The ratios of the 8-OHdG persistency were 0.22, 0.42, and 0.29 (in A549 cells) as well as 0.33, 0.22, and 0.24 (in THP-1 cells) in CZ100, UD 1649, and diesel PM 2975, respectively.

**Table 3.4:** The 8-OHdG persistency in A549 and THP-1 cells.

Cells	Oxidizer		PM		
	Menadione	3-MCPD	CZ100	UD 1649	Diesel PM 2975
A549	0.23 ± 0.03	0.18 ± 0.07	0.22 ± 0.07	0.42 ± 0.10	0.29 ± 0.08
THP-1	0.39 ± 0.12	0.21 ± 0.03	0.33 ± 0.07	0.22 ± 0.03	0.24 ± 0.06

Significantly positive correlations between 8-OHdG persistency and chromosomal instabilities (MN BN and NPB) were observed in A549 cells exposed to diesel PM 2975 and 3-MCPD. Significantly positive correlations between 8-OHdG persistency and NPB were found in THP-1 cells exposed to diesel PM 2975 and menadione (**Figure 3.5**). This indicated that 8-OHdG persistency was an important driving

factor for chromosomal damage, and the induction of genotoxicity by PM may have similar mechanisms to oxidizers. A possible explanation is that the simultaneous removal of multiple 8-OHdG from the DNA helix backbone can cause DNA double-strand breaks leading to MN formation (Fenech et al., 2011). However, the 8-OHdG persistency was negatively correlated with MN MONO in A549 cells exposed to CZ100 and oxidizers as well as in THP-1 cells exposed to menadione. This indicated that 8-OHdG persistency was not the only driving force for chromosomal damage, other factors such as PAHs may also contributed to the detected chromosomal damage. Benzo[a]pyrene is known to cause the formation of DNA-PAH adducts (Zhang et al., 2012) which can be excised from the DNA duplex leading to DNA strand breaks and further induce MN formation as well (Fenech and Neville, 1992; Godschalk et al., 2003). In previous reports, exposure to PAHs caused the increase frequency of MN and NPB in human lymphocytes, respectively (Ada et al., 2013; Duan et al., 2009).

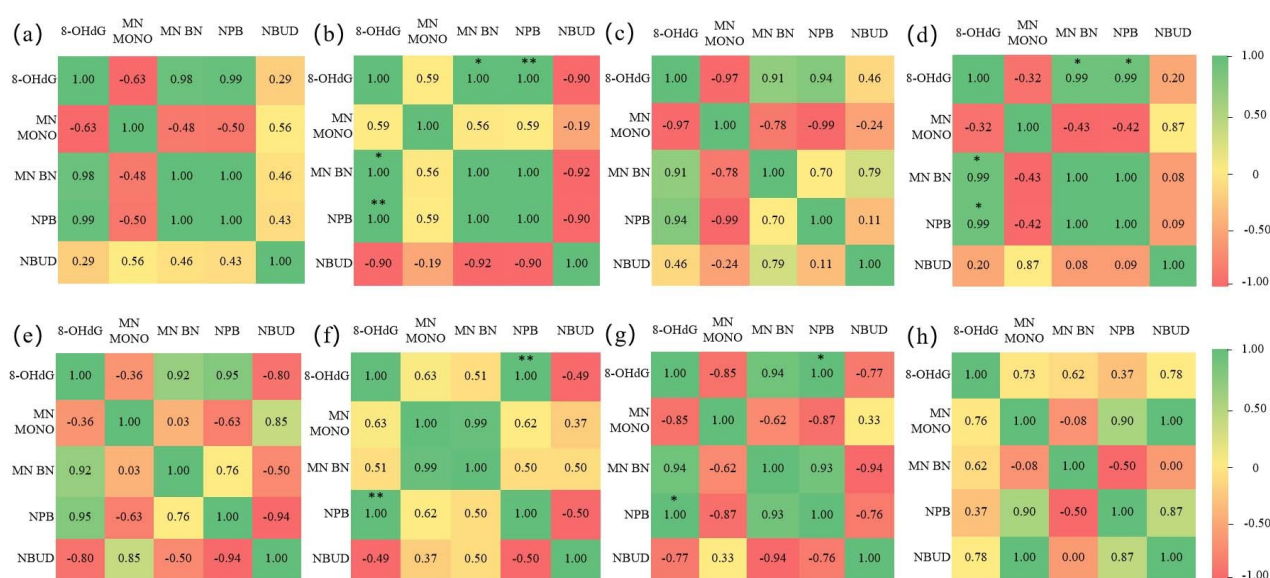


**Figure 3.5:** Pearson correlation coefficients between the 8-OHdG persistency and MN MONO, MN BN, NPB, and NBUD results in A549 cells exposed to (a) CZ100; (b) diesel PM 2975; (c) menadione; (d) 3-MCPD as well as in THP-1 cells exposed to (e) CZ100; (f) diesel PM 2975; (g) menadione; (h) 3-MCPD. \*,  $p < 0.05$ ; \*\*,  $p < 0.01$ .

### 3.7 Epigenetic DNA modifications analysis methods development

Since the concentration levels of 5-hmdC and 6mA in eukaryote cell DNA are very low, a sensitive and reliable analytical method (namely, LC-MS/MS; Publication 3) for their quantification is indispensable. Due to the polarity of the target molecules (cytosine, adenine, and their modifications), they presented poor retention time on reverse phase chromatography. In addition, the MS sensitivity for 5-hmdC and 6mA on MS were not high enough for the detection. Thus, chemical derivatization methods were used in this study to improve the target analyte retention time on LC and their ionization performance on MS. BPAP reacted with the target molecules (i.e. dC, 5-mdC, and 5-hmdC, Ade, and 6mA) forming derivatives for measurement.

**Table 3.5:** The comparison about the retention time and limit of detection (LOD) of target analytes with and without chemical derivatization (n.d., not detected).

Analyte	Without derivatization		derivatization	
	Retention (mins)	LOD (fmol)	Retention (mins)	LOD (fmol)
dC	1.97	1.32	4.47	0.22
5-mdC	2.88	0.83	5.46	0.33
5-hmdC	1.89	1.17	3.70	0.23
Ade	2.00	n.d	13.58	1.48
6mA	2.13	n.d.	15.10	0.67

After derivatization, the retention time behavior of target analytes on LC and the ionization efficiency of target analytes in the MS-source were significantly increased (**Table 3.5**). Until now, different derivative reagents were used for cytosine-related modifications analysis (**Table 2.1**). The limit of detection (LOD) of 5-mdC was at 0.04, 0.1, or 22.7 fmol, respectively, (Xiong et al., 2017; Tang et al., 2015; Torres et al., 2011). The LOD of 5-hmdC was at 0.06 fmol (Xiong et al., 2017; Tang et al., 2015). In this study, the LOD of 5-mdC and 5-hmdC were at 0.33 and 0.23 fmol, respectively. The difference was due to different derivative reagents as well as different instruments. In previous reports, measurements of adenine methylation were conducted by analyzing N6-methyl-2'-deoxyadenosine via LC-MS/MS method. The LOD of N6-methyl-2'-deoxyadenosine were at 0.42, 1.88, or 20 fmol, respectively, (Huang et al., 2015; Liang et al., 2016; Ratel et al., 2006). However, a suitable internal standard for reliable N6-methyl-2'-deoxyadenosine quantification was not included in the above reports and N6-methyl-2'-deoxyadenosine is expensive. Therefore, the determination of 6mA is a good alternative way to measure adenine methylation and 6mA has an additional cost advantage. In our study, the LOD of 6mA is at 0.67 fmol after chemical derivatization.

### 3.8 Epigenetic DNA modifications measurement

The base level of cytosine methylation in the negative control group was about 6.3%. After exposure to CZ100 and UD 1649 for 24 hours, cytosine methylation decreased to 4.8% and 5.2%, respectively (**Figure 3.6a**). After 48 hours, the decreased cytosine methylation was restored to the base level. No cytosine methylation changes were observed upon exposure to diesel PM 2975. After exposure for 24 hours, cytosine hydroxymethylation increased 3.0-, 2.3-, and 1.4-fold in CZ100, UD 1649, and diesel PM 2975, respectively, compared to the negative control group (**Figure 3.6b**). In contrast to cytosine methylation, the increased cytosine hydroxymethylation (2.7 and 2.5-fold of background level) was still observed 48 hours after exposure to UD 1649 and diesel PM 2975. Adenine methylation increased after exposure for 24 hours to CZ100 but not to other PM (**Figure 3.6c**). Taken together, a significantly negative correlation between cytosine methylation and cytosine hydroxymethylation ( $p\text{-value} < 0.001$  and  $R^2=0.1776$ ) was observed (**Figure 3.6d**). No significant correlation was found between cytosine methylation and adenine methylation (**Figure 3.6e**).



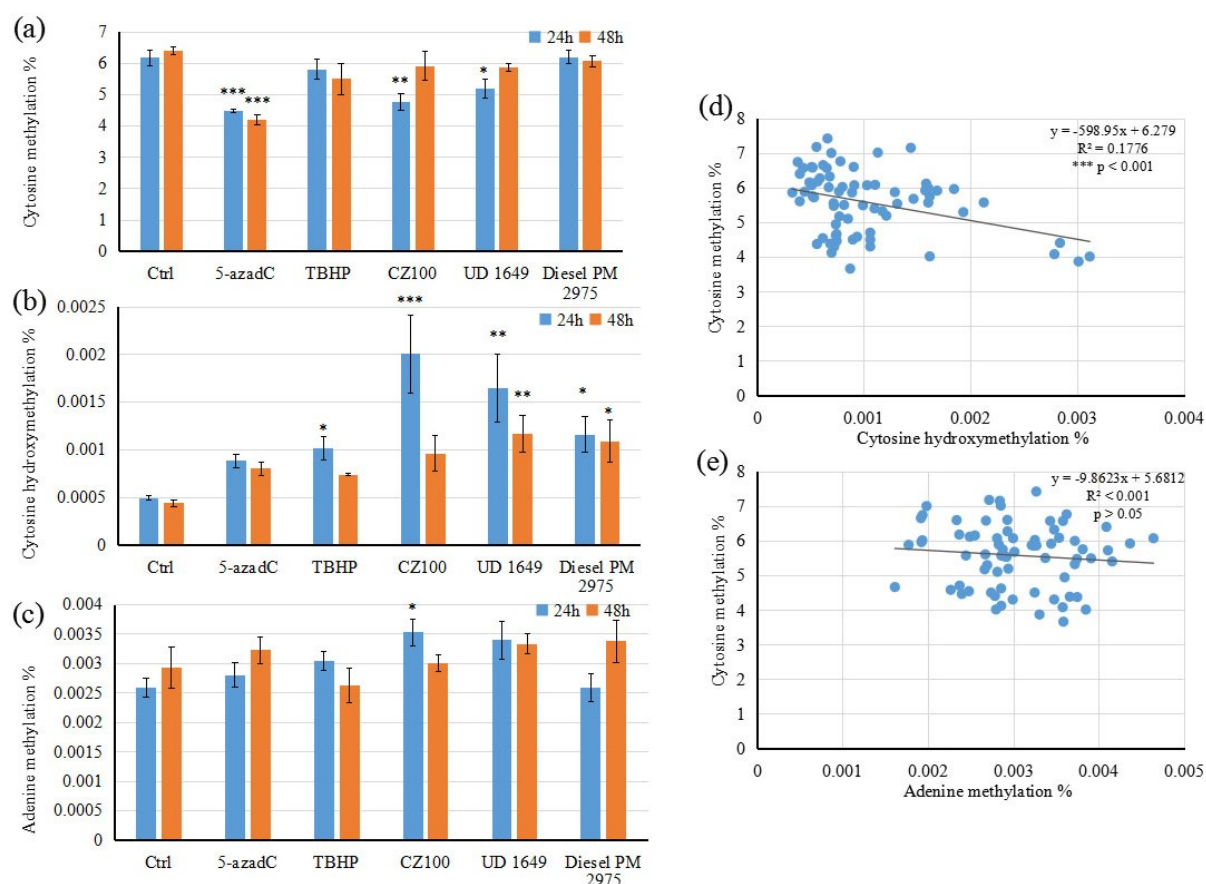


**Figure 3.6:** (a) cytosine methylation; (b) cytosine hydroxymethylation; (c) adenine methylation; (d,e) two-dimensional scatters between different epigenetic modifications. Exposed to 200  $\mu\text{g/mL}$  of CZ100 or UD 1649, or 40  $\mu\text{g/mL}$  of diesel PM 2975. (mean  $\pm$  standard error of mean,  $n=6$ ). 5-azadC = 2.3  $\mu\text{g/mL}$  of 5-aza-2'-deoxycytidine used as positive control for cytosine methylation. TBHP = 9  $\mu\text{g/mL}$  of tert-butyl hydroperoxide used as positive control for cytosine hydroxymethylation. Analysis of variance was used, \* =  $p$ -value  $< 0.05$ , \*\* =  $p$ -value  $< 0.01$ , \*\*\* =  $p$ -value  $< 0.001$ .

**Table 3.6:** Metal elements for each PM, information from certificates (CZ100 and UD1649) or from a literature (diesel PM2975, Ball et al., 2000), or from the ICP-MS analysis. (<sup>a</sup> means data from certificates; <sup>b</sup> means data from a literature; \* means data from ICP-MS)

Metal element	CZ100 (mg/kg)	UD1649 (mg/kg)	Diesel PM 2975 (mg/kg)
As*	8.58 $\pm$ 0.17	78.07 $\pm$ 1.42	1.24 $\pm$ 0.02
Cd*	1.24 $\pm$ 0.02	27.52 $\pm$ 0.14	0.08 $\pm$ 0.01
Cr*	238.13 $\pm$ 6.03	145.02 $\pm$ 1.57	4.22 $\pm$ 0.01
Co	14.3 <sup>a</sup>	16.4 $\pm$ 0.4 <sup>a</sup>	0.1 $\pm$ 0.1 <sup>b</sup>
Cu	462 <sup>a</sup>	223 $\pm$ 7 <sup>a</sup>	0.9 $\pm$ 0.6 <sup>b</sup>
Ni	58 $\pm$ 7 <sup>a</sup>	166 $\pm$ 7 <sup>a</sup>	0.5 $\pm$ 0.7 <sup>b</sup>
Zn	1240 <sup>a</sup>	1680 $\pm$ 40 <sup>a</sup>	16 $\pm$ 4 <sup>b</sup>
Fe	38144 <sup>a</sup>	29800 $\pm$ 700 <sup>a</sup>	0.9 <sup>b</sup>
Sum up	40200	32200	24

In the present study, we found that CZ100 and UD 1649 caused cytosine hypomethylation in cells after exposure to 24 hours but not the case for diesel PM 2975. Both CZ100 and UD 1649 contain higher heavy metal contents (e.g. arsenic, cadmium, and chromium) compared to diesel PM 2975 but have less PAHs and nitro-PAHs compared to diesel PM 2975. In previous reports, arsenic depleted the level of S-adenosylmethionine (SAM) and reduced DNA methyltransferase genes (DNMT1 and DNMT3A) expressions in keratinocyte HaCaT cells, which was responsible for the decreased cytosine methylation level (Reichard et al., 2007). Arsenic also reduced DNA methyltransferase enzymatic activity and caused DNA hypomethylation in rat liver epithelial TRL 1215 cells (Zhao et al., 1997). Cadmium was reported to reduce the DNA methyltransferase activity leading to DNA hypomethylation in liver epithelial TRL 125 cells after a 24 hours treatment period (Takiguchi et al., 2003) and decreased DNA methylation in chronic myelogenous leukemia K562 cells (Huang et al., 2008). Chromium, nickel, and cadmium mixtures in soil caused the reduction of cytosine methylation in plants such as hemp and clover (Aina et al., 2004). On the other hand, DNA oxidation products like 8-oxoguanine located at 5'-C-phosphate-G-3' (CpG) sites can weaken the activities of DNMT3A and DNMT1 proteins (Maltseva et al., 2009; Turk et al., 1995). This mechanism may result in potential hypomethylation as well. We found a significantly negative correlation between cytosine methylation and cytosine hydroxymethylation. The observed decrease of cytosine methylation and increase of cytosine hydroxymethylation may potentially play an important role in gene regulation upon PM exposure. 5-Methylcytosine levels were more than three magnitudes of orders higher than 5-hydroxymethylcytosine levels. The decreased 5-methylcytosine was not likely because of the transformation of 5-methylcytosine to 5-hydroxymethylcytosine, but due to an early aberrant recruitment stage during methylation such as the insufficient S-adenosylmethionine or the deficient DNMTs activities. Taking the above findings and our results into consideration, we assumed that cytosine hypomethylation induced by CZ100 and UD 1649 was due to the heavy metal components such as As, Cr, and Cd (**Table 3.6**) as well as cellular DNA oxidative damage 8-oxoguanine (**Figure 3.7**).

In this study, all PM significantly increased 5-hmdC levels in cells after 24 hours of exposure. Normally, ten-eleven translocation (TET) proteins contribute to the function to transfer 5-mdC into 5-hmdC (Klungland and Roberson, 2017). However, heavy metal components in PM such as As, Cd, and Cr may inhibit the activity of TET proteins (Xiong et al., 2017), which reduced cytosine hydroxymethylation. In addition, stepwise TET oxidation can transfer 5-hmdC into 5-formyl-2'-deoxycytidine (5-fodC) to decrease cytosine hydroxymethylation as well (Klungland and Robertson, 2017). Reductions of 5-hmdC in lung and liver tissues were obtained from a recent *in vivo* study in AJ mice exposed to traffic-related PM (1 hour daily for 3 months) (De Oliveira et al., 2018). Hence, the observed increased cytosine hydroxymethylation may be due to other different mechanisms. One possible explanation for the generation of 5-hmdC could be due to ROS generation (e.g. hydroxyl radical). Hydroxyl radicals can oxidize 5-methylcytosine into 5-hydroxymethylcytosine (Wagner and Cadet, 2010). ROS can be induced by PM via different pathways such as Fenton reaction, metabolism of PAHs, disturbance of

dihyronicotinamide adenine dinucleotide phosphate (NADPH) oxidase-mediated activities, and damage of mitochondria (Winterbourn, 1995; Møller et al., 2010; Lee et al., 2020; Li et al., 2003). An increased amount of 5-hmdC *in vitro* after exposure to PM was mediated by oxidative stress in neuroblast-like SH-SY5Y cells exposed to traffic-related PM (Wei et al., 2017). Considering the above results and previous reports, we assumed that antagonistic effects existed between the generation and reduction of 5-hmdC *in vivo* and *in vitro* systems (**Figure 3.7**). Even the level of 5-hmdC depends on many factors, reported studies show that 5-hmdC is a stable epigenetic modification. And aberrant changes of 5-hmdC are associated with various diseases (Bachmann et al., 2014; Wang et al., 2014). An increase of 5-hmdC was found in prostatic diseases (Grelus et al., 2017). While reductions of 5-hmdC were observed in carcinogenic tissues such as colorectal carcinoma and hepatocellular carcinoma (Tang et al., 2015; Tian et al., 2017; Chen et al., 2013).

The impact of PM on adenine methylation in cells was able to be investigated for the first time in this study. An increased adenine methylation after exposure to CZ100 was documented for the first time. The mechanism of adenine methylation by PM is not yet clear although some studies investigated the associations between adenine methylation and different exogenous factors. Mice brains under stress conditions showed increased DNA N6-methyladenine which may be a response to the environmental stress (Yao et al., 2017). The presence of N6-methyladenine in mice brains was an epigenetic marker which was associated with the development of stress-induced neuropathology (Kigar et al., 2017). The increase of N6-methyladenine levels had positive correlations with special stress-related gene expressions in plants (Zhang et al., 2018). With respect to these reported findings, the increased 6mA in THP-1 cells in this study may be related to the stress condition induced by CZ100.

In addition, we did not see a correlation between cytosine methylation and adenine methylation in cells exposed to PM. This indicated that the two methylation processes were controlled by different mechanisms (Beaulaurier et al., 2019). Cytosine methylation depends on DNMTs enzymes (Lyko, 2018). Adenine methylation requires DNA N6 adenine methyltransferases (DAMTs) enzymes (Li et al., 2019).



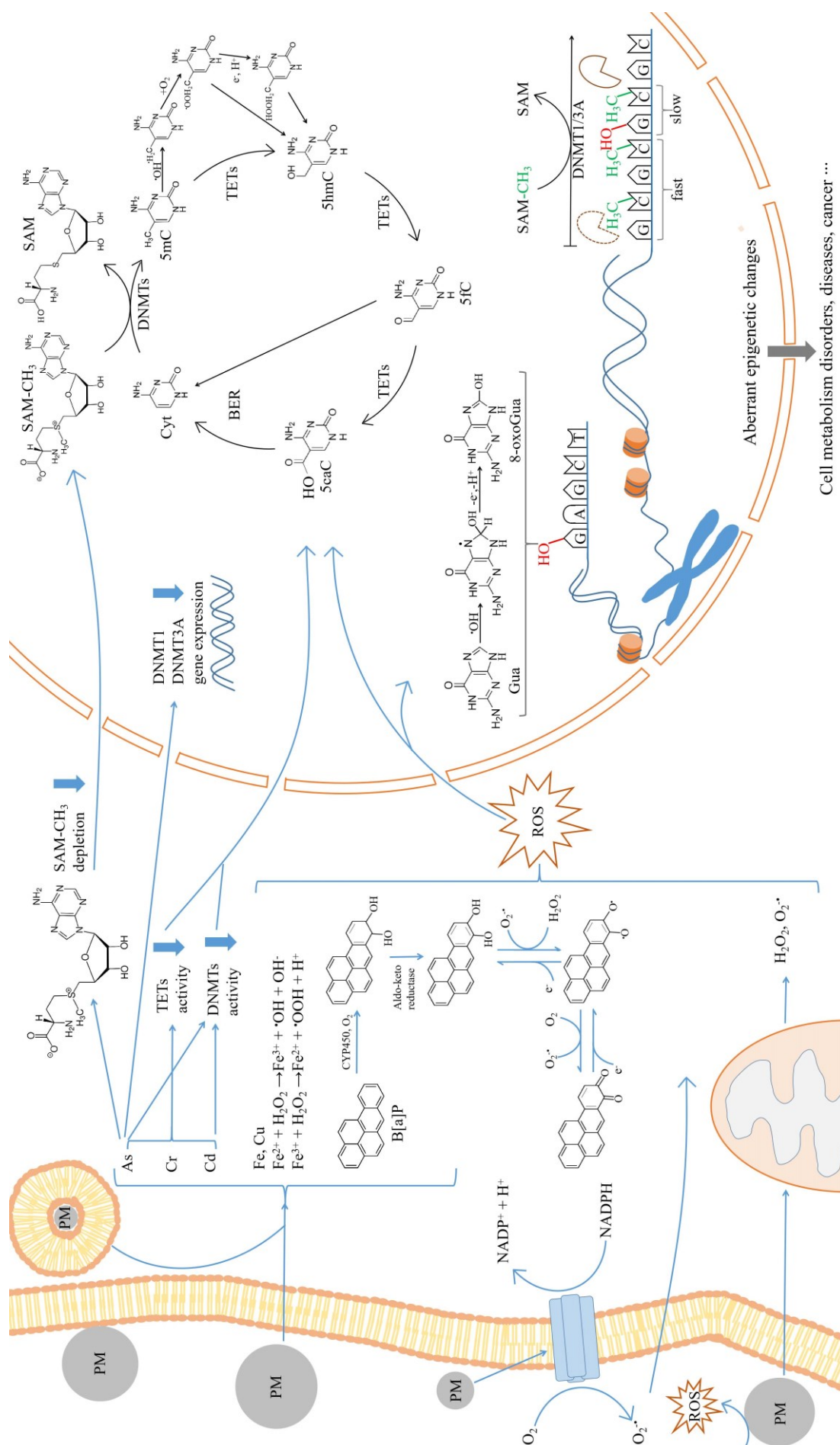


**Figure 3.7:** Illustration of possible mechanisms for cytosine modification exposed to particulate matter.

## 4 Conclusion and outlook

In this work, we analyzed PM<sub>2.5</sub> and PM<sub>10</sub> collected from different districts in Nanjing city. The results showed that PM from different sources containing diverse PAHs and showing different toxic and mutagenic equivalents. To investigate how different PM impact on cells, *in vitro* experiments were operated on human monocytic THP-1 and lung epithelial A549 cells by using three reference PM (i.e. CZ100, UD 1649, and diesel PM 2975) for exposure.

These results showed that diesel PM 2975 was more cytotoxic and genotoxic compared to the other PM, which could be due to its high organic components (e.g. PAHs and nitro-PAHs). All PM induced oxidative DNA damage to a similar level compared to oxidizers. Only CZ100 caused the strong lipid peroxidation which indicated CZ100 had a higher oxidation capacity than the other PM. The persistent DNA oxidation damage was an important driving force for chromosome instability and other factors such as PAHs could also contributed to this process. CZ100 and UD 1649 decreased cytosine methylation which could be due to their high contents of heavy metals. All PM increased cytosine hydroxymethylation which may have relations with the induced oxidative condition. A significant negative correlation between cytosine methylation and cytosine hydroxymethylation suggested potential intracellular interactions affected by PM. The mechanism of increased adenine methylation upon CZ100 exposure was not clarified but we assumed a connection with the stress condition induced by CZ100.

In general, different PM from diverse sources showed different toxicological effects on cells considering the cytotoxicity, genotoxicity, oxidative DNA and lipid damage, and epigenetic DNA modifications. Each toxicological event could be linked to the corresponding components in PM such as PAHs or metals. To further understand how different PM impact human health, more works are still in demand to elucidate the complex intracellular mechanisms. In this thesis, we studied the impact of three PM on THP-1 cells and A549 cells. In the future, we suggest to explore: (1) how other types of PM such as biomass burning PM, residential/indoor PM, or smoking PM impact different cell types; (2) which components in PM contribute to the observed toxicological events (3) and to improve the physiological relevance of the exposure experiments by using the air-liquid interface exposure system.

## 5 References

- Abbas, I., Garçon, G., Saint-Georges, F., Andre, V., Gosset, P., Billet, S., Goff, J. Le, Verdin, A., Mulliez, P., Sichel, F., Shirali, P., 2013. Polycyclic aromatic hydrocarbons within airborne particulate matter (PM<sub>2.5</sub>) produced DNA bulky stable adducts in a human lung cell coculture model. *J. Appl. Toxicol.* 33, 109–119. <https://doi.org/10.1002/jat.1722>
- Ada, A.O., Demiroglu, C., Yilmazer, M., Suzen, H.S., Demirbag, A.E., Efe, S., Alemdar, Y., Iscan, M., Burgaz, S., 2013. Cytogenetic damage in turkish coke oven workers exposed to polycyclic aromatic hydrocarbons: Association with CYP1A1, CYP1B1, EPHX1, GSTM1, GSTT1, and GSTP1 gene polymorphisms. *Arh Hig Rada Toksikol.* 64, 359–369. <https://doi.org/10.2478/10004-1254-64-2013-2328>
- Aga, E., Samoli, E., Touloumi, G., Anderson, H.R., Cadum, E., Forsberg, B., Goodman, P., Goren, A., Kotesovec, F., Kriz, B., Macarol-Hiti, M., Medina, S., Paldy, A., Schindler, C., Sunyer, J., Tittanen, P., Wojtyniak, B., Zmirou, D., Schwartz, J., Katsouyanni, K., 2003. Short-term effects of ambient particles on mortality in the elderly: Results from 28 cities in the APHEA2 project. *Eur. Respir. Journal, Suppl.* 21, 28–33. <https://doi.org/10.1183/09031936.03.00402803>
- Aina, R., Sgorbati, S., Santagostino, A., Labra, M., Ghiani, A., Citterio, S., 2004. Specific hypomethylation of DNA is induced by heavy metals in white clover and industrial hemp. *Physiol. Plant.* 121, 472–480. <https://doi.org/10.1111/j.1399-3054.2004.00343.x>
- Anderson, J.O., Thundiyil, J.G., Stolbach, A., 2012. Clearing the Air: A Review of the Effects of Particulate Matter Air Pollution on Human Health. *J. Med. Toxicol.* 8, 166–175. <https://doi.org/10.1007/s13181-011-0203-1>
- Arden Pope III, C., Burnett, R.T., Turner, M.C., Cohen, A., Krewski, D., Jerrett, M., Gapstur, S.M., Thun, M.J., 2011. Lung cancer and cardiovascular disease mortality associated with ambient air pollution and cigarette smoke: Shape of the exposure-response relationships. *Environ. Health Perspect.* 119, 1616–1621. <https://doi.org/10.1289/ehp.1103639>
- Ayala, A., Muñoz, M.F., Argüelles, S., 2014. Lipid peroxidation: Production, metabolism, and signaling mechanisms of malondialdehyde and 4-hydroxy-2-nonenal. *Oxid. Med. Cell. Longev.* 2014, ID360438. <https://doi.org/10.1155/2014/360438>
- Bachman, M., Uribe-Lewis, S., Yang, X., Williams, M., Murrell, A., Balasubramanian, S., 2014. 5-Hydroxymethylcytosine is a predominantly stable DNA modification. *Nat. Chem.* 6, 1049–1055. <https://doi.org/10.1038/nchem.2064>
- Ball, J.C., Straccia, A.M., Young, W.C., Aust, A.E., 2000. The formation of reactive oxygen species catalyzed by neutral, aqueous extracts of NIST ambient particulate matter and diesel engine particles. *J. Air Waste Manag. Assoc.* 50, 1897–1903. <https://doi.org/10.1080/10473289.2000.10464231>
- Bandowe, B.A.M., Meusel, H., 2017. Nitrated polycyclic aromatic hydrocarbons (nitro-PAHs) in the environment - A review. *Sci. Total Environ.* 581–582, 237–257. <https://doi.org/10.1016/j.scitotenv.2016.12.115>
- Barnes, J.L., Zubair, M., John, K., Poirier, M.C., Martin, F.L., 2018. Carcinogens and DNA damage. *Biochem. Soc. Trans.* 46, 1213–1224. <https://doi.org/10.1042/BST20180519>
- Beaulaurier, J., Schadt, E.E., Fang, G., 2019. Deciphering bacterial epigenomes using modern sequencing technologies. *Nat. Rev. Genet.* 20, 157–172. <https://doi.org/10.1038/s41576-018-0081-3>
- Bellavia, A., Urch, B., Speck, M., Brook, R.D., Scott, J.A., Albeti, B., Behbod, B., North, M., Valeri, L., Bertazzi, P.A., Silverman, F., Gold, D., Baccarelli, A.A., 2013. DNA hypomethylation, ambient particulate matter, and increased blood pressure: Findings from controlled human exposure experiments.

J. Am. Heart Assoc. 2, e000212. <https://doi.org/10.1161/JAHA.113.000212>

Billet, S., Abbas, I., Goff, J. Le, Verdin, A., André, V., Lafargue, P.E., Hachimi, A., Cazier, F., Sichel, F., Shirali, P., Garçon, G., 2008. Genotoxic potential of Polycyclic Aromatic Hydrocarbons-coated onto airborne Particulate Matter (PM<sub>2.5</sub>) in human lung epithelial A549 cells. *Cancer Lett.* 270, 144–155. <https://doi.org/10.1016/j.canlet.2008.04.044>

Bind, M.-A., Baccarelli, A., Zanobetti, A., Tarantini, L., Suh, H., Vokonas, P., Joel, S., 2012. Air pollution and markers of coagulation, inflammation and endothelial function: Associations and epigenvironment interactions in an elderly cohort. *Epidemiology.* 23, 332–340. <https://doi.org/10.1097/EDE.0b013e31824523f0>

Boobis, A., Brown, A., Cronin, M.T.D., Edwards, J., Galli, C.L., Goodman, J., Jacobs, A., Kirkland, D., Luijten, M., Marsaux, C., Martin, M., Yang, C., Hollnagel, H.M., 2017. Origin of the TCC values for compounds that are genotoxic and/or carcinogenic and an approach for their re-evaluation. *Crit. Rev. Toxicol.* 47, 710–732. <https://doi.org/10.1080/10408444.2017.1318822>

Brunekreef, B., Forsberg, B., 2005. Epidemiological evidence of effects of coarse airborne particles on health. *Eur. Respir. J.* 26, 309–318. <https://doi.org/10.1183/09031936.05.00001805>

Cadet, J., Wagner, J.R., 2013. DNA Base Damage by Reactive Oxygen Species, Oxidizing Agents, and UV Radiation. *Cold Spring Harb Perspect Biol.* 5, a012559. <https://doi.org/10.1101/cshperspect.a012559>

Cervena, T., Rossnerova, A., Sikorova, J., Beranek, V., Vojtisek-Lom, M., Ciganek, M., Topinka, J., Rossner, P., 2017. DNA damage potential of engine emissions measured in vitro by micronucleus test in human bronchial epithelial cells. *Basic Clin. Pharmacol. Toxicol.* 121, 102–108. <https://doi.org/10.1111/bcpt.12693>

Chen, J.L., Huang, Y.J., Pan, C.H., Hu, C.W., Chao, M.R., 2011. Determination of urinary malondialdehyde by isotope dilution LC-MS/MS with automated solid-phase extraction: A cautionary note on derivatization optimization. *Free Radic. Biol. Med.* 51, 1823–1829. <https://doi.org/10.1016/j.freeradbiomed.2011.08.012>

Chen, M.L., Shen, F., Huang, W., Qi, J.H., Wang, Y., Feng, Y.Q., Liu, S.M., Yuan, B.F., 2013. Quantification of 5-methylcytosine and 5-hydroxymethylcytosine in genomic DNA from hepatocellular carcinoma tissues by capillary hydrophilic-interaction liquid chromatography/quadrupole TOF mass spectrometry. *Clin. Chem.* 59, 824–832. <https://doi.org/10.1373/clinchem.2012.193938>

Chen, X., Zhang, Li wen, Huang, J. ju, Song, F. ju, Zhang, Luo ping, Qian, Z. min, Trevathan, E., Mao, H. jun, Han, B., Vaughn, M., Chen, K. xin, Liu, Y. min, Chen, J., Zhao, B. xin, Jiang, G. hong, Gu, Q., Bai, Z. peng, Dong, G. hui, Tang, N. jun, 2016. Long-term exposure to urban air pollution and lung cancer mortality: A 12-year cohort study in Northern China. *Sci. Total Environ.* 571, 855–861. <https://doi.org/10.1016/j.scitotenv.2016.07.064>

Chung, M.Y., Lazaro, R.A., Lim, D., Jackson, J., Lyon, J., Rendulic, D., Hasson, A.S., 2006. Aerosol-borne quinones and reactive oxygen species generation by particulate matter extracts. *Environ. Sci. Technol.* 40, 4880–4886. <https://doi.org/10.1021/es0515957>

Colbeck, I., Lazaridis, M., 2014. *Aerosol Science*, Wiley & Sons Ltd., West Sussex, United Kingdom.

Da Silva, C.S., Rossato, J.M., Vaz Rocha, J.A., Vargas, V.M.F., 2015. Characterization of an area of reference for inhalable particulate matter (PM<sub>2.5</sub>) associated with genetic biomonitoring in children. *Mutat. Res. - Genet. Toxicol. Environ. Mutagen.* 778, 44–55. <https://doi.org/10.1016/j.mrgentox.2014.11.006>

Danielsen, P.H., Loft, S., Møller, P., 2008. DNA damage and cytotoxicity in type II lung epithelial (A549) cell cultures after exposure to diesel exhaust and urban street particles. *Part. Fibre Toxicol.* 5, 1–12.

<https://doi.org/10.1186/1743-8977-5-6>

Dao, T., Cheng, R.Y.S., Revelo, M.P., Mitzner, W., Tang, W.Y., 2014. Hydroxymethylation as a Novel Environmental Biosensor. *Curr. Environ. Heal. Reports.* 1, 1–10. <https://doi.org/10.1007/s40572-013-0005-5>

De Oliveira, A.A.F., De Oliveira, T.F., Dias, M.F., Medeiros, M.H.G., Di Mascio, P., Veras, M., Lemos, M., Marcourakis, T., Saldiva, P.H.N., Loureiro, A.P.M., 2018. Genotoxic and epigenotoxic effects in mice exposed to concentrated ambient fine particulate matter (PM<sub>2.5</sub>) from São Paulo city, Brazil. *Part. Fibre Toxicol.* 15, 40. <https://doi.org/10.1186/s12989-018-0276-y>

Dedon, P.C., Plastaras, J.P., Rouzer, C.A., Marnett, L.J., 1998. Indirect mutagenesis by oxidative DNA damage: Formation of the pyrimidopurinone adduct of deoxyguanosine by base propenal. *Proc. Natl. Acad. Sci. U. S. A.* 95, 11113–11116. <https://doi.org/10.1073/pnas.95.19.11113>

Delistraty, D., 1997. Toxic equivalency factor approach for risk assessment of polycyclic aromatic hydrocarbons. *Toxicol. Environ. Chem.* 64, 81–108. <https://doi.org/10.1080/02772249709358542>

Di Bucchianico, S., Gliga, A.R., Åkerlund, E., Skoglund, S., Wallinder, I.O., Fadeel, B., Karlsson, H.L., 2018. Calcium-dependent cyto- and genotoxicity of nickel metal and nickel oxide nanoparticles in human lung cells. *Part. Fibre Toxicol.* 15, 32. <https://doi.org/10.1186/s12989-018-0268-y>

Duan, H., Leng, S., Pan, Z., Dai, Y., Niu, Y., Huang, C., Bin, P., Wang, Y., Liu, Q., Chen, W., Zheng, Y., 2009. Biomarkers measured by cytokinesis-block micronucleus cytome assay for evaluating genetic damages induced by polycyclic aromatic hydrocarbons. *Mutat. Res., Genet. Toxicol. Environ. Mutagen.* 677, 93–99. <https://doi.org/10.1016/j.mrgentox.2009.06.002>

Dumax-Vorzet, A.F., Tate, M., Walmsley, R., Elder, R.H., Povey, A.C., 2015. Cytotoxicity and genotoxicity of urban particulate matter in mammalian cells. *Mutagenesis.* 30, 621–633. <https://doi.org/10.1093/mutage/gev025>

Durant, J.L., Busby, W.F., Lafleur, A.L., Penman, B.W., Crespi, C.L., 1996. Human cell mutagenicity of oxygenated, nitrated and unsubstituted polycyclic aromatic hydrocarbons associated with urban aerosols. *Mutat. Res. - Genet. Toxicol.* 371, 123–157. [https://doi.org/10.1016/S0165-1218\(96\)90103-2](https://doi.org/10.1016/S0165-1218(96)90103-2)

Ehrlich, M., 2009. DNA hypomethylation in cancer cells. *Epigenomics.* 1, 239–259. <https://doi.org/10.2217/epi.09.33>

Elmore, S., 2007. Apoptosis: A Review of Programmed Cell Death. *Toxicol. Pathol.* 35, 495–516. <https://doi.org/10.1080/01926230701320337>

Fenech, M., 2007. Cytokinesis-block micronucleus cytome assay. *Nat. Protoc.* 2, 1084–1104. <https://doi.org/10.1038/nprot.2007.77>

Fenech, M., Kirsch-Volders, M., Natarajan, A.T., Surrallés, J., Crott, J.W., Parry, J., Norppa, H., Eastmond, D.A., Tucker, J.D., Thomas, P., 2011. Molecular mechanisms of micronucleus, nucleoplasmic bridge and nuclear bud formation in mammalian and human cells. *Mutagenesis.* 26, 125–132. <https://doi.org/10.1093/mutage/geq052>

Fenech, M., Neville, S., 1992. Conversion of excision-repairable DNA lesions to micronuclei within one cell cycle in human lymphocytes. *Environ. Mol. Mutagen.* 19, 27–36. <https://doi.org/10.1002/em.2850190106>

Fink, S.L., Cookson, B.T., 2005. Apoptosis, pyroptosis, and necrosis: Mechanistic description of dead and dying eukaryotic cells. *Infect. Immun.* 73, 1907–1916. <https://doi.org/10.1128/IAI.73.4.1907-1916.2005>

Fink, S.P., Reddy, G.R., Marnett, L.J., 1997. Mutagenicity in *Escherichia coli* of the major DNA adduct derived from the endogenous mutagen malondialdehyde. *Proc. Natl. Acad. Sci. U. S. A.* 94, 8652–8657.

<https://doi.org/10.1073/pnas.94.16.8652>

GBD 2019 Risk Factor Collaborators, 2019. Global burden of 87 risk factor in 204 countries and territories, 1990-2019: a systematic analysis for the global burden of disease study 2019. *Lancet*. 396, 1223-1249. [https://doi.org/10.1016/S0140-6736\(20\)30752-2](https://doi.org/10.1016/S0140-6736(20)30752-2)

Godschalk, R.W., Van Schooten, F., Bartsch, H., 2003. A Critical Evaluation of DNA Adducts as Biological Markers for Human Exposure to Polycyclic Aromatic Compounds. *J. Biochem. Mol. Biol.* 36, 1. <https://doi.org/10.5483/bmbrep.2003.36.1.001>

Gouveia, N., Fletcher, T., 2000. Time series analysis of air pollution and mortality: Effects by cause, age and socioeconomic status. *J. Epidemiol. Community Health*. 54, 750-755. <https://doi.org/10.1136/jech.54.10.750>

Grelus, A., Nica, D. V., Miklos, I., Belengeanu, V., Ioiart, I., Popescu, C., 2017. Clinical significance of measuring global hydroxymethylation of white blood cell DNA in prostate cancer: Comparison to PSA in a pilot exploratory study. *Int. J. Mol. Sci.* 18, 2465. <https://doi.org/10.3390/ijms18112465>

Guibert, S., Weber, M., 2013. Functions of DNA Methylation and Hydroxymethylation in Mammalian Development. *Curr. Top. Dev. Biol.* 104, 47-83. <https://doi.org/10.1016/B978-0-12-416027-9.00002-4>

Handy, D., Castro, R., J, L., 2011. Epigenetic Modifications: Basic Mechanisms and Role in Cardiovascular Disease. *Circulation*. 123, 2145-2156. <https://doi.org/10.1161/CIRCULATIONAHA.110.956839>

Hansen, K.D., Timp, W., Bravo, H.C., Langmead, B., McDonald, O.G., Wen, B., Wu, H., Diep, D., Briem, E., Zhang, K., Irizarry, R.A., Feinberg, A.P., 2011. Increased methylation variation in epigenetic domains across cancer types. *Nat. Genet.* 43, 768-775. <https://doi.org/10.1038/ng.865>

Harvey, R.G., 1996. Mechanisms of carcinogenesis of polycyclic aromatic hydrocarbons. *Polycycl. Aromat. Compd.* 9, 1-23. <https://doi.org/10.1080/10406639608031196>

Hattman, S., 2005. DNA-[Adenine] methylation in lower eukaryotes. *Biochem.* 70, 550-558. <https://doi.org/10.1007/s10541-005-0148-6>

He, J., Fan, S., Meng, Q., Sun, Y., Zhang, J., Zu, F., 2014. Polycyclic aromatic hydrocarbons (PAHs) associated with fine particulate matters in Nanjing, China: Distributions, sources and meteorological influences. *Atmos. Environ.* 89, 207-215. <https://doi.org/10.1016/j.atmosenv.2014.02.042>

Ho, C., Lam, C., Chan, M., Cheung, R., Law, L., Lit, L., Ng, K., Suen, M., Tai, H., 2003. Electrospray Ionisation Mass Spectrometry: Principles and Clinical Applications. *Clin. Biochem. Rev.* 24, 3-12. <https://doi.org/PMID: 18568044>

Holländer, A., 2017. Why do we need chemical derivatization? *Plasma Process. Polym.* 14, e1700044. <https://doi.org/10.1002/ppap.201700044>

Hu, B., Tong, B., Xiang, Y., Li, S.R., Tan, Z.X., Xiang, H.X., Fu, L., Wang, H., Zhao, H., Xu, D.X., 2020. Acute 1-NP exposure induces inflammatory responses through activating various inflammatory signaling pathways in mouse lungs and human A549 cells. *Ecotoxicol. Environ. Saf.* 189, 109977. <https://doi.org/10.1016/j.ecoenv.2019.109977>

Huang, D., Zhang, Y., Qi, Y., Chen, C., Ji, W., 2008. Global DNA hydroxymethylation rather than reactive oxygen species (ROS) potential facilitator of cadmium-stimulated K562 cell proliferation. *Toxicol. Lett.* 179, 43-47. <https://doi.org/10.1016/j.toxlet.2008.03.018>

Huang, W., Lan, M.D., Qi, C.B., Zheng, S.J., Wei, S.Z., Yuan, B.F., Feng, Y.Q., 2016. Formation and determination of the oxidation products of 5-methylcytosine in RNA. *Chem. Sci.* 7, 5495-5502. <https://doi.org/doi.org/10.1039/C6SC01589A>

- Huang, W., Xiong, J., Yang, Y., Liu, S.M., Yuan, B.F., Feng, Y.Q., 2015. Determination of DNA adenine methylation in genomes of mammals and plants by liquid chromatography/mass spectrometry. *RSC Adv.* 5, 64046–64054. <https://doi.org/10.1039/c5ra05307b>
- Janssen, B.G., Godderis, L., Pieters, N., Poels, K., Kiciński, M., Cuypers, A., Fierens, F., Penders, J., Plusquin, M., Gyselaers, W., Nawrot, T.S., 2013. Placental DNA hypomethylation in association with particulate air pollution in early life. Part. *Fibre Toxicol.* 10, 22. <https://doi.org/10.1186/1743-8977-10-22>
- Jantzen, K., Roursgaard, M., Desler, C., Loft, S., Rasmussen, L.J., Møller, P., 2012. Oxidative damage to DNA by diesel exhaust particle exposure in co-cultures of human lung epithelial cells and macrophages. *Mutagenesis.* 27, 693–701. <https://doi.org/10.1093/mutage/ges035>
- Ji, J., Zhu, P., Sun, C., Sun, J., An, L., Zhang, Y., Sun, X., 2017. Pathway of 3-MCPD-induced apoptosis in human embryonic kidney cells. *J. Toxicol. Sci.* 42, 43–52. <https://doi.org/10.2131/jts.42.43>
- Katanoda, K., Sobue, T., Satoh, H., Tajima, K., Suzuki, T., Nakatsuka, H., Takezaki, T., Nakayama, T., Nitta, H., Tanabe, K., Tominaga, S., 2011. An association between long-term exposure to ambient air pollution and mortality from lung cancer and respiratory diseases in Japan. *J. Epidemiol.* 21, 132–143. <https://doi.org/10.2188/jea.JE20100098>
- Kigar, S.L., Chang, L., Guerrero, C.R., Sehring, J.R., Cuarenta, A., Parker, L.L., Bakshi, V.P., Auger, A.P., 2017. N6-methyladenine is an epigenetic marker of mammalian early life stress. *Sci. Rep.* 7, 18078. <https://doi.org/10.1038/s41598-017-18414-7>
- Kim, K.H., Kabir, E., Kabir, S., 2015. A review on the human health impact of airborne particulate matter. *Environ. Int.* 74, 136–143. <https://doi.org/10.1016/j.envint.2014.10.005>
- Kirsch-Volders, M., Fenech, M., 2001. Inclusion of micronuclei in non-divided mononuclear lymphocytes and necrosis/apoptosis may provide a more comprehensive cytokinesis block micronucleus assay for biomonitoring purposes. *Mutagenesis.* 16, 51–58. <https://doi.org/10.1093/mutage/16.1.51>
- Klungland, A., Robertson, A.B., 2017. Oxidized C5-methyl cytosine bases in DNA: 5-Hydroxymethylcytosine; 5-formylcytosine; and 5-carboxycytosine. *Free Radic. Biol. Med.* 107, 62–68. <https://doi.org/10.1016/j.freeradbiomed.2016.11.038>
- Kornyushyna, O., Berges, A.M., Muller, J.G., Burrows, C.J., 2002. In vitro nucleotide misinsertion opposite the oxidized guanosine lesions spiroiminodihydantoin and guanidinohydantoin and DNA synthesis past the lesions using Escherichia coli DNA polymerase I (Klenow fragment). *Biochemistry.* 41, 15304–15314. <https://doi.org/10.1021/bi0264925>
- Lee, H.S., Park, H.Y., Kwon, S.P., Kim, B., Lee, Y., Kim, S., Shin, K.O., Park, K., 2020. NADPH oxidase-mediated activation of neutral sphingomyelinase is responsible for diesel particulate extract-induced keratinocyte apoptosis. *Int. J. Mol. Sci.* 21, 1001. <https://doi.org/10.3390/ijms21031001>
- Leonhard, P., Pepelnik, R., Prange, A., Yamada, N., Yamada, T., 2002. Analysis of diluted sea-water at the ng/L level using an ICP-MS with an octopole reaction cell. *J. Anal. At. Spectrom.* 17, 189–196. <https://doi.org/10.1039/b110180n>
- Li, N., Sioutas, C., Cho, A., Schmitz, D., Misra, C., Sempf, J., Wang, M., Oberley, T., Froines, J., Nel, A., 2003. Ultrafine particulate pollutants induce oxidative stress and mitochondrial damage. *Environ. Health Perspect.* 111, 455–460. <https://doi.org/10.1289/ehp.6000>
- Li, Z., Zhao, P., Xia, Q., 2019. Epigenetic methylations on n6-adenine and n6-adenosine with the same input but different output. *Int. J. Mol. Sci.* 20, 2931. <https://doi.org/10.3390/ijms20122931>
- Liang, D., Wang, H., Song, W., Xiong, X., Zhang, X., Hu, Z., Guo, H., Yang, Z., Zhai, S., Zhang, L.H., Ye, M., Du, Q., 2016. The decreased N6-methyladenine DNA modification in cancer cells. *Biochem.*

- Biophys. Res. Commun. 480, 120–125. <https://doi.org/10.1016/j.bbrc.2016.09.136>
- Lintas, C and De Matthaëis, M.C., 1979. Determination of benzo[a]pyrene in smoked, cooked and toasted food products. *Food. Cosmet. Toxicol.* 17, 325–328. [https://doi.org/10.1016/0015-6264\(79\)90323-7](https://doi.org/10.1016/0015-6264(79)90323-7).
- Luo, G.Z., Blanco, M.A., Greer, E.L., He, C., Shi, Y., 2015. DNA N6-methyladenine: A new epigenetic mark in eukaryotes? *Nat. Rev. Mol. Cell Biol.* 16, 705–710. <https://doi.org/10.1038/nrm4076>
- Luukkonen, J., Liimatainen, A., Höytö, A., Juutilainen, J., Naarala, J., 2011. Pre-exposure to 50 HZ magnetic fields modifies menadione-induced genotoxic effects in human SH-SY5Y neuroblastoma cells. *PLoS One*. 6, e18021. <https://doi.org/10.1371/journal.pone.0018021>
- Lyko, F., 2018. The DNA methyltransferase family: A versatile toolkit for epigenetic regulation. *Nat. Rev. Genet.* 19, 81–92. <https://doi.org/10.1038/nrg.2017.80>
- Maltseva, D. V., Baykov, A.A., Jeltsch, A., Gromova, E.S., 2009. Impact of 7,8-dihydro-8-oxoguanine on methylation of the CpG site by dnmt3a. *Biochemistry.* 48, 1361–1368. <https://doi.org/10.1021/bi801947f>
- Mandal, P., Sarkar, R., Mandal, A., Saud, T., 2014. Seasonal variation and sources of aerosol pollution in Delhi, India. *Environ. Chem. Lett.* 12, 529–534. <https://doi.org/10.1007/s10311-014-0479-x>
- Marnett, L.J., Plataras, J.P., 2001. Endogenous DNA damage and mutation. *Trends Genet.* 17, 214–221. [https://doi.org/10.1016/S0168-9525\(01\)02239-9](https://doi.org/10.1016/S0168-9525(01)02239-9)
- Møller, P., Jacobsen, N.R., Folkmann, J.K., Danielsen, P.H., Mikkelsen, L., Hemmingsen, J.G., Vesterdal, L.K., Forchhammer, L., Wallin, H., Loft, S., 2010. Role of oxidative damage in toxicity of particulate. *Free Radic. Res.* 44, 1–46. <https://doi.org/10.3109/10715760903300691>
- Naito, T., Kusano, K., Kobayashi, I., 1995. Selfish behavior of restriction-modification systems. *Science.* 267, 897–899. <https://doi.org/10.1126/science.7846533>
- Nisbet, I.C.T., LaGoy, P.K., 1992. Toxic equivalency factors (TEFs) for polycyclic aromatic hydrocarbons (PAHs). *Regul. Toxicol. Pharmacol.* 16, 290–300. [https://doi.org/10.1016/0273-2300\(92\)90009-X](https://doi.org/10.1016/0273-2300(92)90009-X)
- Nys, S.D., Duca, R., Nawrot, T., Hoet, P., Meerbeek, B.V., Van Landuyt, K.L., Godderis, L., 2017. Temporal variability of global DNA methylation and hydroxymethylation in buccal cells of healthy adults: Association with air pollution. *Environ. Int.* 111, 301–308. <https://doi.org/10.1016/j.envint.2017.11.002>
- OECD, 2016. Test No. 487: In Vitro Mammalian Cell Micronucleus Test, OECD Guidelines for the Testing of Chemicals, Section 4, OECD Publishing, Paris, <https://doi.org/10.1787/9789264264861-en>, 2016)
- Øvrevik, J., Arlt, V.M., Øya, E., Nagy, E., Møllerup, S., Phillips, D.H., Låg, M., Holme, J.A., 2010. Differential effects of nitro-PAHs and amino-PAHs on cytokine and chemokine responses in human bronchial epithelial BEAS-2B cells. *Toxicol. Appl. Pharmacol.* 242, 270–280. <https://doi.org/10.1016/j.taap.2009.10.017>
- Parashar, N.C., Parashar, G., Nayyar, H., Sandhir, R., 2018. N6-adenine DNA methylation demystified in eukaryotic genome: From biology to pathology. *Biochimie.* 144, 56–62. <https://doi.org/10.1016/j.biochi.2017.10.014>
- Park, M., Joo, H.S., Lee, K., Jang, M., Kim, S.D., Kim, I., Borlaza, L.J.S., Lim, H., Shin, H., Chung, K.H., Choi, Y.H., Park, S.G., Bae, M.S., Lee, J., Song, H., Park, K., 2018. Differential toxicities of fine particulate matters from various sources. *Sci. Rep.* 8, 1–11. <https://doi.org/10.1038/s41598-018-35398-0>



- Prahalad, A.K., Inmon, J., Dailey, L.A., Madden, M.C., Ghio, A.J., Gallagher, J.E., 2001. Air pollution particles mediated oxidative DNA base damage in a cell free system and in human airway epithelial cells in relation to particulate metal content and bioreactivity. *Chem. Res. Toxicol.* 14, 879–887. <https://doi.org/10.1021/tx010022e>
- Ratel, D., Ravanat, J.L., Charles, M.P., Platet, N., Breuillaud, L., Lunardi, J., Berger, F., Wion, D., 2006. Undetectable levels of N6-methyl adenine in mouse DNA: Cloning and analysis of PRED28, a gene coding for a putative mammalian DNA adenine methyltransferase. *FEBS Lett.* 580, 3179–3184. <https://doi.org/10.1016/j.febslet.2006.04.074>
- Reichard, J.F., Schneckeburger, M., Alvaro, P., 2007. Long term low-dose arsenic exposure induces loss of DNA methylation. *Biochem. Biophys. Res. Commun.* 352, 188–192. <https://doi.org/10.1016/j.bbrc.2006.11.001>
- Risner, C.H., 1988. The Determination of Benzo[a]pyrene in the Total Particulate Matter of Cigarette Smoke. *J. Chromatogr. Sci.* 26, 113–120. <https://doi.org/10.1093/chromsci/26.3.113>
- Rosefort, C., Fauth, E., Zankl, H., 2004. Mironuclei induced by aneugens and clastogens in mononucleate and binucleate cells using the cytokinesis block assay. *Mutagenesis.* 19, 277–284. <https://doi.org/10.1093/mutage/geh028>
- Rossner, P., Strapacova, S., Stolcpartova, J., Schmuczerova, J., Milcova, A., Neca, J., Vlkova, V., Brzicova, T., Machala, M., Topinka, J., 2016. Toxic effects of the major components of diesel exhaust in human alveolar basal epithelial cells (A549). *Int. J. Mol. Sci.* 17, 1393. <https://doi.org/10.3390/ijms17091393>
- Rudd, C.J., Stromt, K.A., 1981. A spectrophotometric method for the quantitation of Diesel Exhaust Particles in Guinea Pig Lung. *J. Appl. Toxicol.* 1, 83–87. <https://doi.org/10.1002/jat.2550010207>
- Rynning, I., Neca, J., Vrbova, K., Libalova, H., Rossner, P., Holme, J.A., Gützkow, K.B., Afanou, A.K.J., Arnoldussen, Y.J., Hrubá, E., Skare, Ø., Haugen, A., Topinka, J., Machala, M., Møllerup, S., 2018. In vitro transformation of human bronchial epithelial cells by diesel exhaust particles: gene expression profiling and early toxic responses. *Toxicol. Sci.* 166, 51–64. <https://doi.org/10.1093/toxsci/kfy183>
- Sanchez-Guerra, M., Zheng, Y., Osorio-Yanez, C., Zhong, J., Chervona, Y., Wang, S., Chang, D., McCracken, J.P., Díaz, A., Bertazzi, P.A., Koutrakis, P., Kang, C.M., Zhang, X., Zhang, W., Byun, H.M., Schwartz, J., Hou, L., Baccarelli, A.A., 2015. Effects of particulate matter exposure on blood 5-hydroxymethylation: Results from the Beijing truck driver air pollution study. *Epigenetics.* 10, 633–642. <https://doi.org/10.1080/15592294.2015.1050174>
- Schins, R.P.F., Knaapen, A.M., 2007. Genotoxicity of poorly soluble particles. *Inhal. Toxicol.* 19, 189–198. <https://doi.org/10.1080/08958370701496202>
- Sevastyanova, O., Novakova, Z., Hanzalova, K., Binkova, B., Sram, R.J., Topinka, J., 2008. Temporal variation in the genotoxic potential of urban air particulate matter. *Mutat. Res. - Genet. Toxicol. Environ. Mutagen.* 649, 179–186. <https://doi.org/10.1016/j.mrgentox.2007.09.010>
- Shang, Y., Zhou, Q., Wang, T., Jiang, Y., Zhong, Y., Qian, G., Zhu, T., Qiu, X., An, J., 2017. Airborne nitro-PAHs induce Nrf2/ARE defense system against oxidative stress and promote inflammatory process by activating PI3K/Akt pathway in A549 cells. *Toxicol. Vitro.* 44, 66–73. <https://doi.org/10.1016/j.tiv.2017.06.017>
- Sharma, S.K., Mandal, T.K., Sharma, A., Jain, S., Saraswati, Y., 2018. Carbonaceous Species of PM2.5 in Megacity Delhi, India During 2012–2016. *Bull. Environ. Contami. Toxicol.* 100, 695–701. <https://doi.org/10.1007/s00128-018-2313-9>
- Shi, X.C., Keane, M.J., Ong, T.M., Harrison, J.C., Slaven, J.E., Bugarski, A.D., Gautam, M., Wallace, W.E., 2009. Diesel exhaust particulate material expression of in vitro genotoxic activities when

dispersed into a phospholipid component of lung surfactant. *J. Phys. Conf. Ser.* 151, 012021. <https://doi.org/10.1088/1742-6596/151/1/012021>

Steenhof, M., Gosens, I., Strak, M., Godri, K.J., Hoek, G., Cassee, F.R., Mudway, I.S., Kelly, F.J., Harrison, R.M., Lebret, E., Brunekreef, B., Janssen, N.A.H., Pieters, R.H.H., 2011. In vitro toxicity of particulate matter (PM) collected at different sites in the Netherlands is associated with PM composition, size fraction and oxidative potential - the RAPTES project. *Part. Fibre Toxicol.* 8, 1–15. <https://doi.org/10.1186/1743-8977-8-26>

Strober, W., 2015. Trypan Blue Exclusion Test of Cell Viability. *Curr. Protoc. Immunol.* 111, A3.B.1-A3.B.3. <https://doi.org/10.1002/0471142735.ima03bs111>

Sukapan, P., Promnarate P., Avihingsanon, Y., Mutirangura, A., Hirankarn, N., 2014. Types of DNA methylation status of the interspersed repetitive sequences for LINE-1, Alu, HERV-E and HERV-K in the neutrophils from systemic lupus erythematosus patients and healthy controls. *J Hum Genet.* 59, 178–188. <https://doi.org/10.1038/jhg.2013.140>.

Sun, Q., Huang, S., Wang, X., Zhu, Y., Chen, Z., Chen, D., 2015a. N6-methyladenine functions as a potential epigenetic mark in eukaryotes. *Bioessays.* 37, 1155–1162. <https://doi.org/10.1002/bies.201500076>

Sun, X., Zhang, L., Zhang, H., Qian, H., Ji, J., Tang, L., Li, Z., Zhang, G., 2015b. Electrochemical detection of 8-hydroxy-2'-deoxyguanosine as a biomarker for oxidative DNA damage in HEK293 cells exposed to 3-chloro-1,2-propanediol. *Anal. Methods.* 7, 6664–6671. <https://doi.org/10.1039/c5ay01246e>

Takiguchi, M., Achanzar, W.E., Qu, W., Li, G., Waalkes, M.P., 2003. Effects of cadmium on DNA-(Cytosine-5) methyltransferase activity and DNA methylation status during cadmium-induced cellular transformation. *Exp. Cell Res.* 286, 355–365. [https://doi.org/10.1016/S0014-4827\(03\)00062-4](https://doi.org/10.1016/S0014-4827(03)00062-4)

Tang, Y., Zheng, S.J., Qi, C.B., Feng, Y.Q., Yuan, B.F., 2015. Sensitive and Simultaneous Determination of 5-Methylcytosine and Its Oxidation Products in Genomic DNA by Chemical Derivatization Coupled with Liquid Chromatography-Tandem Mass Spectrometry Analysis. *Anal. Chem.* 87, 3445–3452. <https://doi.org/10.1021/ac504786r>

Tian, Y., Lin, A., Gan, M., Wang, H., Yu, D., Lai, C., Zhang, D., Zhu, Y., Lai, M., 2017. Global changes of 5-hydroxymethylcytosine and 5-methylcytosine from normal to tumor tissues are associated with carcinogenesis and prognosis in colorectal cancer. *J. Zhejiang Univ. B.* 18, 747–756. <https://doi.org/10.1631/jzus.B1600314>

Topinka, J., Schwarz, L.R., Wiebel, F.J., Černá, M., Wolff, T., 2000. Genotoxicity of urban air pollutants in the Czech Republic: Part II. DNA adduct formation in mammalian cells by extractable organic matter. *Mutat. Res. - Genet. Toxicol. Environ. Mutagen.* 469, 83–93. [https://doi.org/10.1016/S1383-5718\(00\)00061-9](https://doi.org/10.1016/S1383-5718(00)00061-9)

Torres, A.L., Barrientos, E.Y., Katarzyna, W., Wrobel, K., 2011. Selective derivatization of cytosine and methylcytosine moieties with 2-bromoacetophenone for submicrogram DNA methylation analysis by reversed phase HPLC with spectrofluorimetric detection. *Anal. Chem.* 83, 7999–8005. <https://doi.org/10.1021/ac2020799>

Turk, P.W., Laayoun, A., Smith, S.S., Weitzman, S.A., 1995. DNA adduct 8-hydroxyl-2'-deoxyguanosine (8-hydroxyguanine) affects function of human DNA methyltransferase. *Carcinogenesis.* 16, 1253–1255. <https://doi.org/10.1093/carcin/16.5.1253>

Valavanidis, A., Fiotakis, K., Vlachogianni, T., 2008. Airborne particulate matter and human health: Toxicological assessment and importance of size and composition of particles for oxidative damage and carcinogenic mechanisms. *J. Environ. Sci. Heal. - Part C Environ. Carcinog. Ecotoxicol. Rev.* 26, 339–

362. <https://doi.org/10.1080/10590500802494538>

Vidrio, E., Jung, H., Anastasio, C., 2008. Generation of hydroxyl radicals from dissolved transition metals in surrogate lung fluid solutions. *Atmos. Environ.* 42, 4369–4379. <https://doi.org/10.1016/j.atmosenv.2008.01.004>

Wagner, J.R., Cadet, J., 2010. Oxidation reactions of cytosine DNA components by hydroxyl radical and one-electron oxidants in aerated aqueous solutions. *Acc. Chem. Res.* 43, 564–571. <https://doi.org/10.1021/ar9002637>

Wang, J., Tang, J., Lai, M., Zhang, H., 2014. 5-Hydroxymethylcytosine and disease. *Mutat. Res. Mutat. Res.* 762, 167–175. <https://doi.org/10.1016/j.mrrev.2014.09.003>

Wang, K., Wang, W., Li, L., Li, J., Wei, L., Chi, W., Hong, L., Zhao, Q., Jiang, J., 2020. Seasonal concentration distribution of PM<sub>1.0</sub> and PM<sub>2.5</sub> and a risk assessment of bound trace metals in Harbin, China: Effect of the species distribution of heavy metals and heat supply. *Sci. Rep.* 10, 1–11. <https://doi.org/10.1038/s41598-020-65187-7>

Wang, S., Ye, J., Soong, R., Wu, B., Yu, L., Simpson, A.J., Chan, A.W.H., 2018. Relationship between chemical composition and oxidative potential of secondary organic aerosol from polycyclic aromatic hydrocarbons. *Atmos. Chem. Phys.* 18, 3987–4003. <https://doi.org/10.5194/acp-18-3987-2018>

Wei, H., Feng, Y., Liang, F., Cheng, W., Wu, X., Zhou, R., Wang, Y., 2017. Role of oxidative stress and DNA hydroxymethylation in the neurotoxicity of fine particulate matter. *Toxicology.* 380, 94–103. <https://doi.org/10.1016/j.tox.2017.01.017>

Wilson, A.S., Power, B.E., Molloy, P.L., 2007. DNA hypomethylation and human diseases. *Biochim. Biophys. Acta.* 1775, 138–162. <https://doi.org/10.1016/j.bbcan.2006.08.007>

Winterbourn, C.C., 1995. Toxicity of iron and hydrogen peroxide: the Fenton reaction. *Toxicol. Lett.* 82–83, 969–974. [https://doi.org/10.1016/0378-4274\(95\)03532-x](https://doi.org/10.1016/0378-4274(95)03532-x)

Wu, X., Lintelmann, J., Klingbeil, S., Li, J., Wang, H., Kuhn, E., Ritter, S., Zimmermann, R., 2017. Determination of air pollution-related biomarkers of exposure in urine of travellers between Germany and China using liquid chromatographic and liquid chromatographic-mass spectrometric methods: a pilot study. *Biomarkers.* 22, 525–536. <https://doi.org/10.1080/1354750X.2017.1306753>

Xiong, J., Liu, X., Cheng, Q.Y., Xiao, S., Xia, L.X., Yuan, B.F., Feng, Y.Q., 2017. Heavy Metals Induce Decline of Derivatives of 5-Methylcytosine in Both DNA and RNA of Stem Cells. *ACS Chem. Biol.* 12, 1636–1643. <https://doi.org/10.1021/acscchembio.7b00170>

Yao, B., Cheng, Y., Wang, Z., Li, Y., Chen, L., Huang, L., Zhang, W., Chen, D., Wu, H., Tang, B., Jin, P., 2017. DNA N<sup>6</sup>-methyladenine is dynamically regulated in the mouse brain following environmental stress. *Nat. Commun.* 8, 1122. <https://doi.org/10.1038/s41467-017-01195-y>

Yauk, C., Polyzos, A., Rowan-Carroll, A., Somers, C.M., Godschalk, R.W., Van Schooten, F.J., Berndt, M.L., Pogribny, I.P., Koturbash, I., Williams, A., Douglas, G.R., Kovalchuk, O., 2008. Germ-line mutations, DNA damage, and global hypermethylation in mice exposed to particulate air pollution in an urban/industrial location. *Proc. Natl. Acad. Sci. U. S. A.* 105, 605–610. <https://doi.org/10.1073/pnas.0705896105>

Zhang, L., Jin, Y., Huang, M., Penning, T.M., 2012. The role of human aldo-keto reductases in the metabolic activation and detoxication of polycyclic aromatic hydrocarbons: Interconversion of PAH catechols and PAH o-quinones. *Front. Pharmacol.* 3, 193. <https://doi.org/10.3389/fphar.2012.00193>

Zhang, M.Y., Pace, N., Kerns, E.H., Kleintop, T., Kagan, N., Sakuma, T., 2005. Hybrid triple quadrupole-linear ion trap mass spectrometry in fragmentation mechanism studies: Application to structure elucidation of buspirone and one of its metabolites. *J. Mass Spectrom.* 40, 1017–1029.

---

<https://doi.org/10.1002/jms.876>

Zhang, Q., Liang, Z., Cui, X., Ji, C., Li, Y., Zhang, P., Liu, J., Riaz, A., Yao, P., Liu, M., Wang, Y., Lu, T., Yu, H., Yang, D., Zheng, H., Gu, X., 2018. N<sup>6</sup>-Methyladenine DNA Methylation in Japonica and Indica Rice Genomes and Its Association with Gene Expression, Plant Development, and Stress Responses. *Mol. Plant.* 11, 1492–1508. <https://doi.org/10.1016/j.molp.2018.11.005>

Zhao, C.Q., Young, M.R., Diwan, B.A., Coogan, T.P., Waalkes, M.P., 1997. Association of arsenic-induced malignant transformation with DNA hypomethylation and aberrant gene expression. *Proc. Natl. Acad. Sci. U. S. A.* 94, 10907–10912. <https://doi.org/10.1073/pnas.94.20.10907>

Zhao, H., Barger, M.W., Ma, J.K.H., Castranova, V., Ma, J.Y.C., 2006. Cooperation of the inducible nitric oxide synthase and cytochrome P450 1A1 in mediating lung inflammation and mutagenicity induced by diesel exhaust particles. *Environ. Health Perspect.* 114, 1253–1258. <https://doi.org/10.1289/ehp.9063>

## 6 Appendix

### 6.1 List of abbreviations

3-MCPD	3-chloro-1,2-propanediol
5caC	5-carboxycytosine
5-carboxycytosine	5-formylcytosine
5hmC	5-hydroxymethylcytosine
5mC	5-methylcytosine
5fC	5-formylcytosine
5-azadC	5-aza-2'-deoxycytidine
5-fodC	5-formyl-2'-deoxycytidine
5-hmdC	5-hydroxymethyl-2'-deoxycytidine
5-mdC	5-methyl-2'-deoxycytidine
6mA	N6-methyladenine
8-OHdG	8-hydroxy-2'-deoxyguanosine
ACN	acetonitrile
Ade	adenine
Alu	arthrobacter luteus
BAN	2-bromo-2'-acetonaphthone
B[a]P	benzo[a]pyrene
BER	base excision repair
BN	binucleated cells
BPAP	2-bromo-4'-phenylacetophenone
CBMN Cyt assay	cytokinesis-block micronucleus cytome assay
CBPI	cytokinesis-block proliferation index
CEM	channel electron multiplier
CpG	5'-C-phosphate-G-3'
CYPs	cytochromes P450
CYP1A1	cytochrome P450 family 1 subfamily A polypeptide 1
Cyt	cytosine
CZ100	fine dust ERM-CZ100
DAMTs	DNA N6 adenine methyltransferases
dC	2'-deoxycytidine
dG	2'-deoxyguanosine
diesel PM 2975	diesel PM SRM2975
DMSO	dimethyl sulfoxide
DNMTs	DNA methyltransferases
DNPH	2,4-dinitrophenylhydrazine
EMS	ethyl methanesulfonate
ERM-CZ100	European reference material-CZ100
ESI	electrospray ionization

---

EU	European Union
FBS	fetal bovine serum
Gua	guanine
HNE	4-hydroxynoneal
IARC	International Agency for Research on Cancer
ICP-MS	inductively coupled plasma mass spectrometry
Kd	partition coefficient
LC	liquid chromatography
LC-MS/MS	liquid chromatography tandem mass spectrometry
LC-UV	liquid chromatography ultraviolet/visual
LINE-1	long interspersed element-1
LIT	linear ion trap
LLE	liquid-liquid extraction
LOD	limit of detection
MDA	malondialdehyde
MEF	mutagenic equivalency factor
MEQ	mutagenic equivalent
MI	mitotic index
MN	micronuclei
MONO	mononucleated cells
MRM	multiple reaction monitoring
NADPH	dihydronicotinamide adenine dinucleotide phosphate
NBUD	nuclear bud
NPB	nucleoplasmic bridge
PAHs	polycyclic aromatic hydrocarbons
PBS	phosphate buffered saline
PM	particulate matter
ROS	reactive oxygen species
RPMI	Roswell Park Memorial Institute
SAM	S-adenosylmethionine
SEM	standard error of mean
SPE	solid phase extraction
SRM2975	Standard reference material 2975
TBHP	tert-butyl hydroperoxide
TEA	triethylamine
TEF	toxic equivalency factor
TEQ	Toxic equivalent
TET	ten-eleven translocation
Thy	thymine
UD 1649	urban dust SRM1649

## 6.2 List of figures

**Figure 1.1:** Annual PM<sub>2.5</sub> concentrations in different cities (2008-2020). New Delhi data in 2011 from a report (Mandal et al., 2014) and in 2012-2016 from a report (Sharma et al., 2018) and in 2017-2020 from <https://www.airnow.gov>; Beijing data from <http://www.stateair.net> (2008-2017) and <https://www.airnow.gov> (2018-2020); Hanoi data from <https://www.airnow.gov>; Lima data from <https://www.airnow.gov>; Singapore data from <https://smartairfilters.com/en>; Munich data from <https://www.lfu.bayern.de/index.htm>

**Figure 1.2:** Illustration of possible genotoxicity induced by PM. (ROS, reactive oxygen species; HNE, 4-hydroxynoneal; MDA, malondialdehyde; B[a]P, benzo[a]pyrene)

**Figure 1.3:** (a) Epigenetic cytosine modifications; (b) epigenetic adenine modification. (Cyt, cytosine; 5mC, 5-methylcytosine; 5hmC, 5-hydroxymethylcytosine; 5fC, 5-formylcytosine; 5-caC, 5-carboxycytosine; DNMTs, DNA methyltransferases; TETs, tel-eleven translocations; BER, base excision repair; Ade, adenine, 6mA, N6-methyladenine; DAMTs, DNA N6 adenine methyltransferases)

**Figure 2.1:** Three different reference PM.

**Figure 2.2:** (a) The difference between an alive cell and a dead cell stained by trypan blue; (b) Counting cells by using a hemacytometer.

**Figure 2.3:** Illustration of the work mechanism of a photometer.

**Figure 2.4:** Illustration of the work mechanism of a solid-phase extraction.

**Figure 2.5:** Illustration of the work mechanism of a liquid-liquid extraction.

**Figure 2.6:** Illustration of the chemical derivatization for (a) MDA; (b) cytosine modifications; (c) adenine modifications (the quantification was based on the major adduct).

**Figure 2.7:** Illustration of chemical derivatization for (a) d2-MDA; (b) 5-mdC; (c) Ade and 6mA.

**Figure 2.8:** Illustration of the work mechanism of a liquid chromatography and its complementary connection with a UV detector or mass spectrometry.

**Figure 2.9:** Illustration of the work mechanism of a column.

**Figure 2.10:** Figure 2.10: Illustration of the stationary phase for (a) C18; (b) F5 ;(c) Eurospher HILIC.

**Figure 2.11:** Illustration of the basic components of mass spectrometry.

**Figure 2.12:** Illustration of the mechanism of the electrospray ionization.

**Figure 2.13:** Illustration of the work mechanism of multiple reaction monitoring.

**Figure 2.14:** Typical precursor ions and fragment ions from (a) 8-OHdG; (b) 5-hmdC-BPAP; (c) 6m-Ade-BPAP analyzed in MRM positive mode.

**Figure 2.15:** Illustration of a channel electron multiplier.

**Figure 2.16:** Illustration of the work mechanism of an inductively coupled plasma torch.

**Figure 2.17:** Illustration of the work mechanism of an octopole reaction cell and a quadrupole mass analyzer.

**Figure 2.18:** Illustration of cytokinesis-block micronucleus cytome assay duration.

**Figure 2.19:** Illustration of cytokinesis-block micronucleus cytome assay procedures.

**Figure 3.1:** Cell viability of THP-1 and A549 cells after 24 hours exposure to (a) CZ100; (b) UD 1649; (c) diesel PM 2975; (d) menadione; (e) 3-MCPD. (mean  $\pm$  standard error of mean, n=3)

**Figure 3.2:** (a) 8-OHdG in THP-1 cells; (b) 8-OHdG in A549 cells; (c) MDA in THP-1 cells; (d) MDA in A549 cells. (exposed to 200  $\mu$ g/mL of CZ100 or UD 1649, or 40  $\mu$ g/mL of diesel PM 2975, or 2

µg/mL of menadione or 3-MCPD) mean ± standard error of mean, n=3. Analysis of variance was used, \*= p-value < 0.05, \*\*= p-value < 0.01, \*\*\*= p-value < 0.001.

**Figure 3.3:** Typical microscope graphic of THP-1 cells (a) mononucleated, binucleated and polynucleated cells; (b) a mitotic cell; (c) an apoptotic cell; (d) a necrotic cell; (e) a micronucleus in a mononucleated cell; (f) a micronucleus in a binucleated cell; (g) a nucleoplasmic bridge in a binucleated cell; (h) a nuclear bud in a binucleated cell.

**Figure 3.4:** (a) cytokinesis-block proliferation index (CBPI); (b) mitotic%; (c) apoptotic%; (d) necrotic%; (e) MN in MONO; (f) MN in BN; (g) NPB in BN; (h) NBUD in BN. Exposed to 200 µg/mL of CZ100 or UD 1649, or 40 µg/mL of diesel PM 2975, 2 µg/mL of menadione or 3-MCPD, mean ± standard error of mean, n=3. Solvent control = 0.2% DMSO, positive control = 300 µg/mL of ethyl-methanesulfonate (EMS). Analysis of variance was used, \*, p < 0.05; \*\*, p < 0.01; \*\*\*, p < 0.001.

**Figure 3.5:** Pearson correlation coefficients between the 8-OHdG persistency and MN MONO, MN BN, NPB, and NBUD results in A549 cells exposed to (a) CZ100; (b) diesel PM 2975; (c) menadione; (d) 3-MCPD as well as in THP-1 cells exposed to (e) CZ100; (f) diesel PM 2975; (g) menadione; (h) 3-MCPD. \*, p < 0.05; \*\*, p < 0.01.

**Figure 3.6:** (a) cytosine methylation; (b) cytosine hydroxymethylation; (c) adenine methylation; (d,e) two-dimensional scatters between different epigenetic modifications. Exposed to 200 µg/mL of CZ100 or UD 1649, or 40 µg/mL of diesel PM 2975. (mean ± standard error of mean, n=6). 5-azadC = 2.3 µg/mL of 5-aza-2'-deoxycytidine used as positive control for cytosine methylation. TBHP = 9 µg/mL of tert-butyl hydroperoxide used as positive control for cytosine hydroxymethylation. Analysis of variance was used, \*, p-value < 0.05, \*\*= p-value < 0.01, \*\*\*= p-value < 0.001.

**Figure 3.7:** Illustration of possible mechanisms for cytosine modification exposed to particulate matter.



### 6.3 List of tables

**Table 2.1:** Derivative reagents used for cytosine and its modifications.

**Table 2.2:** Toxic equivalency factor (No. 1-17 from Nisbet and Lagoy, 1992; No. 18-33 from Delistraty, 1997) and mutagenic equivalency factor (Durant et al., 1996) for PAHs and their derivatives.

**Table 3.1:** Concentrations of PAHs in PM<sub>2.5</sub> and the calculated TEQ and MEQ of PM<sub>2.5</sub>.

**Table 3.2:** Concentrations of PAHs in PM<sub>10</sub> and the calculated TEQ and MEQ of PM<sub>10</sub>.

**Table 3.3:** Particle deposition values for A549 cells exposed to different PM (mean  $\pm$  standard error of mean, n=3)

**Table 3.4:** The 8-OHdG persistency in A549 and THP-1 cells.

**Table 3.5:** The comparison about retention time and limit of detection (LOD) of target analytes with and without chemical derivatization (n.d., not detected).

**Table 3.6:** Metal elements for PM, information from certificates (CZ100 and UD1649) or from literature (diesel PM2975, Ball et al., 2000), or from the ICP-MS analysis. (superscript a means from certificates; superscript b means from a literature; \* means from ICP-MS)

## 6.4 List of publications

### 6.4.1 Publication 1

**Title:** Analysis of PAHs Associated with PM10 and PM2.5 from Different Districts in Nanjing.

**Authors:** Xiansheng Liu, Jürgen Schnelle-Kreis, Brigitte Schlöter-Hai, Lili Ma, Pengfei Tai, Xin Cao, Cencen Yu, Thomas Adam, Ralf Zimmermann.

**Journal:** Aerosol and Air Quality Research, 19: 2294–2307

**Year:** 2019

<p><b>Contributions:</b> For this publication, Xin Cao helped to make data process and revised the manuscript.</p>
--



## Analysis of PAHs Associated with PM<sub>10</sub> and PM<sub>2.5</sub> from Different Districts in Nanjing

Xiansheng Liu<sup>1,2,3</sup>, Jürgen Schnelle-Kreis<sup>2</sup>, Brigitte Schlöter-Hai<sup>2</sup>, Lili Ma<sup>1\*</sup>, Pengfei Tai<sup>4</sup>, Xin Cao<sup>2,3</sup>, Cencen Yu<sup>1</sup>, Thomas Adam<sup>2,5</sup>, Ralf Zimmermann<sup>2,3</sup>

<sup>1</sup> School of Environment, Nanjing Normal University, Nanjing 210023, China

<sup>2</sup> Joint Mass Spectrometry Center, Cooperation Group Comprehensive Molecular Analytics, Helmholtz Zentrum München, Neuherberg 85764, Germany

<sup>3</sup> Joint Mass Spectrometry Center, Chair of Analytical Chemistry, University of Rostock, Rostock 18059, Germany

<sup>4</sup> Geomatics College, Shandong University of Science and Technology, Shandong, Qingdao 266590, China

<sup>5</sup> Bundeswehr University Munich, Neubiberg 85577, Germany

### ABSTRACT

Nanjing has areas with different degrees of pollution and is therefore predestined for the analysis of particle phase polycyclic aromatic hydrocarbons (P-PAHs) in different functional areas and their correlation with the latter. The functional sites include a background area (BGA), an industrial area (IDA), a traffic area (TFA), a business area (BNA) and a residential area (RDA), where parameters such as PAH composition, content, carcinogenic and mutagenic potencies were analyzed. The results revealed increasing P-PAH contents (PM<sub>2.5</sub>, PM<sub>10</sub>) in the following order: BGA (14.02 ng m<sup>-3</sup>, 38.45 ng m<sup>-3</sup>) < BNA (16.33 ng m<sup>-3</sup>, 44.13 ng m<sup>-3</sup>) < TFA (17.13 ng m<sup>-3</sup>, 48.31 ng m<sup>-3</sup>) < RDA (21.11 ng m<sup>-3</sup>, 61.03 ng m<sup>-3</sup>) < IDA (50.00 ng m<sup>-3</sup>, 93.08 ng m<sup>-3</sup>). Thereby, the P-PAH content in the industrial area was significantly higher than in the other functional zones ( $P < 0.01$ ). Furthermore, the gas phase PAH concentrations were also estimated by the G/P partitioning model and the total PAH toxicity was assessed applying toxicity equivalent factors ( $\Sigma$ BaP<sub>TEF</sub>) and mutagenicity equivalent factors ( $\Sigma$ BaPM<sub>EF</sub>). Finally, the incremental lifetime cancer risk (ILCR) value of children and adolescents in Nanjing was higher than that of adults.

**Keywords:** Particle phase PAHs; Different functional areas; Toxicity assessment; Incremental lifetime cancer risk.

### INTRODUCTION

It is well-known, that the primary particles are emitted directly as liquids or solids from sources such as biomass burning, incomplete combustion of fossil fuels, volcanic eruptions, and wind-driven or traffic-related suspension of road, soil, and mineral dust, sea salt, and biological materials (Abdel-Shafy *et al.*, 2016; Du *et al.*, 2017). Ambient particulate matter (PM) is a growing concern worldwide due to its associations between elevated concentrations and increased incidences of cardiopulmonary disease (Ning *et al.*, 2010), including chronic obstructive pulmonary disease (Zhang *et al.*, 2017). According to the Global Burden of Disease study, fine particulate matter (PM<sub>2.5</sub>) is the seventh largest important death risk factor in the world and the fourth largest important death risk factor in China (Cohen *et al.*, 2005; Lim *et al.*,

2012).

Many studies suggest that organic carbon constituents may play a significant role in PM-induced health effects (Li *et al.*, 2003). Recently, polycyclic aromatic hydrocarbons (PAHs) have brought great environmental concerns as they are ubiquitous in the ambient air and the presence of PAH directly affects humans, especially to vulnerable groups such as the elderly and children (Brook *et al.*, 2010; Beelen *et al.*, 2014; Wang *et al.*, 2017a; Wright *et al.*, 2018). In addition, some PAH-compounds, such as benzo[a]pyrene and benz[a]anthracene, are well known carcinogens (Nisbet *et al.*, 1992; Goldstein, 2001; Li *et al.*, 2009). So it is important to investigate the PAHs in the atmosphere and reduce human exposure to these toxic chemicals.

EPA Carcinogenicity Risk Assessment Endeavor Work Group has verified the carcinogenicity classifications in 1994 (U.S. EPA, 1994), indicating that BaA, BbF, BkF, BaP, Chr, DahA and IcdP are considered to be probable human carcinogens. It has been found that the PAHs are carcinogenic and that BaP is the most serious (Garban *et al.*, 2002) among the listed carcinogens. Moreover, some special PAHs are mutagenic (Durant *et al.*, 1996) associated with

\*Corresponding author.

Tel.: +49 15237060510

E-mail address: malifeng19830615@126.com

some health effects, i.e., pulmonary diseases (DeMarini *et al.*, 2004). Many studies have attempted to estimate the carcinogenic potency of PAHs using BaP equivalent concentration, but less attention was given to mutagenicity. Therefore, in the studies, mutagenicity should be given similar attention when attempting to estimate the carcinogenic potency of PAHs.

In recent decades, with the rapid increase in energy consumption, public health has been a matter of great concern to scientists and policy makers in China. The PAHs occur in the atmosphere as complex mixtures of congeners with different molecular weights: Lighter PAHs (2–3 aromatic rings) are almost exclusively present in the vapor phase, whereas PAHs with higher molecular weights ( $\geq 4$  rings) are almost completely adsorbed to the particulate matter (Cheruiyot *et al.*, 2015; Manoli *et al.*, 2016). Meanwhile, the carcinogenic contributions of particle phase PAHs is much higher than those of gas phase PAHs. The current research focuses mainly on particulate matter. Nevertheless, in order to take the concentration of PAHs fully into account, this study estimated the concentration of PAHs in the gas phase by using the gas/particle partitioning model (Xie *et al.*, 2013; Gao *et al.*, 2015) and focused primarily on the higher molecular weight PAHs (4–6 rings). Due to the fact that the atmospheric pollution is a persistent problem in Nanjing (Wang *et al.*, 2006), numerous studies were conducted in the Nanjing area, such as sources of PAHs in the atmosphere, analysis of concentration distribution of particulate matter, meteorological factors and the seasonal trends of indoor fine particulate matter (Wang *et al.*, 2006; He *et al.*, 2014; Shao *et al.*, 2017; Wang *et al.*, 2017b). However, very few studies have considered the different functional areas (Jiang *et al.*, 2018; Simayi *et al.*, 2018) and the distribution characteristics of PAHs in the atmospheric particulate matter for a comprehensive comparison and analysis, one example for PAHs is the study of Manoli *et al.* (2016), who compared the PAH levels between traffic and urban background. Another purpose of the study was to support future epidemiology and health impact research. Therefore, the carcinogenic and mutagenic potencies were assessed as well to estimate their potential impact on human health. In addition, a lifetime lung cancer risk assessment in relation to different groups was carried out.

## EXPERIMENTAL

### Sampling Area and Site Description

The sampling sites were located in Nanjing in eastern China in the heartland of the drainage area of the lower reaches of the Yangtze River, with longitudes and latitudes of 118°22′–119°14′ and 31°14′–32°36′, respectively. Its area is 4,736 km<sup>2</sup> with 140 km in length (west–east direction) and 80 km in width (north–south direction). The mean annual temperature and precipitation are 15.7 °C and 1106.5 mm, respectively (Xu *et al.*, 2007). The four seasons are distinct, with damp conditions throughout the year, very hot and muggy summers, cold and damp winters, and in between, spring and autumn are of reasonable length. A detailed description of the sampling areas is listed in Table 1.

### Sampling Collection

Sampling was carried out in Nanjing at five sites during 47 days. High volume air samplers (KC-1000, flow rate 1.05 m<sup>3</sup> min<sup>-1</sup>) with glass fiber filters (GFF) were used to collect particle phase PAHs in PM<sub>10</sub> and PM<sub>2.5</sub>, respectively. All filters have been baked at 450°C for 4 h in a muffle furnace (MF-2.5-10A, Shanghai) and stabilized for 24 h under constant temperature (21°C) using a dryer. Samples were collected in triplicate every 24 h. All filters were weighed before and after sampling and finally stored at -1°C until analysis.

### Analytical Procedure

For the PAH analysis, brown glass tubes were cleaned three times with tap water and ethyl alcohol prior to use. Impurities were removed with a clean brush used only for this study. Each filter was cut into small pieces and extracted by Soxhlet with 200 mL dichloromethane at 46°C for 16 h. Rotary evaporator (R-201, Shanghai, China) was adopted to purify the concentrated solution with water at 37°C. In order to reduce the loss, the extraction was concentrated altogether three times with dichloromethane in a flat bottom flask. The total extracts were subsequently transferred to alumina silica gel columns for purification, consisting of 3 cm alumina, 6 cm silica gel and 1 cm anhydrous sodium sulfate. Prior to purification, the alumina silica gel column has been washed for two times using a 20 mL 1:1 mixture of n-hexane and acetone. After the sample transfer, the bottom flasks have

**Table 1.** Characteristic of the sampling sites in Nanjing.

Functional area	Sampling site	Regional characteristics
Background area (BGA)	Nanjing Sport Institute 32°2′36.72″N; 118°52′1.04″E	Scenic tourist area; few vehicles; many trees
Residential area (RDA)	Ruijin Country of Nanjing 32°1′54.55″N; 118°48′44.34″E	Densely populated; many vehicles; city center
Business area (BNA)	Nanjing Institute of Aerospace Management 32°1′11.72″N; 118°47′10.96″E	Commercial network intensive area; large flow of people
Traffic area (TFA)	Nanjing Normal University of Suiyuan Campus 32°3′12.55″N; 118°45′58.94″E	city center, many vehicles, convenient transportation
Industrial area (IDA)	Nanjing Yangzi Vocational Training Co. Ltd. 32°14′35.76″N; 118°45′46.83″E	Chemical plant gathering area



been cleaned three times with dichloromethane. The eluted mixture from the column was brought to approximately 1 mL by rotary evaporator at 37°C. Finally, they were diluted with n-hexane to exactly 1 mL, sealed in vials and stored at -18°C before PAH analysis.

#### Determination of PAHs

PAH levels were determined by GC/MS according to previous studies (Xia *et al.*, 2013; Wu *et al.*, 2014) using the Agilent 7890A/5975MSD (Agilent, USA) with a J&W Scientific column DB-5MS (30 m × 0.25 mm ID × 0.25 μm film, Agilent, USA). The GC was running under following conditions: 1 min at 40°C, heated from 40°C to 200°C at a rate of 10°C min<sup>-1</sup> and heated from 200°C to 310°C at 5°C min<sup>-1</sup>, then held at 310°C for 5 min. The sample was injected on a splitless mode at the injector temperature of 280°C. The EI-MS conditions were as follows: ion-source temperature, 230°C; ionizing voltage, 70 eV; scan range, m/z 40–350 amu; cycle time, 0.5 s. 10 PAHs were determined listed by the IARC as class 1, class 2A, 2B and class 3 (fluoranthene, pyrene, benz[a]anthracene, chrysene, benzo[b]fluoranthene, benzo[k]fluoranthene, benzo[a]pyrene, benzo[g,h,i]perylene, indeno[1,2,3-cd]pyrene and dibenz[a,h]anthracene), mainly associated to the particle-phase.

#### Prediction of Gas-phase PAH Concentrations

The semi-volatile organic compounds of PAHs encounter gas-particle phase distribution when transported in the atmosphere. In order to fully understand the concentration of PAHs in Nanjing, the concentration of PAHs in the gas phase was calculated by the gas/particle (G/P) partitioning theory (Pankow, 1994a, b). The theory was described in detail elsewhere (Xie *et al.*, 2013; Gao *et al.*, 2015; Xie *et al.*, 2015), which was defined as follows:

$$K_{p,OM} = \frac{K_p}{f_{OM}} = \frac{F/M_{OM}}{A} \quad (1)$$

$$K_{p,OM} = \frac{RT}{10^6 \overline{MW}_{OM} \xi_{OM} P_L^0} \quad (2)$$

$$A = \frac{10^6 \overline{MW}_{OM} \xi_{OM} P_L^0 F}{RT} \times \frac{1}{M_{OM}} \quad (3)$$

where  $K_{p,OM}$  represents the absorptive G/P partitioning coefficient of each PAH.  $K_p$  is the G/P partitioning coefficient and  $f_{OM}$  is the weight fraction of the absorptive OM phase in the total PM phase.  $F$  and  $A$  are a concentration of each PAH in the particle phase (ng m<sup>-3</sup>) and a concentration of each PAH in the gas phase (ng m<sup>-3</sup>).  $\overline{MW}_{OM}$  and  $\overline{MW}_{OM}$  are the concentrations of the particle-phase OM (μg m<sup>-3</sup>) and the average molecular weight (MW) of the absorbing OM phase (g mol<sup>-1</sup>). Referring to Xie *et al.*, (2013),  $\overline{MW}_{OM}$  is 200 g mol<sup>-1</sup> and referring to Zhai *et al.*, (2016), this work estimated that the  $M_{OM}$  concentration was equal to the 50% of the PM

concentration.  $R$  is the ideal gas constant (m<sup>3</sup> atm K<sup>-1</sup> mol) and  $T$  is the ambient temperature (K).  $\xi_{OM}$  and  $P_L^0$  are the mole fraction scale activity coefficient of each compound in the absorbing OM phase and vapor pressure of each pure compound.

#### Quality Control and Analysis

All procedures were strictly quality-controlled, with quality control and blank control samples added into the sequence in order to assess the data repeatability, and no significant contamination was found. Quantification of PAHs was standardized by the retention times and peak areas of the calibration standards. It was performed by the internal standard method using 2-fluoro-1,10-biphenyl and p-terphenyl-d14 (2.0 mg mL<sup>-1</sup>; J&K Chemical, Beijing, China). The instruments were calculated using at least five standard concentrations covering the concentration of interest for ambient air work and the analytical precision, measured as the relative standard deviation, was < 10% (Liu *et al.*, 2017a).

Data analysis was performed using the Statistical Package of the Social Sciences 18.0 (SPSS 18.0) Software for Windows (SPCC Co., 2001). For the mathematical statistics analysis, the one-way analysis of variance (ANOVA) and correlation analysis with Bivariate Correlations Analysis were completed. The relationships between the concentrations of compounds were subsequently explored by linear correlation analysis.

#### Data Processing

##### Coefficient of Divergence ( $CD_{jk}$ )

Recent research shows that the intraurban spatial distributions of PM concentrations in some study areas are heterogeneous. Therefore, a coefficient of variation (CV) or a coefficient of divergence (CD) is used for the heterogeneous distributions of particulates to describe relative intra urban concentration heterogeneity (Wilson, *et al.*, 2005). The  $CD_{jk}$  method for identifying the differences of PAH composition profiles was described in detail elsewhere (Wongphatarakul, 1998), which was defined as follows:

$$CD_{jk} = \sqrt{\frac{1}{p} \sum_{i=1}^p \left( \frac{X_{ij} - X_{ik}}{X_{ij} + X_{ik}} \right)^2} \quad (4)$$

where  $x_{ij}$  represents the average concentration for a chemical component  $i$  at site  $j$ ,  $j$  and  $k$  represent two sampling sites, and  $p$  is the number of chemical components. If the value of  $CD_{jk}$  approaches zero, the PAH composition in  $j$  and  $k$  is similar, and if it approaches one, it is significantly different (Wongphatarakul, 1998). Kong *et al.* (2012) found that if the value of  $CD_{jk}$  is lower than 0.2, the source of the two sites is the same.

##### Diagnostic Ratios of PAH

The binary ratio method for PAH source identification was described in detail elsewhere (Ravindra *et al.*, 2008), which involves comparing ratios of pairs of frequently found PAH emissions. The diagnostic ratio method can also characterize the diversity in PAH sources and distinguishing

emissions (Venkataraman *et al.*, 1994; Harrison *et al.*, 1996; Ravindra *et al.*, 2008).

#### Toxic and Mutagenic Equivalent Factors

The carcinogenic risk of a PAH mixture is often expressed by its BaP equivalent concentration ( $BaP_{TEQ}$ ) (Han *et al.*, 2011). To normalize the toxicity of different PAHs in  $PM_{2.5}$  and  $PM_{10}$ , it has been calculated by the equivalent mass concentration based on BaP and the value of toxic equivalency factors, TEFs (Table 2). Similarly, just with the replacement of TEF with MEF (Mutagenic Equivalency Factors), the mutagenicity related to BaP ( $BaP_{MEQ}$ ) was calculated as well.

And the  $BaP_{TEQ}$  and  $BaP_{MEQ}$  of the air were calculated according to Eqs. (5) and (6):

$$\sum BaP_{TEQ} = \sum_{i=1}^n C_i \times TEF_i \quad (5)$$

$$\sum BaP_{MEQ} = \sum_{i=1}^n C_i \times MEF_i \quad (6)$$

where  $C_i$  = concentration of PAH congener  $i$ ;  $TEF_i$  = the toxic equivalency factors (TEFs) of PAH congener  $i$ ;  $MEF_i$  = the mutagenic equivalency factors (MEFs) of PAH congener  $i$ . The toxicity assessment of PAHs was determined by benzo(a)pyrene, an equivalent for carcinogenicity ( $\sum BaP_{TEF}$ ) and mutagenicity ( $\sum BaP_{MEF}$ ).

In urban areas, the citizens were divided into three population groups according to the age and gender: children and adolescents (1–18 years), male (19–71.95 years) and female (19–77.06 years). Daily inhalation exposure level ( $E$ ) for each population group was calculated as follows in Eq. (7):

$$E = \sum_{i=1}^n BaP_{TEQ_i} \times IR_i \times T_i \quad (7)$$

where  $T_i$  = daily exposure time span in the  $i$ th area (for all groups of the urban area on one day: they spend the whole day in the urban area, thus  $n = 1$ ,  $i = 1$  refers to urban area,  $T_1 = 1$ );  $BaP_{TEQ_i}$  = B(a)P equivalent concentration of 10 PAHs in the  $i$ th area ( $ng\ m^{-3}$ ) (for all groups of urban area:  $n = 1$ ,  $i = 1$  refers to urban area);  $IR$  = inhalation rate ( $m^3\ day^{-1}$ ) (Table 3) (Xia *et al.*, 2013; Lin, 2016; Zhang *et al.*, 2019).

#### Cancer Risk Estimates

The incremental lifetime cancer risk (ILCR) of population groups in Nanjing caused by PAHs inhalation exposure was calculated based on Eqs. (8) and (9):

$$LADD = \frac{C_i \times EF}{AT} \times \left( \frac{IR_{child} \times ED_{child}}{BW_{child}} + \frac{IR_{adult} \times ED_{adult}}{BW_{adult}} \right) \quad (8)$$

$$ILCR = q \times LADD \quad (9)$$

where  $LADD$  = Lifetime Average Daily Doses;  $C_i$  =

**Table 2.** Abbreviations used for PAHs in this paper and carcinogenic and mutagenic potencies of PAHs (Nisbet and LaGoy, 1992; Malcom and Dobson, 1994; Durant *et al.*, 1996).

PAH	PAH abbreviation	IARC class	TEFs	MEFs
Fluoranthene	Flu	3	0.001	/
Pyrene	Pyr	3	0.001	/
Benz[a]anthracene	BaA	2B	0.1	0.082
Chrysene	Chr	2B	0.01	0.017
Benzo[b]fluoranthene	BbF	2B	0.1	0.25
Benzo[k]fluoranthene	BkF	2B	0.1	0.11
Benzo[a]pyrene	BaP	1	1	1
Dibenz[a,h]anthracene	Daha	2A	1	0.29
Benzo[ghi]perylene	BghiP	3	0.01	0.19
Indeno[1,2,3-cd]pyrene	IcdP	2B	0.1	0.31

a Agents Classified by the IARC Monographs, Volumes 1e100 (IARC, 2012): 1, Carcinogenic to humans; 2A, Probably carcinogenic to humans; 2B, Possibly carcinogenic to humans; 3, Not classifiable as to its carcinogenicity to humans.

**Table 3.** Exposure parameters for different age and gender groups of Nanjing city.

Parameter	Children and adolescents	Male	Female	Units
$T_i$	1	1	1	
$C_i$	/	/	/	$mg\ m^{-3}$
$IR$	8.6	18	14.5	$m^3\ d^{-1}$
$EF$	365	365	365	$d\ a^{-1}$
$ED$	1–18	19–71.95	19–77.06	a
$AT$	365•18	365•71.95	365•77.06	d
$BW$	16	65	56.8	kg
$q$	3.14	3.14	3.14	

2298

Liu et al., *Aerosol and Air Quality Research*, 19: 2294–2307, 2019

$\Sigma \text{BaP}_{\text{TEQ}}$  ( $\text{mg m}^{-3}$ ); EF = the exposure frequency ( $\text{day year}^{-1}$ ); ED = exposure duration (year); BW = body weight (kg); AT = average lifespan for carcinogens (day).

ILCR = the incremental cancer risk of the inhalation exposure (dimensionless); q = the cancer slope factor for BaP inhalation exposure [a lognormal distribution with a geometric mean of  $3.14 (\text{mg kg}^{-1} \text{ day}^{-1})^{-1}$  and a geometric standard deviation of 1.80] (Chen and Liao 2006).

## RESULTS AND DISCUSSION

### Pollution Level of Particle PAHs (P-PAHs) in $\text{PM}_{2.5}$ and $\text{PM}_{10}$

Descriptive statistics for all valid observations of P-PAH

concentration-ratios in  $\text{PM}_{2.5}$  and  $\text{PM}_{10}$  from 5 sites in Nanjing are summarized in Fig. 1. The average 24-h total P-PAH concentrations of  $\text{PM}_{2.5}$  and  $\text{PM}_{10}$  were in the ranges of  $10.95\text{--}59.10 \text{ ng m}^{-3}$  and  $35.38\text{--}97.33 \text{ ng m}^{-3}$ , respectively. Among the 5 sites, the average mass of carcinogenic PAHs (C-PAHs) including BaA, BbF, BkF, BaP, Icdp and Daba, at the Business area reached the highest proportion (61.19% for  $\text{PM}_{2.5}$  and 53.57% for  $\text{PM}_{10}$ , respectively), apparently affected by many area emission sources distributed around the business district. However, the highest average 24-h C-PAH concentrations appeared in the industrial area, with  $20.13 \pm 5.39 \text{ ng m}^{-3}$  for  $\text{PM}_{2.5}$  and  $36.31 \pm 5.35 \text{ ng m}^{-3}$  for  $\text{PM}_{10}$ . The results suggest that C-PAHs may be related with the coal combustion and coal processing industries.

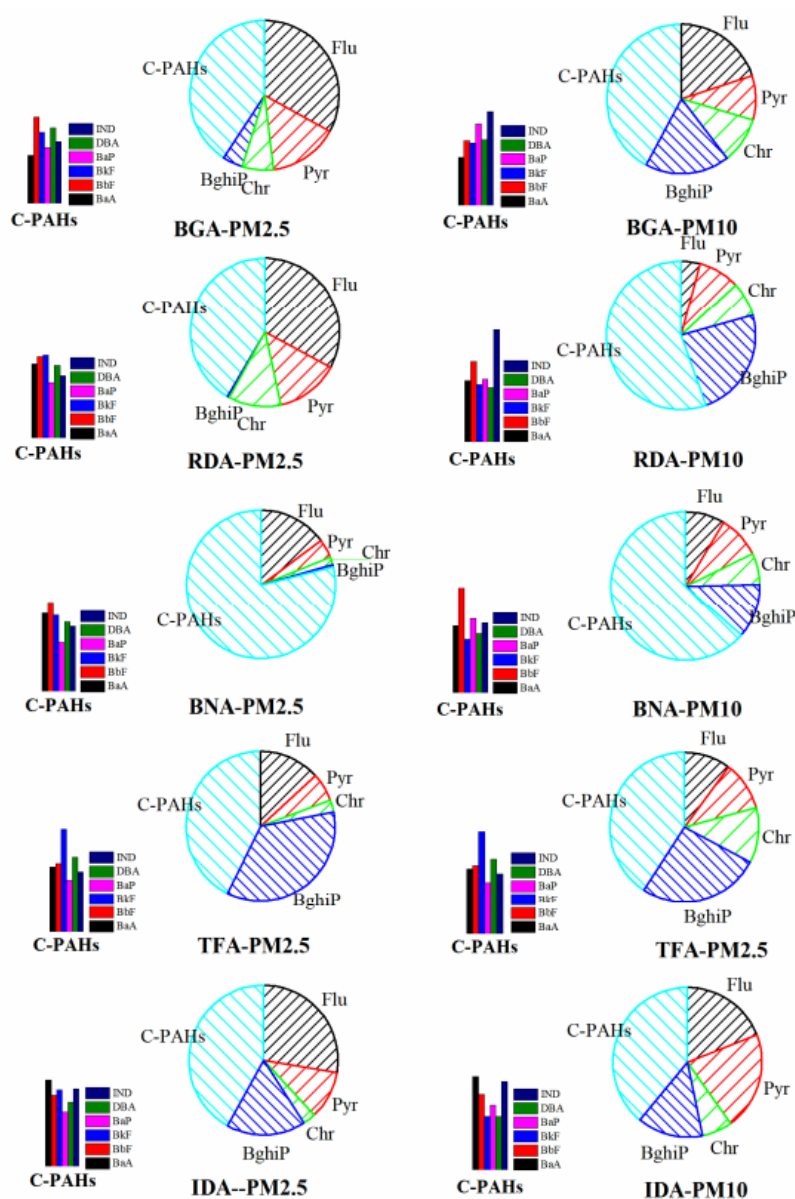


Fig. 1. The proportion of each P-PAH in different functional areas in  $\text{PM}_{2.5}$  and  $\text{PM}_{10}$ .



Among the 10 P-PAHs analyzed, the average concentrations of middle molecular weight PAHs (Flu, Pyr, BaA, Chr), and high molecular weight PAHs (BbF, BkF, BaP, Icdp, Bghip, Daba) (Yang *et al.*, 1998) ranged from 4.72 to 24.91 ng m<sup>-3</sup> and 5.07 to 23.08 ng m<sup>-3</sup>, respectively, for PM<sub>2.5</sub>. The corresponding values were 14.63 to 54.77 ng m<sup>-3</sup>, and 21.49 to 44.95 ng m<sup>-3</sup>, respectively, for PM<sub>10</sub>.

A one-way ANOVA was also used to test the significant differences using the BaP and total P-PAH data. This analysis suggests that the BaP levels were not statistically different for each site (ANOVA,  $p > 0.05$ ) while clear regional trends were observed for the total P-PAH levels ( $p < 0.01$ ). Meanwhile, there was a significant correlation between BaP and total P-PAHs in PM<sub>2.5</sub> ( $R = 0.713$ ,  $p < 0.01$ ) and the correlation of total P-PAH in PM<sub>2.5</sub> and PM<sub>10</sub> was also significant ( $R = 0.783$ ,  $p < 0.01$ ).

### Spatial Variation

Fig. 2 shows the box plot of the Spearman rank correlation coefficients of each P-PAH and the total P-PAHs between five sites. In general, the medians of the correlation coefficients for all P-PAHs in PM<sub>2.5</sub> and PM<sub>10</sub>, respectively, were approximately below 0.50 and 0.55. This means that the spatial correlations between all sites are not strong in Nanjing, especially for TFA in terms of PM<sub>2.5</sub> and BGA in terms of PM<sub>10</sub>. In order to measure the spread of the data

points for two datasets, mass concentrations characterized between different sites for  $j$  against  $k$  are also presented in Fig. 2. Low  $CD_{jk}$  values ( $< 0.2$ ) have been shown to indicate a high level of homogeneity between sites, while  $CD_{jk}$  values larger than 0.2 indicate heterogeneous sites (Wilson *et al.*, 2005). As can be seen, the median PM<sub>2.5</sub> -  $CD_{jk}$  values ranged from 0.41 to 0.53 and PM<sub>10</sub> -  $CD_{jk}$  values ranged from 0.27 to 0.37 suggesting a heterogeneous distribution of PM<sub>2.5</sub> and PM<sub>10</sub> in the 5 sites, indicating significant differences in PAH composition.

For the comparison of P-PAHs between PM<sub>2.5</sub> and PM<sub>10</sub>, the diagrams characterized by scatter plots of P-PAHs component mass concentrations between PM<sub>2.5</sub> and PM<sub>10</sub> for  $j$  against  $k$  are also presented in Fig. 3. The  $CD_{jk}$  values of BGA, RDA, BNA, TFA and IDA were 0.523, 0.566, 0.603, 0.584, and 0.426, being also higher than 0.2. It can be concluded that the P-PAHs compositions at the sites in PM<sub>2.5</sub> and PM<sub>10</sub> are different, indicating the influence of different sources.

### Source Identification and Source Contribution Assessment

Molecular diagnostic ratios, firstly used in organic geochemistry, have been a convenient approach to help identifying possible emission sources. Yunker *et al.* (1996) has used fluoranthene/pyrene and phenanthrene/anthracene

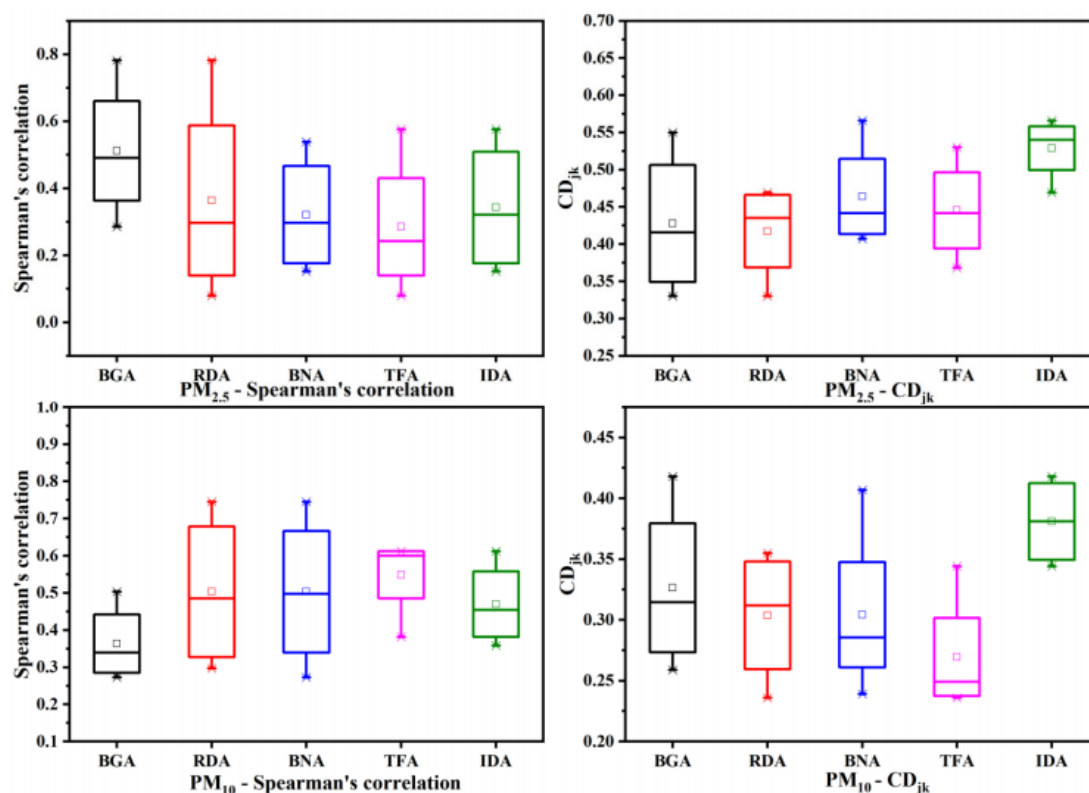


**Fig. 2.** Box plots of Spearman rank correlation coefficients (left) and coefficient of divergence ( $CD_{jk}$ , right) based on individual P-PAHs and the total P-PAHs concentrations between five different measurement sites. The box plots indicate the maximum, 75<sup>th</sup> percentile, the median, 25<sup>th</sup> percentile, and the minimum of all the data, respectively.



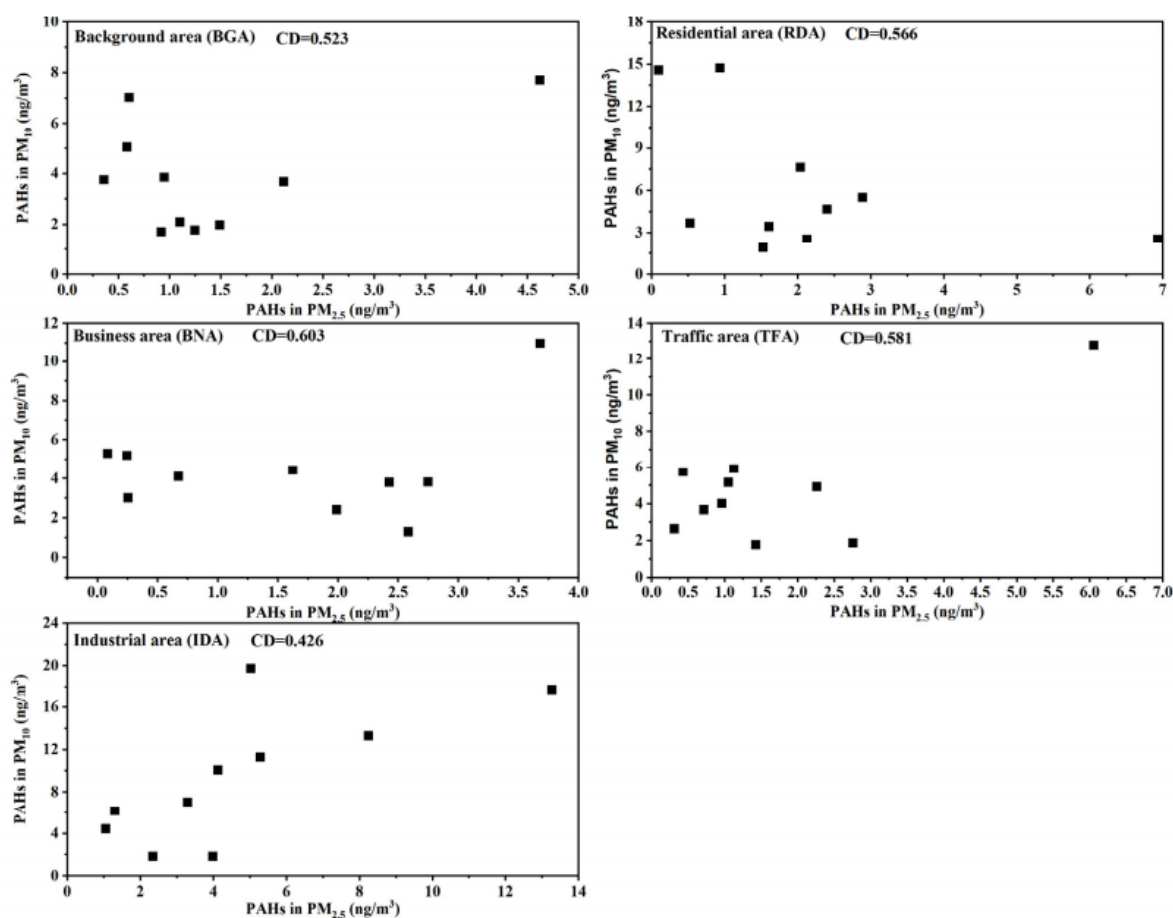


**Fig. 3.** Comparison of average concentrations of P-PAHs between  $PM_{2.5}$  and  $PM_{10}$  for different sites in Nanjing.

to ascertain emission sources in sediment samples. Simoneit *et al.* (2004) and Andreou *et al.* (2008) have used this method to investigate the origin of organic species in the atmosphere.

Studies have revealed that the ratio of Flu/(Flu + Pyr) is lower than 0.40 for the petroleum source, and higher than 0.50 for biomass and coal combustion, and between 0.4 and 0.5 for fuel emissions caused by the exhaust (Li *et al.*, 2006a; Ravindra and Grieken, 2008). Kavouras *et al.* (2001) has found the value of Icdp/(Icdp + BghiP) ratio is between 0.35 and 0.7 for diesel emissions. For both  $PM_{2.5}$  and  $PM_{10}$ , the ratios of P-PAHs values for the background site and other sites are shown in Fig. 4.

As shown in Fig. 4, different ratios of compounds indicate different sources. However, the main source of pollution is the combustion of fossil fuels for  $PM_{2.5}$  and  $PM_{10}$ . It is clear that the main sources are diesel emissions in BGA and pyrolytic sources in RDA, BNA, TFA and IDA. However, there is some difference between  $PM_{2.5}$  and  $PM_{10}$ . It can be found that the main source is focusing on traffic emissions for  $PM_{10}$ . And several sources of ambient PM (Laden *et al.*, 2000; Hoek *et al.*, 2002) are under investigation, especially of interest are emissions from combustion sources with focus on traffic emissions (Mudway *et al.*, 2004; Peters *et al.*, 2004).

Meanwhile, the isomer ratio of a more reactive PAH to a stable PAH, such as BaA/Chr, can be employed to illustrate whether the air masses collected are fresh or aged (Ding *et al.*, 2007). The values of the BaA/Chr were 1.32, 0.67, 10.74, 2.22 and 4.03 for BGA, RDA, BNA, TFA and IDA in  $PM_{2.5}$ , respectively. The high values were found in BNA, TFA and IDA, indicating relatively little photochemical reaction and a major impact from local sources. However, the low values were found in BGA and RDA, meaning more degradation happened in situ or during the process of air transport (He *et al.*, 2014).

#### **Predicted Gas-phase PAH Concentrations**

The total PAH concentration data is the sum of the concentration of P-PAHs and gaseous PAHs (G-PAHs). The calculation of G-PAHs is presented in detail in Section 1.5. According to Zhai *et al.* (2016), the average gas-phase fraction of each PAH was calculated and listed in Table 4. By comparison, the total predicted PAH concentrations found in this study are consistent with those reported by Li *et al.* (2006b) and Gao *et al.* (2015), who found that the total PAH concentrations in  $PM_{2.5}$  ranged from 10 to 40  $ng\ m^{-3}$  in December 2001 in Guangzhou, and 7.1 to 72.6  $ng\ m^{-3}$  in November–December 2009, respectively.

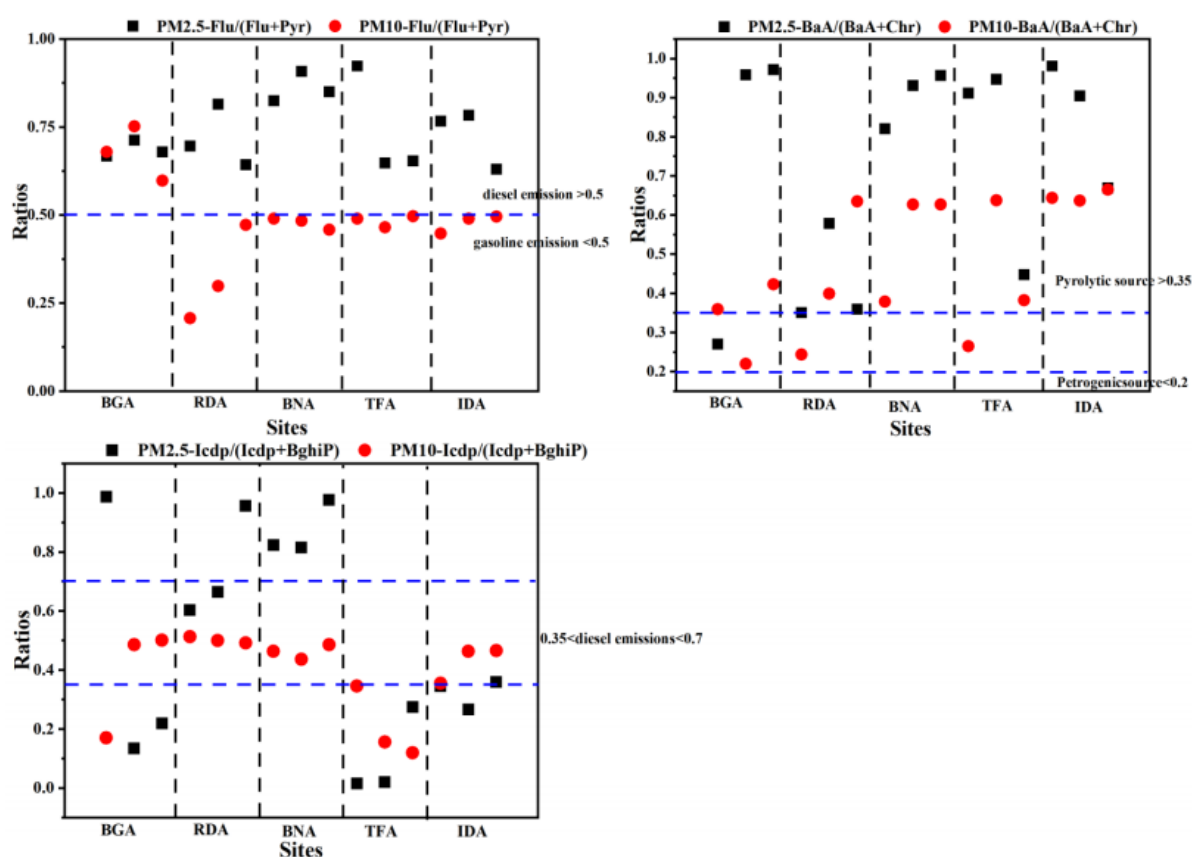


**Fig. 4.** Diagnostic ratios for Flu/(Flu + Pyr), BaA/(BaA + Chr) and Icdp/(Icdp + BghiP) of the five sites for PM<sub>2.5</sub> and PM<sub>10</sub> in Nanjing.

### Health Risk of PAHs

#### Carcinogenic and Mutagenic Potencies

As shown in Fig. 5, the BaP<sub>TEQ</sub> and BaPM<sub>EQ</sub> values were computed applying the modified lists of TEFs and MEFs (Table 2) in all five investigated sites. There were higher carcinogenic risks of total PAHs in Nanjing, with average values of  $3.14 \pm 1.27 \text{ ng m}^{-3}$  for PM<sub>2.5</sub> and  $8.23 \pm 1.55 \text{ ng m}^{-3}$  for PM<sub>10</sub>, respectively. European countries have been established the target annual mean values of BaP to range between 0.7 and  $1.3 \text{ ng m}^{-3}$  (Ballesta, *et al.*, 1999) and it has been suggested a concentration of  $0.1 \text{ ng m}^{-3}$  of BaP as a health-based guideline in ambient air (Boström *et al.*, 2002). The value of the  $\Sigma\text{BaP}_{\text{TEQ}}$  in Nanjing has exceeded the standard value of  $1 \text{ ng m}^{-3}$ , indicating that many of the more toxic compounds are threatening human health in the urban city, nowadays. For mutagenic potencies, the average concentrations of  $\Sigma\text{BaPM}_{\text{EQ}}$  were  $3.14 \pm 1.85 \text{ ng m}^{-3}$  for PM<sub>2.5</sub> and  $11.23 \pm 2.70 \text{ ng m}^{-3}$  for PM<sub>10</sub>, being higher than those at the Chinese background sites ( $1.26 \pm 1.75 \text{ ng m}^{-3}$  for PM<sub>2.5</sub> and  $1.41 \pm 1.98 \text{ ng m}^{-3}$  for PM<sub>10</sub>) (Wang *et al.*, 2015).

As PAHs can be classified on different standard levels, this study has classified the total PAHs according to their number of aromatic rings to quantify the BaP<sub>TEQ</sub> and BaPM<sub>EQ</sub>. It can be found that the BaP<sub>TEQ</sub> of total PAHs with 4, 5 and 6 rings are dominant in both PM<sub>2.5</sub> and PM<sub>10</sub>. Among

all functional sites, 5-rings account for absolutely high ratios, up to nearly 80% or more. This may indicate that the high-numbered ring PAHs are the predominant compounds in PM.

Regarding the different functional areas, the values of  $\Sigma\text{BaP}_{\text{TEQ}}$  and  $\Sigma\text{BaPM}_{\text{EQ}}$  in the background area (BGA) were the lowest. Meanwhile, the high molecular weight compounds (6-ring compounds) have not been detected as frequently in the background site, TEF values of low-numbered ring compounds are lower than the high-numbered rings, and MEFs only belong to special PAHs. Certainly, this is also related to inconspicuous anthropogenic sources and more plants in the background site. For IDA and BNA, it should be noticed that 5-ring and 4-ring PAHs exhibit the highest mass percentages when compared with other sites. Ravindra *et al.* (2006) indicated that the major sources for BaP, BbF, BghiP and Icdp are gasoline vehicles.

#### Lung Cancer Risk of Assessment

With the average equivalent BaP concentration of total PAHs in PM<sub>2.5</sub> and PM<sub>10</sub> (Fig. 5) and the variables of exposure parameters (Table 3), the value of the lifetime carcinogenic risk for children and adolescents, males and females in Nanjing has been calculated (Table 5).

As shown in Table 5, the LADD of children and adolescents

**Table 4.** Average predicted g-PAH profile based on the P-PAH data sets of the five sampling sites in Nanjing (unit: ng m<sup>-3</sup>).

PAHs	Background area (BGA)		Residential area (RDA)		Business area (BNA)		Traffic area (TFA)		Industrial area (IDA)	
	G-PAH-PM <sub>2.5</sub>	G-PAH-PM <sub>10</sub>	G-PAH-PM <sub>2.5</sub>	G-PAH-PM <sub>10</sub>	G-PAH-PM <sub>2.5</sub>	G-PAH-PM <sub>10</sub>	G-PAH-PM <sub>2.5</sub>	G-PAH-PM <sub>10</sub>	G-PAH-PM <sub>2.5</sub>	G-PAH-PM <sub>10</sub>
Flu	0.1	0.1	0.2	0.04	0.03	0.03	0.03	0.04	0.1	0.1
Pyr	0.1	0.1	0.1	0.2	0.02	0.02	0.02	0.08	0.1	0.3
BaA	0.01	0.01	0.01	0.02	0.01	0.01	0.004	0.01	0.02	0.03
Chr	0.005	0.01	0.01	0.02	0.001	0.01	0.001	0.01	0.003	0.01
BbF	0.01	0.01	0.02	0.04	0.01	0.03	0.004	0.02	0.01	0.02
BkF	0.01	0.01	0.03	0.02	0.01	0.005	0.01	0.007	0.02	0.005
BaP	0.002	0.01	0.002	0.01	0.001	0.008	0.001	0.004	0.002	0.005
DBA	0.02	0.03	0.03	0.03	0.02	0.02	0.01	0.01	0.02	0.01
BghiP	0.003	0.02	0.001	0.04	0.001	0.008	0.01	0.02	0.02	0.02
IND	0.01	0.03	0.01	0.09	0.008	0.01	0.003	0.01	0.02	0.03

were approximately 1.6 times and 1.7 times higher than that of males and females. This may be due to the fact that children's and adolescents' breathing rate is greater than that of adults, while their bodyweight is lower. Furthermore, the ranking of ILCR in decreasing order basically was children and adolescents, males and females, indicating children and adolescents being a population group sensitive to health risks by pollutants (Martí-Cid *et al.*, 2008). So, there are security risks for humans, especially children and adolescents, although the values are within an acceptable range ( $10^{-4}$ – $10^{-6}$  made by U.S. EPA (1989)).

#### Comparison with Other Studies

According to previous study (Wang *et al.*, 2006), there has been a decrease in P-PAH concentration in Nanjin since 2001, based on the average between the five study sites (Table 6). The P-PAHs concentrations in PM<sub>2.5</sub> were similar to those analyzed by Ningbo (Mo *et al.*, 2018) in winter and in spring in Shanghai (Liu *et al.*, 2017b). In comparison, the total P-PAH concentrations found in this study are lower than those reported by Simayi *et al.* (2018), who also analyzed the P-PAHs in different functional areas. However, the average concentrations of  $\Sigma$  P-PAHs in PM<sub>2.5</sub> and PM<sub>10</sub> were approximately 7 and 14 times higher than those in the background of China (Wang *et al.*, 2015) and in Hong Kong (Guo *et al.*, 2003). When comparing the P+G PAHs, values are significantly lower in Nanjing than in Guangzhou (Yang *et al.*, 2010), indicating that the G-PAHs are also noteworthy. Therefore, in the future, gas-phase samples should be collected for the analysis. It is worth noting that the values were higher as compared to those of the urban centre at the same sampling period in Taiwan (Fang *et al.*, 2005) and much higher than those of Nanjing in summer (Sun *et al.*, 2016).

Similarly, compared to the study by Wang *et al.*, (2006), the average concentrations of  $\Sigma$ BaP<sub>TEQ</sub> for PM<sub>2.5</sub> and PM<sub>10</sub> decreased, similar to Jinhua (Mo *et al.*, 2018) and Shanghai (Liu *et al.*, 2017b). However, they were approximately 4 and 9 times higher than those in the backgrounds of China (Wang *et al.*, 2015) and much higher than those of Nanjing in summer (Sun *et al.*, 2016). The average concentrations of  $\Sigma$ BaP<sub>MEQ</sub> for PM<sub>2.5</sub> and PM<sub>10</sub> were approximately 2 and 8 times higher than those in the backgrounds of China. In PM<sub>2.5</sub>, the  $\Sigma$ BaP<sub>MEQ</sub> concentration was similar to that in Venice-Mestre (Masiol *et al.*, 2012). The calculated ILCR average values for PM<sub>2.5</sub> and PM<sub>10</sub> in Nanjing were also higher than those in Thessaloniki (Northeastern Greece) (Manoli *et al.*, 2016) but lower than those in Xiamen (Zhang *et al.*, 2018).

#### SUMMARY AND CONCLUSIONS

In this manuscript, daily ambient samples of particle PAHs were collected in Nanjing to examine chemical characteristics, regional variation, emission sources and the related carcinogenicity, mutagenicity and risks for human health. Total P-PAH concentrations ranged from 14.02 to 50.00 ng m<sup>-3</sup> and from 38.45 to 93.08 ng m<sup>-3</sup> in PM<sub>2.5</sub> and PM<sub>10</sub>, respectively. Thereby, the main source of pollution was the combustion of fossil fuels. Furthermore, the gas



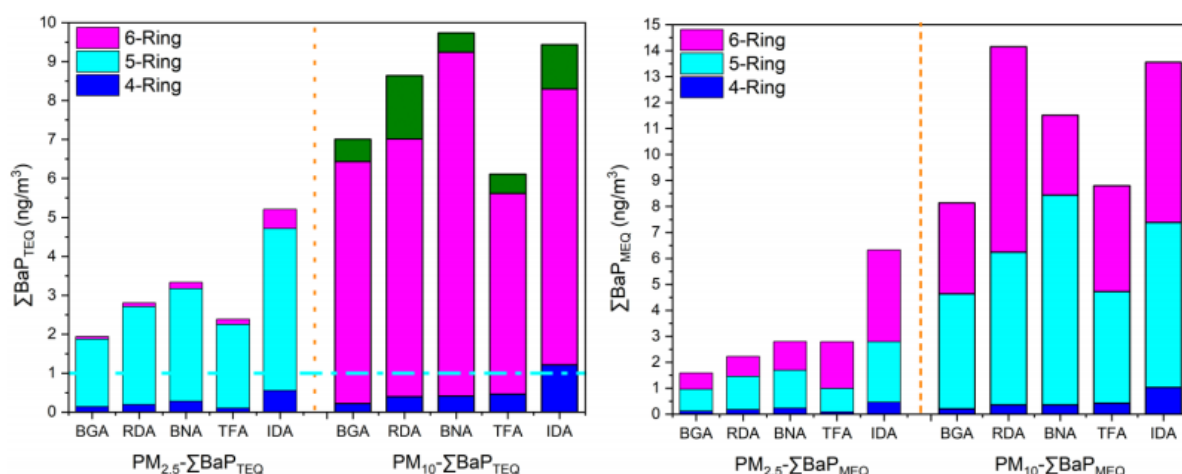


Fig. 5.  $\Sigma\text{BaP}_{\text{TEQ}}$  and  $\Sigma\text{BaP}_{\text{MEQ}}$  concentrations of PAHs in  $\text{PM}_{2.5}$  and  $\text{PM}_{10}$  at the five sites.

Table 5. LADD and ILCR for different groups of Nanjing city.

Groups	Children and adolescents		Males		Females	
	$\text{PM}_{2.5}$	$\text{PM}_{10}$	$\text{PM}_{2.5}$	$\text{PM}_{10}$	$\text{PM}_{2.5}$	$\text{PM}_{10}$
E (ng)	26.93	70.39	56.38	147.34	45.42	118.69
LADD/mg (kg d) <sup>-1</sup>	$1.68 \cdot 10^{-6}$	$4.39 \cdot 10^{-6}$	$1.07 \cdot 10^{-6}$	$2.80 \cdot 10^{-6}$	$1.01 \cdot 10^{-6}$	$2.63 \cdot 10^{-6}$
ILCR	$5.29 \cdot 10^{-6}$	$1.38 \cdot 10^{-5}$	$3.36 \cdot 10^{-6}$	$8.79 \cdot 10^{-6}$	$3.16 \cdot 10^{-6}$	$8.25 \cdot 10^{-6}$

Table 6. Comparison of the four factors analysed in the present study and with values reported in the literature.

Compounds	Mean concentrations in $\text{PM}_{2.5}$	Mean concentrations in $\text{PM}_{10}$	Area and Time	Source
P-PAHs	62.6 ng m <sup>-3</sup>	86.0 ng m <sup>-3</sup>	Nanjing in 2001–2002	Wang et al., 2006
P-PAHs	29.5 ng m <sup>-3</sup>	-	Shanghai in Spring 2012	Liu et al., 2017b
P-PAHs	25.34 ng m <sup>-3</sup>	34.2 ng m <sup>-3</sup>	Hong Kong in 2000–2001	Guo et al., 2003
P-PAHs	4.30 ng m <sup>-3</sup>	4.73 ng m <sup>-3</sup>	Four background sites of China in 2013	Wang et al., 2015
P-PAHs	16.35 ng m <sup>-3</sup>	37.47 ng m <sup>-3</sup>	Tunghai University in Mar.–Apr. 2002	Fang et al., 2005
P-PAHs	128.10 ng m <sup>-3</sup>	173.08 ng m <sup>-3</sup>	Urumqi in Nov. 2015–Mar. 2016	Simayi et al., 2018
P-PAHs	25.56 ng m <sup>-3</sup>	-	Ningbo in winter 2015	Mo et al., 2018
P-PAHs	-	7.49 ng m <sup>-3</sup>	Nanjing in Summer, 2015	Sun et al., 2016
P-PAHs	23.31 ng m <sup>-3</sup>	57.01 ng m <sup>-3</sup>	Nanjing in Mar.–Apr. 2017	<b>This study</b>
P+G-PAHs	-	129 ng m <sup>-3</sup>	Guangzhou in Apr. 2005–Mar. 2006	Yang et al., 2010
P+G-PAHs	23.34 ng m <sup>-3</sup>	57.34 ng m <sup>-3</sup>	Nanjing in Mar.–Apr. 2017	<b>This study</b>
BaP <sub>TEQ</sub>	7.10 ng m <sup>-3</sup>	9.3 ng m <sup>-3</sup>	Nanjing in 2001–2002	Wang et al., 2006
BaP <sub>TEQ</sub>	1.5 ng m <sup>-3</sup>	1.5 ng m <sup>-3</sup>	Urban traffic site in Feb.–Mar. 2012	Manoli et al., 2016
BaP <sub>TEQ</sub>	3.6 ng m <sup>-3</sup>	/	Shanghai in Spring 2012	Liu et al., 2017b
BaP <sub>TEQ</sub>	0.82 ng m <sup>-3</sup>	0.91 ng m <sup>-3</sup>	Four background sites of China in Spring 2013	Wang et al., 2015
BaP <sub>TEQ</sub>	3.1 ng m <sup>-3</sup>	-	Jinhua in winter 2015	Mo et al., 2018
BaP <sub>TEQ</sub>	3.14 ng m <sup>-3</sup>	8.23 ng m <sup>-3</sup>	Nanjing in Mar.–Apr. 2017	<b>This study</b>
BaP <sub>MEQ</sub>	3.10 ng m <sup>-3</sup>	/	Venice-Mestre in Mar. 2009	Masiol et al., 2012
BaP <sub>MEQ</sub>	1.26 ng m <sup>-3</sup>	1.41 ng m <sup>-3</sup>	Four background sites of China in Spring 2013	Wang et al., 2015
BaP <sub>MEQ</sub>	3.13 ng m <sup>-3</sup>	11.20 ng m <sup>-3</sup>	Nanjing in Mar.–Apr. 2017	<b>This study</b>
ILCR	$1.7 \cdot 10^{-6}$	$1.6 \cdot 10^{-6}$	Urban traffic site in Feb.–Mar. 2012	Manoli et al., 2016
ILCR	$1.1 \cdot 10^{-4}$	-	Xiamen in Winter	Zhang et al., 2018
ILCR	$4.0 \cdot 10^{-6}$	$1.0 \cdot 10^{-5}$	Nanjing in Mar.–Apr. 2017	<b>This study</b>

PAHs were also estimated by the G/P partitioning model. The annual average concentrations of BaP<sub>TEQ</sub> was larger than both the Chinese national standard and the WHO guideline. Similarly, the annual average concentrations of

BaP<sub>MEQ</sub> have exceeded the background sites of China many times. ILCR values caused by particle phase PAHs for humans were all greater than the significant level ( $10^{-6}$ ), indicating a high potential lung cancer risk. Moreover, it is

2304

Liu et al., *Aerosol and Air Quality Research*, 19: 2294–2307, 2019

necessary to pay more attention to children and adolescents, whose ILCR values were higher than those of adults.

## ACKNOWLEDGEMENTS

We are very grateful to the anonymous referees and editor for their valuable suggestions which have helped to improve the paper. This research was supported by the National Natural Science Foundation of China (No. 41603114), Natural Science Foundation of Jiangsu Province (No. BK20161017) and Natural Science Foundation of the Higher Education Institutions of Jiangsu Province, China (No. 15KJD610004) and the China Scholarship Council (CSC) under the State Scholarship Fund (File No. 201706860028).

## REFERENCES

- Abdel-Shafy, H.I. and Mansour, M.S.M. (2016). A review on polycyclic aromatic hydrocarbons: Source, environmental impact, effect on human health and remediation. *Egypt. J. Pet.* 25: 107–123.
- Andreou, G., Alexiou, S.D., Loupa, G. and Rapsomanikis, S. (2008). Identification, abundance and origin of aliphatic hydrocarbons in the fine atmospheric particulate matter of Athens, Greece. *Water Air Soil Pollut. Focus* 8: 99–106.
- Ballesta, P.P., Saeger, E.D. and Kotzias, D. (1999). State of the art of the PAHs' analysis in ambient air. *Fresenius Environ. Bull.* 8: 499–505.
- Beelen, R., Raaschou-Nielsen, O., Stafoggia, M., Andersen, Z.J., Weinmayr, G., Hoffmann, B. et al. (2014). Effects of long-term exposure to air pollution on natural-cause mortality: an analysis of 22 European cohorts within the multicentre ESCAPE project. *Lancet* 383: 785–795.
- Boström, C.E., Gerde, P., Hanberg, A., Jernström, B., Johansson, C., Kyrklund, T., Rannug, A., Törnqvist, M., Victorin, K. and Westerholm, R. (2002). Cancer risk assessment, indicators, and guidelines for polycyclic aromatic hydrocarbons in the ambient air. *Environ. Health Perspect.* 110: 451–488.
- Brook, R.D., Rajagopalan, S., Pope III, C.A., Brook, J.R., Bhatnagar, A., Diez-Roux, A.V., Holguin, F., Hong, Y., Luepker, R.V. and Mittleman, M.A. (2010). Particulate matter air pollution and cardiovascular disease: An update to the scientific statement from the American Heart Association. *Circulation* 121: 2331–2378.
- Chen, S.C. and Liao, C.M. (2006). Health risk assessment on human exposed to environmental polycyclic aromatic hydrocarbons pollution sources. *Sci. Total Environ.* 366: 112–123.
- Cheruiyot, N.K., Lee, W.J., Mwangi, J.K., Wang, L.C., Lin, N.H., Lin, Y.C., Cao, J., Zhang, R. and Chang-Chien, G.P. (2015). An overview: Polycyclic aromatic hydrocarbon emissions from the stationary and mobile sources and in the ambient air. *Aerosol Air Qual. Res.* 15: 2730–2762.
- Cohen, A.J., Ross Anderson, H., Ostro, B., Pandey, K.D., Krzyzanowski, M., Künzli, N., Gutschmidt, K., Pope, A., Romieu, I., Samet, J.M. and Smith, K. (2005). The global burden of disease due to outdoor air pollution. *J. Toxicol. Environ. Health A* 68: 1301–1307.
- Demarini, D.M., Brooks, L.R., Warren, S.H., Takahiro, K., Ian, G.M. and Pramila, S. (2004). Bioassay-directed fractionation and salmonella mutagenicity of automobile and forklift diesel exhaust particles. *Environ. Health Perspect.* 112: 814–819.
- Ding, X., Wang, X.M., Xie, Z.Q., Xiang, C.H., Mai, B.X., Sun, L.G., Zheng, M., Sheng, G.Y., Fu, J.M. and Pöschl, U. (2007). Atmospheric polycyclic aromatic hydrocarbons observed over the North Pacific Ocean and the Arctic area: Spatial distribution and source identification. *Atmos. Environ.* 41: 2061–2072.
- Du, W., Zhang, Y., Chen, Y., Xu, L., Chen, J., Deng, J., Hong, Y. and Xiao, H. (2017). Chemical characterization and source apportionment of PM<sub>2.5</sub> during spring and winter in the Yangtze River Delta, China. *Aerosol Air Qual. Res.* 17: 2165–2180.
- Durant, J.L., Busby, W.F., Lafleur, A.L., Penman, B.W. and Crespi, C.L. (1996). Human cell mutagenicity of oxygenated, nitrated and unsubstituted polycyclic aromatic hydrocarbons associated with urban aerosols. *Mutat. Res.* 371: 123–157.
- Fang, G.C., Wu, Y.S., Chen, J.C., Fu, P.P.C., Chang, C.N., Ho, T.T. and Chen, M.H. (2005). Characteristic study of polycyclic aromatic hydrocarbons for fine and coarse particulates at Pastureland near Industrial Park sampling site of central Taiwan. *Chemosphere* 60: 427–433.
- Gao, B., Wang, X.M., Zhao, X.Y., Ding, X., Fu, X.X., Zhang, Y.L., He, Q.F., Zhang, Z., Liu, T.Y., Huang, Z.Z., Chen, L.G., Peng, Y. and Guo, H. (2015). Source apportionment of atmospheric PAHs and their toxicity using PMF: Impact of gas/particle partitioning. *Atmos. Environ.* 103: 114–120.
- Garban, B., Blanchoud, H., Motelay-Massei, A., Chevreuil, M. and Ollivon, D. (2002). Atmospheric bulk deposition of PAHs onto France: Trends from urban to remote sites. *Atmos. Environ.* 36: 5395–5403.
- Goldstein, L.S. (2001). To BaP or not to BaP? That is the question. *Environ. Health Perspect.* 109: A356–A357.
- Guo, H., Lee, S.C., Ho, K.F., Wang, X.M. and Zou, S.C. (2003). Particle-associated polycyclic aromatic hydrocarbons in urban air of Hong Kong. *Atmos. Environ.* 37: 5307–5317.
- Han, B., Ding, X., Bai, Z., Kong, S. and Guo, G. (2011). Source analysis of particulate matter associated polycyclic aromatic hydrocarbons (PAHs) in an industrial city in northeastern China. *J. Environ. Monit.* 13: 2597–2604.
- Harrison, R.M., Smith, D.J.T. and Luhana, L. (1996). Source apportionment of atmospheric polycyclic aromatic hydrocarbons collected from an urban location in Birmingham, U.K. *Environ. Sci. Technol.* 30: 825–832.
- He, J., Fan, S., Meng, Q., Sun, Y., Zhang, J. and Zu, F. (2014). Polycyclic aromatic hydrocarbons (PAHs) associated with fine particulate matters in Nanjing, China: Distributions, sources and meteorological influences. *Atmos. Environ.* 89: 207–215.
- Hoek, G., Brunekreef, B., Goldbohm, S., Fischer, P. and van den Brandt, P.A. (2002). Association between mortality and indicators of traffic-related air pollution in the



- Netherlands: A cohort study. *Lancet* 360: 1203–1209.
- IARC (International Agency for Research on Cancer) (2012). Agents Classified by the IARC Monographs. List of Classifications by Alphabetical Order, vol. 1e105 <http://monographs.iarc.fr/ENG/Classification/ClassificationsAlphaOrder.pdf>, Last Access: January 2012.
- Jiang, N., Yin, S., Guo, Y., Li, J., Kang, P., Zhang, R. and Tang, X. (2018). Characteristics of mass concentration, chemical composition, source apportionment of PM<sub>2.5</sub> and PM<sub>10</sub> and health risk assessment in the emerging megacity in China. *Atmos. Pollut. Res.* 9: 309–321.
- Kavouras, I.G., Koutrakis, P., Tsapakis, M., Lagoudaki, E., Stephanou, E.G., Von Baer, D. and Oyola, P. (2001). Source apportionment of urban particulate aliphatic and polynuclear aromatic hydrocarbons (PAHs) using multivariate methods. *Environ. Sci. Technol.* 35: 2288–2294.
- Kong, S., Lu, B., Ji, Y., Bai, Z., Xu, Y., Liu, Y. and Jiang, H. (2012). Distribution and sources of polycyclic aromatic hydrocarbons in size-differentiated re-suspended dust on building surfaces in an oilfield city, China. *Atmos. Environ.* 55: 7–16.
- Laden, F., Neas, L.M., Dockery, D.W. and Schwartz, J. (2000). Association of fine particulate matter from different sources with daily mortality in six US cities. *Environ. Health Perspect.* 108: 941–947.
- Li, G., Xia, X., Yang, Z., Wang, R. and Voulvoulis, N. (2006a). Distribution and sources of polycyclic aromatic hydrocarbons in the middle and lower reaches of the Yellow River, China. *Environ. Pollut.* 144: 985–993.
- Li, J., Zhang, G., Li, X.D., Qi, S.H., Liu, G.Q. and Peng, X.Z. (2006b). Source seasonality of polycyclic aromatic hydrocarbons (PAHs) in a subtropical city, Guangzhou, South China. *Sci. Total Environ.* 355: 145–155.
- Li, N., Sioutas, C., Cho, A., Schmitz, D., Misra, C., Sempf, J., Wang, M., Oberley, T., Froines, J. and Nel, A. (2003). Ultrafine particulate pollutants induce oxidative stress and mitochondrial damage. *Environ. Health Perspect.* 111: 455–460.
- Li, Z., Porter, E.N., Sjödin, A., Needham, L.L., Lee, S., Russell, A.G. and Mulholland, J.A. (2009). Characterization of PM<sub>2.5</sub>-bound polycyclic aromatic hydrocarbons in Atlanta—Seasonal variations at urban, suburban, and rural ambient air monitoring sites. *Atmos. Environ.* 43: 4187–4193.
- Lim, S.S., Vos, T., Flaxman, A.D., Danaei, G., Shibuya, K., Adair-Rohani, H. et al. (2012). A comparative risk assessment of burden of disease and injury attributable to 67 risk factors and risk factor clusters in 21 regions, 1990–2010: a systematic analysis for the Global Burden of Disease study 2010. *Lancet* 380: 2224–2260.
- Lin, X. (2016) Chemical composition characteristics and source apportionment in PM<sub>2.5</sub> in Autumn of Nanchang City. Huaqiao University (in Chinese).
- Liu, X., Shi, C., Xu, X., Li, X., Xu, Y., Huang, H., Zhao, Y., Zhou, Y., Shen, H., Chen, C. and Wang, G. (2017a). Spatial distributions of  $\beta$ -cyclocitral and  $\beta$ -ionone in the sediment and overlying water of the west shore of Taihu Lake. *Sci. Total Environ.* 579: 430–438.
- Liu, Y., Yan, C., Ding, X., Wang, X., Fu, Q., Zhao, Q., Zhang, Y., Duan, Y., Qiu, X. and Zheng, M. (2017b). Sources and spatial distribution of particulate polycyclic aromatic hydrocarbons in Shanghai, China. *Sci. Total Environ.* 584: 307–317.
- Malcolm, H.M. and Dobson, S. (1994). The calculation of an Environmental Assessment Level (EAL) for atmospheric PAHs using relative potencies. Department of the Environment, London.
- Manoli, E., Kouras, A., Karagkiozidou, O., Argyropoulos, G., Voutsas, D. and Samara, C. (2016). Polycyclic aromatic hydrocarbons (PAHs) at traffic and urban background sites of northern Greece: Source apportionment of ambient PAH levels and PAH-induced lung cancer risk. *Environ. Sci. Pollut. Res.* 23: 3556–3568.
- Martíćid, R., Llobet, J.M., Castell, V. and Domingo, J.L. (2008). Evolution of the dietary exposure to polycyclic aromatic hydrocarbons in Catalonia, Spain. *Food Chem. Toxicol.* 46: 3163–3171.
- Masiol, M., Hofer, A., Squizzato, S., Piazza, R., Rampazzo, G. and Pavoni, B. (2012). Carcinogenic and mutagenic risk associated to airborne particle-phase polycyclic aromatic hydrocarbons: A source apportionment. *Atmos. Environ.* 60: 375–382.
- Mo, Z., Wang, Z., Mao, G., Pan, X., Wu, L., Xu, P., Chen, S., Wang, A., Zhang, Y., Luo, J., Ye, X., Wang, X., Chen, Z. and Lou, X. (2019). Characterization and health risk assessment of PM<sub>2.5</sub>-bound polycyclic aromatic hydrocarbons in 5 urban cities of Zhejiang Province, China. *Sci. Rep.* 9: 7296.
- Mudway, I.S., Stenfors, N., Duggan, S.T., Roxborough, H., Zielinski, H., Marklund, S.L., Blomberg, A., Frew, A.J., Sandström, T. and Kelly, F.J. (2004). An in vitro and in vivo investigation of the effects of diesel exhaust on human airway lining fluid antioxidants. *Arch. Biochem. Biophys.* 423: 200–212.
- Ning, Z. and Sioutas, C. (2010). Atmospheric processes influencing aerosols generated by combustion and the inference of their impact on public exposure: A review. *Aerosol Air Qual. Res.* 10: 43–58.
- Nisbet, I.C. and Lagoy, P.K. (1992). Toxic equivalency factors (TEFs) for polycyclic aromatic hydrocarbons (PAHs). *Regul. Toxicol. Pharm.* 16: 290–300.
- Pankow, J.F. (1994a). An absorption model of gas/particle partitioning of organic compounds in the atmosphere. *Atmos. Environ.* 28: 185–188.
- Pankow, J.F. (1994b). An absorption model of the gas/aerosol partitioning involved in the formation of secondary organic aerosol. *Atmos. Environ.* 28: 189–193.
- Peters, A., von Klot, S., Heier, M., Trentinaglia, I., Hörmann, A., Wichmann, H.E. and Löwel, H. (2004). Exposure to traffic and the onset of myocardial infarction. *N. Engl. J. Med.* 351: 1721–1730.
- Ravindra, K., Bencs, L., Wauters, E., de Hoog, J., Deutsch, F., Roekens, E., Bleux, N., Berghmans, P. and Van Grieken, R. (2006). Seasonal and site-specific variation in vapour and aerosol phase PAHs over Flanders (Belgium) and their relation with anthropogenic activities. *Atmos. Environ.* 40: 771–785.

2306

Liu et al., *Aerosol and Air Quality Research*, 19: 2294–2307, 2019

- Ravindra, K. and Grieken, S.R.V. (2008). Atmospheric polycyclic aromatic hydrocarbons: Source attribution, emission factors and regulation. *Atmos. Environ.* 42: 2895–2921.
- Ravindra, K., Wauters, E. and Van Grieken, R. (2008). Variation in particulate PAHs levels and their relation with the transboundary movement of the air masses. *Sci. Total Environ.* 396: 100–110.
- Shao, Z., Bi, J., Ma, Z. and Wang, J. (2017). Seasonal trends of indoor fine particulate matter and its determinants in urban residences in Nanjing, China. *Build. Environ.* 125: 319–325.
- Simayi, M., Yahefu, P. and Han, M. (2018). Spatiotemporal variation, source analysis, and health risk assessment of particle-bound PAHs in Urumqi, China. *Aerosol Air Qual. Res.* 18: 2728–2740.
- Simoneit, B.R.T., Kobayashi, M., Mochida, M., Kawamura, K., Lee, M., Lim, H.J., Turpin, B.J. and Komazaki, Y. (2004). Composition and major sources of organic compounds of aerosol particulate matter sampled during the ACE-Asia campaign. *J. Geophys. Res.* 109: D19S10.
- SPCC Co. (2001). SPSS for Windows in medical science. Ma, B.R. (Ed.), Science Press, Beijing (207 pp).
- Sun, S., Xia, Z., Wang, T., Wu, M., Zhang, Q., Yin, J., Zhou, Y., Yang, H., Wang, W., Yu, Y., Xu, J. and Chen, C. (2016). Pollution level, sources, and lung cancer risk of PM<sub>10</sub>-bound polycyclic aromatic hydrocarbons (PAHs) in summer in Nanjing, China. *J. Chem.* 2016: 4546290.
- U.S. EPA (1989). Risk assessment guidance for Superfund, Volume I, Human health evaluation manual (Part A). U.S. Environmental Protection Agency.
- U.S. EPA (1994). Peer review and peer involvement at the U.S. Environmental Protection Agency. Science Policy Council, Office of the Science Advisor, United States Environmental Protection Agency, ID 2872, <http://epa.gov/osa/spc/htm/perevmem.htm>.
- Venkataraman, C., Lyons, J.M. and Friedlander, S.K. (1994). Size distributions of polycyclic aromatic hydrocarbons and elemental carbon. 1. sampling, measurement methods, and source characterization. *Environ. Sci. Technol.* 28: 555–562.
- Wang, C., Dao, X., Zhang, L.L., Lv, Y.B. and Teng, E.J. (2015). Characteristics and toxicity assessment of airborne particulate polycyclic aromatic hydrocarbons of four background sites in China. *China Environ. Sci.* 35: 3543–3549 (in Chinese).
- Wang, G., Huang, L., Zhao, X., Niu, H. and Dai, Z. (2006). Aliphatic and polycyclic aromatic hydrocarbons of atmospheric aerosols in five locations of Nanjing urban area, China. *Atmos. Res.* 81: 54–66.
- Wang, J., Guinot, B., Dong, Z., Li, X., Xu, H., Xiao, S., Ho, S.S.H., Liu, S. and Cao, J. (2017a). PM<sub>2.5</sub>-bound polycyclic aromatic hydrocarbons (PAHs), oxygenated-PAHs and phthalate esters (PAEs) inside and outside middle school classrooms in Xi'an, China: Concentration, Characteristics and health risk assessment. *Aerosol Air Qual. Res.* 17: 1811–1824.
- Wang, T., Xia, Z., Wu, M., Zhang, Q., Sun, S., Yin, J., Zhou, Y. and Yang, H. (2017b). Pollution characteristics, sources and lung cancer risk of atmospheric polycyclic aromatic hydrocarbons in a new urban district of Nanjing, China. *J. Environ. Sci.* 55: 118–128.
- Wilson, J.G., Kingham, S., Pearce, J. and Sturman, A.P. (2005). A review of intraurban variations in particulate air pollution: Implications for epidemiological research. *Atmos. Environ.* 39: 6444–6462.
- Wongphatarakul, V., Friedlander, S.K. and Pinto, J.P. (1998). A comparative study of PM<sub>2.5</sub> ambient aerosol chemical databases. *Environ. Sci. Technol.* 32: 3926–3934.
- Wright, L.P., Zhang, L., Cheng, I., Aherne, J. and Wentworth, G.R. (2018). Impacts and effects indicators of atmospheric deposition of major pollutants to various ecosystems-A review. *Aerosol Air Qual. Res.* 18: 1953–1992.
- Wu, D., Wang, Z., Chen, J., Kong, S., Fu, X., Deng, H., Shao, G. and Wu, G. (2014). Polycyclic aromatic hydrocarbons (PAHs) in atmospheric PM<sub>2.5</sub> and PM<sub>10</sub> at a coal-based industrial city: Implication for PAH control at industrial agglomeration regions, China. *Atmos. Res.* 149: 217–229.
- Xia, Z., Duan, X., Tao, S., Qiu, W., Liu, D., Wang, Y., Wei, S., Wang, B., Jiang, Q., Lu, B., Song, Y. and Hu, X. (2013). Pollution level, inhalation exposure and lung cancer risk of ambient atmospheric polycyclic aromatic hydrocarbons (PAHs) in Taiyuan, China. *Environ. Pollut.* 173: 150–156.
- Xie, M., Barsanti, K.C., Hannigan, M.P., Dutton, S.J. and Vedral, S. (2013). Positive matrix factorization of PM<sub>2.5</sub> - eliminating the effects of gas/particle partitioning of semivolatile organic compounds. *Atmos. Chem. Phys.* 13: 7381–7393.
- Xie, M., Hannigan, M.P. and Barsanti, K.C. (2014). Impact of gas/particle partitioning of semivolatile organic compounds on source apportionment with positive matrix factorization. *Environ. Sci. Technol.* 48: 9053–9060.
- Xu, C., Liu, M., Zhang, C., An, S., Yu, W. and Chen, J.M. (2007). The spatiotemporal dynamics of rapid urban growth in the Nanjing metropolitan region of China. *Landscape Ecol.* 22: 925–937.
- Yang, H.H., Lee, W.J., Chen, S.J. and Lai, S.O. (1998). PAH emission from various industrial stacks. *J. Hazard. Mater.* 60: 159–174.
- Yang, Y., Guo, P., Zhang, Q., Li, D., Zhao, L. and Mu, D. (2010). Seasonal variation, sources and gas/particle partitioning of polycyclic aromatic hydrocarbons in Guangzhou, China. *Sci. Total Environ.* 408: 2492–2500.
- Yunker, M.B., Snowdon, L.R., Macdonald, R.W., Smith, J.N., Fowler, M.G., Skibo, D.N., McLaughlin, F.A., Danyushevskaya, A.I., Petrova, V.I. and Ivanov, G.I. (1996). Polycyclic aromatic hydrocarbon composition and potential sources for sediment samples from the Beaufort and Barents Seas. *Environ. Sci. Technol.* 30: 1310–1320.
- Zhai, Y., Li, P., Zhu, Y., Xu, B., Peng, C., Wang, T., Li, C. and Zeng, G. (2016). Source apportionment coupled with gas/particle partitioning theory and risk assessment of polycyclic aromatic hydrocarbons associated with size-segregated airborne particulate matter. *Water Air Soil Pollut.* 227: 44.
- Zhang, J., Li, S., Li, S., Chen, Y., Lei, Z. and Zhang, Z.



*Liu et al., Aerosol and Air Quality Research*, 19: 2294–2307, 2019

2307

- (2017). Therapeutic effects of stemonine on particulate matter 2.5-induced chronic obstructive pulmonary disease in mice. *Exp. Ther. Med.* 14: 4453.
- Zhang, N., Cao, J., Li, L., Ho, S. S. H., Wang, Q., Zhu, C. and Wang, L. (2018). Characteristics and source identification of polycyclic aromatic hydrocarbons and n-alkanes in PM<sub>2.5</sub> in Xiamen. *Aerosol Air Qual. Res.* 18: 1673–1683.
- Zhang, Y., Yang, L., Zhang, X., Li, J., Zhao, T., Gao, Y., Jiang, P., Li, Y., Chen, X. and Wang, W. (2019). Characteristics of PM<sub>2.5</sub>-bound PAHs at an urban site and a suburban site in Jinan in North China Plain. *Aerosol Air Qual. Res.* 19: 871–884.

*Received for review, June 12, 2019*

*Revised, September 11, 2019*

*Accepted, September 14, 2019*



### 6.4.2 Publication 2

**Title:** A comparative study of persistent DNA oxidation and chromosomal instability induced in vitro by oxidizers and reference airborne particles

**Authors:** Xin Cao, Sara Padoan, Stephanie Binder, Stefanie Bauer, Jürgen Orasche, Corina-Marcela Rus, Ajit Mudan, Anja Huber, Evelyn Kuhn, Sebastian Oeder, Jutta Lintelmann, Thomas Adam, Sebastiano Di Bucchianico, Ralf Zimmermann

**Journal:** Mutation Research - Genetic Toxicology and Environmental Mutagenesis

**Year:** Accepted (2022)

<p><b>Contribution:</b> For this publication, Xin Cao carried out the experiments, made data process, and wrote the manuscript.</p>
---

**A comparative study of persistent DNA oxidation and chromosomal instability induced *in vitro* by oxidizers and reference airborne particles**

Xin Cao <sup>a,b</sup>, Sara Padoan <sup>a,c</sup>, Stephanie Binder <sup>a,b</sup>, Stefanie Bauer <sup>a</sup>, Jürgen Orasche <sup>a</sup>, Corina-Marcela Rus <sup>b,d</sup>, Ajit Mudan <sup>c</sup>, Anja Huber <sup>a</sup>, Evelyn Kuhn <sup>a</sup>, Sebastian Oeder <sup>a</sup>, Jutta Lintelmann <sup>c</sup>, Thomas Adam <sup>a,c</sup>, Sebastiano Di Bucchianico <sup>a,\*</sup>, Ralf Zimmermann <sup>a,b</sup>

<sup>a</sup> Joint Mass Spectrometry Center, Comprehensive Molecular Analytics, Helmholtz Zentrum München, Neuherberg, Germany.

<sup>b</sup> Joint Mass Spectrometry Center at Analytical Chemistry, Institute of Chemistry, University of Rostock, Rostock, Germany.

<sup>c</sup> Institute of Chemistry and Environmental Engineering, University of the Bundeswehr Munich, Neubiberg, Germany.

<sup>d</sup> Centogene GmbH, Rostock, Germany.

<sup>e</sup> Research Unit of Molecular Endocrinology and Metabolism, Helmholtz Zentrum München, Neuherberg, Germany.

\* Corresponding author: dibucchianico@helmholtz-muenchen.de (Sebastiano Di Bucchianico)

**Abstract**

Adverse health effects driven by airborne particulate matter (PM) are mainly associated with reactive oxygen species formation, pro-inflammatory effects, and genome instability. Therefore, a better understanding of the underlying mechanisms is needed to evaluate health risks caused by exposure to PM. The aim of this study was to compare the genotoxic effects of two oxidizing agents (menadione and 3-chloro-1,2-propanediol) with three different reference PM (fine dust ERM-CZ100, urban dust SRM1649, and diesel PM SRM2975) on monocytic THP-1 and alveolar epithelial A549 cells. We assessed DNA oxidation by measuring the oxidized derivative 8-hydroxy-2'-deoxyguanosine (8-OHdG) following short and long exposure times to evaluate the persistency of oxidative DNA damage. Cytokinesis-block micronucleus cytome assay was performed to assess chromosomal instability, cytostasis, and cytotoxicity. Particles were characterized by inductively coupled plasma mass spectrometry in terms of selected elemental content, the release of ions in cell medium and the cellular uptake of metals. PM deposition and cellular dose were investigated by a spectrophotometric method on adherent A549 cells. The level of lipid peroxidation was evaluated via malondialdehyde concentration measurement. Despite differences in the tested concentrations, deposition efficiency, and lipid peroxidation levels, all reference PM samples caused oxidative DNA damage to a similar extent as the two oxidizers in terms of magnitude but with different oxidative DNA damage persistence. Diesel particles were more effective in inducing chromosomal instability with respect to fine and urban dust highlighting the role of polycyclic aromatic hydrocarbons derivatives on chromosomal instability. The persistence of 8-OHdG lesions strongly correlated with different types of chromosomal damage and revealed distinguishing sensitivity of cell types as well as specific features of particles versus oxidizing agent effects. In conclusion, this study revealed that an interplay between DNA oxidation persistence and chromosomal damage is driving particulate matter-induced genome instability.

### *Keywords*

Oxidative DNA damage; Genotoxicity; Micronuclei; Reference particulate matter; Oxidizing agents.

### *Abbreviations*

PM, particulate matter; CZ100, fine dust ERM-CZ100; UD 1649, urban dust SRM1649; diesel PM2975, diesel PM SRM2975; 3-MCPD, 3-chloro-1,2-propanediol; 8-OHdG, 8-hydroxy-2'-deoxyguanosine; PAHs, polycyclic aromatic hydrocarbons; MAPK, mitogen-activated protein kinase; MDA, malondialdehyde; NF- $\kappa$ B, nuclear factor  $\kappa$ B; AP-1, activator protein 1; MN, micronuclei; NPB, nucleoplasmic bridge; NBUD, nuclear bud; ROS, reactive oxygen species; EMS, ethyl methanesulfonate; FBS, fetal bovine serum; PBS, phosphate buffered saline; DMSO, dimethyl sulfoxide; dG, 2'-deoxyguanosine; TE buffer, tris-EDTA buffer; SPE, solid phase extraction; LC-MS/MS, liquid chromatography tandem mass spectrometry; MRM, multiple reaction monitoring; LC-UV, liquid chromatography ultraviolet detection; CBMN Cyt assay, cytokinesis-block micronucleus cytome assay; SEM, standard error of mean; CBPI, cytokinesis-block proliferation index; MI, mitotic index; mono, mononucleated cells; BN, binucleated cells; CYP1A1, cytochrome P450 family 1 subfamily A polypeptide 1.

## **1. Introduction**

A number of studies have linked airborne particulate matter (PM) exposure with a wide range of human diseases including cardiopulmonary failure, type II diabetes mellitus, neurological disorders and cancer [1,2,3]. PM-induced adverse effects involve oxidative stress and inflammation, which in turn may lead to different genetic alterations [4]. DNA damage and repair play a pivotal role in the pathogenesis of asthma and the telomeric erosion caused by oxidative stress was proven as a mechanism underlying PM related cardiovascular disease [5,6]. Particularly in susceptible populations, PM is an important environmental factor that exacerbates inflammatory processes by cellular responses to PM-induced oxidative stress [7]. It is widely recognized that the adverse health effects of PM exposure are mediated by oxidative stress and the induction of inflammation is mediated by signaling pathways (e.g. MAPK) and transcription factors (e.g. NF- $\kappa$ B, AP-1) [8]. Airborne PM contains a complex mixture of toxic compounds – including polycyclic aromatic hydrocarbons (PAHs), their derivatives such as nitrated PAHs (nitro-PAHs) and transition metals – and it is composed of different size fractions that may induce diverse toxic mechanisms of action and effects. While the PAHs compounds in PM can form stable bulky DNA adducts, which inhibit DNA replication and transcription, metals primarily act as oxidizing agents inducing 8-hydroxy-2'-deoxyguanosine (8-OHdG) formation as well as DNA single and double strand breaks [9,10,11].

Chromatin is a dynamic entity that responds to environmental cues in terms of structure and function and its organization may be disrupted *inter alia* by, for example, the formation of DNA strand breaks. Failure of subsequent repairing processes and cell cycle checkpoints may lead to mutations and chromosomal rearrangements that result in phenotypic changes or ultimately result in cell death [12,13]. In particular, DNA double strand breaks are considered as a critical primary lesion for the formation of chromosomal aberrations [14]. In this context, the present study aimed at investigating the correlation between PM-induced persistent oxidative DNA damage, evaluated via measurements of 8-OHdG formation, and chromosomal instability as determined in terms of micronuclei (MN), nucleoplasmic bridges (NPB), and nuclear buds (NBUD) induction as well as mitotic dysfunction and



cell death. Oxidative stress, considered as the underlying mechanism of PM-induced genotoxicity, was detected by measuring one of the end product of lipid peroxidation, malondialdehyde (MDA). This study also focused on the role of bioavailable metals in PM induced toxic effects versus the total PM metal content. For this scope, nine elements, namely vanadium, chromium, manganese, iron, nickel, copper, zinc, arsenic, cadmium, and lead were determined by inductively coupled plasma mass spectrometry (ICP-MS) in PM samples. Additionally, relative levels of those metals were determined intra- and extracellularly following cell exposures to reference PM.

To address the role of different PAHs and metals in driving persistent oxidative DNA damage and subsequent chromosomal instability on different functional levels, two cell models were used: human monocytes THP-1 and alveolar epithelial A549 cell lines. Monocyte-like THP-1 cells represent an immune-competent cell model to elucidate the influence of immunological mechanisms on particles induced toxicity [15]. The widely used A549 type II pulmonary epithelial cells may give rise to a better understanding of particle-induced mutagenicity/carcinogenicity on lung cells, which is associated with oxidative stress and chromosomal instability. To study the variability of biomarkers for genetic toxicology, which are potentially induced by different ambient PM with diverse chemical identity and similar size distribution, three standard reference materials (SRM) were chosen: i) fine dust ERM-CZ100 (referred to as CZ100 in this paper); ii) urban dust SRM 1649 (UD 1649); iii) diesel PM SRM 2975 (diesel PM). CZ100 consisted of road dust collected in a tunnel in Poland and was released in 2010. It is rich in metals with a similar PAH distribution as UD 1649, an airborne dust from the Washington urban area collected in the late '70s. The NIST-certified diesel PM consists of diesel combustion emissions from diesel-powered forklifts and was distributed as diesel reference material since the year 2000. The diesel PM can be characterized as nitro- and alkyl-PAH rich PM mixture. Typically, these diesel particles contain less amount of PAH with five or more condensed aromatic rings (e.g. Benz[a]pyrene). Certified values of certain PAHs and their derivatives are shown in table S1 and the certified elements composition are presented in table S2 of supplementary material.

We compared the effects of the three reference PM with two oxidative and genotoxic substances: menadione and 3-chloro-1,2-propanediol (3-MCPD). Both compounds are known to promote the generation of reactive oxygen species and to induce cellular oxidative stress [16,17]. Possible correlations between the persistence of DNA oxidation and genotoxic endpoints were analyzed by Pearson correlation coefficients.

## 2. Material and methods

### 2.1 Materials and reagents

8-OHdG, 2'-deoxyadenosine, 2'-deoxyguanosine monohydrate, thymidine, malondialdehyde tetra butylammonium salt, 2,4-dinitrophenylhydrazine, ammonium acetate, formic acid, 3-chloro-1,2-propanediol, ethyl methanesulfonate, dimethyl sulfoxide, and fine dust ERM-CZ100 were purchased from Sigma (Taufkirchen, Germany). 2'-Deoxycytidine was obtained from Alfa Aesar (Kandel, Germany). Internal standard  $^{15}\text{N}_5$ -8-OHdG and 1,1,3,3-Tetraethoxypropane (1,3-d2) were purchased from Cambridge Isotope Laboratories, Inc. (Massachusetts, USA). Menadione was purchased from AppliChem (Damstadt, Germany). LC-MS grade acetonitrile and methanol were obtained from ChemSolute (Munich, Germany). LC-MS grade water was generated by a Milli-Q Reference System from Merck (Darmstadt, Germany). THP-1 cells were bought from ECACC (No. 88081201). A549 cells were from Leibniz Institute DSMZ (Braunschweig, Germany, ACC 107). LiChrolut® EN 200MG 3 mL cartridges were purchased from Merck (Darmstadt, Germany). Acrodisc® Syringe Filters 13 mm, 0.2 µm GHP were obtained from Waters (New York, USA). Degradase Plus™ were from Zymo Research (Freiburg, Germany). Urban dust SRM1649 and diesel PM SRM2975 were from the

National Institute of Standards and Technology (Gaithersburg, USA). N-hexane (GC-grade) was obtained from VWR (Darmstadt, Germany).

## 2.2 Cell culture, particle exposures, and cell viability

THP-1 and A549 cells were cultured in Roswell Park Memorial Institute medium (supplemented with 10% Fetal Bovine Serum, 2 mM L-glutamine, and 1 % penicillin/streptomycin solution) and incubated at 37 °C, 5% CO<sub>2</sub> in a humidified atmosphere and sub-cultured at 80% confluency. Particulate matter suspension (1 mg/mL) in cell culture medium without FBS were prepared freshly before exposure and dispersed using an ultrasonic bath for 20 min. Menadione and 3-MCPD stock solutions (10 mg/mL) were prepared in DMSO and water, respectively, and diluted in culture medium with FBS before exposure. Concentration-response curves of the tested compounds were made to find the concentration which results in approximately 90% cell viability for subsequent endpoints in order to avoid cytotoxic conditions. THP-1 and A549 cell viability was evaluated using trypan blue dye exclusion after exposure to different concentrations of the test substances for 24 h. Briefly, A549 and THP-1 cells (0.06 and 0.12 million cells/cm<sup>2</sup> in T25 flasks 24 h prior to exposure) were exposed to different concentrations of menadione (0.1-10 µg/mL, 0.2 % DMSO (v/v) final concentration), 3-MCPD (0.1-10 µg/mL), CZ100 (1-1000 µg/mL), UD 1649 (1-1000 µg/mL) and diesel PM (1-100 µg/mL). For the following experiments, 2 µg/mL menadione or 3-MCPD, 200 µg/mL (40 µg/cm<sup>2</sup>) of CZ100 or UD1649, and 40 µg/mL (8 µg/cm<sup>2</sup>) of diesel PM were chosen as the concentrations giving rise to approx. 90% cell viability.

## 2.3 Particle deposition analysis

Particle deposition analysis was performed in adherent A549 cells according to a previous report by Rudd with minor modifications [18]. Briefly, A549 cells (0.06 million cells/cm<sup>2</sup> in T-25 flasks) were seeded 24h prior the exposure to different PM (200 µg/mL CZ100 or UD 1649 or 40 µg/mL diesel PM) for 48h in three independent experiments. Cells were washed twice with PBS and collected by centrifugation after trypsinization. The cell pellet was resuspended in 1 mL of 4N KOH: ethanol (1:1, v/v) by using an ultrasonic bath for 20 min. The suspension was kept in a Thermomixer C (Eppendorf, Germany) at room temperature overnight at 1000 rpm for cell digestion. Afterwards, the suspension was centrifuged at 9390 rcf for 20 min (in 2 mL eppendorf tube). The supernatant was discarded and the pellet was resuspended in 1 mL of water in an ultrasonic bath for 20 min. Finally, the sample absorbance was measured at 748 nm in a Multiskan™ FC Microplate Photometer (Thermo Scientific™, Germany) and the deposited dose was calculated by using standard curves.

## 2.4 Elemental composition analysis by inductively coupled plasma mass spectrometry (ICP-MS)

Following 48h exposure to 200 µg/mL of CZ100 or UD 1649, and 40 µg/mL of diesel PM, the cellular uptake of the elements arsenic, cadmium, chromium, vanadium, manganese, copper, nickel, zinc and lead and the release of their respective ions from the particles into cell culture medium was quantified by ICP-MS. At the end of the exposure, cell culture supernatants were collected and A549 and THP-1 cells were harvested and counted. Then, A549 and THP-1 supernatants as well as the collected cells were acidified with a mixture of nitric acid (69%) and hydrogen peroxide (35%). Subsequently, they were digested by a Microwave speedwave ENTRY (Berghof, Germany) and diluted to a final concentration of 5% of HNO<sub>3</sub>. All samples were filtered through a 0.2 µm syringe filter and analyzed by an Agilent 7700 Series ICP-MS. Calibration standard curves of 0.1, 1, 10, 100 and 300 µg/L for all measured elements except iron were used for the quantification. For iron, a calibration standard curve of 10, 100, 1000, 10000 and 30000 µg/L was used. The calibration curves were prepared from the initial calibration verification standard (Agilent, USA): 10 ppm for arsenic, cadmium, chromium,



vanadium, manganese, copper, nickel, zinc, lead and 100 ppm for iron in a matrix of 5% of nitric acid. All samples were spiked with 20 µg/L of scandium and rhodium and used as internal standards. For each sample 3 technical repetitions were performed. The Detection Limit (DL) for V, Cr, Mn, Ni, Cu, As, Cd and Pb was lower than 0.01 µg/L both in the supernatants and in the cell fractions. For Fe and Zn the DL it was lower than 0.4 µL in both phases. All samples were measured above the detection limits.

## 2.5 Membrane lipid peroxidation estimation

The formation of malondialdehyde (MDA) was used to evaluate membrane lipid peroxidation as a biomarker of oxidative stress. MDA derivatization was performed according to a published method developed by our group with minor modifications [19]. Briefly, after 4h, 48h or 72h exposures 20 µL of cell culture medium was mixed with 25 µL of 100 ng/mL d2-MDA (internal standard solution in water) and 500 µL of 0.5 mM DNPH (in 1% formic acid solution). The mixture was kept at 37 °C and 300 rpm for 70 min in a Thermomixer C (Eppendorf, Germany). After derivatization, 700 µL of n-hexane was added and the mixture was vigorously shaken and centrifuged at 9390 rcf for 5 min in a Heraeus™ Biofuge Pico® Centrifuge (Thermo scientific, Germany). The n-hexane supernatant was transferred to a new 2 mL tube and 700 µL of fresh n-hexane was added to the mixture. Then the extraction procedure was repeated and both n-hexane supernatants were combined and dried by nitrogen in a Vapotherm basis mobil I (Barkey, Germany) at room temperature. The dried residue was re-dissolved in 50 µL of methanol:0.1% formic acid (80:20, v/v).

The MDA adduct (MDA-DNPH) was analyzed using a triple quadrupole mass spectrometer Qtrap 4000 (AB Sciex, USA) equipped with a Turbo V™ Source (Sciex, USA) enabling electrospray ionization and coupled to an HPLC system (Agilent 1290 HPLC, Agilent Technologies, USA) including a degasser, a binary pump, an autosampler, and a column compartment. The used mass spectrometer parameters were a capillary voltage of 4.5 kV, a source temperature of 350 °C, a nebulizer gas at 40 psi, heater gas 50 psi, curtain gas 20 psi, and collision gas 11 psi. The column compartment was set to 20 °C. The autosampler was set to 10 °C. The measurement was performed using multiple reaction monitoring in positive ion mode. Two transitions were selected (Table S3, supplement information). The first transition was used for quantification and the second transition was used for qualification. The separation column was a Kinetex C18 (2.6 µm, 100 Å, 100×3 mm i.d., Phenomenex, Germany). The mobile phase was methanol:0.1% formic acid (80:20, v/v) with a constant flow of 200 µL/min. Ten µL of each sample were injected twice into the HPLC column, and the solvent fraction eluting from 1.5 to 3.5 min from the analytical column was infused into the MS for measurement. A standard calibration curve was set up for quantification (0.4, 0.8, 2, 4, 8, 20 ng/ml). The MDA background in the blank medium without cells was subtracted from the concentration in the sample with cells and further normalized by using the respective cell number.

## 2.6 DNA extraction, and DNA hydrolysis

A549 and THP-1 cells were seeded and treated as described in the subsection 2.2 for 4h and 72h with 2 µg/mL of menadione or 3-MCPD, 200 µg/mL of CZ100 or UD 1649, or 40 µg/mL of diesel PM. DNA extraction was performed according to a salting out procedure [20]. Quantity and purity of DNA were measured spectrophotometrically (Nanodrop, Thermo Fisher, Germany). For DNA hydrolysis, 200 µg of DNA (dissolved in 400 µL of TE buffer) was mixed with 2 µL of DNA degradase plus™ according to the manufacturer's protocol and kept on an Eppendorf Thermo Mixer C with 850 rpm at 37 °C for 24 h. After DNA hydrolysis, the mixture was heated to 70 °C for 20 min to deactivate the enzyme. An aliquot of the hydrolysate was processed by solid phase extraction (using LiChrolut® EN 200MG 3 mL cartridges) and analyzed by LC-MS/MS for 8-OHdG. A second aliquot of the

hydrolysate was filtered (using Acrodisc® Syringe filters) and analyzed by LC-UV for 2'-deoxyguanosine.

### 2.6.1 Solid phase extraction

The DNA hydrolysate (350 µL) was mixed with 50 µL of water and 100 µL of internal standard solution (<sup>15</sup>N<sub>5</sub>-8-OHdG, 10 ng/mL). The mixture was diluted to a total volume of 3 mL with water and the pH was adjusted to 5.0 for SPE. Firstly, 3 mL of acetonitrile, 3 mL of methanol, and 3 mL of water were used for conditioning and equilibration of the SPE cartridge. Secondly, the sample was loaded. Thirdly, 3 mL of water and 2 mL of acetonitrile were used for washing. Finally, 3 mL of methanol was applied for elution of 8-OHdG. The eluate was dried under a gentle nitrogen flow at room temperature and re-dissolved in 60 µL of the mobile phase (acetonitrile:water, 80:20, v/v) for LC-MS/MS analysis.

### 2.6.2 Determination of 8-OHdG levels

The LC-MS/MS-system used for the determination of 8-OHdG consisted of an HPLC coupled with a QTrap 4000 triple quadrupole mass spectrometer. The HPLC (Agilent 1290 HPLC, Agilent Technologies, USA) included a degasser, a binary pump, an autosampler, and a column compartment. The Qtrap 4000 was equipped with a Turbo V™ Source (Sciex, USA) enabling electrospray ionization. The following instrumental parameters were used for the mass spectrometric detection: capillary voltage, 5 kV; source temperature, 500 °C; nebulizer gas, 40 psi; heater gas, 50 psi; curtain gas, 20 psi. The measurements were carried out using multiple reaction monitoring in positive ion mode. Further parameters and the transition used are shown in Table S3. Analyst 1.6.2 software was used for instrumental control, data acquisition, and data analysis. A Eurospher II 100-3 HILIC column (3 µm, 100 Å, 100×3 mm i.d., Knauer, Germany) was utilized for chromatographic separation. The mobile phase consisted of a mixture of acetonitrile and water (80:20, v/v) with ammonium acetate (2 mM) at a constant flow rate of 300 µL/min. Both column oven and autosampler were set to 20 °C during analysis. The injection volume was 10 µL. Each sample was injected three times. The quantification of 8-OHdG in cells was done using a calibration curve based on relations between peak areas of the internal standard and 8-OHdG (0.16, 0.4, 1.0, 1.6, 4.0, 10, 16, 40, 100 ng/mL). For the separation and quantification of dG, an HPLC-UV system (UltiMate 3000, ThermoFisher, USA) was used. It consisted a degasser, a pump, an autosampler, a column compartment, and a UV-Vis detector. A Eurospher II 100-3 HILIC column (3 µm, 100 Å, 100×3 mm i.d., Knauer, Germany) was applied for the separation. The eluent was a mixture of acetonitrile and water (90:10, v/v) with ammonium acetate (20 mM) at a constant flow rate of 600 µL/min. The column oven and the autosampler were kept at 20 °C, and the detection wavelength for dG was 260 nm. The quantification of dG was performed using external calibration (dG, 0.5, 1, 2, 5, 10, 20 µg/mL).

### 2.7 Cytokinesis-block Micronucleus Cytome Assay

CBMN Cyt assay was performed according to Di Bucchianico et al. [21]. Briefly, A549 and THP-1 cells were seeded, as described in the subsection 2.2, 24h prior to exposure to different compounds (2 µg/mL of menadione or 3-MCPD, 200 µg/mL of CZ100 or UD 1649, or 40 µg/mL of diesel PM). Twenty hours after exposure, a final concentration of 5 µg/mL cytochalasin-B (Sigma-Aldrich) was used to block cytokinesis. Cells were harvested after an additional 28h culture for a total of 48h exposure to the tested compounds. 300 µg/mL ethyl methanesulfonate (EMS) was used as positive control while 0.2 % DMSO (v/v) was used as solvent control for menadione exposures. Two slides per condition were examined in three independent experiments. The cytokinesis-block proliferation index (CBPI) indicates the average number of cell cycles during the exposure and was evaluated as a measure of cytostasis. The number of apoptotic (APO), necrotic (NEC) and mitotic (MI) cells were



scored to evaluate the induced cytotoxicity. Micronuclei were evaluated in both binucleated (MN BN) and mononucleated (MN mono) cells to distinguishing between aneuploidogenic and clastogenic effects [22]. Additionally, nucleoplasmic bridges (NPB) and nuclear buds (NBUD) were also scored as biomarkers of chromosomal rearrangements and DNA repair, respectively [21].

## 2.8 Statistical analysis

Statistical analysis was performed using GraphPad Prism 9.1.2. One-way analysis of variance followed by multiple comparison versus control group (Dunnett's method) was used to test the statistical significance of results expressed as mean  $\pm$  standard error of mean of three independent experiments ( $n=3$ ). Pearson correlation coefficients were used for the correlation studies between MDA levels ratio, genotoxic effects and 8-OHdG persistence.

## 3. Results

### 3.1 ICP-MS elemental particles analysis

The elemental composition is available in the material certificates for few selected elements in UD 1649 and CZ100, or in Ball et al. for diesel PM [23]. Recently we published the mass fraction values of epigenetically active elements like As, Cd and Cr for the investigated reference materials [24]. For the present study, we conducted new ICP-MS analysis to evaluate the elemental concentration of V, Cr, Mn, Fe, Ni, Cu, Zn, and Pb, which could play an important role in inducing geno-toxicological effects. As shown in Table 1, UD 1649 contains the highest amount of metals, notably V, As, and Pb, with respect to CZ100 which in contrast contains higher fractions of Cr, Mn, Fe and Cu. Overall the mass fraction of metals in diesel PM was low compared to the other two PM samples, however, we detected considerable amounts of Fe and Zn.

Table 1. Determination of elemental concentrations (mg/kg) in the reference particles CZ100, UD 1649, and diesel PM as evaluated by ICP-MS. Data are shown as mean  $\pm$  standard deviation of three measurements. \*, measured in our previous study [24].

	Elements (mg/kg)		
	CZ100	UD 1649	diesel PM
Vanadium (V)	60 $\pm$ 1	349 $\pm$ 4	$\approx$ 0.1
Chromium (Cr)*	238 $\pm$ 6	145 $\pm$ 2	$\approx$ 4
Manganese (Mn)	586 $\pm$ 16	282 $\pm$ 2	$\approx$ 4
Iron (Fe)	38251 $\pm$ 920	28705 $\pm$ 335	602 $\pm$ 2
Nickel (Ni)	105 $\pm$ 3	177 $\pm$ 4	$\approx$ 3
Copper (Cu)	434 $\pm$ 12	273 $\pm$ 2	$\approx$ 9
Zinc (Zn)	1335 $\pm$ 28	2089 $\pm$ 16	737 $\pm$ 5
Arsenic (As)*	$\approx$ 9	78 $\pm$ 1	$\approx$ 1
Cadmium (Cd)*	$\approx$ 1	$\approx$ 28	$\approx$ 0.1
Lead (Pb)	117 $\pm$ 1	13393 $\pm$ 110	$\approx$ 10
Total (g/Kg)	$\approx$ 41	$\approx$ 46	$\approx$ 1.4

### 3.2 Cell viability assay

All tested compounds decreased cell viability in both epithelial A549 and monocytic THP-1 cells with increasing mass concentrations following 24h exposure (Fig. 1). Interestingly, the oxidizers menadione and 3-MCPD caused a severe decrease of cell viability in THP-1 cells, but not in A549 cells, starting from concentrations above 2  $\mu$ g/mL (Fig. 1a and 1b). 6  $\mu$ g/mL of menadione and 8



$\mu\text{g/mL}$  of 3-MCPD treatments caused a decrease of A549 cell viability to 90%. In contrast, THP-1 cell viability was reduced to 90 % with 2  $\mu\text{g/mL}$  of menadione and 3-MCPD exposures. These cell-type specific effects were not observed in exposures to PM (Fig. 1c-e). The cell viability of A549 and THP-1 cells decreased to 90% when treated with 200  $\mu\text{g/mL}$  of CZ100 or UD 1649 compared to 40  $\mu\text{g/mL}$  of diesel PM. To avoid cytotoxic conditions and the resulting confounding effects, we chose 2  $\mu\text{g/mL}$  of menadione or 3-MCPD, 200  $\mu\text{g/mL}$  of CZ100 or UD 1649, and 40  $\mu\text{g/mL}$  of diesel PM in the subsequent exposure experiments.

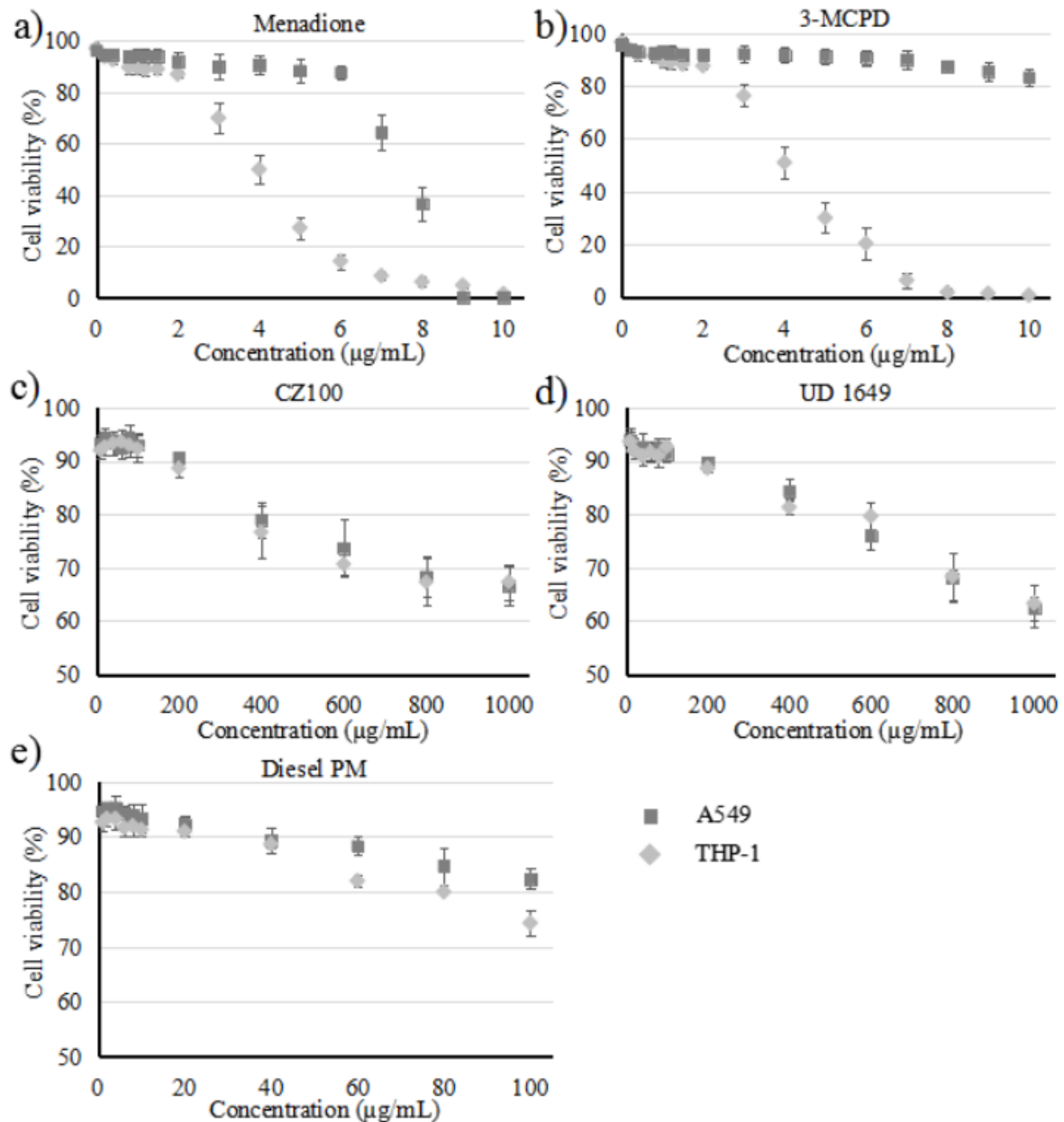


Fig. 1. Concentration-response curves for determining the concentrations of tested compounds for subsequent cell exposures. % cell viability of A549 and THP-1 cells is shown as mean  $\pm$  standard error from three independent experiments following 24h exposures to (a) menadione (b) 3-MCPD (c) fine dust CZ100 (d) urban dust UD 1649 (e) diesel PM.

### 3.3 Particle deposition analysis

UV-Vis spectrophotometric analysis of PM deposition on adherent A549 exposures was based on the detected amount of particles per surface area. In this study, 200  $\mu\text{g/mL}$  of CZ100 or UD 1649, or 40

$\mu\text{g/mL}$  of diesel PM were used with nominal concentrations in terms of mass per surface of  $40 \mu\text{g/cm}^2$ ,  $40 \mu\text{g/cm}^2$ , and  $8 \mu\text{g/cm}^2$ , respectively. Spectrophotometric deposition analysis revealed different deposition efficiencies among tested PM and the deposited mass were calculated as  $26 \pm 2 \mu\text{g/cm}^2$ ,  $34 \pm 2 \mu\text{g/cm}^2$ , and  $6 \pm 0.3 \mu\text{g/cm}^2$  for CZ100, UD 1649, and diesel PM, corresponding to a percentages of deposited particles of approximately 65 %, 85 %, and 76 %, respectively. Due to difficulties in removing particles not interacting with cells, UV-Vis spectrophotometric evaluation was not possible in suspension cultures performed with THP-1 cells.

### 3.4 ICP-MS ion release in cell culture medium and cellular uptake

In order to characterize the dissolution/ion release of selected elements in cell culture medium and their cellular uptake, ICP-MS analysis was conducted in both cell culture supernatants and cell pellets following 48h exposure to  $200 \mu\text{g/mL}$  of CZ100 or UD 1649, and  $40 \mu\text{g/mL}$  of diesel PM, of both A549 (Fig. 2a-c) and THP-1 cells (Fig. 2d-f). A similar distribution trend for V, Cr, Mn, Fe and Ni between the supernatant and the cells was observed following both A549 and THP-1 exposure to CZ100, where these elements are mostly taken up by cells. In comparison, the cellular content of Cu, As, Cd and Pb was equal or lower with respect to the supernatant content (Fig. 2a and 2d). However, for CZ100 exposure a different Zn distribution between supernatants and cells was noticed in the two used cell models, and THP-1 cells showed higher Zn uptake efficacy (ca. 85%) with respect to A549 cells (ca. 30%). This clear difference could not be observed following UD 1649 exposures where approx. 46% of Zn was taken up by A549 cells and approx. 36% by THP-1 cells (Fig. 2b and 2e). After exposure to diesel PM, A549 cells were taking up Fe more efficiently than monocytic THP-1 while the opposite effect was observed for V and Zn (Fig. 2c and 2f).

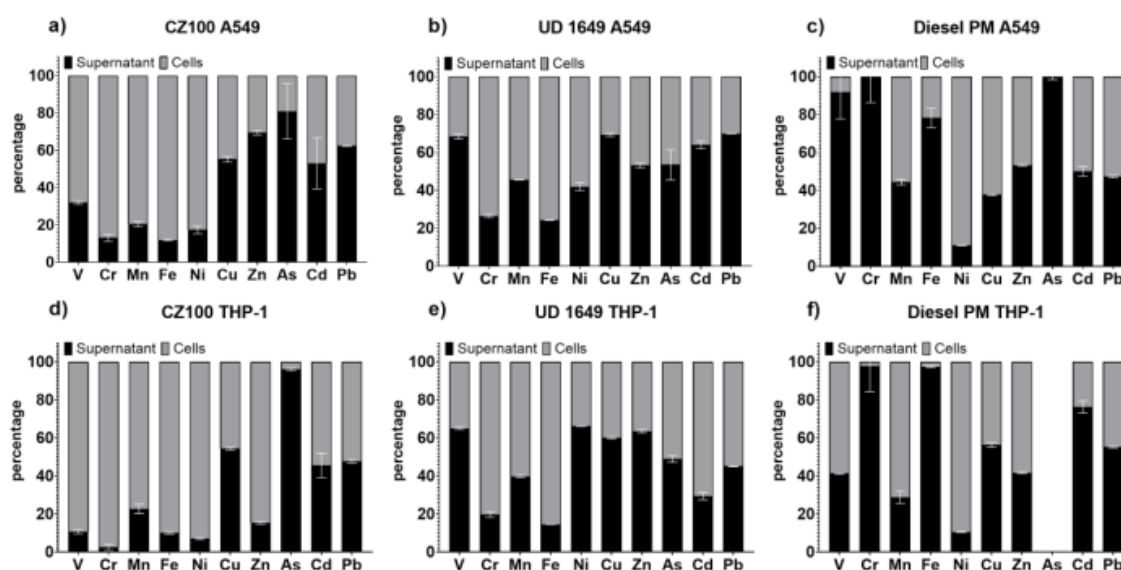


Fig. 2. The amount of selected elements was analyzed by ICP-MS following 48h exposure of A549 cells to CZ100 (a), UD 1649 (b), Diesel PM (c), and THP-1 cells to CZ100 (d), UD 1649 (e), and Diesel PM (f). Data are expressed as mean % distribution of elements in supernatant (black) and cells (gray)  $\pm$  SD.

The cellular associated elemental content was measured as  $\mu\text{g/L}$  and calculated as ng per  $10^6$  cells in both THP-1 (Fig. 3a) and A549 cells (Fig. 3b). The most abundant elements, which might differentiate between cell types and reference particles exposures, were Mn, Fe, Ni, Cu, Zn and Pb. However, both THP-1 and A549 cells took up considerable amount of V and Cr following exposures to CZ100 or UD 1649. No differences on Mn uptake were observed between the cell types and the higher cellular

content of Mn after CZ100 treatments was in line with the higher Mn content of CZ100 particle compared to that of UD 1649. Interestingly this coherency was not observed for Fe uptake, since no clear differences on iron cellular content could be shown after CZ100 or UD 1649 exposures despite the diverse particles content of Fe. This was especially the case in monocytic THP-1 exposure. Furthermore, the cellular Fe content was ten times higher, ca. 0.7 ng/10<sup>6</sup> cells, following A549 exposure to Diesel PM compared to THP-1 treatments. Clear differences between cell types as well as among reference particle treatments could be seen for Zn cellular content. Untreated A549 cells contained a larger amount of Zn compared to monocytic THP-1, ca. 52 ng/10<sup>6</sup> A549 cells versus ca. 28 ng/10<sup>6</sup> THP-1 cells. Following exposures to PM, the cellular content of Zn was decreasing in A549 cells regardless of the particle types and their relative Zn content, while after THP-1 exposures to PM, up to 6-fold and 4-fold increase of Zn uptake was observed for CZ100 and Diesel PM treatments, respectively, regardless the relative Zn particles content. As expected, Pb uptake significantly increased following exposure to UD 1649 due to the significantly higher Pb content of these reference particles. However, considerable cellular content of Pb was observed following CZ100 and Diesel PM exposures.

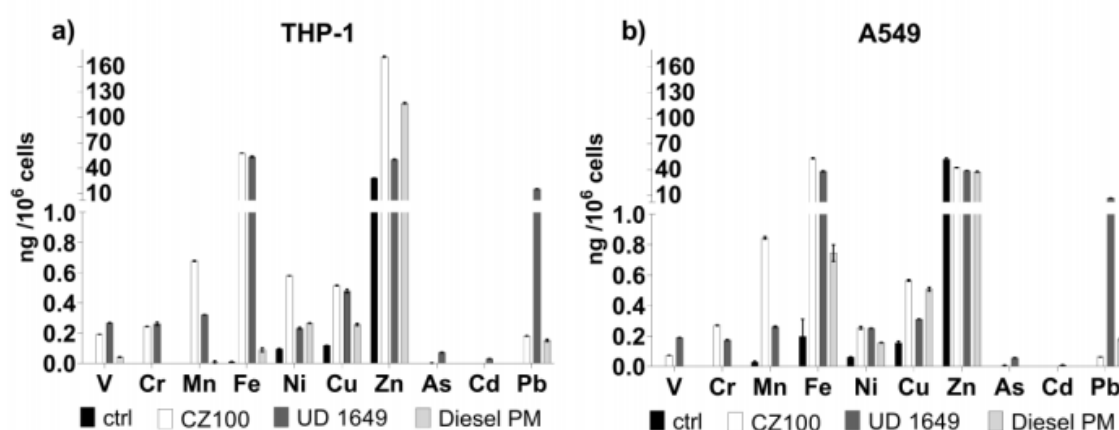


Fig. 3. Cellular content of selected elements was analyzed by ICP-MS following 48h exposure of THP-1 (a) and A549 cells (b) to CZ100, UD 1649, or Diesel PM. Data are expressed as mean  $\pm$  SD.

### 3.5 CZ100 is more effective in inducing lipid peroxidation

To assess oxidative stress induced by PM and oxidizers we evaluated MDA levels following 4, 48, and 72h exposures (Fig. 4). The fine dust CZ100 particles significantly increased MDA levels with a decreasing trend from 4h to 72h exposure in THP-1 cells while the oxidizer 3-MCPD showed a significant MDA release only after the shorter exposure time (Fig. 4a). A slight increase of MDA level was observed following 4h exposure of THP-1 cells to Diesel PM (Fig. 4a). Following A549 treatments with CZ100 the released amount of MDA was approximately doubled and similar over the exposure times, but a statistical significant increase was only observed following 4h treatment (Fig. 4b). A slight increase of MDA was noticed after both 4h and 72h exposures of A549 to UD 1649. The oxidizer 3-MCPD induced a significant MDA release on 4h treated A549 to a similar extent found for THP-1 while menadione was inducing a double amount of MDA production with respect to untreated A549 without statistical significance (Fig. 4b).



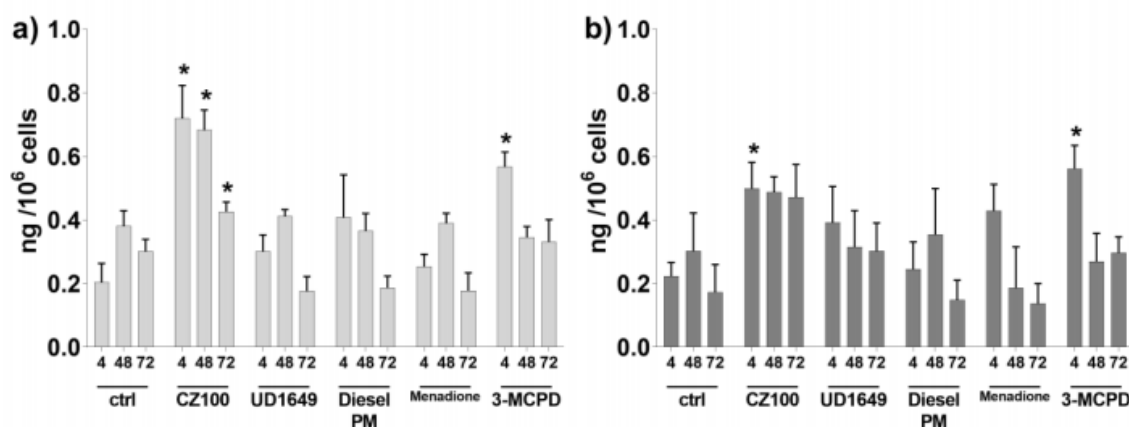


Fig. 4. MDA levels expressed as ng per million of cells in monocytic THP-1 cells (a) and A549 (b) following 4h, 48h and 72h exposures. Data are shown as mean  $\pm$  standard error from three independent experiments. \* =  $p$ -value < 0.05 compared to the relative untreated control (ctrl).

### 3.6 Reference PM induce persistent 8-OHdG lesions

The basal amount of oxidative 8-OHdG lesions in both THP-1 and A549 cells equaled approximately five lesions per 10<sup>6</sup> nucleobases (Fig. 5). Representative mass spectra for the analysis of 8-OHdG is shown in Fig. S1. Elevated oxidative stress levels were accompanied by an increase in the levels of 8-OHdG lesions in both THP-1 (Fig. 5a) and A549 cells (Figure 5b) following both short and long exposure times, indicating a persistent DNA oxidation. In THP-1 cells both reference particles and oxidizers induced significant DNA oxidation in a similar extent, but differences were observed in terms of DNA oxidation persistence measured as the ratio between the effects detected following 72h and 4h exposures. In fact, DNA oxidation induced by CZ100 decreased by 3.3 fold during time with a ratio of 0.33, similar to the 3.8 fold decrease observed upon menadione treatments (ratio of 0.39). The effects induced by UD 1649 and diesel PM decreased by 4.7 and 4.9 fold, with a ratio of 0.22 and 0.24 respectively, indicating a lower persistency of DNA oxidation with respect to both CZ100 and menadione treatments (Table 2). All exposures induced significant DNA oxidation in A549 cells after both 4h and 72h exposures (Fig. 5b) whereas diesel PM was more effective than UD 1649 and the oxidizer menadione after the shorter exposure time. Also following 72h exposure diesel PM treatments were more effective than CZ100 and the two oxidizers in inducing DNA oxidation. However, the effects induced by UD 1649 were more persistent over the exposure time as indicated by a 2.6 fold changes between 4h and 72h exposures corresponding to a ratio of 0.42 (Table 2). In general, considering the lower exposure concentration and deposition, diesel PM showed the highest DNA oxidative capacity with respect to both UD 1649 and CZ100. After treatments, THP-1 cells generally showed higher DNA oxidation levels compared to those of A549 cells.

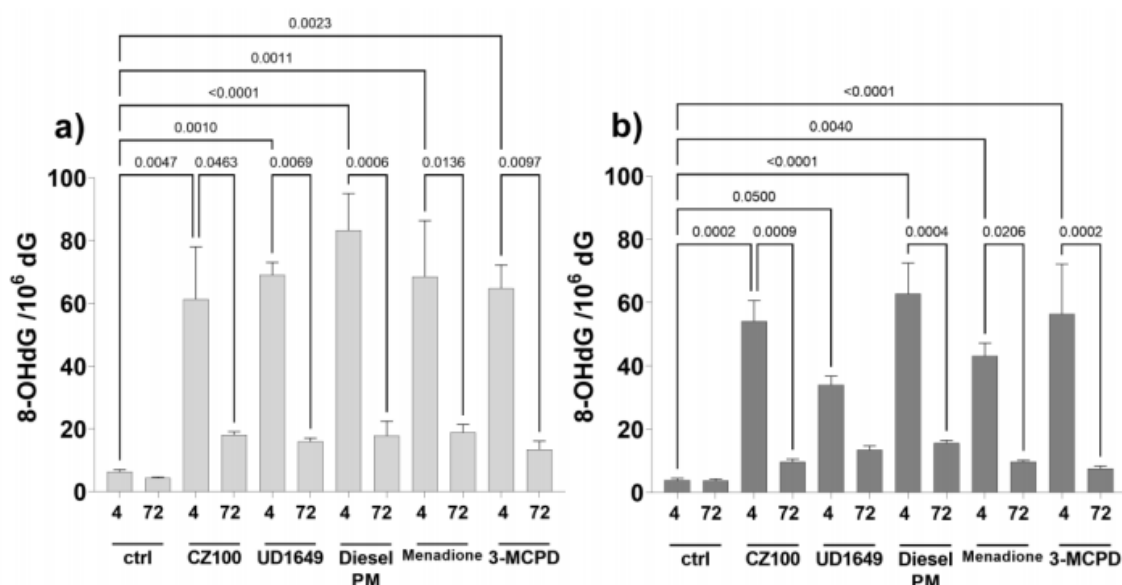


Fig. 5. 8-OHdG levels in THP-1 (a) and A549 (b) cells unexposed (ctrl) and exposed for 4h or 72h to 200  $\mu\text{g/mL}$  of CZ100 or UD 1649, or 40  $\mu\text{g/mL}$  of diesel PM, or 2  $\mu\text{g/mL}$  of menadione or 3-MCPD,. Results are shown as mean  $\pm$  standard error of three independent experiments and p-values indicate statistical significance differences.

Table 2. Mean values ( $\pm$  standard error) of 8-OHdG persistency in THP-1 and A549 cells exposed to different substance calculated as the ratio between the effects observed following 72h and 4h treatments.

Cells	Ctrl	Particles			Oxidizers	
		CZ100	UD 1649	Diesel PM	Menadione	3-MCPD
THP-1	$0.79 \pm 0.25$	$0.33 \pm 0.07$	$0.22 \pm 0.03$	$0.24 \pm 0.06$	$0.39 \pm 0.12$	$0.21 \pm 0.03$
A549	$1.0 \pm 0.1$	$0.22 \pm 0.07$	$0.42 \pm 0.10$	$0.29 \pm 0.08$	$0.23 \pm 0.03$	$0.18 \pm 0.07$

### 3.7 CBMN cyt assay

A representative distribution of mononucleated, binucleated, and polynucleated cells used to calculate the CBPI is shown in Fig. 6a while a typical mitotic cell used to evaluate the mitotic index is shown in Fig. 6b. Apoptotic and necrotic cells are shown in Fig. 6c and 6d, respectively, and were used to assess the cytotoxic potential of oxidizers and PM. Micronuclei formation in both mononucleated (Fig. 6e) and binucleated cells (Fig. 6f) was analyzed as a hallmark of aneuploidogenic and clastogenic effects, respectively [22,25]. Nucleoplasmic bridges (Fig. 6g) as well as nuclear buds (Fig. 6h) were scored as biomarkers of chromosome rearrangements or telomere end-fusion and as biomarker of amplified DNA elimination, respectively [21].

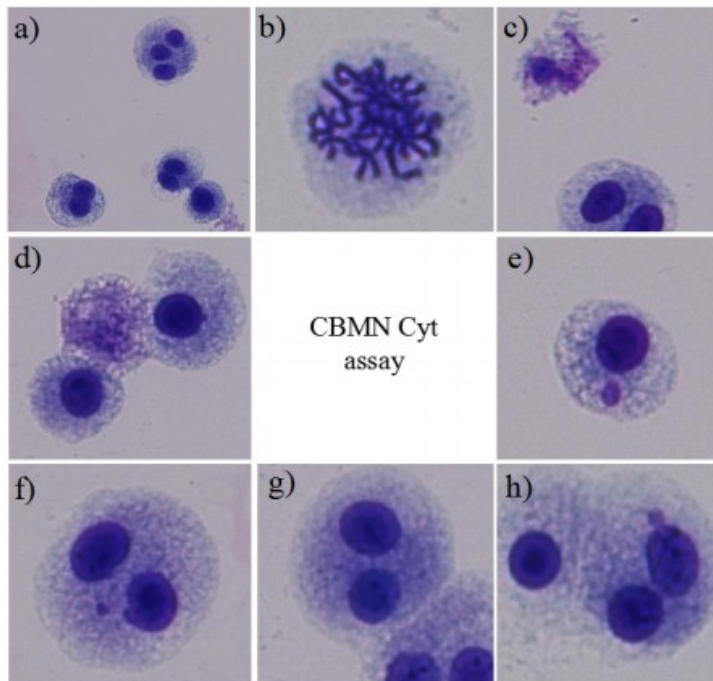


Figure 6. (a) Exemplary distribution of mononucleated, binucleated and polynucleated THP-1 cells (b) mitotic cell (c) apoptotic cell (d) necrotic cell used to assess cytostasis and cytotoxicity by CBMN Cyt assay (e) micronucleus in mononucleated THP-1 cell (f) micronucleus in binucleated THP-1 cell (g) nucleoplasmic bridge (NPB) (h) and nuclear bud (NBUD) were evaluated in order to comprehensively detect induced genotoxic mechanisms.

Besides menadione, which reduced cell proliferation in THP-1 cells, none of the tested compounds showed anti-proliferative effects (Fig. 7a). While all PM samples and oxidizers significantly reduced the mitotic index in THP-1 cells from 4.8 % in control cells to approximately 3 % (Fig. 7b), only minor cytotoxic changes in terms of apoptotic and necrotic effects were noticed (Fig. 7c and 7d).

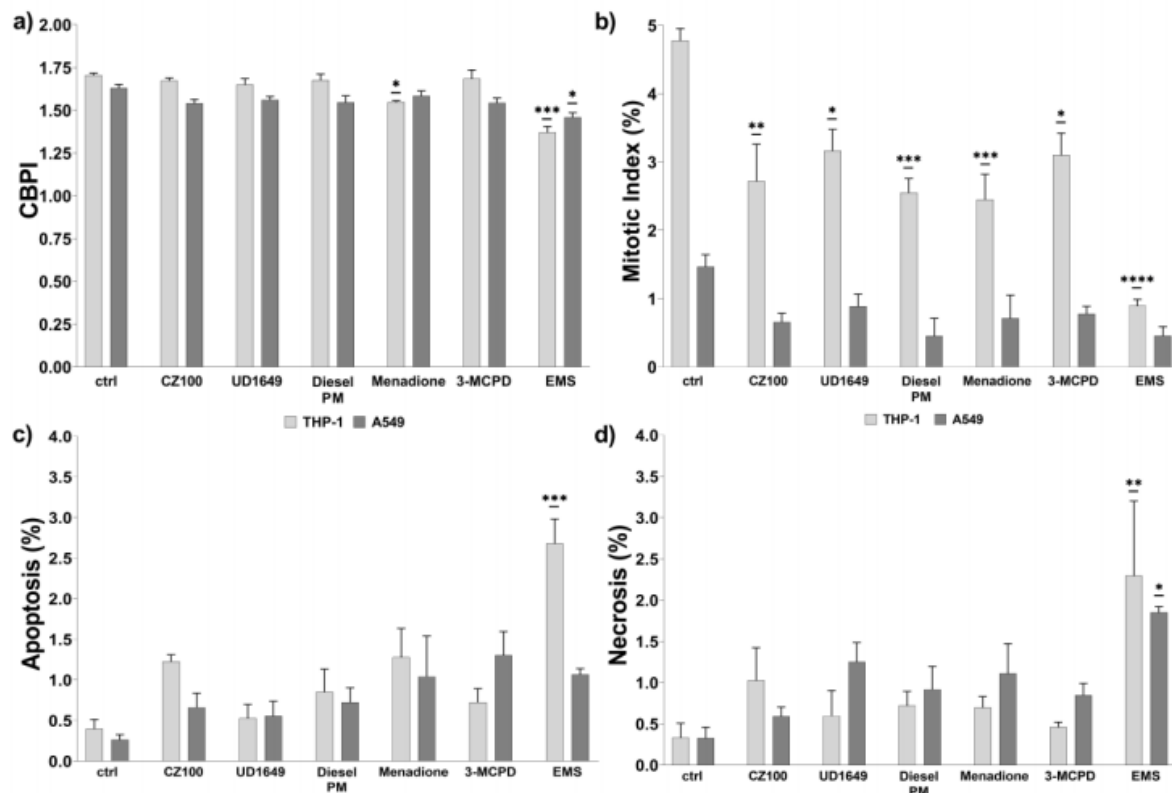


Fig. 7. CBMN Cyt assay, cytostasis and cytotoxicity. The cytokinesis-block proliferation index (CBPI, a), the % of mitotic (b), apoptotic (c) and necrotic cells (d) are presented as mean  $\pm$  standard error from three independent experiments (2  $\mu$ g/mL of menadione or 3-MCPD, 200  $\mu$ g/mL of CZ100 or UD 1649, or 40  $\mu$ g/mL of Diesel PM). \*,  $p < 0.05$ ; \*\*,  $p < 0.01$ ; \*\*\*,  $p < 0.001$ . Underlined asterisks denote statistical significance for both cell types with respect to their relative controls.

In terms of genotoxic potential, a significant induction of MN in mono- and binucleated cells was observed in A549 exposed to diesel PM and oxidizers (Fig. 8a and 8b). Only after exposure to menadione a significant increase of MN in binucleated cells was observed in THP-1 cells (Fig. 7b). In contrast, a significant induction of NPB formation occurred in both cell types following exposure to CZ100 and oxidizers (Fig. 8c). Diesel PM exposure significantly induced NPB formation on A549 cells. On the other hand, NBUD slightly increased in both THP-1 and A549 cells (Fig. 8d). Generally, diesel PM and oxidizers were more effective in inducing chromosomal damage compared to CZ100 and UD 1649 particles.



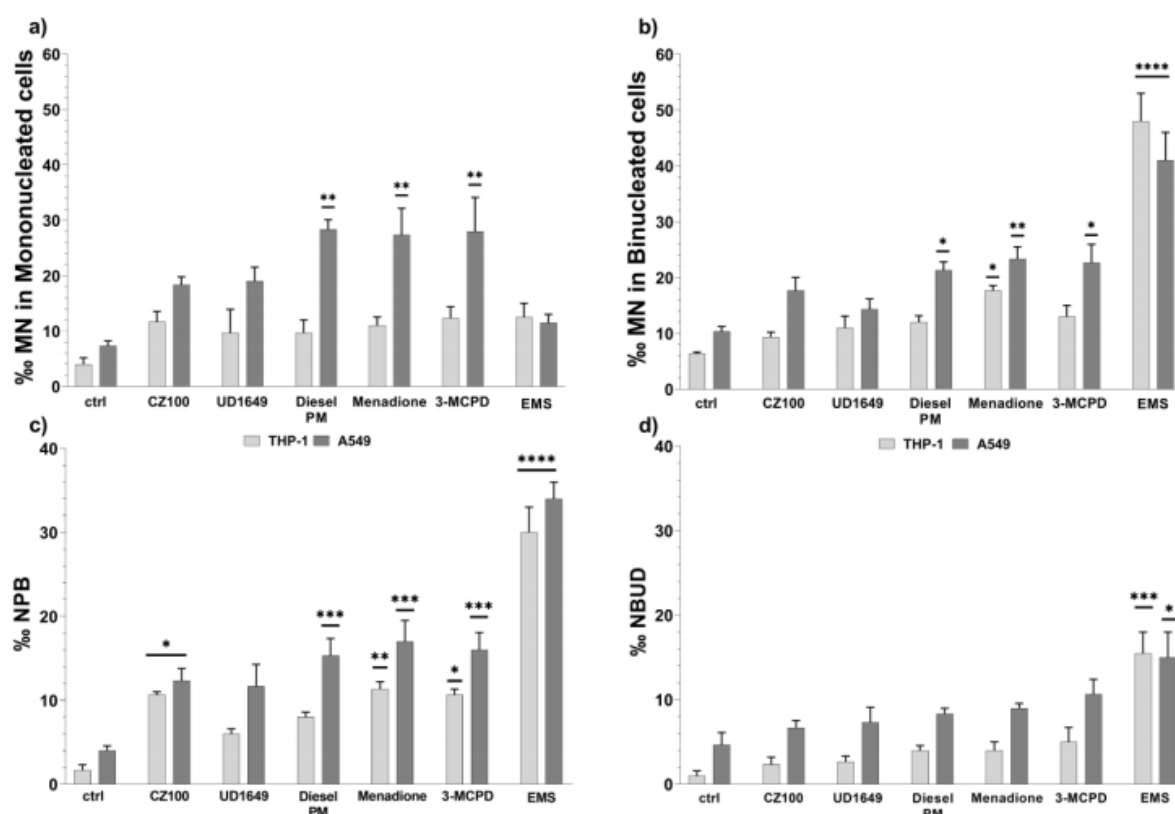


Fig. 8. CBMN Cyt assay, chromosomal damage and rearrangements. Micronuclei in mononucleated cells (a) and in binucleated cells (b), nucleoplasmic bridges (c) and nuclear buds (d) frequencies are presented as mean  $\pm$  SEM from three independent experiments (2  $\mu$ g/mL of menadione or 3-MCPD, 200  $\mu$ g/mL of CZ100 or UD 1649, or 40  $\mu$ g/mL of diesel PM). 300  $\mu$ g/mL ethyl methanesulfonate (EMS) was used as positive control. \*,  $p < 0.05$ ; \*\*,  $p < 0.01$ ; \*\*\*,  $p < 0.001$ , \*\*\*\*,  $p < 0.0001$  with respect to the relative controls (ctrl).

### 3.8 Correlations between 8-OHdG persistency, chromosomal instability and oxidative stress

8-OHdG persistence was evaluated based on the ratio between 72h and 4h exposures of 8-OHdG/ $10^6$  dG values (Table 2) in order to depict possible correlations among 8-OHdG formation dynamics and the genotoxic biomarkers as well as with MDA levels ratio between 72h and 4h exposures. Pearson correlation data are shown for CZ100, diesel PM, menadione and 3-MCPD treatments on A549 (Fig. 9a, 9b, 9c, 9d) and THP-1 cells (Fig. 9e, 9f, 9g, 9h). Correlations following exposure to UD 1649 were due to the lack of significantly increased chromosomal instability and therefore considered as not relevant and are not displayed. There was a significant positive correlation between 8-OHdG persistence and MN in binucleated cells (MN BN) following A549 exposures to diesel PM ( $R^2=0.998$ ,  $p=0.021$ ; Fig. 9b) and the oxidizer 3-MCPD ( $R^2=0.984$ ,  $p=0.05$ ; Fig. 9d). A strong positive correlation was observed between the DNA oxidation persistency and NPB formation after A549 exposures to diesel PM ( $R^2=1.0$ ,  $p=0.001$ ; Fig. 9b) and to 3-MCPD ( $R^2=0.988$ ,  $p=0.05$ ; Fig. 9d), as well as after THP-1 treatments with diesel PM ( $R^2=1.0$ ,  $p=0.005$ ; Fig. 9f) and menadione ( $R^2=1.0$ ,  $p=0.017$ ; Fig. 9g). We also observed that the induction of NPB had a strong positive correlation with MN induction in binucleated A549 cells after exposure to CZ100 ( $R^2=1.0$ ,  $p=0.018$ ; Fig. 9a), diesel PM ( $R^2=0.998$ ,  $p=0.021$ ; Fig. 9b), and the oxidizer 3-MCPD ( $R^2=1.0$ ,  $p=0.009$ ; Fig. 9d). The lipid peroxidation biomarker MDA was positively correlated with MN BN after A549 treatments with CZ100 ( $R^2=0.994$ ,  $p=0.05$ ; Fig. 9a) and menadione ( $R^2=1.0$ ,  $p=0.017$ ; Fig. 9c), and negatively correlated with MN mono in A549 cells following 3-MCPD treatment ( $R^2=1.0$ ,  $p=0.013$ ; Fig. 9d).



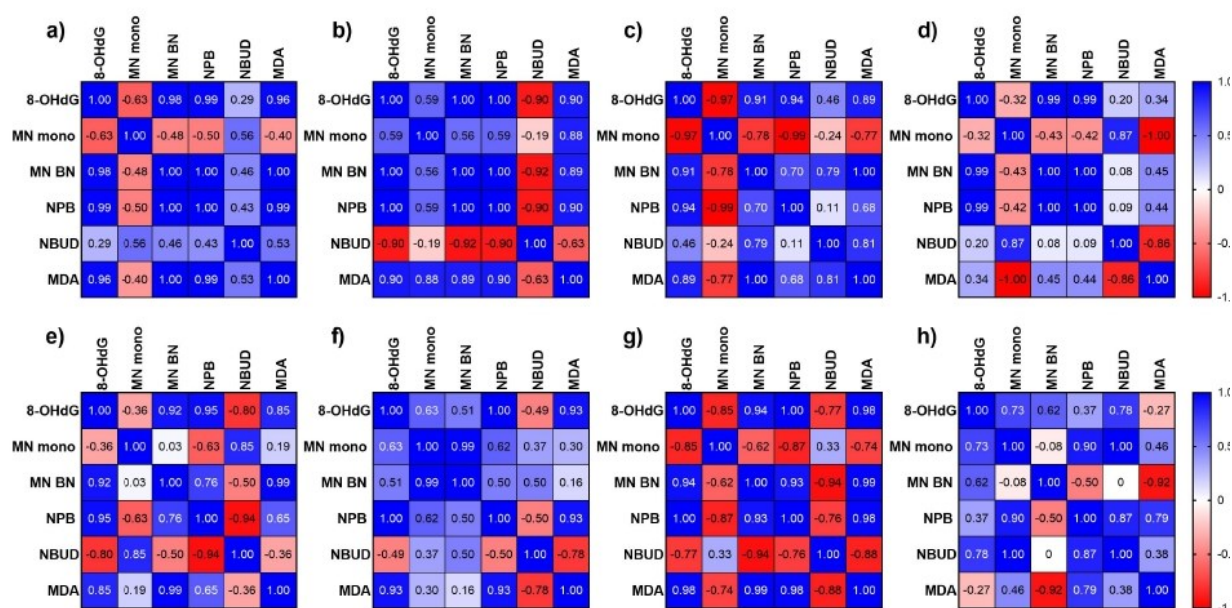


Fig. 9. Pearson's correlation coefficients of 8-OHdG persistency (ratio between 72h and 4h effects), MN in mononucleated cells (MN mono), MN in binucleated cells (MN BN), nucleoplasmic bridges (NPB), nuclear buds (NBUD), and the ratio of malondialdehyde (MDA) production between 72h and 4h exposures of A549 to CZ100 (a), diesel PM (b), menadione (c), 3-MCPD (d), and following monocytic THP-1 exposures to CZ100 (e), diesel PM (f), menadione (g), and 3-MCPD (h).

#### 4. Discussion

Recently we showed that the content of metals and PAHs of reference particulate matter differently shapes epigenetic DNA modifications on monocytic THP-1 cells and that CZ100 was more effective than UD 1649, diesel SRM2975, and the oxidizer tert-butyl hydroxiperoxide in inducing cytosine demethylation, cytosine hydroxymethylation, and adenine methylation [24]. CZ100 is characterized by a similar distribution of PAHs with respect to UD 1649, but with a lower amount of toxic compounds such as benzo(a)pyrene and benzo(a)anthracene among others (Table S1). CZ100 is also the applied PM with the highest content of metals with a total elemental content 3.4 times higher than UD 1649 as reported in the respective material certificates, and particularly rich in Cr, Mn, Fe, and Cu as confirmed by the present study (Table 1 and S2). On the other hand, UD 1649 is particularly abundant in toxic elements like V, Ni, Zn, As, Cd and Pb, while having a lower total metal content compared to CZ100. Diesel PM is characterized by a lower amount of PAHs compared to CZ100 and UD 1649, but it contains larger amount of nitro-PAHs, e.g. the high toxic 1,6-dinitropyrene, and considerable amounts of Zn and Fe (Table 1 and S1). Despite the different metal content of the particles, we have shown that the ion release into cell culture media can vary among particle types as well as among cell model systems. For instance, this behavior was translated into a similar Fe cellular uptake in epithelial A549 cells following CZ100 and UD 1649 exposures despite the particle iron content, which is 1.4 times higher in CZ100 compared to UD 1649. Furthermore, even though UD 1649 contained the highest amount of Zn, the cellular content of Zn in monocytic THP-1 was much higher following exposures to CZ100 and diesel PM compared to the Zn content after exposure to UD 1649. Such observations call for more in-depth studies on physico-chemical, structural, and electronic properties of PM that can regulate metal bioaccessibility. Recently, the importance of bioaccessible metal fractions versus the total metal content was highlighted as an important aspect for calculating the carcinogenic and non-carcinogenic risk indexes of several airborne PM sources, demonstrating that health risks can be accurately predicted by the fraction of bioaccessible metals rather than the total



metal content [26]. However, the variety of inorganic and organic compounds of PM samples could be specifically responsible for different PM-induced genotoxic mechanisms of action. For instance, transition metals can induce intracellular ROS via Fenton-like reactions while the metabolism of PAHs can produce reactive intermediates able to undergo redox cycling mechanisms, which are subsequently responsible for oxidative stress conditions, or generating highly reactive molecules that are directly reacting with biomolecules including DNA.

In the present study we have shown that CZ100 and the oxidizer 3-MCPD significantly induced lipid peroxidation in both cell types with 4h exposure more effective than 72h, while all other tested materials slightly increased MDA levels following the shorter exposure time. Neutral aqueous extracts of UD 1649 and diesel SRM2975 were previously used to evaluate ROS induction via the formation of MDA from 2-deoxyribose [23]. This study showed that UD 1649 was more effective than diesel SRM2975 in generating MDA and that this effect was inhibited by the chelating agent deferoxamine, therefore suggesting that transition metals are catalyzing the formation of ROS [23]. Accordingly, lipid peroxidation observed in our study might be explained by the higher metal content of CZ100 and the subsequent higher elemental cellular uptake observed in both cell types. However, the efficacy of CZ100 in inducing lipid peroxidation, as well as its more pronounced effects with respect to UD 1649 and diesel PM treatments, was more evident in monocytic THP-1 compared to alveolar epithelial A549 cells. Recently, further research has shown that organic extracts from airborne PM reduce lipid peroxidation, as evaluated by 15-F2t-Isoprostane, via aryl hydrocarbon receptor inhibition of prostaglandin endoperoxide synthase 2 expression in A549 cells. This effect was not observed in normal human embryonic lung fibroblasts HEL12469, suggesting that processes related to lipid peroxidation are highly specific for different cell lines [27,28]. These observations also suggest a complex interplay between metal and organic particle content induced effects and their pro-oxidant potential. For instance, the observed 8-OHdG formation could not be exclusively attributed to the particles metal content since Diesel PM was the most effective in inducing DNA oxidation in both cell types. Indeed, we have shown that all tested reference particles and oxidizers promoted the generation of 8-OHdG in both monocytic THP-1 and epithelial A549 cells with a DNA oxidation persistence varying among particles and cell types in sub-cytotoxic conditions.

The organic content of PM samples and its pro-oxidant activity could also constitute a driving factor for DNA oxidation and chromosomal instability. For instance, we observed a significant induction of MN in A549 cells after exposure to diesel PM and both tested oxidizers (menadione and 3-MCPD) which were positively correlated with 8-OHdG lesions persistency. Moreover, in both cell lines, we found significantly increased NPB formation after CZ100 and oxidizer treatments showing that both fine dust and the oxidizers might share similar mechanisms of genotoxicity. NPB formation was positively correlated with 8-OHdG persistence in both cell types, with a significant correlation following diesel PM and oxidizers. NPB originating from dicentric chromosomes and centric ring chromosomes are a sensitive measure of chromosomal damage induced by ROS, and positive correlations of NPB with MN and NBUD were shown in previous studies on oxidative stress and genotoxicity in human lymphoblastoid WIL2-NS cell line [29,30]. However, we found conflicting correlations between NPB and NBUD with varying treatments and cell type, and no significant increase of NBUD was noticed.

In particular for UD 1649 treatments, the increase of 8-OHdG levels in THP-1 cells was higher than in A549, in terms of absolute frequencies, asking for a better understanding of the role of cell-specific metabolism with regards to the different PAHs and metal content of tested particles. In fact, besides CZ100, which showed a similar DNA oxidation capacity between the two distinct cell models, UD 1649 induced DNA oxidation was more persistent in A549 than monocytic THP-1 cells. Prahalad et

al. reported that the level of 8-OHdG in bronchial BEAS-2B cells treated for 2h with urban dust particles (UD 1649) increased 1.7-fold compared to untreated controls [31]. However, the oxidative capacity of UD 1649 could not be attributed to the total metal content but to its water-soluble fraction since both metal ion chelators and hydroxyl radical scavenger particle pretreatments were ineffective in inhibiting the induced DNA hydroxylation in cell-free systems [31]. Similarly, diesel SRM2975 generated oxidative DNA damage in A549 cells in a dose-dependent manner but was not able to induce 8-oxodG in calf thymus DNA even following co-exposure with H<sub>2</sub>O<sub>2</sub>, indicating the lack of metal-catalyzed reactions in the solvent because of low levels of transition metals in SRM2975 [32].

Coherently, in the current study all PM samples increased 8-OHdG levels in both cell types, which could be explained by their PAHs and nitro-PAHs content due to the low amount of metals in diesel particles and its slightly higher effectiveness in inducing DNA oxidation. This assumption is supported by the role played by CYP1A1 enzymes, mainly responsible for metabolism or oxidation of PAHs, as previously shown in murine embryonic fibroblasts and alveolar macrophages, where UD 1649 and diesel SRM2975 caused an increased CYP1A1 expression [33,34]. Moreover, Shi and co-authors investigated diesel SRM2975 induced chromosomal damage mechanisms on V79 fibroblasts and found that the particle organic solvent extracts significantly increased MN frequency, while no effects were observed after particle washing [35]. This indicates that the genotoxicity of diesel SRM2975 can be attributed to its organic components PAHs and nitro-PAHs. Specifically, nitro-PAHs are more toxic than PAHs [36]. For instance, by comparing the cytotoxicity of benzo[a]pyrene, 1-nitropyrene, and 3-nitrofluoranthene it was shown that both nitro-PAHs induced higher cytotoxicity than benzo[a]pyrene [37]. One of the most abundant nitro-PAHs in diesel SRM2975, 1-nitropyrene, induced strong DNA damage and oxidative stress *in vivo*, and greatly promoted inflammation, apoptosis and necrosis in human bronchial epithelial BEAS-2B cells *in vitro* [38,39]. A direct comparison of PAHs and nitro-PAHs was conducted on BEAS-2B cells showing that 1-nitropyrene and 3-nitrobenzanthrene were more effective than benzo(a)pyrene in inducing micronuclei formation [40]. Furthermore, 1-nitropyrene and 3-nitrofluoranthene were shown to be genotoxic and cause ROS generation and inflammatory processes by activating PI3K/Akt signaling in A549 cells [41,42].

Chromosomal instability can result from persistent DNA oxidation since the simultaneous removal of multiple 8-OHdG can cause DNA double-strand breaks leading to MN formation [43]. It is important to note that persistent activation of DNA damage-related signaling was found in response to complex mixtures of air PM extract fractions containing PAHs with more than four aromatic rings but without polar compounds [44]. However, the relative PAHs composition of PM is not conserved in the atmosphere but is subjected to dynamic atmospheric aging processes, which in turn induce changes on the bioaccessibility of PAHs. Whereas UD 1649 particles could be affected mainly by the photo-oxidation reactions during daytime, CZ100 could be a result of accumulation of nitro-PAHs by diesel engine emissions and the fresh formation of nitro-PAHs, since mainly dark reactions are taking place in a tunnel and the exclusion of ozone and UV light prevents fast degradation of nitro-PAH. For instance, precursor PAH can react with nitrate radicals and further with NO<sub>2</sub> to form nitro-PAH [36]. The atmospheric ageing of particles collected for UD 1649 surely included similar dark reactions during nighttime but photo-oxidation during daytime can lead to both the formation and the decay of nitro-PAH. The formation of nitro-PAH is due to reaction with hydroxyl radicals and subsequent reaction with NO<sub>2</sub> [45]. However, a concurrent pathway of precursor PAH leads to the formation of oxygenated PAH by reaction with ozone or hydroxyl radicals which are responsible for the decay reactions [46] possibly explaining the lower genotoxic potential of UD 1649 with respect to CZ100 and diesel PM.



## 5. Conclusions

In this study, we investigated the oxidative capacity and persistency of reference PM fine dust CZ100, urban dust UD 1649, and Diesel PM compared to the oxidizers menadione, and 3-MCPD on epithelial A549 and monocytic THP-1 cells. Despite differences in PM tested concentrations and cellular metal uptake, all reference PM samples induced oxidative DNA damage in a comparable magnitude of order compared to the two tested oxidizers but with different persistence. Diesel particles are more genotoxic compared to fine and urban dust highlighting the role of PAH derivatives on chromosomal instability. Furthermore, we explored the correlation between 8-OHdG lesion persistency and biomarkers of chromosomal damage showing that the NPB measure is a sensitive indicator of genotoxicity induced by airborne particles and oxidative stress, and that a connection between DNA oxidation and chromosomal instability is associated with PM exposure. Additionally, a complex interplay between bioaccessible metals and PAHs particle content was shown pointing out the importance of PAH derivatives in driving reference airborne particle induced genotoxicity.

## Funding

The Helmholtz Virtual Institute of Complex Molecular Systems in Environmental Health (HICE) via the Helmholtz Association of German Research Centers (HFG), the aeroHEALTH Helmholtz International Lab., and the China Scholarship Council funded this work.

## Declaration of Competing Interest

The authors declare that they have no competing interests.

## References

- [1] F. Liu, G. Chen, W. Huo, C. Wang, S. Liu, N. Li, S. Mao, Y. Hou, Y. Lu, H. Xiang, Associations between long-term exposure to ambient air pollution and risk of type 2 diabetes mellitus: A systematic review and meta-analysis, *Environ. Pollut.* 252 (2019) 1235–1245. <https://doi.org/10.1016/j.envpol.2019.06.033>.
- [2] R.B. Hayes, C. Lim, Y. Zhang, K. Cromar, Y. Shao, H.R. Reynolds, D.T. Silverman, R.R. Jones, Y. Park, M. Jerrett, J. Ahn, G.D. Thurston, PM<sub>2.5</sub> air pollution and cause-specific cardiovascular disease mortality, *Int. J. Epidemiol.* (2019) 1–11. <https://doi.org/10.1093/ije/dyz114>.
- [3] N. Wang, K. Mengersen, M. Kimlin, M. Zhou, S. Tong, L. Fang, B. Wang, W. Hu, Lung cancer and particulate pollution: A critical review of spatial and temporal analysis evidence, *Environ. Res.* 164 (2018) 585–596. <https://doi.org/10.1016/j.envres.2018.03.034>.
- [4] L. Risom, P. Møller, S. Loft, Oxidative stress-induced DNA damage by particulate air pollution, *Mutat. Res., Fundam. Mol. Mech. Mutagen.* 592 (2005) 119–137. <https://doi.org/10.1016/j.mrfmmm.2005.06.012>.
- [5] Y. Wang, J. Lin, J. Shu, H. Li, Z. Ren, Oxidative damage and DNA damage in lungs of an ovalbumin-induced asthmatic murine model, *J. Thorac. Dis.* 10 (2018) 4819–4830. <https://doi.org/10.21037/jtd.2018.07.74>.
- [6] T.J. Grahame, R.B. Schlesinger, Oxidative stress-induced telomeric erosion as a mechanism underlying airborne particulate matter-related cardiovascular disease, *Part. Fibre Toxicol.* 9:21 (2012). <https://doi.org/10.1186/1743-8977-9-21>.
- [7] N. Li, T. Xia, A.E. Nei, The role of oxidative stress in ambient particulate matter-induced lung diseases and its implications in the toxicity of engineered nanoparticles, *Free Radicals Biol. Med.* 44 (2008) 1689–1699. <https://doi.org/10.1016/j.freeradbiomed.2008.01.028>.
- [8] K. Donaldson, L. Tran, L.A. Jimenez, R. Duffin, D.E. Newby, N. Mills, W. MacNee, V. Stone, Combustion-derived nanoparticles: a review of their toxicology following inhalation exposure, *Part. Fibre Toxicol.* 2:10 (2005). <https://doi.org/10.1186/1743-8977-2-10>.

- [9] H.L. Karlsson, J. Nygren, L. Möller, . Genotoxicity of airborne particulate matter: the role of cell-particle interaction and of substances with adduct-forming and oxidizing capacity, *Mutat. Res. , Genet. Toxicol. Environ. Mutagen.* 565 (2004) 1–10. <https://doi.org/10.1016/j.mrgentox.2004.07.015>.
- [10] I. Abbas, G. Garçon, F. Saint-Georges, V. Andre, P. Gosset, S. Billet, J. Le Goff, A. Verdin, P. Mulliez, F. Sichel, P. Shirali, Polycyclic aromatic hydrocarbons within airborne particulate matter (PM<sub>2.5</sub>) produced DNA bulky stable adducts in a human lung cell coculture model, *J. Appl. Toxicol.* 33 (2013) 109–119. <https://doi.org/10.1002/jat.1722>.
- [11] G. Çakmak, P. Ertürk Arı, E. Emerce, A. Arı, M. Odabaşı, R. Schins, S. Burgaz, E.O. Gaga, Investigation of spatial and temporal variation of particulate matter in vitro genotoxicity and cytotoxicity in relation to the elemental composition, *Mutat. Res. , Genet. Toxicol. Environ. Mutagen.* 842 (2019) 22–34. <https://doi.org/10.1016/j.mrgentox.2019.01.009>.
- [12] W.J. Cannan, D.S. Pederson, Mechanisms and Consequences of Double-Strand DNA Break Formation in Chromatin, *J. Cell. Physiol.* 231 (2016) 3–14. <https://doi.org/10.1002/jcp.25048>.
- [13] N. Chatterjee, G.C. Walker, Mechanisms of DNA damage, repair, and mutagenesis. *Environ. Mol. Mutagen, Environ. Mol. Mutagen.* 58 (2017) 235–263. <https://doi.org/10.1002/em.22087>.
- [14] P. Pfeiffer, W. Goedecke, G. Obe, Mechanisms of DNA double-strand break repair and their potential to induce chromosomal aberrations, *Mutagenesis.* 15 (2000) 289–302. <https://doi.org/10.1093/mutage/15.4.289>.
- [15] A. Murphy, A. Casey, G. Byrne, G. Chambers, O. Howe O, Silver nanoparticles induce pro-inflammatory gene expression and inflammasome activation in human monocytes. *J Appl Toxicol.* 36 (2016) 1311-20. <https://doi.org/10.1002/jat.3315>.
- [16] D.N. Criddle, S. Gillies, H.K. Baumgartner-Wilson, M. Jaffar, E.C. Chinje, S. Passmore, M. Chvanov, S. Barrow, O. V. Gerasimenko, A. V. Tepikin, R. Sutton, O.H. Petersen, Menadione-induced reactive oxygen species generation via redox cycling promotes apoptosis of murine pancreatic acinar cells, *J. Biol. Chem.* 281 (2006) 40485–40492. <https://doi.org/10.1074/jbc.M607704200>.
- [17] X. Sun, L. Zhang, H. Zhang, H. Qian, J. Ji, L. Tang, Z. Li, G. Zhang, Electrochemical detection of 8-hydroxy-2'-deoxyguanosine as a biomarker for oxidative DNA damage in HEK293 cells exposed to 3-chloro-1,2-propanediol, *Anal. Methods.* 7 (2015) 6664–6671. <https://doi.org/10.1039/c5ay01246e>.
- [18] C.J. Rudd, K.A. Stromt, A spectrophotometric method for the quantitation of Diesel Exhaust Particles in Guinea Pig Lung, *J. Appl. Toxicol.* 1 (1981) 83–87. <https://doi.org/10.1002/jat.2550010207>.
- [19] X. Wu, J. Lintelmann, S. Klingbeil, J. Li, H. Wang, E. Kuhn, S. Ritter, R. Zimmermann, Determination of air pollution-related biomarkers of exposure in urine of travellers between Germany and China using liquid chromatographic and liquid chromatographic-mass spectrometric methods: a pilot study, *Biomarkers.* 22 (2017) 525-536. <https://doi.org/10.1080/1354750X.2017.1306753>.
- [20] S.A. Miller, D.D. Dykes, H.F. Polesky, A simple salting out procedure for extracting DNA from human nucleated cells, *Nucleic. Acids. Res.* 16 (1988) 1215. <https://doi.org/doi:10.1093/nar/16.3.1215>.
- [21] S. Di Bucchianico, A.R. Gliga, E. Åkerlund, S. Skoglund, I.O. Wallinder, B. Fadeel, H.L. Karlsson, Calcium-dependent cyto- and genotoxicity of nickel metal and nickel oxide nanoparticles in human lung cells, *Part. Fibre Toxicol.* 15 (2018) 32. <https://doi.org/10.1186/s12989-018-0268-y>.
- [22] C. Rosefort, E. Fauth, H. Zankl, Micronuclei induced by aneugens and clastogens in mononucleate and binucleate cells using the cytokinesis block assay, *Mutagenesis.* 19 (2004) 277-84. <https://doi.org/10.1093/mutage/geh028>.
- [23] J.C. Ball, A.M. Straccia, W.C. Young, A.E. Aust, The formation of reactive oxygen species catalyzed by neutral, aqueous extracts of NIST ambient particulate matter and diesel engine particles, *J. Air Waste Manag. Assoc.* 50 (2000) 1897-903. <https://doi.org/10.1080/10473289.2000.10464231>.
- [24] X. Cao, J. Lintelmann, S. Padoan, S. Bauer, A. Huber, A. Mudan, S. Oeder, T. Adam, S. Di Bucchianico, R. Zimmermann, Adenine derivatization for LC-MS/MS epigenetic DNA modifications studies on monocytic THP-



- 1 cells exposed to reference particulate matter, *Anal. Biochem.* 618 (2021) 114127. <https://doi.org/10.1016/j.ab.2021.114127>.
- [25] M. Kirsch-Volders, M. Fenech, Inclusion of micronuclei in non-divided mononuclear lymphocytes and necrosis/apoptosis may provide a more comprehensive cytokinesis block micronucleus assay for biomonitoring purposes, *Mutagenesis*. 16 (2001) 51–58. <https://doi.org/10.1093/mutage/16.1.51>.
- [26] X. Liu, W. Ouyang, Y. Shu, Y. Tian, Y. Feng, T. Zhang, W. Chen, Incorporating bioaccessibility into health risk assessment of heavy metals in particulate matter originated from different sources of atmospheric pollution. *Environ. Pollut.* 254, Part B (2019) 113113. <https://doi.org/10.1016/j.envpol.2019.113113>.
- [27] P. Rossner, H. Libalova, T. Cervena, K. Vrbova, F. Elzeinova, A. Milcova, A. Rossnerova, Z. Novakova, M. Ciganek, M. Pokorna, A. Ambroz, J. Topinka, The processes associated with lipid peroxidation in human embryonic lung fibroblasts, treated with polycyclic aromatic hydrocarbons and organic extract from particulate matter. *Mutagenesis*. 29 (2019) 153–164. <https://doi.org/10.1093/mutage/gez004>.
- [28] P. Rossner, H. Libalova, K. Vrbova, T. Cervena, A. Rossnerova, F. Elzeinova, A. Milcova, Z. Novakova, J. Topinka, Genotoxicant exposure, activation of the aryl hydrocarbon receptor, and lipid peroxidation in cultured human alveolar type II A549 cells. *Mutat. Res.* 853 (2020) 503173. <https://doi.org/10.1016/j.mrgentox.2020.503173>.
- [29] P. Thomas, K. Umegaki, M. Fenech, Nucleoplasmic bridges are a sensitive measure of chromosome rearrangement in the cytokinesis-block micronucleus assay, *Mutagenesis*. 18 (2003) 187–94. <https://doi.org/10.1093/mutage/18.2.187>.
- [30] K. Umegaki, M. Fenech, Cytokinesis-block micronucleus assay in WIL2-NS cells: a sensitive system to detect chromosomal damage induced by reactive oxygen species and activated human neutrophils, *Mutagenesis*. 15 (2000) 261–9. <https://doi.org/10.1093/mutage/15.3.261>.
- [31] A.K. Prahalad, J. Inmon, L.A. Dailey, M.C. Madden, A.J. Ghio, J.E. Gallagher, Air pollution particles mediated oxidative DNA base damage in a cell free system and in human airway epithelial cells in relation to particulate metal content and bioreactivity, *Chem. Res. Toxicol.* 14 (2001) 879–887. <https://doi.org/10.1021/tx010022e>.
- [32] P.H. Danielsen, S. Loft, P. Møller, DNA damage and cytotoxicity in type II lung epithelial (A549) cell cultures after exposure to diesel exhaust and urban street particles, *Part. Fibre Toxicol.* 5:6 (2008). <https://doi.org/10.1186/1743-8977-5-6>.
- [33] A.F. Dumax-Vorzet, M. Tate, R. Walmsley, R.H. Elder, A.C. Povey, Cytotoxicity and genotoxicity of urban particulate matter in mammalian cells, *Mutagenesis*. 30 (2015) 621–633. <https://doi.org/10.1093/mutage/gev025>.
- [34] H. Zhao, M.W. Barger, J.K.H. Ma, V. Castranova, J.Y.C. Ma, Cooperation of the inducible nitric oxide synthase and cytochrome P450 1A1 in mediating lung inflammation and mutagenicity induced by diesel exhaust particle, *Environ. Health Perspect.* 114 (2006) 1253–1258. <https://doi.org/10.1289/ehp.9063>.
- [35] X. Shi, M.J. Keane, O. TM., J. Harrison, S. JE., A. Bugarski, M. Gautam, W. Wallace, Diesel exhaust particulate material expression of in vitro genotoxic activities when dispersed into a phospholipid component of lung surfactant, *J. Phys. Conf. Ser.* 151 (2009) 012021. <https://doi.org/10.1088/1742-6596/151/1/012021>.
- [36] B.A.M. Bandowe, H. Meusel, Nitrated polycyclic aromatic hydrocarbons (nitro-PAHs) in the environment - A review, *Sci. Total Env.* 581–582 (2017) 237–257. <https://doi.org/10.1016/j.scitotenv.2016.12.115>.
- [37] P. Rossner, S. Strapacova, J. Stolcpartova, J. Schmuczerova, A. Milcova, J. Neca, V. Vlkova, T. Brzicova, M. Machala, J. Topinka, Toxic effects of the major components of diesel exhaust in human alveolar basal epithelial cells (A549), *Int. J. Mol. Sci.* 17 (2016) 1393. <https://doi.org/10.3390/ijms17091393>.
- [38] R. Li, L. Zhao, L. Zhang, M. Chen, C. Dong, Z. Cai, DNA damage and repair, oxidative stress and metabolism biomarker responses in lungs of rats exposed to ambient atmospheric 1-nitropyrene, *Environ. Toxicol. Pharmacol.* 54 (2017) 14–20. <https://doi.org/10.1016/j.etap.2017.06.009>.



- [39] J. Øvrevik, V.M. Arlt, E. Øya, E. Nagy, S. Møllerup, D.H. Phillips, M. Låg, J.A. Holme, Differential effects of nitro-PAHs and amino-PAHs on cytokine and chemokine responses in human bronchial epithelial BEAS-2B cells, *Toxicol. Appl. Pharmacol.* 242 (2010) 270–280. <https://doi.org/10.1016/j.taap.2009.10.017>.
- [40] T. Cervena, A. Rossnerova, J. Sikorova, V. Beranek, M. Vojtisek-Lom, M. Ciganek, J. Topinka, P. Rossner, DNA damage potential of engine emissions measured in vitro by micronucleus test in human bronchial epithelial cells, *Basic Clin. Pharmacol. Toxicol.* 121 (2017) 102–108. <https://doi.org/10.1111/bcpt.12693>.
- [41] Y. Shang, Q. Zhou, T. Wang, Y. Jiang, Y. Zhong, G. Qian, T. Zhu, X. Qiu, J. An, Airborne nitro-PAHs induce Nrf2/ARE defense system against oxidative stress and promote inflammatory process by activating PI3K/Akt pathway in A549 cells, *Toxicol. Vitro* 44 (2017) 66–73. <https://doi.org/10.1016/j.tiv.2017.06.017>.
- [42] B. Hu, B. Tong, Y. Xiang, S.R. Li, Z.X. Tan, H.X. Xiang, L. Fu, H. Wang, H. Zhao, D.X. Xu, Acute 1-NP exposure induces inflammatory responses through activating various inflammatory signaling pathways in mouse lungs and human A549 cells, *Ecotoxicol. Environ. Saf.* 189 (2020) 109977. <https://doi.org/10.1016/j.ecoenv.2019.109977>.
- [43] M. Fenech, M. Kirsch-Volders, A.T. Natarajan, J. Surrallés, J.W. Crott, J. Parry, H. Norppa, D.A. Eastmond, J.D. Tucker, P. Thomas, Molecular mechanisms of micronucleus, nucleoplasmic bridge and nuclear bud formation in mammalian and human cells, *Mutagenesis* 26 (2011) 125–132. <https://doi.org/10.1093/mutage/geq052>.
- [44] I.W. Jarvis, C. Bergvall, M. Bottai, R. Westerholm, U. Stenius, K. Dreij, Persistent activation of DNA damage signaling in response to complex mixtures of PAHs in air particulate matter. *Toxicol Appl Pharmacol.* 266 (2013) 408–18. <https://doi.org/10.1016/j.taap.2012.11.026>.
- [45] N. Jariyasopit, M. McIntosh, K. Zimmermann, J. Arey, R. Atkinson, P.H. Cheong, R.G. Carter, T.W. Yu, R.H. Dashwood, S.L. Massey Simonich. Novel nitro-PAH formation from heterogeneous reactions of PAHs with NO<sub>2</sub>, NO<sub>3</sub>/N<sub>2</sub>O<sub>5</sub>, and OH radicals: prediction, laboratory studies, and mutagenicity. *Environ Sci Technol.* 48 (2014) 412–9. <https://doi.org/10.1021/es4043808>
- [46] C. Walgraeve, K. Demeestere, J. Dewulf, R. Zimmermann, H. Van Langenhove. Oxygenated polycyclic aromatic hydrocarbons in atmospheric particulate matter: Molecular characterization and occurrence. *Atmospheric Environment*. 44 (2010) 1831–46. <https://doi.org/10.1016/j.atmosenv.2009.12.004>

### 6.4.3 Publication 3

**Title:** Adenine Derivatization for LC-MS/MS Epigenetic DNA Modifications Studies on Monocytic THP-1 Cells Exposed to Reference Particulate Matter

**Author:** Xin Cao, Jutta Lintelmann, Sara Padoan, Stefanie Bauer, Anja Huber, Ajit Mudan, Sebastian Oeder, Thomas Adam, Sebastiano Di Bucchianico, Ralf Zimmermann

**Journal:** Analytical biochemistry, 618: 114127

**Year:** 2021

**Contribution:** For this publication, Xin Cao carried out the experiments, made data process, and wrote the manuscript.



Contents lists available at ScienceDirect

Analytical Biochemistry

journal homepage: [www.elsevier.com/locate/yabio](http://www.elsevier.com/locate/yabio)

## Adenine derivatization for LC-MS/MS epigenetic DNA modifications studies on monocytic THP-1 cells exposed to reference particulate matter

Xin Cao<sup>a,d</sup>, Jutta Lintelmann<sup>b,\*\*</sup>, Sara Padoan<sup>c,a</sup>, Stefanie Bauer<sup>a</sup>, Anja Huber<sup>a</sup>, Ajit Mudan<sup>c</sup>, Sebastian Oeder<sup>a</sup>, Thomas Adam<sup>c,a</sup>, Sebastiano Di Bucchianico<sup>a,\*</sup>, Ralf Zimmermann<sup>a,d</sup>

<sup>a</sup> Joint Mass Spectrometry Center (JMSC) at Comprehensive Molecular Analytics (CMA), Helmholtz Zentrum München, Neuherberg, Germany

<sup>b</sup> Research Unit of Molecular Endocrinology and Metabolism, Helmholtz Zentrum München, Neuherberg, Germany

<sup>c</sup> University of the Bundeswehr Munich, Institute for Chemistry and Environmental Engineering, Neubiberg, Germany

<sup>d</sup> Joint Mass Spectrometry Center (JMSC) at Analytical Chemistry, Institute of Chemistry, University of Rostock, Rostock, Germany

### ARTICLE INFO

#### Keywords:

Cytosine methylation  
Cytosine hydroxymethylation  
Adenine methylation  
Particulate matter  
LC-MS/MS  
Chemical derivatization

### ABSTRACT

The aim of this study was to explore the impact of three different standard reference particulate matter (ERM-CZ100, SRM-1649, and SRM-2975) on epigenetic DNA modifications including cytosine methylation, cytosine hydroxymethylation, and adenine methylation. For the determination of low levels of adenine methylation, we developed and applied a novel DNA nucleobase chemical derivatization and combined it with liquid chromatography tandem mass spectrometry. The developed method was applied for the analysis of epigenetic modifications in monocytic THP-1 cells exposed to the three different reference particulate matter for 24 h and 48 h. The mass fraction of epigenetic active elements As, Cd, and Cr was analyzed by inductively coupled plasma mass spectrometry. The exposure to fine dust ERM-CZ100 and urban dust SRM-1649 decreased cytosine methylation after 24 h exposure, whereas all 3 p.m. increased cytosine hydroxymethylation following 24 h exposure, and the epigenetic effects induced by SRM-1649 and diesel SRM-2975 were persistent up to 48 h exposure. The road tunnel dust ERM-CZ100 significantly increased adenine methylation following the shorter exposure time. Two-dimensional scatters analysis between different epigenetic DNA modifications were used to depict a significantly negative correlation between cytosine methylation and cytosine hydroxymethylation supporting their possible functional relationship. Metals and polycyclic aromatic hydrocarbons differently shapes epigenetic DNA modifications.

### 1. Introduction

Exposure to particulate matter (PM) is associated with an increasing prevalence and exacerbation of respiratory diseases and cardiovascular risks [1,2]. The cellular damages induced by PM include the generation of reactive oxygen species (ROS), which can severely disturb the balance between antioxidants and free radicals, which can oxidize macromolecules, namely DNA, lipids, and proteins. PM itself can cause many adverse effects, and additionally, numerous chemicals that are adsorbed on the surface of the particles can act as harmful pollutants. A very prominent class of such pollutants are polycyclic aromatic hydrocarbons (PAHs), such as benzo[a]pyrene (B[a]P), pyrene, fluoranthene and others. PAHs can be metabolized by cytochromes p450 (CYPs) enzymes resulting in dione-derivates or diol epoxide-derivates. These chemically

activated substances can then form PAH-glutathione (PAH-GSH) adducts or PAH-DNA adducts which can cause G-T transversion [3,4]. Investigations of fine PM from different combustion and non-combustion sources showed that diesel exhaust particles had the highest toxicological potential compared with other PM such as biomass and coal combustion or gasoline exhaust PM [5]. A comparison between particles of different size collected in traffic area showed that fine particles (<2.5 µm) were more cytotoxic than coarse particles (2.5–10 µm) [6]. The results of the mentioned studies show that the PM toxicity depends on multiple physico-chemical characteristics like particle size and chemical identity.

Previous studies on PM induced-effects mainly focused on cytotoxicity, genotoxicity, and oxidative-stress *in vivo* or *in vitro*. In contrast, the impact of PM exposure on epigenetic DNA modifications is studied to a

\* Corresponding author.

\*\* Corresponding author.

E-mail addresses: [lintelmann@helmholtz-muenchen.de](mailto:lintelmann@helmholtz-muenchen.de) (J. Lintelmann), [dibucchianico@helmholtz-muenchen.de](mailto:dibucchianico@helmholtz-muenchen.de) (S. Di Bucchianico).

<https://doi.org/10.1016/j.ab.2021.114127>

Received 9 September 2020; Received in revised form 18 January 2021; Accepted 29 January 2021

Available online 8 February 2021

0003-2697/© 2021 Elsevier Inc. All rights reserved.



much lesser extent. Cytosine methylation (5 mC) and cytosine hydroxymethylation (5 hmC) are widely known as two important epigenetic DNA markers because they have a significant impact on gene regulation [7]. The abnormal alterations of 5 mC and 5 hmC levels are linked to different pathologies, e.g. cancer, and can be used as diagnostic or prognostic indicators [8–10]. However, much less knowledge is available for other epigenetic changes of nucleobases like adenine. Recently, Sun et al. reported that N6-methyladenine may be a potential epigenetic marker associated with gene expression in eukaryotes [11]. Until now, the research about epigenetic DNA modifications caused by PM exposure has mainly focused on cytosine methylation and cytosine hydroxymethylation. For instance, Janssen et al. found that global cytosine hypomethylation levels in placental tissues were associated with residential PM exposure [12]. Bellavia and co-workers compared the effects of different sizes of PM collected from downtown streets (fine <2.5  $\mu\text{m}$ ; coarse 2.5–10  $\mu\text{m}$ ) on blood DNA cytosine methylation and found decreased levels of 5 mC level after exposure to fine PM [13]. Nys et al. showed that both ambient  $\text{PM}_{10}$  and  $\text{PM}_{2.5}$  had negative associations with 5-hmC levels in human buccal cells [14].

The impact of PM on adenine methylation is still unknown and understanding the effects of PM exposure on complex epigenetic DNA modifications and their endogenous relations will help to understand how PM affects cell metabolism and functions. Since the expected concentration levels of methylated adenine in eukaryote cell DNA are very low, a sensitive and reliable analytical method for their quantification is an indispensable tool. One possibility to improve the detection sensitivity is the chemical derivatization prior to chromatographic separation and mass spectrometric detection. This was shown in recent works where chemical derivatization combined with LC-MS/MS was applied for the analysis of cytosine derivatives including 5-methylcytosine and 5-hydroxymethylcytosine. For instance, those methods used derivatives containing a bromoacetone functional group, which specifically reacts with cytosine on the 4-N and 3-N position forming penta-cyclic derivatives [15–17]. Guo et al. used a different derivative containing an anhydride group, which reacts with the primary amine group on the 4-N position of cytosine [18]. After derivatization both the retention behavior of the derivatives during liquid chromatography and the ionization efficiency of derivatives in the MS-source were significantly improved. The mentioned methods did not use internal standards, even though it is widely accepted that the use of internal standards with similar physical and chemical properties as the target analytes is indispensable for a reliable quantification in LC-MS/MS. We used 2-bromo-4'-phenylacetophenone (BPAP) as reagent for the derivatization of 2'-deoxycytidine (dC), 5-methyl-2'-deoxycytidine (5-mdC), and 5-hydroxymethyl-2'-deoxycytidine (5-hmC). BPAP also reacts with adenine (Ade) and N6-methyladenine (6 mA) forming 3-N derivatives (minor product) and 9-N derivatives (major product, used for quantification) [19]. To further improve the reliability of the method, substituted internal standards were synthesized by using 2-bromo-2'-acetophenone (BAN) reagent for the derivatization of 5-mdC, Ade, and 6 mAde. The LC-MS methods were validated and used for the analysis of epigenetic DNA modifications in THP-1 cells. THP-1 cells were chosen because they are human monocytic cells and they offer a very broad application range for example as a cancer cell model in *in vitro* studies [20], to study the macrophage differentiation processes [21], or to explore the macrophage physiological-related activities *in vitro* [22].

Aimed to comprehensively analyze epigenetic DNA modifications, the levels of 5-mdC, 5-hmC, and 6 mA in THP-1 cells after exposure to three reference PM, fine dust ERM-CZ100, urban dust SRM-1649, and diesel SRM-2975 were determined. To further explore the need of specific positive controls for distinct DNA modifications, the epigenetic modifier 5-aza-2'-deoxycytidine (5-azadC), and the oxidizer tert-butyl hydroperoxide (TBHP) were used. Inductively coupled plasma mass spectrometry (ICP-MS) analysis of epigenetically relevant metals as Arsenic, Chromium and Cadmium [23] was performed to depict the role

of different metal content in the reference materials.

## 2. Materials and methods

### 2.1. Reagents

2'-Deoxycytidine (dC) was purchased from Alfa Aesar (Kandel, Germany). 5-Methyl-2'-deoxycytidine (5-mdC) and 5-hydroxymethyl-2'-deoxycytidine (5-hmC) were obtained from Jena Bioscience (Jena, Germany). Adenine (Ade), guanine (Gua), cytosine (Cyt), thymine (Thy), triethylamine (TEA), acetic acid, fine dust ERM-CZ100 (CZ100, ERM® certified reference material), BAN, BPBP, 5-azadC, and TBHP were bought from Sigma-Aldrich (Taufkirchen, Germany). Diesel PM SRM2975 (diesel PM, NIST® SRM® 2975) and urban dust SRM1649 (UD 1649, NIST® SRM® 1649) were from the National Institute of Standards and Technology (Gaithersburg, USA). N6-methyladenine (6 mA) was obtained from Cayman Chemical Company (Michigan, USA). Dimethyl sulfoxide (DMSO) was purchased from Biomol (Hamburg, Germany). Formic acid was bought from VWR international (Leuven, Belgium). Monocytic THP-1 cells were from ECACC (No. 88081201). DNA Degradase Plus™ and DNA degradase™ were obtained from Zymo Research (Freiburg, Germany). Acetonitrile (ACN) and methanol (LC-MS grade) were from ChemSolute (Munich, Germany). LC-MS-grade water was generated by a Milli-Q Reference System from Merck Millipore (Burlington, Massachusetts, US). Nitrogen was provided by a liquid nitrogen tank (Linde, Munich, Germany).

### 2.2. Cell culture, particle exposure, and DNA extraction

THP-1 cells were cultured in Roswell Park Memorial Institute (RPMI) medium (containing 10% Fetal Bovine Serum (FBS), 2 mM L-glutamine, and 1% penicillin/streptomycin solution) at 37 °C with 5% CO<sub>2</sub> in a humidified atmosphere. PM suspensions (1 mg/mL) were freshly prepared in medium without FBS by using an ultrasonic bath for 20 min directly before exposure. 5-azadC and tert-butyl hydroperoxide (1 mg/mL, TBHP) stock solutions were prepared in water and used as positive controls. The prepared suspensions were added into the medium to reach a final exposure concentration of 200  $\mu\text{g/mL}$  for ERM-CZ100 and SRM1649, 40  $\mu\text{g/mL}$  for SRM2975, 2.3  $\mu\text{g/mL}$  (10  $\mu\text{M}$ ) of 5-aza-2'-deoxycytidine, or 9  $\mu\text{g/mL}$  (10  $\mu\text{M}$ ) of tert-butyl hydroperoxide. THP-1 cells (0.12 million cells/cm<sup>2</sup> in T-75 flasks, 24 h prior to exposure) were treated with these PM suspensions or the positive control substances for 24 or 48 h. The established concentrations of PM caused 90% cell viability after 24 h exposure according to concentration-response pre-tests performed beforehand. Finally, THP-1 cells were harvested and washed with 10 mL of phosphate buffer solution. For DNA extraction, we followed a protocol published by Miller et al. [24] Quantity and purity of DNA were determined on a NanoDrop™ One/One<sup>c</sup> (Thermo Scientific, Germany). Following 24 h and 48 h THP-1 exposures, approximately 300  $\mu\text{g}$  and 500  $\mu\text{g}$  of DNA were extracted, respectively, and three independent analytical runs per condition were performed.

### 2.3. Epigenetic DNA modifications

#### 2.3.1. Liquid chromatography-mass spectrometry

LC-MS/MS measurements were carried out on an Agilent 1100 HPLC system consisting of a degasser, a binary pump, an autosampler, and a column compartment (Agilent Technologies, USA). Mass spectrometry was performed on a QTrap 4000 equipped with an ESI source (Sciex, USA). A Kinetex® C18 (2.6  $\mu\text{m}$ , 100 Å, 100 × 2.1 mm i.d., Phenomenex, USA) analytical column was used for the analysis of methylated and hydroxymethylated cytosine. Mobile phase A was water. Mobile phase B was acetonitrile. Gradient elution with a flow of 250  $\mu\text{L/min}$  was applied as follows: 0 min 65% A; in 7 min–50% A; from 8–17 min to 10% A; from 18–23 min to 65% A (equilibration). The eluent between 3 and 7 min was infused into the MS, the other gradient fractions were eluted to the



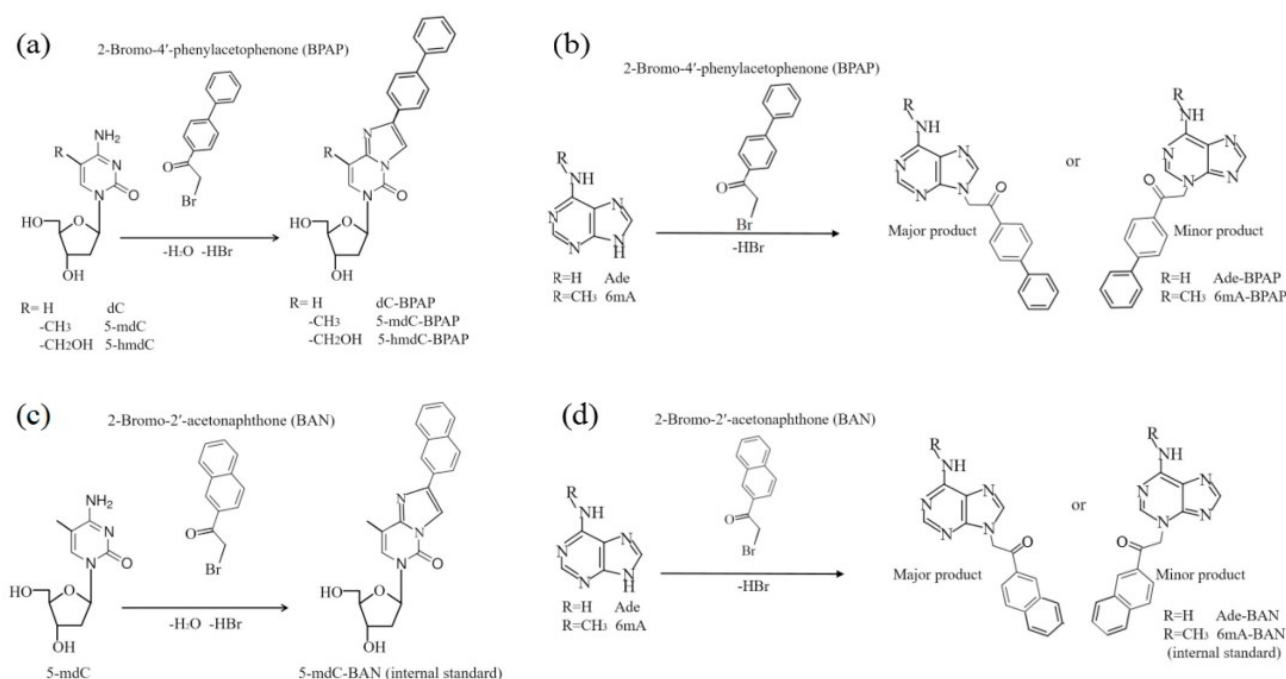


**Fig. 1.** Proposed reactions of (a) target analytes dC-BPAP, 5-mdC-BPAP, and 5-hmdC-BPAP (b) target analytes Ade-BPAP and 6 mA-BPAP (c) internal standard 5-mdC-BAN (d) internal standard Ade-BAN and 6 mA-BAN.

waste. A Kinetex® F5 (2.6  $\mu$ m, 100 Å, 100  $\times$  3.0 mm i.d., Phenomenex, USA) was used for the analysis of adenine methylation. Mobile phase A was 0.1% acetic acid. Mobile phase B was acetonitrile. Gradient elution with a flow of 250  $\mu$ L/min was used as follows: 0 min 85% A; in 18 min–50% A; from 19–28 min to 10% A; from 29 to 34 min 85% A (equilibration). Only the elution fraction from 9 to 18 min was infused into the MS.

### 2.3.2. Nucleobases methylation and hydroxymethylation

DNA (30  $\mu$ g) was dissolved in 60  $\mu$ L of tris-EDTA (TE) buffer containing 1  $\mu$ L of DNA degradase plus™ and 2  $\mu$ L of reaction buffer for cytosine modification studies and in 0.5  $\mu$ L of DNA degradase and 2.5  $\mu$ L of reaction buffer (Zymo research, Germany) for adenine methylation studies, respectively. The mixture was kept at 37 °C for 24 h at 800 rpm on a Thermo mixer C (Eppendorf, Germany). Afterwards, the DNA hydrolysate was heated at 70 °C for 20 min to deactivate the enzymes. DNA hydrolysate was dried under a gentle nitrogen flow in a Vapotherm basis mobil I (Barkey, Germany) at room temperature. For cytosine methylation and hydroxymethylation studies 10  $\mu$ L of BPAP solution (10 mg/mL) and 50  $\mu$ L of ACN containing 0.04% of glacial acetic acid were added to hydrolysed DNA, and kept at 80 °C for 4 h at 850 rpm on a ThermoMixer C. Then the mixture was moved to a fridge and stored at –20 °C for 10 min. After centrifugation at 10 000 rpm for 10 min in a Heraeus™ Biofuge Pico® Centrifuge (Thermo Scientific, Germany), 30  $\mu$ L of supernatant was mixed with 20  $\mu$ L of internal standard solution (Section 1.2, supporting information) for the measurement of 5-hmdC. Another 3  $\mu$ L of supernatant was diluted in a total volume of 300  $\mu$ L ACN, and 30  $\mu$ L of diluted supernatant was mixed with 20  $\mu$ L of internal standard solution (Section 1.2, supporting information) for the measurement of dC and 5-mdC. Each sample was injected three times into the LC-MS system with an injection volume of 10  $\mu$ L. Cytosine methylation and hydroxymethylation were calculated based on mole values as follows [25]:

$$\text{Cytosine methylation \%} = \frac{5\text{-mdC}}{5\text{-mdC} + \text{dC}} \times 100\% \quad (1)$$

$$\text{Cytosine hydroxymethylation \%} = \frac{5\text{-hmdC}}{5\text{-mdC} + \text{dC}} \times 100\% \quad (2)$$

For adenine methylation studies, 100  $\mu$ L of 88% formic acid was added to hydrolysed DNA and kept at 20 °C for 2 h at 800 rpm. Thereafter the mixture was dried under a gentle nitrogen flow at room temperature and dissolved in 10  $\mu$ L of DMSO. The solution was mixed with 50  $\mu$ L of BPAP solution (4 mg/mL), 10  $\mu$ L of TEA solution (2 mg/mL), and kept at 80 °C for 11 h at 1500 rpm on a ThermoMixer C. Afterwards the reaction solution was stored in a fridge at –20 °C for 10 min. The mixture was centrifuged at 10 000 rpm for 10 min in a Heraeus™ Biofuge Pico® Centrifuge after adding 30  $\mu$ L of internal standard solution (Section 1.4, supporting information). Then 60  $\mu$ L of supernatant was taken into a glass vial for the measurement of 6 mA. Another 3  $\mu$ L of supernatant was diluted in a total volume of 300  $\mu$ L ACN. 70  $\mu$ L of this acetonitrile solution was mixed with 30  $\mu$ L internal standard solution (Section 1.4, supporting information) for the measurement of Ade. Each sample was injected three times into the LC-MS system with an injection volume of 10  $\mu$ L. Adenine methylation was calculated based on mole values as follows [26]:

$$\text{Adenine methylation \%} = \frac{6\text{mA}}{\text{Ade}} \times 100\% \quad (3)$$

### 2.4. ICP-MS

The Standard Reference NIST Materials SRM-1649, ERM-CZ100 and SRM-2975 have been weighed and acidified with a mixture of nitric acid (69%) and hydrogen peroxide (30%). Subsequently the acidified samples have been digested by a Microwave speedwave ENTRY (Berghof, Germany) and diluted to a final concentration of 13% of HNO<sub>3</sub>. All the samples have been filtered through a 0.45  $\mu$ m syringe filter and analyzed by an Agilent 7700 Series ICP-MS. Calibration standard curves of 1, 10, 100 and 300  $\mu$ g/L for arsenic, cadmium and chromium have been used for the quantification. The calibration standard lines have been prepared from the initial calibration verification standard (Agilent, USA): 10 ppm for arsenic, cadmium and chromium in a matrix of 5% of nitric acid. In

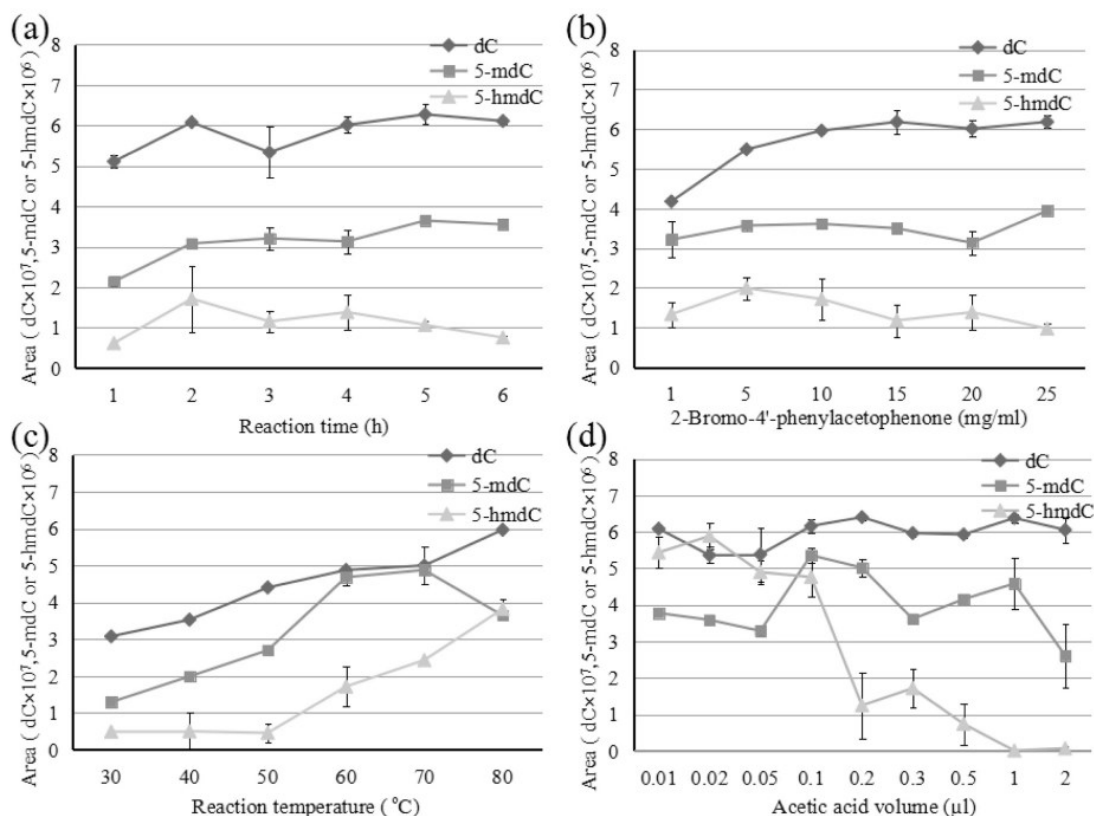


**Fig. 2.** Optimization of target analyte reactions between dC, 5-mdC, 5-hmdC, and BPAP, mean  $\pm$  standard error ( $n = 3$ ). (a) Reaction time with 20 mg/mL of BPAP solution, 0.3  $\mu$ L of glacial acetic acid, and 80  $^{\circ}$ C; (b) Different concentrations of BPAP at constant 0.3  $\mu$ L of glacial acetic acid, 4 h, and 80  $^{\circ}$ C; (c) Different temperatures with constant 10 mg/mL of BPAP, 0.3  $\mu$ L of glacial acetic acid, and 4 h; (d) Different volumes of acetic acid with constant 10 mg/mL of BPAP, 4 h, and 80  $^{\circ}$ C.

all samples 20  $\mu$ g/L of scandium and rhodium have been spiked and were used as internal standards. For every samples 4 technical repetitions have been performed. The detection limits for arsenic, cadmium and chromium were estimated as  $<0.005$   $\mu$ g/L,  $<0.0017$   $\mu$ g/L, and 0.0069  $\mu$ g/L, respectively.

### 2.5. Statistical analysis

The statistical data was processed by SPSS 20.0 software (SPSS, Inc). For clustered columns, the analysis of variance was calculated between the control and exposed groups. For two-dimensional scatters, linear regression, coefficient of determination, and p-value were evaluated between different epigenetic modifications. Data difference was considered to be significant when p-values were less than 0.05.

## 3. Results

### 3.1. Method development

The proposed reactions and mechanisms for chemical derivatization of cytosine and adenine are shown in Fig. 1 and – more detailed – in Fig. S1, supporting information. Chemical derivatizations of dC, 5-mdC, and 5-hmdC (Fig. 1a) were optimized concerning the following parameters: reaction time, concentration of BPAP, volume of acetic acid, and reaction temperature (Section 1.1, supporting information, and Fig. 2). The production of dC and 5-mdC derivatives reached an equilibrium after 4 h with 15 mg/mL of BPAP, which were then chosen as final reaction time and BPAP concentration. The generation of dC and 5-hmdC

derivatives was most effective at 80  $^{\circ}$ C which was selected as the reaction temperature. If the volume of acetic acid was higher than 0.1  $\mu$ L, the amount of 5-hmdC derivative decreased more than 80%. Finally, 0.02  $\mu$ L of acetic acid was selected. In order to study adenine methylation levels, a novel chemical derivatization of 6 mA was developed. BPAP was used to react with adenine and 6 mA to generate Ade-BPAP and 6 mA-BPAP derivatives (Fig. 1b). Adenine chemical derivatization was then optimized considering the reaction time, the concentration of BPAP, the concentration of TEA, and the reaction temperature (Section 1.3, supporting information, and Fig. 3). The production of the adenine derivative reached an optimum at 11 h, 4 mg/mL, and 80  $^{\circ}$ C, which were selected as the optimized conditions. The adenine derivative was in equilibrium between 0.05 and 4 mg/mL of TEA. If the concentration of TEA was higher than 4 mg/mL, the production of the adenine derivative decreased about 20%. Finally, 2 mg/mL of TEA was selected. Similar to the chemical derivatization of dC, the reaction between 5-mdC and BAN, used to produce the internal standard 5-mdC-BAN, was also optimized in terms of reaction time, temperature and concentration of acetic acid and BAN (Fig. 1c). The resulting conditions were 2 h, 15 mg/mL of BAN, 0.1  $\mu$ L of acetic acid, and 80  $^{\circ}$ C (Fig. S2, supporting information). The reaction time, temperature and concentrations of TEA and BAN for adenine and 6 mA derivatives, used as internal standards (Fig. 1d), were also optimized. Optimum conditions were 11 h, 2 mg/mL of BAN, 2 mg/mL of TEA, and 80  $^{\circ}$ C (Fig. S3, supporting information).

### 3.2. MS characterization

The parameters for mass spectrometric detection of each standard



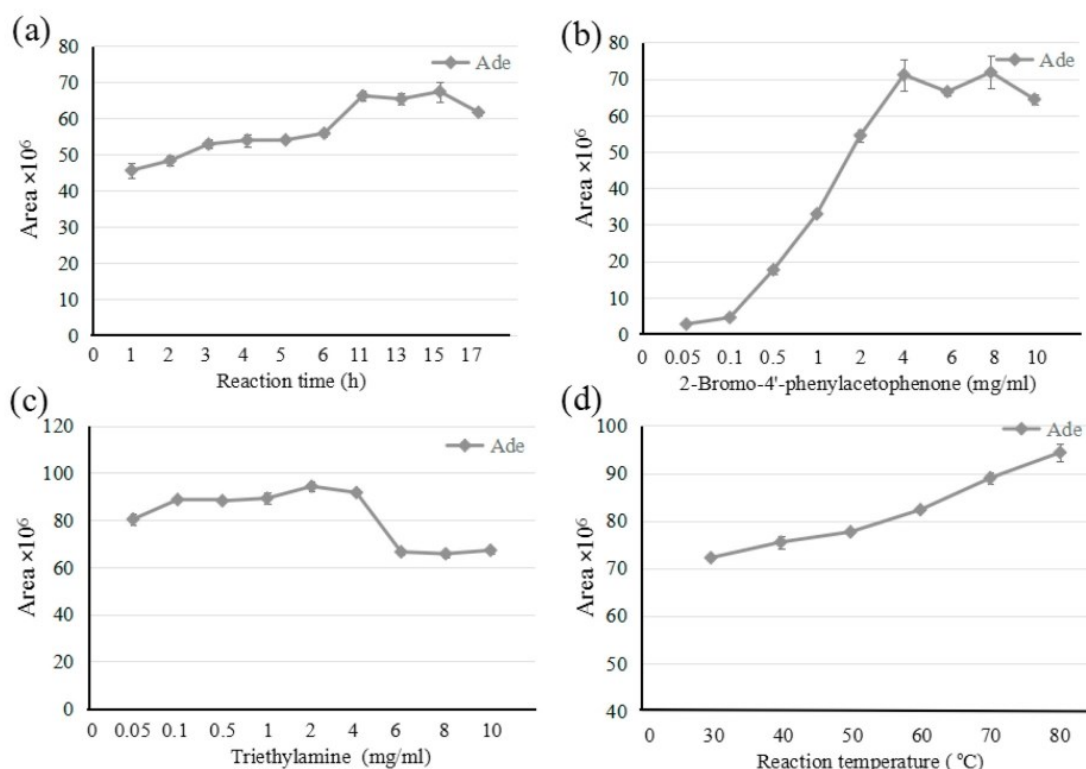


**Fig. 3.** Optimization of target analyte reactions between Ade and BPAP, mean  $\pm$  standard error ( $n = 3$ ). (a) Reaction time at constant 6 mg/mL of BPAP, 6 mg/mL of TEA, and 80 °C; (b) Different concentrations of BPAP with 6 mg/mL of TEA for 11 h, and 80 °C; (c) Different concentrations of TEA at constant 4 mg/mL of BPAP for 11 h, and 80 °C; (d) Different reaction temperatures at constant 4 mg/mL of BPAP, 2 mg/mL of TEA, and 11 h.

and its respective derivative were optimized, and the quantification was performed using multiple reaction monitoring (MRM) in the positive ion mode. For dC and its derivatives, the most intensive transition was the loss of deoxyribose moieties from nucleosides. For 5-hmdC and 5-hmdC derivatives, the fragment ions at  $m/z$  142.2 and 318.9 were not stable and easily lost a water molecule further generating new fragment ions at  $m/z$  124.1 and 300.7, respectively. For Ade and 6 mA, the typical fragment ions were at  $m/z$  94.1 and  $m/z$  119.1. Similarly, the derivatives had the most sensitive fragment ions at  $m/z$  136.2 and  $m/z$  150.4 which were  $[\text{Ade} + \text{H}]^+$  and  $[\text{6 mA} + \text{H}]^+$ . For each analyte, two transitions were selected for the detection using MRM. The first transition was used for quantification and the second one was used for qualification. Tuning parameters are summarized in Table S1, supporting information. Representative mass spectra obtained by collision induced fragmentation are shown in Figs. S4 and S5, supporting information.

### 3.3. Method validation

Methods were validated considering linearity, accuracy, precision, and the instrument limits of detection and quantification (Section 1.5, supporting information). Calibration curves showed good linearity with  $R^2 > 0.99$ . Three concentration levels (low, med, and high) were selected to evaluate accuracy and precision. Comparison between derivatized and non-derivatized target molecules showed that both the chromatographic retention of the target analytes during liquid chromatography and the detection performance of the target analytes by MS were greatly improved after derivatization (Tables S2 and S3, supporting information). The methods were applied to the analysis of THP-1 cell samples after exposure experiments. Typical MRM traces are shown in Fig. 4. Ade and 6 mA formed two derivatives with BPAP and BAN, respectively, showing two peaks for Ade-BPAP, Ade-BAN, 6 mA-BPAP,

and 6 mA-BAN in Fig. 4c–e. The chromatograms underline the capacity of the analytical methods to detect and quantify the low concentration of the target analytes.

### 3.4. Epigenetics modification in THP-1 cells

The background cytosine methylation in controls are about 6.3%. After 24 h exposure to CZ100 and UD 1649, the cytosine methylation significantly decreased to about 4.8% and 5.2%, respectively (Fig. 5a). However, the cytosine hypomethylation was restored after 48 h exposure. All 3 p.m. significantly increased cytosine hydroxymethylation by about 4-fold, 3.3-fold, and 2.4-fold of control levels after 24 h exposure to CZ100, UD 1649, and diesel PM, respectively (Fig. 5b). Even after 48 h exposure, increased cytosine hydroxymethylation was observed after exposure to UD 1649 and diesel PM with 2.7-fold and 2.5-fold of control levels (Fig. 5b). Significantly increased adenine methylation levels were observed after 24 h exposure to CZ100 while adenine methylation level was restored following 48 h exposures (Fig. 5c). Correlation analysis between different epigenetic modifications were performed, and a significantly negative correlation was found between cytosine methylation and cytosine hydroxymethylation ( $R^2 = 0.1776$ ,  $p\text{-value} < 0.001$ , Fig. 6a). In contrast, no significant relationships were found between cytosine methylation and adenine methylation (Fig. 6b).

### 3.5. ICP-MS

The certified mass fraction values of elements are available for SRM-1649, ERM-CZ100, and SRM-2975, however the most epigenetic active elements As, Cd and Cr were not analyzed in SRM-2975 particles (diesel PM). The average mass concentration of As, Cd and Cr in the used reference PM samples was analyzed by ICP-MS and the results are shown

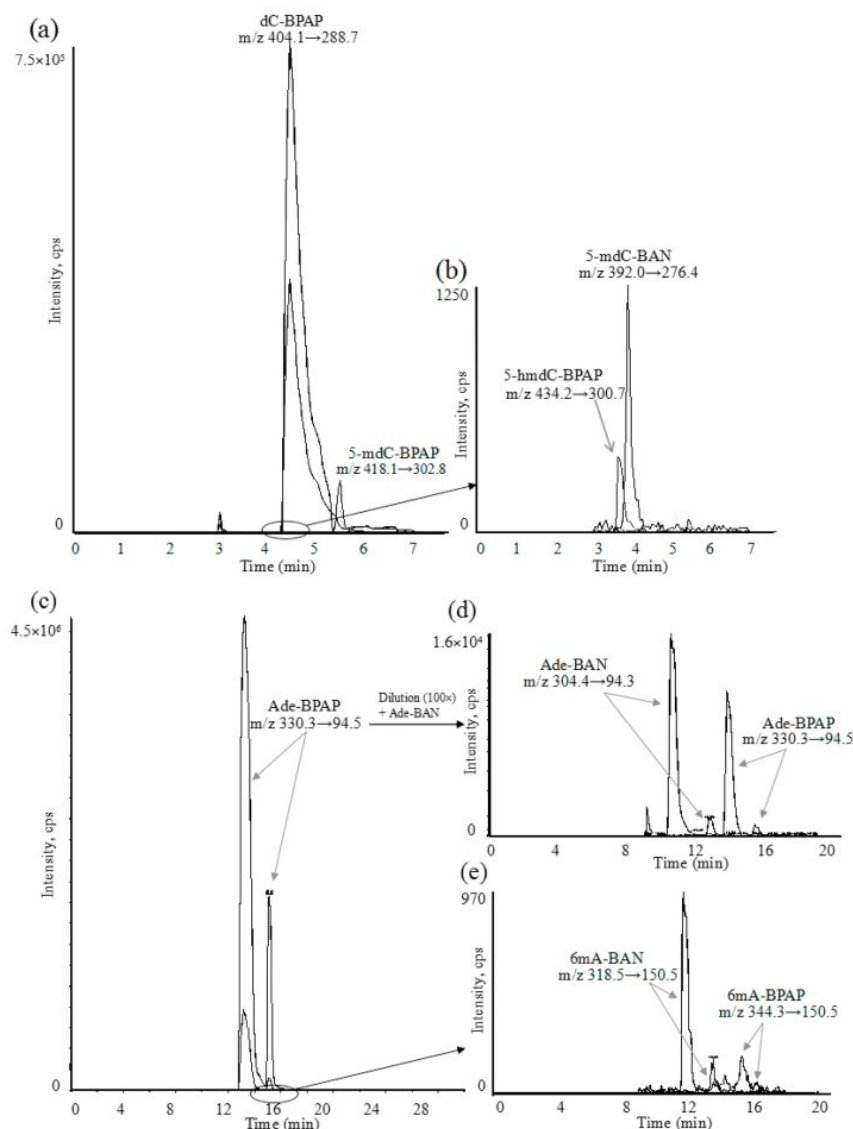


**Fig. 4.** MRM-traces of (a) target analytes dC-BPAP, 5-mdC-BPAP, 5-hmdC-BPAP, and internal standard 5-mdC-BAN (b) target analyte 5-hmdC-BPAP and internal standard 5-mdC-BAN (c) target analytes Ade-BPAP and 6 mA-BPAP, and internal standard 6 mA-BAN (d) target analyte Ade-BPAP and internal standard Ade-BAN (e) target analyte 6 mA-BPAP and internal standard 6 mA-BAN. The analytes were determined in control samples.

in Table 1. As expected diesel PM SRM-2975 do not contain high content of metals, however a non-negligible concentration of Cr was found. The fine dust ERM-CZ100 contains the largest amount of chromium while the urban dust particles SRM-1649 are characterized for having the largest amount of arsenic. With respect to the total amount of considered epigenetic active elements, no significant differences can be observed between CZ-100 and UD-1649, however ERM CZ-100 contains higher total amount of elements with respect to the other tested reference PM.

#### 4. Discussion

In the current study, we explored the impact of three standard reference PM on epigenetic DNA modifications (cytosine methylation, cytosine hydroxymethylation, and adenine methylation). A novel chemical derivatization method was developed for the analysis of 6 mA. To improve the retention behaviour of adenine and 6 mA in reversed phase liquid chromatography, we used BPAP to generate Ade-BPAP and

6 mA-BPAP derivatives in order to introduce a hydrophobic biphenyl group. The limits of detection (LOD) of all target analytes was also significantly improved compared to those found without derivatization. For instance, the LOD for 5-mdC and 5-hmdC decreased 2.5- and 5-fold respectively after derivatization, compared to the detection without proceeding derivatization (Table S2, supporting information) due to the improved ionization efficiency of the target analytes in the MS-source.

Until now, different derivative reagents have been used to analyze cytosine-related modifications in DNA and RNA. For instance, very low LODs for 5-mdC and 5-hmdC were obtained after derivatization with 2-bromo-1-(4-diethylamino-phenyl)-ethanone resulting in 0.04 fmol and 0.06 fmol, respectively [17]. Similarly, LODs values like 0.10 fmol for 5-mdC and 0.06 fmol for 5-hmdC were calculated by using 2-Bromo-1-(4-dimethylamino-phenyl)-ethanone [16]. In our study we used BPAP and BAN, and we reached LODs of 0.33 and 0.23 fmol for 5-mdC and 5-hmdC, respectively (Table 2). The observed difference can be attributed to both different derivatizing reagents and different



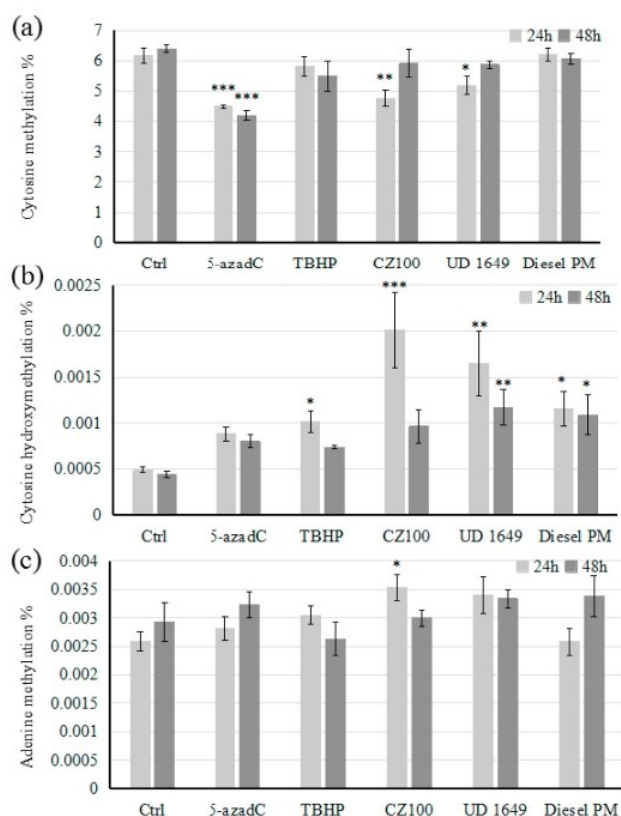


**Fig. 5.** Percentages of cytosine methylation (a) cytosine hydroxymethylation (b) adenine methylation (c) in untreated cells (Ctrl) and following 24 h or 48 h THP-1 exposures to 5-azadC (5-aza-2'-deoxycytidine), TBHP (tert-butyl hydroperoxide), CZ100 (ERM-CZ100), UD 1649 (urban dust SRM-1649), Diesel PM (diesel PM SRM-2975). Data are shown as mean  $\pm$  standard error ( $n = 6$ ), \* =  $p$ -value  $< 0.05$ , \*\* =  $p$ -value  $< 0.01$ , \*\*\* =  $p$ -value  $< 0.001$ .

instruments. In previous studies, the investigation of adenine methylation levels was mainly based on N6-methyl-2'-deoxyadenosine by using LC-MS/MS with LOD values ranging from 0.42 fmol to 20 fmol [28–30]. However, N6-methyl-2'-deoxyadenosine is expensive and a suitable internal standard for N6-methyl-2'-deoxyadenosine is difficult to obtain. In contrast, N6-methyladenine (6 mA) is cheap and thus adenine methylation studies based on N6-methyladenine evaluation are an ideal alternative approach. A disadvantage of using 6 mA is its poor retention in LC (on both reverse and normal phase chromatography) and its low mass spectrometric intensity. In this study, we could develop a novel derivatization method for 6 mA prior to LC leading to significantly improved retention behavior and increased mass spectrometric detectability. The LOD achieved (0.67 fmol) is the lowest reported detection

limit for 6 mA applying LC-MS/MS. With the aim to increase the reliability of the quantification, suitable internal standards were synthesized (5-mdC-BAN for cytosine modification analysis; Ade-BAN and 6 mA-BAN for adenine modification) and successfully applied in our study.

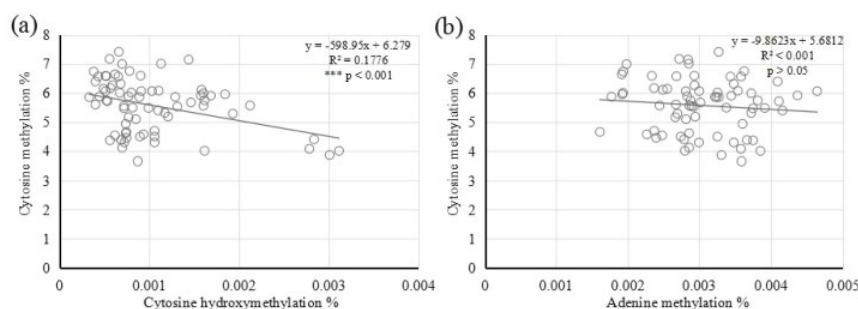
The application of optimized LC-MS methods including the novel chemical derivatization allowed a comprehensive evaluation of epigenetic DNA modifications induced by reference PM in monocytic THP-1 cells.

Global DNA hypomethylation is associated with aging and cancer [31], and it is therefore suggested to be a useful biomarker for carcinogenesis [32–34]. In the present study, we found that at non-cytotoxic conditions, both fine dust ERM-CZ100 and urban dust SRM-1649 significantly induced a transient cytosine hypomethylation and increased the levels of cytosine hydroxymethylation to a similar extent, while diesel SRM-2975 was irreversibly acting only on cytosine hydroxymethylation levels. These reference PM samples contain various epigenetically active chemical components such as the analyzed metals arsenic, cadmium and chromium, and also other elements and organic compounds like PAHs and nitro-PAHs (Table 1, Table S4 and material certificates). It was previously shown that exposure to arsenic induces a depletion of S-adenosylmethionine (SAM) and inhibits DNA methyltransferase gene expression (DNMT1 and DNMT3A) leading to DNA hypomethylation in HaCaT keratinocytes and a decreased enzymatic activity of DNA methyltransferase in rat liver TRL 1215 cells [35,36]. Cadmium is considered to be an epigenetic carcinogen perturbing DNA methylation levels via indirect mechanisms such as ROS generation and DNA repair inhibition while chromium inhibits histone-remodelling and alters gene expression via its genotoxic effects [37,38]. While higher levels of metal content in urban dust and fine dust materials can explain the higher efficacy in inducing hypomethylation, the higher content of nitro-PAHs in diesel SRM-2975 particles could explain its efficient and irreversible induction of cytosine hydroxymethylation. In fact, despite a 5 fold lower tested concentration of diesel PM with respect to the cell treatments with fine and urban dust PMs, the extremely high concentrations of nitro-PAHs, as reported in the material certificates, are

**Table 1**

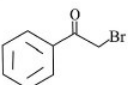
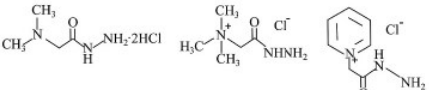
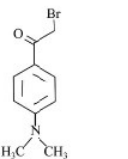
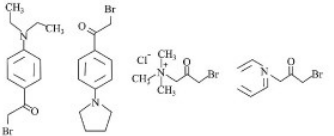
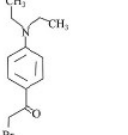
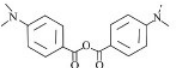
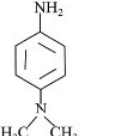
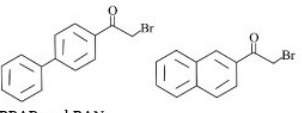
Mass fraction values (mg/Kg) of As, Cd, and Cr as evaluated by ICP-MS in the present study and as reported in CZ-100 and UD-1649 NIST certificates, or in Ball et al. for diesel PM SRM-2975 [27]. \*, not measured in our study.

	CZ-100	UD-1649	Diesel PM
As	8.58 $\pm$ 0.17	78.07 $\pm$ 1.42	1.24 $\pm$ 0.02
Cd	0.97 $\pm$ 0.02	27.52 $\pm$ 0.14	0.08 $\pm$ 0.01
Cr	238.13 $\pm$ 6.03	145.02 $\pm$ 1.57	4.22 $\pm$ 0.01
Co*	14.3	16.4 $\pm$ 0.4	0.1 $\pm$ 0.1
Cu*	462	223 $\pm$ 7	0.9 $\pm$ 0.6
Ni*	58 $\pm$ 7	166 $\pm$ 7	0.5 $\pm$ 0.7
Zn*	1240	1680 $\pm$ 40	16 $\pm$ 4
Fe*	38144	29800 $\pm$ 700	0.9
Total	$\approx$ 40200	$\approx$ 32200	$\approx$ 24



**Fig. 6.** Two-dimensional scatters between different epigenetic modifications based on six independent experiments for each exposure.

**Table 2**  
Summary for the used derivative reagents for cytosine-related modifications.

Target	Derivative reagent	LOD (dC, 5-mdC, 5-hmC, Ade, and 6mA)	Reference
cytidine; dC; 5-methylcytidine; 5-mdC;	 2-bromoacetophenone	15.3 fmol (dC) 22.7 fmol (5-mdC)	[15]
5-fodC; 5-cadC;	 Girard's D, T, P	no	[50]
5-mdC; 5-hmC; 5-fodC; 5-cadC;	 2-bromo-1-(4-(dimethylamino)phenyl)ethanone	0.10 fmol (5-mdC) 0.06 fmol (5-hmC)	[16]
5-methylcytidine; 5-hydroxymethylcytidine; 5-formylcytidine; 5-carboxycytidine;	 2-bromo-1-(4-(diethylamino)phenyl)ethanone 2-bromo-1-(4-(1-pyrrolidinyl)phenyl)ethanone 3-bromoacetonyltrimethylammonium bromide ω-bromoacetylpyridinium bromide	no	[51]
5-mdC; 5-hmC; 5-fodC; 5-cadC; 5-methylcytidine; 5-hydroxymethylcytidine; 5-formylcytidine; 5-carboxycytidine;	 2-bromo-1-(4-(dimethylamino)phenyl)ethanone	0.04 fmol (5-mdC) 0.06 fmol (5-hmC)	[17]
5-mdC; 5-hmC; 5-fodC; 5-cadC;	 4-(dimethylamino) benzoic anhydride	2.24 fmol (5-mdC) 2.53 fmol (5-hmC)	[18]
cytidine 5'-mono-phosphate; 2'-deoxycytidine 5'-monophosphate; 5-methylcytidine 5'-monophosphate; 5-methyl-2'-deoxycytidine 5'-monophosphate;	 N,N-Dimethyl-p-phenylenediamine	no	[52]
dC; 5-mdC; 5-hmC; Ade; 6mA;	 BPAP and BAN	0.22 fmol (dC) 0.33 fmol (5-mdC) 0.23 fmol (5-hmC) 1.48 fmol (Ade) 0.67 fmol (6mA)	Current study

differentiating diesel PM from urban dust and fine dust PM. This is related to freshly collected diesel combustion particles, not exposed to any atmospheric photo-oxidation reactions. *In vitro*, an increased amount of 5-hmC after exposure to traffic-related fine PM and its organic extracts was also observed in neuroblastoma SH-SY5Y cells [39]. Interestingly, the authors showed that the induced DNA hydroxymethylation was oxidative-stress mediated and was involved in neuronal pathology. However, the oxidizer TBHP used in our study only reversibly induced increased 5-hmC levels. A recent *in vivo* study in mice exposed to traffic-related PM (1 h daily for 3 months) showed decreased 5-hmC levels in lung and liver but no effects in the kidney,

and no significant differences on 5 mC levels in all analyzed internal organs [40]. In the latter study the 5mC/5-hmC ratio in the lung DNA of exposed mice increased suggesting that the loss of 5-hmC can be an early event in carcinogenesis [40]. Even if 5-hmC levels depend on many factors, intensive studies showed that 5-hmC is a stable epigenetic modification, and aberrant changes of 5-hmC levels have been associated with diseases such as cancer and Rett syndrome [41,42]. An increase of 5-hmC was, for example, found in the peripheral blood of patients with non-cancerous prostate diseases while decreased levels of 5-hmC were observed in human colorectal carcinoma tissues, with respect to tumor-adjacent normal tissues, and in hepatocellular



carcinoma tissues as well [16,43–45]. In the present study, we found a significant negative correlation between cytosine methylation and hydroxymethylation indicating a crosstalk between the two epigenetic mechanisms. In fact, TET proteins play a pivotal role in epigenetic processes through modification of 5 mC to 5-hmC which has a functional link with DNA elimination during genome rearrangements [46,47].

A reversibly increased level of 6 mA was observed only following fine dust ERM-CZ100 exposures and no effects were observed after exposure with the demethylating agent 5-aza-2'-deoxycytidine, or the oxidizing agent tert-butyl hydroperoxide, asking for specific adenine methylation related positive controls. Furthermore, we did not observe a correlation between cytosine and adenine methylation levels indicating that the two methylation processes are controlled by different mechanisms. The mechanism of adenine methylation modifications influenced by PM is not studied yet although some studies have shown associations between adenine methylation and different exogenous factors like environmental stress on mouse brains and the development of stress-induced neuropathology [48,49].

In summary, exposure to different PM reference materials, with distinct chemical composition, results in dissimilar epigenetic changes. Metal-rich PM exposures (ERM-CZ100 and SRM-1649) reversibly decreased cytosine methylation levels and increased adenine methylation content while all tested PM induced cytosine hydroxymethylation as observed, with smaller magnitude, following the treatments with the oxidizer TBHP. Oxidative stress is largely recognized as the major cause of many chronic diseases and plays a pivotal role in the pathogenesis of environmental lung diseases. The crosslinks between oxidative stress and epigenetic mechanisms need to be further investigated as well as the role of the chemical composition of different airborne PM in inducing genotoxicity and immunotoxicity.

## 5. Conclusions

In this study, we explored the impact of three reference PM on epigenetic DNA modifications in monocytic THP-1 cells. LC-MS/MS methods with preceding chemical derivatization of target analytes were optimized and a novel chemical derivatization for N6-methyladenine was developed. The derivatization significantly improved the retention behavior of the target analytes during chromatographic separation and increased the sensitivity of these targets during mass spectrometric detection. The methods were validated and subsequently applied for the quantification of epigenetic DNA modifications in monocytic THP-1 cellular DNA. Cell exposure to fine dust ERM-CZ100 and urban dust SRM-1649 decreased global cytosine methylation levels, while all tested PM increased cytosine hydroxymethylation. The two epigenetic processes were significantly negatively associated. A reversible increase of adenine methylation was observed after exposure to fine dust ERM-CZ100, which was independent compared to the observed cytosine methylation changes. Further studies are needed to investigate the epigenetic impact of PM exposure on human health, especially considering the different elemental/organic carbon content of PM as well as its metal content. An emphasis of such studies should be the examination of PM originating from break wear or abrasion particles from e-cars at emission sources.

## CRedit authorship contribution statement

**Xin Cao:** performed the majority of cell culture work LC-MS/MS, Formal analysis, and manuscript, preparation, Supervision, LC-MS/MS experiments. **Jutta Lintelmann:** Supervision, LC-MS/MS experiments. **Sara Padoan:** performed the ICP-MS, Formal analysis. **Stefanie Bauer:** supported cell culture work. **Anja Huber:** supported cell culture work. **Ajit Mudan:** performed the ICP-MS, Formal analysis. **Sebastian Oeder:** were involved in data interpretation. **Thomas Adam:** performed the ICP-MS, Formal analysis. **Sebastiano Di Bucchianico:** Supervision, cell experiments and was involved in the data interpretation and, Writing -

original draft, preparation.

## Declaration of competing interest

The authors declare that they have no competing interests.

## Acknowledgements

This work was supported by the Helmholtz Virtual Institute of Complex Molecular Systems in Environmental Health (HICE) via the Helmholtz Association of German Research Centers (HFG), the aero-HEALTH Helmholtz International Lab, and China Scholarship Council.

## Appendix A. Supplementary data

Supplementary data to this article can be found online at <https://doi.org/10.1016/j.ab.2021.114127>.

## References

- [1] A.B. Machin, L.F. Nascimento, K. Mantovani, E.B. Machin, Effects of exposure to fine particulate matter in elderly hospitalizations due to respiratory diseases in the South of the Brazilian Amazon, *Braz. J. Med. Biol. Res.* 52 (2019), e8130.
- [2] Y. Du, X. Xu, M. Chu, Y. Guo, J. Wang, Air particulate matter and cardiovascular disease: the epidemiological, biomedical and clinical evidence, *J. Thorac. Dis.* 8 (2016), E8–E19.
- [3] J.L. Barnes, M. Zubair, K. John, M.C. Poirier, F.L. Martin, Carcinogens and DNA damage, *Biochem. Soc. Trans.* 46 (2018) 1213–1224.
- [4] L. Zhang, Y. Jin, M. Huang, T.M. Penning, The role of human aldo-keto reductases in the metabolic activation and detoxication of polycyclic aromatic hydrocarbons: interconversion of PAH catechols and PAH o-quinones, *Front. Pharmacol.* 3 (2012) 193.
- [5] M. Park, H.S. Joo, K. Lee, M. Jang, S.D. Kim, I. Kim, L.J.S. Borlaza, H. Lim, H. Shin, K.H. Chung, Y.H. Choi, S.G. Park, M.S. Bae, J. Lee, H. Song, K. Park, Differential toxicities of fine particulate matters from various sources, *Sci. Rep.* 8 (2018) 17007.
- [6] W.L.W. Hsiao, Z. Mo, M. Fang, X. Shi, F. Wang, Cytotoxicity of PM2.5 and PM2.5–10 ambient air pollutants assessed by the MTT and the Comet assays, *Mutat. Res. Genet. Toxicol. Environ. Mutagen* 471 (2000) 45–55.
- [7] S. Guibert, M. Weber, Functions of DNA methylation and hydroxymethylation in mammalian development, *Curr. Top. Dev. Biol.* 104 (2013) 47–83.
- [8] A.S. Wilson, B.E. Power, P.L. Molloy, DNA hypomethylation and human diseases, *Biochim. Biophys. Acta* 1775 (2007) 138–162.
- [9] M. Ehrlich, DNA hypomethylation in cancer cells, *Epigenomics* 1 (2009) 239–259.
- [10] T. Dao, R.Y.S. Cheng, M.P. Revelo, W. Mitzner, W.Y. Tang, Hydroxymethylation as a novel environmental biosensor, *Curr. Environ. Health Rep.* 1 (2014) 1–10.
- [11] Q. Sun, S. Huang, X. Wang, Y. Zhu, Z. Chen, D. Chen, N6-methyladenine functions as a potential epigenetic mark in eukaryotes, *Bioessays* 37 (2015) 1155–1162.
- [12] B.G. Janssen, L. Godderis, N. Pieters, K. Poels, M. Kiciński, A. Cuyper, F. Fierens, J. Penders, M. Plusquin, W. Gyselaers, T.S. Nawrot, Placental DNA hypomethylation in association with particulate air pollution in early life, *Part. Fibre Toxicol.* 10 (2013) 22.
- [13] A. Bellavia, B. Urch, M. Speck, R.D. Brook, J.A. Scott, B. Albeti, B. Behbod, M. North, L. Valeri, P.A. Bertazzi, F. Silverman, D. Gold, A.A. Baccarelli, DNA hypomethylation, ambient particulate matter, and increased blood pressure: findings from controlled human exposure experiments, *J. Am. Heart Assoc.* 2 (2013), e000212.
- [14] S. De Nys, R.C. Duca, T. Nawrot, P. Hoet, B. Van Meerbeek, K.L. Van Landuyt, K. L. Van Landuyt, L. Godders, Temporal variability of global DNA methylation and hydroxymethylation in buccal cells of healthy adults: association with air pollution, *Environ. Int.* 111 (2018) 301–308.
- [15] A. L. Torres, E.Y. Barrientos, K. Wrobel, K. Wrobel, Selective derivatization of cytosine and methylcytosine moieties with 2-bromoacetophenone for submicrogram DNA methylation analysis by reversed phase HPLC with spectrofluorimetric detection, *Anal. Chem.* 83 (2011) 7999–8005.
- [16] Y. Tang, S.J. Zheng, C.B. Qi, Y.Q. Feng, B.F. Yuan, Sensitive and simultaneous determination of 5-methylcytosine and its oxidation products in genomic DNA by chemical derivatization coupled with liquid chromatography-tandem mass spectrometry analysis, *Anal. Chem.* 87 (2015) 3445–3452.
- [17] J. Xiong, X. Liu, Q.Y. Cheng, S. Xiao, L.X. Xia, B.F. Yuan, Y.Q. Feng, Heavy metals induce decline of derivatives of 5-methylcytosine in both DNA and RNA of stem cells, *ACS Chem. Biol.* 12 (2017) 1636–1643.
- [18] M. Guo, X. Li, L. Zhang, D. Liu, W. Du, D. Yin, N. Lyu, G. Zhao, C. Guo, D. Tang, Accurate quantification of 5-Methylcytosine, 5-Hydroxymethylcytosine, 5-Formylcytosine, and 5-Carboxymethylcytosine in genomic DNA from breast cancer by chemical derivatization coupled with ultra performance liquid chromatography-electrospray quadrupole time of flight mass spectrometry analysis, *Oncotarget* 8 (2017) 91248–91257.



- [19] D.M.-J.S. Buysen, Alkylation of Adenine: A Synthetic and Computational Study of the Reaction Mechanism, Master's thesis. University of Pretoria, Pretoria, RSA, 2015. Retrieved from, <http://hdl.handle.net/2263/64255>.
- [20] T.L. Chao, T.Y. Wang, C. H Lee, S.J. Yiin, C.T. Ho, S.H. Wu, H.L. You, C.L. Chern, Anti-cancerous effect of Inonotus taiwanensis polysaccharide extract on human acute monocytic leukemia cells through ROS-independent intrinsic mitochondrial pathway, *Int. J. Mol. Sci.* 19 (2018) 393.
- [21] J. Auwerx, The human leukemia cell line, THP-1: a multifaceted model for the study of monocyte-macrophage differentiation, *Experientia* 47 (1991) 22–31.
- [22] D. Wang, V. Hiebl, A. Ladurner, S.L. Latkolik, F. Bucar, E.H. Heib, V.M. Dirsch, A. G. Atanasov, 6-Dihydroparadol, a ginger constituent, enhances cholesterol efflux from THP-1-derived macrophages, *Mol. Nutr. Food Res.* 62 (2018) 1800011.
- [23] H.W. Ryu, D.H. Lee, H.R. Won, K.H. Kim, Y.J. Seong, S.H. Kwon, Influence of toxicologically relevant metals on human epigenetic regulation, *Toxicol. Res.* 31 (2015) 1–9.
- [24] S.A. Miller, D.D. Dykes, H.F. Polesky, A simple salting out procedure for extracting DNA from human nucleated cells, *Nucleic Acids Res.* 16 (1988) 1215.
- [25] T. Le, K.P. Kim, G. Fan, K.F. Faull, A sensitive mass spectrometry method for simultaneous quantification of DNA methylation and hydroxymethylation levels in biological samples, *Anal. Biochem.* 412 (2011) 203–209.
- [26] Z. Liang, L. Shen, X. Cui, S. Bao, Y. Geng, G. Yu, F. Liang, S. Xie, T. Lu, X. Gu, H. Yu, DNA N6-adenine methylation in Arabidopsis thaliana, *Dev. Cell* 45 (2018) 406–416.
- [27] J.C. Ball, A.M. Straccia, W.C. Young, A.E. Aust, The formation of reactive oxygen species catalyzed by neutral, aqueous extracts of NIST ambient particulate matter and diesel engine particles, *J. Air Waste Manag. Assoc.* 50 (2000) 1897–1903.
- [28] W. Huang, J. Xiong, Y. Yang, S.M. Liu, B.F. Yuan, Y.Q. Feng, Determination of DNA adenine methylation in genomes of mammals and plants by liquid chromatography/mass spectrometry, *RSC Adv.* 5 (2015) 64046–64054.
- [29] D. Liang, H. Wang, W. Song, X. Xiong, X. Zhang, Z. Hu, H. Guo, Z. Yang, S. Zhai, L. H. Zhang, M. Ye, Q. Du, The decreased N6-methyladenine DNA modification in cancer cells, *Biochem. Biophys. Res. Commun.* 480 (2016) 120–125.
- [30] D. Ratel, J.L. Ravanat, M.P. Charles, N. Platet, L. Breuillaud, J. Lunardi, F. Berger, D. Wion, Undetectable levels of N6-methyl adenine in mouse DNA: cloning and analysis of PRED28, a gene coding for a putative mammalian DNA adenine methyltransferase, *FEBS Lett.* 580 (2006) 3179–3184.
- [31] S. Gonzalo, Epigenetic alterations in aging, *J. Appl. Physiol.* 109 (2010) 586–597.
- [32] S. Friso, S. Udali, P. Guarini, C. Pellegrini, P. Pattini, S. Moruzzi, D. Girelli, F. Pizzolo, N. Martinelli, R. Corrocher, O. Olivieri, S.W. Choi, Global DNA hypomethylation in peripheral blood mononuclear cells as a biomarker of cancer risk, *Cancer Epidemiol. Biomarkers Prev.* 22 (2013) 348–355.
- [33] S. Lisanti, W.A.W. Omar, B. Tomaszewski, S. De Prins, G. Jacobs, G. Koppen, J. C. Mathers, S.A.S. Langie, Comparison of methods for quantification of global DNA methylation in human cells and tissues, *PLoS One* 8 (2013), e79044.
- [34] W. Huang, C.B. Qi, S.W. Lv, M. Xie, Y.Q. Feng, W.H. Huang, B.F. Yuan, Determination of DNA and RNA methylation in circulating tumor cells by mass spectrometry, *Anal. Chem.* 88 (2016) 1378–1384.
- [35] J.F. Reichard, M. Schnakenburger, P. Alvaro, Long term low-dose arsenic exposure induces loss of DNA methylation, *Biochem. Biophys. Res. Commun.* 352 (2007) 188–192.
- [36] C.Q. Zhao, M.R. Young, B.A. Diwan, T.P. Coogan, M.P. Waalkes, Association of arsenic-induced malignant transformation with DNA hypomethylation and aberrant gene expression, *Proc. Natl. Acad. Sci. U.S.A.* 94 (1997) 10907–10912.
- [37] A. Arita, M. Costa, Epigenetics in metal carcinogenesis: nickel, arsenic, chromium and cadmium, *Metal* 1 (2019) 222–228.
- [38] M. Venza, M. Visalli, C. Biondo, R. Oteri, F. Agliano, S. Morabito, G. Caruso, Maria Caffo, D. Teti, I. Venza, Epigenetic effects of cadmium in cancer: focus on melanoma, *Curr. Genom.* 15 (2014) 420–435.
- [39] H. Wei, Y. Feng, F. Liang, W. Cheng, X. Wu, R. Zhou, Y. Wang, Role of oxidative stress and DNA hydroxymethylation in the neurotoxicity of fine particulate matter, *Toxicology* 380 (2017) 94–103, <https://doi.org/10.1016/j.tox.2017.01.017>.
- [40] A.A.F. De Oliveira, T.F. De Oliveira, M.F. Dias, M.H.G. Medeiros, P. Di Mascio, M. Veras, M. Lemos, T. Marcourakis, P.H.N. Saldiva, A.P.M. Loureiro, Genotoxic and epigenotoxic effects in mice exposed to concentrated ambient fine particulate matter (PM<sub>2.5</sub>) from São Paulo city, Brazil, *Part. Fibre Toxicol.* 15 (2018) 40.
- [41] M. Bachman, S. Uribe-Lewis, X. Yang, M. Williams, A. Murrell, S. Balasubramanian, 5-Hydroxymethylcytosine is a predominantly stable DNA modification, *Nat. Chem.* 6 (2014) 1049–1055.
- [42] J. Wang, J. Tang, M. Lai, H. Zhang, 5-Hydroxymethylcytosine and disease, *Mutat. Res. Rev. Mutat. Res.* 762 (2014) 167–175.
- [43] A. Grelus, D.V. Nica, I. Miklos, V. Belengescu, I. Ioiart, C. Popescu, Clinical significance of measuring global hydroxymethylation of white blood cell DNA in prostate cancer: comparison to PSA in a pilot exploratory study, *Int. J. Mol. Sci.* 18 (2017) 2465.
- [44] Y. Tian, A. Lin, M. Gan, H. Wang, D. Yu, C. Lai, D. Zhang, Y. Zhu, M. Lai, Global changes of 5-hydroxymethylcytosine and 5-methylcytosine from normal to tumor tissues are associated with carcinogenesis and prognosis in colorectal cancer, *J. Zhejiang Univ. - Sci. B* 18 (2017) 747–756.
- [45] M.L. Chen, F. Shen, W. Huang, J.H. Qi, Y. Wang, Y.Q. Feng, S.M. Liu, B.F. Yuan, Quantification of 5-methylcytosine and 5-hydroxymethylcytosine in genomic DNA from hepatocellular carcinoma tissues by capillary hydrophilic-interaction liquid chromatography/quadrupole TOF mass spectrometry, *Clin. Chem.* 59 (2013) 824–832.
- [46] M. Tahiliani, K.P. Koh, Y. Shen, W.A. Pastor, H. Bandukwala, Y. Brudno, S. Agarwal, L.M. Lyer, D.R. Liu, L. Aravind, A. Rao, Conversion of 5-methylcytosine to 5-hydroxymethylcytosine in mammalian DNA by MLL partner TET1, *Science* 324 (2009) 930–935.
- [47] J.R. Bracht, D.H. Perlman, L.F. Landweber, Cytosine methylation and hydroxymethylation mark DNA for elimination in *Oxytricha trifallax*, *Genome Biol.* 13 (2012) R99.
- [48] B. Yao, Y. Cheng, Z. Wang, Y. Li, L. Chen, L. Huang, W. Zhang, D. Chen, H. Wu, B. Tang, P. Jin, DNA N6-methyladenine is dynamically regulated in the mouse brain following environmental stress, *Nat. Commun.* 8 (2017) 1122.
- [49] S.L. Kigar, L. Chang, C.R. Guerrero, J.R. Sehring, A. Cuarenta, L.L. Parker, V. P. Bakshi, A.P. Auger, N6-methyladenine is an epigenetic marker of mammalian early life stress, *Sci. Rep.* 7 (2017) 18078.
- [50] Y. Tang, J. Xiong, H.P. Jiang, S.J. Zheng, Y.Q. Feng, B.F. Yuan, Determination of oxidation products of 5-methylcytosine in plants by chemical derivatization coupled with liquid chromatography/tandem mass spectrometry analysis, *Anal. Chem.* 86 (2014) 7764–7772.
- [51] W. Huang, M.D. Lan, C.B. Qi, S.J. Zheng, S.Z. Wei, B.F. Yuan, Y.Q. Feng, Formation and determination of the oxidation products of 5-methylcytosine in RNA, *Chem. Sci.* 7 (2016) 5495–5502.
- [52] H. Zeng, C.B. Qi, T. Liu, H.M. Xiao, Q.Y. Cheng, H.P. Jiang, B.F. Yuan, Y.Q. Feng, Formation and determination of endogenous methylated nucleotides in mammals by chemical labeling coupled with mass spectrometry analysis, *Anal. Chem.* 89 (2017) 4153–4160.



## 6.5 Contributions to conferences

- (1) Xin Cao, Jutta Lintelmann, Sebastian Oeder, Anja Huber, Stefanie Bauer, Sebastiano Di Bucchianico, Ralf Zimmermann

*Determination of DNA Damage and Modifications in Cells Exposed to Particulate Matter*

European aerosol conference (EAC), poster presentation, 25-30. Aug. 2019, Gothenburg, Sweden

---

## 6.6 Curriculum vitae

Name           Xin Cao

Date of birth    3<sup>rd</sup> Jan, 1990

Place of birth   Shandong, China

### Education

Since 11. 2016	PhD student	Helmholtz Zentrum Munich and Rostock University
09. 2013-06. 2016	Student (Master, chemistry)	Beijing Forestry University
09. 2009-06. 2013	Student (Bachelor, chemistry)	Tianjin University of Technology
Until 2009	Pupil	Schools in Shandong